Titre: Title:	Seismic analysis design of taller eccentrically braced frames
Auteur: Author:	Simona Olivia David
Date:	2009
Type:	Mémoire ou thèse / Dissertation or Thesis
Référence: Citation:	David, S. O. (2009). Seismic analysis design of taller eccentrically braced frames [Mémoire de maîtrise, École Polytechnique de Montréal]. PolyPublie. https://publications.polymtl.ca/8302/

UNIVERSITÉ DE MONTRÉAL

SEISMIC ANALYSIS DESIGN OF TALLER ECCENTRICALLY BRACED FRAMES

SIMONA OLIVIA DAVID
DÉPARTEMENT DES GÉNIES CIVIL, GÉOLOGIQUE ET DES MINES
ÉCOLE POLYTECHNIQUE DE MONTRÉAL

MÉMOIRE PRÉSENTÉ EN VUE DE L'OBTENTION
DU DIPLÔME DE MAÎTRISE ÈS SCIENCES APPLIQUÉES
(GÉNIE CIVIL)
FÉVRIER 2009

Your file Votre référence
ISBN: 978-0-494-49434-9
Our file Notre référence
ISBN: 978-0-494-49434-9

UNIVERSITÉ DE MONTRÉAL

ÉCOLE POLYTECHNIQUE DE MONTRÉAL

Ce mémoire intitulé:

SEISMIC ANALYSIS AND DESIGN OF TALLER ECCENTRICALLY BRACED FRAMES

présenté par : DAVID Simona Olivia

en vue de l'obtention du diplôme de : Maîtrise ès sciences appliquées

a été dûment accepté par le jury d'examen constitué de :

M. BOUAANANI Najib, Ph.D., président

Mme KOBOEVIC Sanda, Ph.D., membre et directeur de recherche

M. HAN Xue Ming, P.Eng., membre

DEDICATION

To my fiancé, Nicolae

To my parents and sister

AKNOWLEDGEMENTS

I would like to express my most sincere thanks to my research supervisor, Prof. Sanda Koboević, for her moral and financial support during my research, for her advices and efforts invested in this project.

The author gratefully acknowledges the financial support provided by the Steel Structures Education Foundation of the Canadian Institute of Steel Construction for the current research project.

The provision of acceleration data by Prof. R. Tremblay of École Polytechnique de Montréal and Prof. G. Atkinson of Carleton University is gratefully acknowledged.

My thanks are extended to my graduate colleagues Carmen Bara, Camelia Nedisan and Jonathan Rozon for their help and collaboration during the process of this study. And finally but not least, I would like to thank my family for their love and support.

RESUMÉ

Les travaux présentés dans ce mémoire étudient le comportement sismique des cadres à contreventement excentrique de grande hauteur (CCE) et les prescriptions actuelles de conception du Code National du Canada 2005 et de la norme d'acier CAN/CSA S16-01(S16S1-05). Les CCE de type chevron avec poutres de liaison qui plastifie en cisaillement ont été conçu pour des bâtiments ayant quatorze, vingt et vingt-cinq étages situés à Montréal et Vancouver, qui représentent les conditions sismiques typiques pour l'est et pour l'ouest de l'Amérique du Nord. Pour chaque emplacement, l'importance des différents critères de conception est discutée. Les demandes reliées aux exigences de conception générale comme la résistance, la rigidité et la stabilité globale ont été comparées à la demande exigée selon la conception par capacité. Il a été découvert que les exigences de ductilité ne contrôlent pas la conception. En utilisent l'agrandissent de la masse structurale comme indicateur, il a été établis que pour Vancouver l'exigence du déplacement inter-étages inélastiques gouverne la conception du cadre, tendis ce que pour Montréal il est critique d'assuré la stabilité globale du cadre. Contrairement aux différences significatives relatives au cisaillement sismique de conception à la base, la masse de la configuration finale pour la même hauteur de cadre a été quasi identique. Suite à ces découvertes, la séquence appropriée de conception a été suggérée pour des zones avec activité sismique haute et modérée. L'impact de la distribution de la force sismique latérale (statique équivalente ou distribution spectrale) dans la sélection des membrures a été aussi investigué. Il a été démontré que les deux distributions conduisent à des sélections de membrures similaires.

La réponse sismique des cadres a été investiguée en utilisant des analyses non linéaires temporelles pour évaluer si les procédures de conception amènent à la réponse souhaitée du cadre. Les analyses ont été effectuées pour le set de séismes calibrés en concordance avec le spectre de conception pour les emplacements étudiés. La réponse de la poutre de

liaison a été enregistrée en utilisent les forces normalisées de cisaillement de la poutre de liaison et les rotations inélastiques en cisaillement. Le comportement global du cadre a été observé à travers le comportement des segments extérieurs des poutres et des diagonales, des forces axiales et des moments dans les poteaux, le profile de la force sismique, les profiles des déplacements inter-étages et la relation entre le déplacement inter-étage total et la rotation inélastique de la poutre de liaison. La performance sismique des structures situées dans l'ouest du Canada a été trouvée adéquat, à l'exception des étages supérieurs où les déformations plastiques excèdent les déformations envisagées dans la phase de conception. L'ampleur de la sur-résistance, introduite pendent la phase de conception pour les structures localisées dans l'est du Canada, a entraîné des exigences de ductilité réduites dans les poutres de liaison et a conduit à des cadres moins efficients de point de vue sismique.

ABSTRACT

The study presented in this thesis investigates the seismic behavior of taller eccentrically braced frames (EBFs) and current Canadian design procedures specified in 2005 National Building Code of Canada and steel design standard CAN/CSA S16-01(S16S1-05). Chevron-type EBFs with shear-critical links were designed for fourteen-, twenty- and twenty-five storey buildings in Montreal and Vancouver, representing typical eastern and western North-American seismic conditions. For each design location the importance of different design criteria is discussed. The demands related to the general design requirements such as strength, stiffness and the global stability were compared to the demand imposed by the capacity design. It was found that ductility requirements did not control design. Using an increase of the structural mass as indicator it was established that for Vancouver total inter-storey drift requirements governed frame design while for Montreal ensuring the global frame stability was critical. In spite of the large differences in seismic design base shears, the mass of final designs for the same frame height were almost identical. In view of these findings, the appropriate design sequence was suggested for zones with higher and moderate seismic activity. The impact of lateral force distribution (equivalent static or spectral distribution) on member selection was also investigated. It was shown that both distributions yielded similar selection of frame elements.

The seismic response of the frames was investigated using the non-linear time-history analysis to assess if the design procedures achieved desired frame response. The analyses were done for the sets of earthquake records calibrated to match design spectra at studied locations. The link response was monitored through maximum normalized link shear forces and inelastic shear rotations. The global frame behavior was observed tracing the behavior of the outer beams segment and braces, the axial forces and moments in the columns, the seismic force profile, inter-storey drift profiles and the relationship between

the total inter-storey drifts and the inelastic link rotations. The seismic performance of the structures situated in west of Canada was found to be adequate, except for the top storeys where the plastic deformations exceeded the deformations predicted in the design. The extent of seismic overstrength introduced during the design phase for the structures located in the eastern Canada caused the ductility demands in the links to be reduced and lead to seismically less efficient frames.

CONDENSÉ EN FRANÇAIS

Le cadre à contreventement excentrique (CCE) est un système de résistance aux charges latérales économique et efficace. La dissipation d`énergie sismique pour ce système est réalisée à travers la plastification en cisaillement et/ou flexion d`un segment spécial de poutre nommé lien de la poutre. Les autres éléments du cadre, les parties externes de poutres les diagonales et les colonnes seront conçues pour rester élastiques pendant l`activité sismique.

Les principaux objectifs de ce projet étaient d'étudier la performance sismique pour les cadres à contreventement excentrique de grande hauteur, établir l'importance de différentes règles de conception et les caractéristiques de conception pour l'est et l'ouest du Canada, d'investiguer la nécessité de limiter la hauteur de CCE et valider la procédure de calcul du CAN/CSA-S16S1-05 pour la rotation inélastique du lien de poutre.

Les études antérieures documentées dans la littérature ont principalement investigué des cadres à basse et moyenne hauteur, conçues pour l'ouest du Canada. Les analyses dynamiques indiquent que le comportement souhaité du cadre n'a pas été obtenu tout le temps. Les liens dans les étages supérieurs ont développé de plus grandes déformations et plus grands efforts de cisaillement qu'anticipé dans la conception. Le CNBC2005 impose des limitations de hauteur pour certains systèmes utilisés dans les applications sismiques. Un des objectifs de ce projet est d'investiguer la nécessité de limiter la hauteur de CCE pour empêcher les phénomènes d'étage faible.

Les cadres de grande hauteur développent des larges déformations et en conséquence assurer la rigidité et la stabilité du cadre devient un critère de conception important.
Les règles de conception canadiennes anticipent une grande ductilité dans les liens, comportement qui est peu probable dans les zones de modérée et basse sismicité. Dans

ces zones, la conception peut être gouvernée par d'autres exigences que la ductilité. Alors, il est important d'établir quelles sont les exigences qui gouvernent la conception pour l'est et l'ouest du Canada.

Les CCE sont le seul type de cadre en acier pour lequel l'explicite vérification de la ductilité doit se faire dans la phase de conception. La rotation inélastique du lien est calculée basé sur des estimées de déplacements inter étages qui sont calculés en utilisant les déplacements inter étages élastiques et en appliquant le principe des déplacements égaux. Plus des donnes seront nécessaires, incluent celles des cadres de grande hauteur pour proposer une approche plus réaliste de vérification de la ductilité.

La méthodologie suivante a été appliquée :

- Revue de littérature : études antérieures, normes de conception
- Pour chaque ville sélectionnée, deux différentes conceptions pour cadres aient 14, 20 et 25 étages, ont été effectué a fin d'évaluer l`impact de la distribution de la force sismique latérale dans la sélection des membrures
- Sélection et calibration d'ensemble des séismes qui seront utilisés dans les analyses dynamiques
- Des analyses temporelles non linéaires : résultats et interprétation
- Conclusions et recommandations

La majorité des études analytiques menées à ce jour, ont été effectué pour des cadres de faible à modérée hauteur, située dans des fortes zones sismiques. Les dispositions des codes canadiennes et américaines reflètent dans la conception par ductilité ces études. Aussi, les structures mentionnées ont été conçues en débutant avec la conception par ductilité, comme il a été observé que pour les cadres modérément élevés, la ductilité domine les exigences de la conception, et ensuite les cadres ont été vérifiés pour la résistance et la rigidité. Le but de cette étude est d'investiguer l'importance des différentes étapes de conception dans le cas des structures de grande hauteur.

Plusieurs études antérieures adressent le comportement des cadres à contreventement excentrique et en particulier le comportement cyclique des liens. La configuration et les proportions initiales du cadre sont basées sur des considérations trouvées dans la littérature comme: la position des diagonales dans le cadre, l'angle entre la diagonale et la poutre extérieure, la longueur du segment de lien. Le type de CCE utilisé dans cette étude a le lien placé au centre de la poutre (type Chevron) entre les points de la connexion poutres diagonales. L'étude présente se concentre sur des CCE avec des liens qui plastifient seulement en cisaillement. Plusieurs chercheurs recommandent cette configuration pour le comportement inélastique stable du lien de poutre.

Le développement théorique de l'élément lien de poutre est basé sur l'approche proposée par Ricles et Popov (1987b, 1994). Leur formulation de l'élément lien prédit avec succès le comportement en flexion et en cisaillement du lien. Le modèle comprend la plastification en cisaillement et en flexion et tient compte d'un écrouissage anisotrope, où le durcissement combiné cinématique et isotrope survient pendant la plastification en cisaillement, et seulement le durcissement cinématique pour la plastification en flexion.

L'élément est constitué d'un seul élément poutre linéaire élastique, avec des rotules plastiques non linéaires à chaque extrémité (Figure 2.3). Les déformations plastiques de l'élément sont retenues à la fin de l'élément dans les rotules plastiques, où la déformation de cisaillement et de flexion a lieu. Le comportement des rotules plastiques est décrit à travers une relation rigide - plastique force déformation et moment - rotation. La relation multilinéaire utilisée pour la rotule plastique (Figure 2.5) a été adoptée de Ricles (1994) et elle a été calibrée en fonction des essais expérimentaux récemment effectués pour l'acier ASTM A992 (Okazaki et al. 2004; Okazaki et al. 2005).

La méthodologie de conception par capacité utilisée dans cette étude est adoptée de Popov (1988, 1989) et le Kasaï (1997a). Pour les CCE la conception par capacité assume

deux étapes différentes : la première est de dimensionner le lien pour les charges anticipées selon sa résistance pondérée et la deuxième assume de dimensionner les autres membrures pour la résistance probable du lien, résistance probable du lien qui incluant l'écrouissage du lien.

La première étape est la sélection des liens de poutre : des sections pour les liens qui devaient être class 1 pour l'âme et class 1 ou 2 pour les ailes. Le lien qui plastifie en cisaillement sera choisi tel que la longueur du lien e < $1.6M_p/V_p$. et que la résistance pondérée ($V_r=\phi$ 0.55 wdF_y) de la section soit supérieure à la charge sismique du CNBC. Pour la rotation inélastique du lien le CAN/CSA-S16-05 précise une limite de 0.08 rad pour le lien plastifié en cisaillement. Dans le but de calculer cette rotation nous devrons utiliser un déplacement inélastique qui est précisé dans la norme comme étant égal à 3 fois le déplacement élastique, déplacement qui est déterminé pour les charges sismiques pondérées de conception.

Dans une deuxième étape on procède à :

- La conception des diagonales et poutres hors lien selon les charges amplifiées du lien, $V_{ultimé} = V_r*R_y* 1/ \phi *1.30$, ou V_r est la résistance pondérée du lien;
- Et la conception des colonnes selon les charges amplifiées du lien, avec un facteur d'écrouissage de 1.30 pour les deux étages supérieurs et 1.15 pour tous les autres étages. Les colonnes seront conçues pour leur capacité axiale en utilisent les formules montrées :
    - $C_f/C_r < 0.65$ pour la section de colonne du toit, pas d'effet cumulatif des efforts transmis par les liens.
    - $C_f/C_r < 0.85$ pour les autres sections de colonne, il est anticipé qu'un effet cumulatif des efforts transmis par les liens est moins probable à se produire pour touts les liens. Les liens ne seront pas tous plastifiés dans le même temps.

Les bâtiments étudiés dans ce projet ont été conçus pour deux sites (Vancouver et Montréal) et trois hauteurs de cadre : 14, 20 et 25 étages. Les plans typiques et les élévations pour les trois hauteurs des cadres utilisés sont présentés dans la Figure 3.1. Les CCE sont placés symétriquement dans le noyau central du bâtiment, deux dans chaque direction, ce qui permet l'analyse indépendante dans chaque direction. Les cadres ont des portées de 9 m, avec des hauteurs des étages type de 3.7m sauf le premier étage qui a 4.5m. La longueur du lien a été établie à 800 mm suite aux études paramétriques.

La procédure de conception implique la vérification de différents critères de conception tels que : la résistance, la rigidité, et la ductilité. Pour optimiser le processus de conception, il est souhaitable d'utiliser la séquence qui nécessiterait le moins de modifications entre les différentes phases de conception. Basé sur des processus de conception discutées dans la littérature et tenant compte du fait que la conception ce fait pour des cadres de grande hauteur (donc une plus grande importance des déplacements), la séquence suivante des phases de conception a été choisi :

- Sélection initiale du lien, basée sur des critères de conception ductiles.
- Avec les sections de poutres imposées, le choix des autres membres du cadre est fondé sur des critères de résistance.
- Les sections des membrures du cadre sont vérifiées pour la rigidité et la stabilité et des modifications sont effectuées si nécessaire.
- La stabilité globale de l'CCE est vérifiée au moyen d'une force sismique latérale amplifiée avec les effets P-Δ.
- Les poutres extérieures, les diagonales et les colonnes sont ensuite vérifiées pour la capacité en cisaillement des liens.
- Les rotations inélastiques des liens sont calculées et comparées avec les limites du code.

Les liens doivent être sélectionnés pour une résistance inélastique en cisaillement aussi proche que possible de la force de cisaillement induite par les charges sismiques pondérées. Les Tableaux 3.7 et 3.8 indiquent les valeurs de α (alpha) qui est le ratio de la résistance du lien divise par la charge sismique pondérée dans le lien. Le facteur alpha devrait être aussi proche que possible de l'unité, pour minimiser la sur résistance dans le lien et alpha doit être gardé constant sur la hauteur du cadre pour assurer des déformations inélastiques uniformément réparties. Le facteur alpha a des valeurs plus grandes dans le cas de Vancouver parce que le choix des liens est gouverné par les charges de gravité ou les forces sismiques dans les étages supérieurs, et les forces du vent dans le milieu et à la base du cadre. Les structures situées à Montréal ont des valeurs plus grandes du facteur alpha en raison des forces du vent qui contrôlent la conception dans le milieu du cadre et les étages bas ou par les forces de gravité dans les étages supérieurs.

Une fois que les sections des liens ont été choisies, les sections des poutres à l'extérieur des liens ont été fixées et la conception des autres membres a été réalisée à l'aide du logiciel Visual Design. La conception a été effectuée sur un modèle 2D du CCE. Les membres du cadre sont déterminés afin d'obtenir une structure avec une résistance suffisante pour toutes les combinaisons de charges. La combinaison de charge critique est différente pour les structures situées dans l'est ou l'ouest du Canada. Pour Vancouver, la combinaison des charges qui contrôlé la conception est généralement la combinaison des forces sismiques, tandis qu'à Montréal les combinaisons avec les charges de gravité ou les charges de vent dominent la sélection des membres.

Dans l'étape suivante, les déplacements inter - étages totaux ont été vérifiés par rapport à la limite du code 0.025 h_s, vérification effectuée pour les combinaisons de charge sismique. Les déplacements dus aux charges de vent ont été vérifie par la suite, pour que ça soit plus petites que 1/500 h_s. Les sections sélectionnées à la fin de cette phase de conception sont indiquées dans les tableaux 3.9 à 3.14. Les sections présentées sont celles qui satisfont les limites de déflexions pour la combinaison de la charge sismique, car

l'augmentation de la masse en raison de conditions de vent est pratiquement négligeable. Pour toutes les structures, quel que soit l'emplacement géographique du bâtiment, les valeurs maximales des déplacements ont été observées dans les étages supérieurs.

Pour vérifier la stabilité globale de la structure, deux méthodes sont utilisées dans le présent projet : (i) une procédure itérative dans laquelle les charges horizontales sont amplifiées en fonction des déplacements développés à chaque étage et (ii) la procédure NBCC 2005 dans laquelle un facteur de U_2 est calculé à l'aide d'une procédure d'une seule étape et comparée à une valeur maximale admissible. Pour satisfaire les exigences de la stabilité globale, il était nécessaire de modifier toutes les membrures du cadre y compris les liens. Alors que les modifications des liens de poutres ont été requises que localement, une augmentation significative des sections de colonnes et de diagonales a été nécessaire pour contrôler les déplacements et l'amplification des forces provoquées par les effets P-Δ. Les valeurs du coefficient de U2 ont été calculées sur la structure obtenue après le calcul des forces P-Δ, en utilisent ces forces sismiques amplifiées. Plusieurs modifications de sections ont été nécessaires pour maintenir la valeur de U2 dans la limite du code.

La dernière étape de la procédure de conception est la conception par capacité du cadre. La conception par capacité a été choisie comme dernière étape parce qu'on pense que les étapes précédentes (c'est-à-dire la résistance, la rigidité, la stabilité) sont plus exigeantes dans le cas des cadres de grande hauteur. Les formules pour déterminer les forces dans chaque type d'élément sont examinées en détail dans la mémoire. Étant donné que les liens de poutre ont été choisis du debout en considérant les critères de conception par capacité, il reste à vérifier seulement les capacités des autres éléments. Uniquement les diagonales à la base de la structure devaient être modifiées, tandis que les colonnes ont des grandes réserves de résistance à cause des autres critères de conception considérés avant. La dernière vérification de la conception par capacité est la rotation inélastique du lien, qui est calculée à partir des déplacements élastiques inter étages obtenus d'une

analyse statique sur les charges sismiques amplifies. Les valeurs de la rotation inélastique du lien sont calculées basé sur les déplacements inter étages qui exclu les déformations axiales des colonnes, ce qui explique les valeurs de gamma plus petites au sommet des cadres.

Les masses structurales obtenues en différentes étapes de conception pour tous les cadres sont en ordre croissant pour la suite des phases de conception choisie. On voit une différence significative entre les masses de la phase de résistance et rigidité pour les structures à Vancouver, donc on conclu que la rigidité est l'étape de conception critique pour Vancouver et une grande augmentation de masse entre la phase de rigidité et stabilité pour les structures à Montréal, qui nous amené a dire que l'étape critique pour Montréal est la stabilité.

Une deuxième conception en utilisant la distribution spectrale de la force sismique a été effectuée. Les analyses spectrales pour obtenir la force sismique ont été réalisées en utilisant des modèles 3D dans le logiciel Visual Design. Les étapes de conception décrites auparavant ont été suivies et les CCE conçu pour la distribution spectrale de la force sismique sont comparées avec les cadres conçus dans la conception initiale avec une distribution empirique de la force sismique. Les différences observes sont mineures et on peut conclure que pour les CCE de grande hauteur la distribution de la force sismique sur la hauteur du cadre n'influence pas la sélection des sections de membrures.

Deux études de sensibilité ont été effectuées dans cette étape : la première pour établir la sensibilité de la distribution spectrale aux modes supérieures de vibration, et la deuxième à la sélection des membrures du cadre.

- Influence des modes supérieures, qui sont plus évidentes dans le cas de Montréal. On peut observer l'influence significative de premier et deuxième mode, et moindre à partir de troisième mode.

- L'influence de la sélection des membrures dans la configuration du cadre est observée en comparent les forces spectrales de 3 cadres différents:
    1. Structure 1 dans laquelle les diagonales et les colonnes sont choisies sur le critère de résistance.
    2. Structure 2 les diagonales et les colonnes entièrement compatibles avec toutes les exigences de conception.
    3. les mêmes sections pour toutes les diagonales et les colonnes, identiques à ceux qui sont choisis au premier étage de la structure 1

On observe des influences mineures dans le profil spectral.

Les observations concernant la conception sont les suivantes :

- La séquence de conception établie (résistance, rigidité, stabilité et conception par ductilité) est jugée appropriée pour la gamme de hauteurs de cadre et les lieux étudiés.
- Pour les bâtiments, à Vancouver, le déplacement inélastique inter étages est le critère de conception principal ($\Delta \leq 0.025h_s$).
- Pour les bâtiments, à Montréal, le critère critique de conception, la vérification de la stabilité, a été gouverné par l'obligation de limiter le coefficient de U_2 à la limite du CNBC.
- Dans la phase de conception par capacité, seules les diagonales situées à la base des structures ont été modifiées.
- La vérification des rotations inélastiques du lien n'a pas été un critère critique dans la conception des cadres.
- La variante de la conception en utilisant la distribution spectrale de la force rapporte des configurations de cadres presque identiques. Les configurations semblables des cadres sont justifiées par le fait que des critères de conception comme la rigidité et la stabilité globale gouvernent la sélection des membrures.

Aux fins de cette étude, 10 séismes historiques et 10 artificiels ont été sélectionnés pour la ville de Vancouver et 10 séismes artificiels pour Montréal. Les séismes représentent des combinaisons de magnitude et des distances épicentrales qui contribuent le plus significativement au risque sismique de l'emplacement choisi. Les séismes artificiels sont choisis à partir de la base de données d'Atkinson et l'ensemble de dix records historiques a été sélectionné à partir de la base de données PEER. La calibration des séismes historiques: a été effectué à l'aide d'une méthode hybride qui consiste en : obtenir une aire sous le spectre identique à celui du CNBC sur une période déterminée par l'utilisateur (variable). En général deux plages de périodes structurales 0.2 à 1.0 sec et 1.0 sec à 2.5 sec ont été choisies. La calibration se fait basée sur l'égalité des aires (intensité spectrale) calculées en dessous de la ligne du spectre de réponse.

Les analyses temporales non linéaires ont été réalisées avec le logiciel ANSR1, dans lequel les liens seront modélisés comme des éléments élastiques dans la partie centrale avec une rotule inélastique à chaque extrémité, incluant l'écrouissage. La rotule plastique est composée des 3 sous rotules plastiques qui permettent d'obtenir la relation cisaillement – rotation appropriée. Les poutres seront modélisées comme des éléments poutre – colonne inélastiques. Les diagonales et les colonnes seront modélisées à l'aide des éléments poutre – colonne élastiques. La méthode d'analyse employée est la méthode de l'accélération constante moyenne de Newmark.

Les analyses dynamiques ont été effectuées et les suivantes paramètres de réponse sismique ont été étudiées :

- Les rotations inélastiques maximales des liens (γmax)
- Les forces de cisaillement dans les liens normalisés
- Les déplacements totaux inter étages
- La force sismique latérale
- Le comportement des autres membrures du EBF et l'amplitude des efforts développés dans ces membrures

- La relation entre le déplacement total inter étage et la rotation inélastique de lien

Pour quantifier le comportement inélastique des liens deux paramètres ont été étudiés : les rotations inélastiques maximales des liens et les forces de cisaillement dans les liens normalisés. Les rotations inélastiques maximums des liens pour les structures de Vancouver sont toutes allées au-delà de la limite de code dans les étages supérieurs et parfois dans les étages bas, tandis que dans les autres étages les rotations développées sont inférieures à la limite de 0.08 radian. On observe le dépassement de la limite du code pour le 50-émé percent des résultats dans le cas de la structure de 14 étages Vancouver. Les rotations inélastiques maximales des liens (γ_{max})- pour les structures à Montréal sont en général autour de 0.01rad, à l'exception des derniers étages ou les rotations atteindrent environ un tiers de la limite de code, soit 0.03 radian.

Les forces de cisaillement normalisées dans les liens sont calculées comme V_{max}/V_p et sont présentes dans des graphiques. Le facteur d'amplification de la force développée dans le lien a été trouvée à proximité de la valeur recommandée dans le standard CAN / CSA S16-05 de 1.30 avec des dépassements faibles aux derniers étages pour toutes les trois structures situées à Vancouver. Pour les structures à Montréal les facteurs d'amplification de la force de cisaillement dans les liens attendent la valeur recommande dans le code de 1.30 seulement aux derniers étages, et pour le reste des liens on observe des valeurs autour de 1.0 ou moindres, ce qui veut dire que les liens restant élastiques.

Les déplacements inter étages totaux ont la même tendance que les rotations inélastiques de liens : des valeurs plus élevées pour les structures situées à Vancouver, en particulier aux derniers étages et des valeurs faibles pour les structures à Montréal. Les profils de la force sismique latérale obtenus des analyses temporales ont été comparés avec les forces latérales empiriques et spectrales. Une ressemblance plus près est observée avec la force spectrale qu'avec la force empirique et aussi des différences importantes avec les deux profils des forces pour les derniers étages et les étages bas du cadre. Le profile de la force

dynamique pour les structures à Montréal, est moins lisse que celles des forces spectrales et statiques, caractéristique plus évidente due à l'influence des modes supérieures de vibration.

Les réponses de poutres, les diagonales et les colonnes ont été analysées en détail afin de localiser l'activité inélastique des membrures et pour valider les spécifications du code concernent la conception par ductilité. Le comportement des autres membrures du CCE peut être résumé comme suite:

- L'activité inélastique dans les poutres à l'extérieur du lien est très faible et elle est présente seulement dans le cadre de 14 étages à Vancouver.
- L'activité inélastique dans les diagonales et colonnes est isolée et elle se produise sans développent des larges rotules plastiques dans ces éléments.
- Les efforts dans les diagonales ont des valeurs plus grandes que celles estimées dans la phase de conception.
- Les colonnes dans les structures situées à Vancouver développent des moments fléchissants plus grands que les valeurs estimées dans la conception pendent que les colonnes pour les structures à Montréal ont des moments plus petits que prévu.

Une relation entre Δmax (déplacement total inter étages) et γmax (rotation inélastique du lien) a été établi dont la formule est pressente :

$$\Delta/hs=0.10\ \gamma+0.0033$$

Cette formule représente une moyenne entre les résultats des structures analysées. La formule est basée sur un mécanisme plastic – rigide et pour lequel le point de la première plastification est située à un index du déplacement inter étage de 0.33. Des graphiques exposent la comparaison entre les résultats de l'analyse dynamique et les prévisions de la rotation inélastique du lien en cisaillement à l'aide de la formule énoncée. Une bonne et conservative prédiction pour les valeurs de gamma est observée.

Les conclusions concernant la conception et l'analyse dynamique sont les suivantes :

- La séquence conception adoptée (sélection du lien, résistance, rigidité, stabilité et conception par capacité) de a été établie comme étant le plus approprié.
- La conception par capacité n'est pas un critère critique dans la conception sismique des CCE (EBF) de grande hauteur. La modification des sections du cadre n'est pas nécessaire pour se conformer au critère imposé sur la rotation en cisaillement du lien.
- Les critères de rigidité et de stabilité peuvent influencer significatif la conception.
- Les deux distributions des forces (statiques et spectrales) donnent des configurations des cadres presque identiques.

Dans l'ensemble la performance sismique des grandes CCE (EBF) est satisfaisante, à l'exception :

- Les liens dans les étages supérieurs qui ont des déformations plus grandes que prévu dans la phase de conception.
- La plastification dans les autres membrures de CCE, plastification qui est par contre limitée et confinée à certains étages.
- Les moments de flexion développés dans les colonnes de la structure située à Vancouver sont plus élevés dans les étages supérieurs que les valeurs estimées dans la phase conception, valeur qui est égale à 0.3Mp.
- Les structures à Montréal n'ont pas atteint le niveau prévu de la performance sismique.

TABLE OF CONTENTS

LIST OF TABLES

LIST OF FIGURES

LIST OF APPENDICES

LIST OF SYMBOLS

A	area
C_f	compressive force in a member
C_r	factored compressive resistance of a member
d	depth of the section
D	dead load
D_{nx}	plan dimension of building at level x perpendicular to the direction of seismic loading
e	length of the link
e_x	distance measured perpendicular to the direction of earthquake loading between center of mass and center of rigidity at the level considered
E	elastic modulus of steel; earthquake load
EBF	eccentrically braced frame
F_t	portion of V to be concentrated at the top of the structure
F_x	lateral force applied to level x
F_y	yield strength
g	acceleration due to gravity
G	shear modulus of steel
h_i, h_x	the height above the base to level i or x
h_n	total building height
h_s	storey height
HSS	hollow structural section
I	moment of inertia
I_a	Arias intensity
I_E	earthquake importance factor of a structure
K_x	effective length factor for in-plane action
K_y	effective length factor for out-of plane action
L	span of the EBF frame; live load

M_y yielding moment in a member

M_{beam} bending moment in the beam

M_f bending moment in a member

M_{link} moment in the link segment

M_p plastic moment resistance

M_r factored moment resistance of a member

M_{trans} bending moment transferred from link

M_v factor to account for higher mode effect on base shear

M magnitude of the ground motion

NLTHA nonlinear time history analysis

P_E Euler buckling strength

P_{beam} axial force in the beam

P_{brace} axial force in the brace

P_{col} axial force in the column

P_f factored axial force in link

PGA peak ground acceleration expressed as a ratio to gravitational acceleration

PS_a spectral acceleration of the ground motion

PS_v spectral velocity of the ground motion

r response ratio RE; radius of gyration; ratio of stiffness between beam and brace

R hypocentral distance of the ground motion

R_d ductility related force modification factor

R_o overstrength related force modification factor

R_y factor applied to F_y to estimate the probable yield stress

s second; stiffness reduction factor

S snow load

S the design spectral response acceleration

$S_a(T)$ the 5% damped spectral response acceleration

STE plain square sections

S_f scaling factor applied to ground motions to match the 2005 NBCC spectrum

T_a fundamental lateral period of vibration of the building

T_f tension force in a member

UHS uniform hazard spectra

U_2 amplification factor to account for second-order effects of gravity loads acting on the laterally displaced storey

V lateral earthquake design force at the base of the structure as determined in equivalent static force procedure; shear force in member

V_{beam} shear force in the exterior beam

V_{cum} cumulated lateral shear force

V_d lateral earthquake design force at the base of the structure as determined in dynamic analysis procedure

V_e lateral earthquake elastic force at the base of the structure as determined in dynamic analysis procedure

V_f factored shear force in the link

V_{max} maximum shear force in the link induced by earthquake

V_{min} minimum shear force in the structure

V_n nominal shear resistance

V_p plastic shear resistance

V_r factored shear resistance

V_u ultimate link shear force

V_y yielding shear force

W the weight of the building; wide flange section; wind load

WWF welded wide flange section

W_i, W_x portion of W which is located at level i or x

w thickness of the web

Z plastic section modulus

ΣC_f sum of factored axial compressive loads of all columns in the storey

ΣV_f sum of factored lateral loads above the storey; total first order storey shear

α value of link resistance to force demand

β angle between beam and brace

γ inelastic link rotation

Δ_f	inter storey drift
Δ_{in}	inelastic drift for factored seismic loading
Δ_{el}	elastic drift for factored seismic loading
ϕ	resistance factor
θ	storey drift angle
ψ	factor related to brace lower end constraint condition

CHAPTER 1. INTRODUCTION

1.1 Problematic

The development of the earthquake engineering field has increased the necessity to use structural systems that can provide significant ductility. The eccentrically braced frame (EBF) is an effective and economical seismic resistant system which stands out among other conventional steel framing systems by the extraordinary combination of high ductility, stiffness and strength. Some typical configurations of EBFs are illustrated in Figure 1.1. The system is detailed so as to provide energy dissipation through the shear and/or flexural yielding of a special segment of the beam called link, thus limiting the forces transmitted to the other elements of the structure. In the chevron-type EBF, which is the object of the present study, links are centrally placed between the brace-to-beam connection points. Under seismic solicitation all the other frame members, including outer beam segments, braces and columns are expected to remain elastic. The elastic braces contribute significantly to the high rigidity of this system.

Previous studies reported in literature investigated mainly the response of lower to medium height EBFs (four to fourteen storeys) designed for western North-American locations. It was shown that, for the regions with higher seismicity, it was possible to obtain efficient designs. In general, frame members were highly utilized while providing adequate structural strength, stiffness and ductility. Non-linear time-history analyses suggested however that desired frame behavior was not always obtained; links in the upper storeys developed higher shear forces and deformations than anticipated in design, columns, braces and outer beam segments showed inelastic behavior and the total inter-storey drifts remained well bellow the values predicted in design.

Little information on the behavior of taller EBFs can be found in literature. Such frames would normally experience larger deflections under lateral loading and thus, providing the adequate stiffness and global structural stability could become an important design consideration. On the other hand, Canadian design requirements anticipate severe ductility demand in yielding links, the behavior that is not probable to be obtained in zones with moderate or lower seismic activity. In such zones design could be governed by wind or gravity loads. Consequently, it is expected that taller EBFs will be differently proportioned compared to the lower EBFs which might significantly alter their seismic behavior. It is therefore necessary to study the seismic response of taller EBFs, both for western and eastern North-American seismic conditions and establish to which extent current design procedures achieve desired behavior and how the building height influences the seismic response.

National building Code of Canada (NBCC 2005)imposes limitation of height for the number of seismic load resisting systems, such as for instance concentrically braced frames or the shear walls. These limits were defined in response to the results of studies which indicated that large concentration of plastic deformations occurred only in one or two storeys (soft storey formation) when certain height of the structure was exceeded. Although the similar observations were reported in literature for EBFs, no limitation of height is defined for EBFs. On the other hand, it is well known that the increase in the number of floors in a building will lead to an exponentially increase in the quantity of steel, thus questioning the effectiveness of the selected framing system to provide sufficient resistance to wind and earthquake loads with the minimum steel quantity possible. It is therefore of interest to conduct a detailed study of the non-linear seismic behavior of taller eccentrically braced frames and establish if height limits are necessary for this structural system.

The eccentrically braced frames are also the only traditional steel seismic resisting system for which the explicit verification of ductility has to be done at design stage. This

verification is done by estimating the link inelastic rotations using the empirical formula provided in CAN/CSA-S16S1-05 and comparing the obtained values to the limits prescribed by the same standard. The procedure for the calculation of the inelastic link rotation is based on the assumption of the development of a rigid-plastic mechanism, and uses the estimates on total inter-storey drifts. The latter are calculated simply by multiplying the elastic inter-storey drifts by the factors R_0 and R_d. Previous studies on EBFs of lower to medium height showed the strong positive correlation between the maximum values of total inter-storey drifts and maximum inelastic shear rotations. However the relations between elastic and total inter-storey drifts were poorly predicted. More scientific data is required including those for taller EBFs in order to propose a more rational approach to perform ductility verifications.

1.2 Objectives

The main objectives of this research project are:

- Study the seismic response of tall EBF's designed following the Canadian design requirements and thereby validates design procedures for taller EBFs. It is anticipated to give recommendations on the most appropriate design sequence for this type of the structures
- Investigate the differences in the design and seismic behavior of the structures situated in west and east of Canada.
- Evaluate the necessity to define height limits for eccentrically braced frame systems.
- Validate the CAN/CSA-S16S1-05 procedure for the calculation of the link inelastic rotation for taller EBFs and suggest more rational approach to perform theses calculations.

1.3 Methodology

To accomplish the above objectives, buildings having 14, 20 and 25 storey were designed and analyzed for two locations: Vancouver to represent a strong seismic zone and Montreal for moderate seismic zone. The 14 storey structures were studied in greater detail to validate a number of assumptions used in the design process. The following methodology was applied:

- A comprehensive literature review was performed including the past experimental and analytical studies carried out on eccentrically braced frames, the seismic provisions of the 2005 National Building Code of Canada and the seismic design requirements of CAN/CSA-S16S1-05;
- For each selected location, two variant designs for 14, 20 and 25-storey frames were done to evaluate the impact of lateral seismic force distribution on member selection. The load profiles studied, both prescribed by NBCC 2005, included the one obtained from equivalent static force procedure as well as 3D response spectrum analysis.
- An ensemble of seismic ground motions specific for the west and east of Canada was selected, including 14 historic accelerograms. The ground motion were scaled to represent the design level specified in the NBCC 2005 and subsequently used to perform the nonlinear dynamic analyses;
- Nonlinear time history analyses were performed on the designed EBFs, to study their seismic performance and validate ductility requirements given in Canadian design standards. A special attention will be given to the inelastic link rotation – total inter-storey drift relation (γ-Δ relation) to assess the validity of the relation recommended in the code CAN/CSA-S16S1-05 for the tall EBF.

1.4 Organization

This thesis consists of six chapters. The first chapter presents the problem statement and sets the objectives and the methodology for the study. The second chapter provides the background on the development of seismic design and analysis of eccentrically braced frames and outlines Canadian design requirements for this specific structural system. In the third chapter, the design of six frames studied is presented and the appropriate design sequence is proposed. The sensibility of design to the choice of lateral load distribution is discussed. The fourth chapter describes the methodology used to select and scale the ground motions and presents the modeling used to carry out nonlinear time-history dynamic analyses. The results obtained from the nonlinear time-history analyses and the local and global frame behaviors are presented in the fifth chapter. The conclusions of the studies and the recommendations for further research are summarized in the sixth chapter.

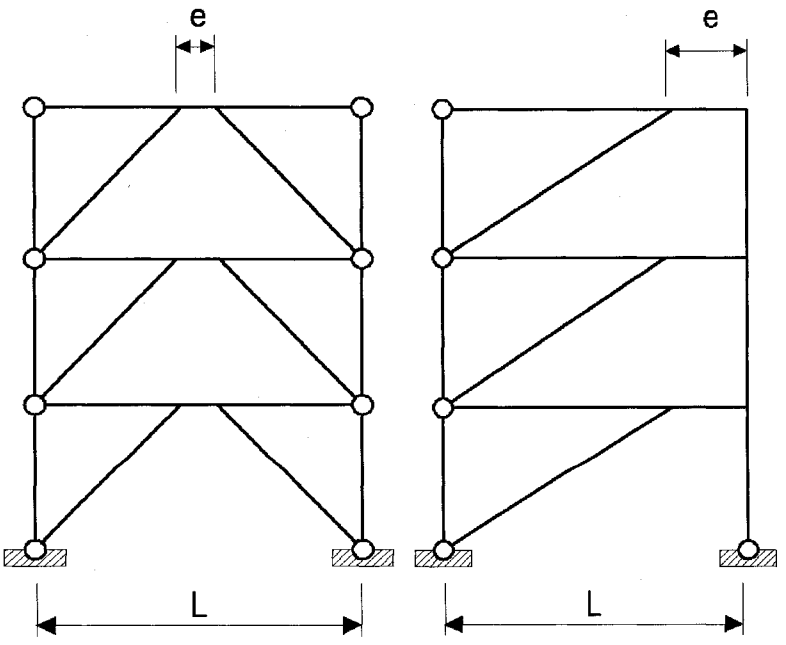

Figure 1.1 Typical configurations of EBFs

CHAPTER 2. LITERATURE REVIEW

This chapter begins with a comprehensive review of the previous analytical and experimental studies on seismic design and behavior of the eccentrically braced frames. The second part of the chapter summarizes the seismic provisions of the 2005 National Building Code of Canada as well as the seismic design requirements of CAN/CSA S16S01-05 relevant for the eccentrically braced frames.

2.1 Past studies on eccentrically braced frames

2.1.1 Generalities

The first objective of this project is to extend the previous studies on the EBF system and provide data regarding the seismic behavior of high rise structures that go above 14 storeys. The majority of the analytical studies carried out so far, were done for low to moderate frame heights and in strong seismic zones; and the provisions of design from the Canadian and American codes reflect those studies. Also the previous mentioned structures were conceived starting with ductility design, as it was observed that for moderately high frames the ductility requirements dominate the design, and afterwards verified for strength and stiffness. The intent of this study is to exanimate the importance of the design steps in the case of high rise structures.

Several past studies addressed the behavior of eccentrically braced frames and particularly the cyclic behavior of individual links. The code limitation for the inelastic rotation capacity of the link is based on experimental tests conducted at the University of California, Berkeley, during more then a decade, under the guidance of professor E.P.Popov (Engelhardt et al. 1992; Hjelmstad and Popov 1983; Kasai and Popov 1986b; Malley and Popov 1984; Popov et al. 1989). These UCB researchers recommend as a preferred EBF configuration the one presented in Figure 2.1 with links that develop pure

shear deformation. Experiments realized by Engelhardt and Popov (1989) found poor performance in the case of link-to-column connection or the long links and they recommended to avoid these connections.

Starting with the results of the research done in California, Canadian researchers have continued the work by developing new link models or improving the understanding of the structural behavior of EBF (Ghobarah and Ramadan 1990; Kasai and Han 1997a; Koboevic and Redwood 1997; Ramadan and Ghobarah 1995). The analytical link model developed by Ramadan and Ghobarah (1995) can be successfully used in various computer programs for analysis of nonlinear structural response. The studies effectuated by Han (1998) and Koboevic (2000) support the development of the design procedure in the Canadian building code and improve the understanding of EBFs seismic behavior.

Lately a new research project has started in the United States consisting of two main parts: a series of experimental tests (Okazaki et al. 2004; Okazaki et al. 2005) conducted at the University of Texas at Austin, followed by analytical studies effectuated by the researchers form University of California, San Diego. The experimental tests are meant to verify the satisfactory behavior of the new A992 steel grade, commonly used in the USA for seismic resistant structures. The analytical studies conducted by professor Uang (Richards and Uang 2006) investigate the impact of the loading protocol on the cumulative rotation demands of the links and propose a reformulated shear link element.

2.1.2 Frame proportioning and global structural response

To achieve an effective EBF design it is essential to select the frame configuration including initial proportioning considerations as: the bracing arrangement in the frame, the brace to beam angle, the length of the link segment. These design principles are key elements to a proper overall EBF behavior (Popov and Engelhardt 1988).

The chevron type of frame in which the two braces are disposed symmetrically and the link is positioned at the middle of the beam is preferred to the link adjacent to the column. The link to column connection develops unequal end moments and axial force in the link, which can lead to poor hysteretic behavior and fracture. The tests on long links positioned in the vicinity of columns have shown development of fractures on the link flange near the flange to column weld (Engelhardt and Popov 1989). Ghobarah and Ramadan (1990) also investigated the performance of short versus long links. Through finite element models, the performance of the short links was found to be better in terms of maximum deformation angle and energy dissipation capacity. Another general design recommendation (Popov and Engelhardt 1988) referring to the bracing arrangement is to keep the brace-to-beam angle higher than 40 degrees to avoid large axial forces in the outside beam.

The capacity design methodology used in this study is adopted from Popov (1988; 1989) and Kasai (1997a). Capacity design of a structure aims at designing elements from the system to provide the most ductile response after yielding while limiting the inelastic behavior of the other elements from the structure and avoiding potential brittle failure modes and global instability. The ductile eccentrically braced frames dissipate the energy by yielding of the link segments, yielding that can be either in flexure or shear, while the other elements of the frame will be chosen to resist the forces developed from the yielding of the links. In the papers published by Popov (1988; 1989) and Kasai (1997a) problems as the concentrations of yielding at a particular storey, the modelisation of the beam as elastic or inelastic element and the verifications of code recommendations for the inelastic link rotation are discussed.

In the process of links selection, the sections chosen can have higher strengths than the demand, thus a high overstrength due to several factors. When the capacity design is applied, this link overstrength factor, α is recommended by the above mentioned authors, to be kept constant in all storeys in order to obtain uniformly distributed link inelastic

deformations. The simultaneous link yielding assures a uniform distributed demand on the other elements of the frame. The design procedure to calculate the forces in all the members of the frame, when the link develops ultimate shear force is described in Kasai and Han (1997a). A particularity of the method is that the possible inelastic behavior of the outer beam is accepted. The modeling of the beam as inelastic is supported by other studies (Koboevic 2000) where it was observed that the plastic rotation of the beam is in general small when the brace is strong enough to remain elastic during the earthquake. Also in the recent studies realized in 2003 at the University of California, San Diego (Richards and Uang 2003) the response of the other members of the frame during the time-history analyses was in general elastic. A more detailed description of the capacity design procedure and the formulas used in this study to calculate the forces can be found in Chapter 3.2.6.

The frame proportioning is important in the calculation of the inelastic link rotation. The link rotation is calculated assuming the formation of a rigid plastic collapse mechanism (Figure 2.2), where the link length variation influences the elastic stiffness of the frame and the link rotation demand. The frame stiffness decreases with the increase of the e/L ratio, where L is the span of the EBF. For the link rotation demand the effect is opposite: the increase of the e/L ratio determines a lower value for the link rotation. In conclusion, keeping a reasonable balance between these two factors is an attempt of optimum design.

Recently a number of European researchers have published the results of their studies regarding the general behavior of EBF structures. In these papers subjects as the type of collapse mechanism and the influence of seismic load distribution are discussed. The Italian researchers Rossi and Lombardo (2007) have studied the influence of the link overstrength factor on the seismic response of EBFs, and they observed that the collapse configurations of the high-rise buildings are characterized by plastic concentrations in the upper storeys only. The same observations on the EBF response can be found in the work of the Canadian researchers (Koboevic 2000). Rossi and Lombardo (2007) also found

that the buildings designed with the static approach the normalized overstrength factor of links at the upper storeys exhibit overestimated values.

The differences between a simple EBF resisting system and a dual system, EBF coupled with moment resisting frame, have been studied by Bosco and Melina (2004). The results show that high-rise EBFs are likely to develop soft-storey mechanisms, caused by large plastic deformations in links and bending moment demand in columns. It was acknowledged that for the coupled system the additional stiffness provided by the Moment Resisting Frame, determines a uniform plastic deformation over the height of the building.

Static pushover analyses with different load patterns (Marino et al. 2003) were employed to determine the relevance of providing good evaluation on the seismic response. Empirical load patterns and load patterns that are resulting from the dynamic properties of the structures are examined in the study. The conclusion was that only the load patterns derived from the modal storey shears and bending moments lead to reliable results.

2.1.3 Link behavior and model

2.1.3.1 Link behavior in experimental tests

The investigation of the inelastic link behavior was extensively carried out in the past two decades. Link detailing provisions such as the stiffeners, the lateral bracing or the flange slenderness ratio were found to be important parameters in design modeling process to obtain satisfactory inelastic behavior of the link. It was demonstrated by Popov and Engelhardt (1988) that the lack of web stiffeners and axial force in the link can cause significant deterioration of the link hysteretic behavior.

Experimental tests carried out on short links (Hjelmstad and Popov 1983; Kasai and Popov 1986a; Malley and Popov 1984) investigated the link response under monotonically and cyclic increasing loading. The following general findings from their studies can be summarized:

a) Inelastic web buckling of the link will lead to loss in strength capacity and energy dissipation. The improvement of the hysteretic behavior is obtained by positioning web stiffeners. Properly stiffened links can achieve rotation of 0.20 radians under monotonically increasing load and ±0.10 radians under cyclic load. The range of inelastic rotations (maximum positive rotation added to maximum negative rotation) can reach 0.18 radians.
b) The largest shear force that the link can achieve after strain hardening is forty to fifty percent higher than the initial shear yield V_p. The ultimate shear strength of the short link tends to be higher than the maximum developed strength of flexural links.
c) The presence of axial force in the link during the cyclic loading leads to a deterioration of hysteretic behavior. The axial force in the link can be neglected in a properly designed EBF framing and with chevron type bracing.
d) The provision of lateral bracing for the link determines the state of in-plane deformations, thus eliminating the out-of-plane bending and the torsion moment.
e) The fracture in the web occurred after large deformations of web or flange buckling.

All the above mentioned tests were done on wide-flange shapes of ASTM A36 steel. In the current design codes and in practice the use of higher strength steel as ASTM A992 is mandatory for energy dissipating elements.

Twenty three experimental tests were carried out by Arce and Okazaki (2005) in order to investigate the effect of flange slenderness, the degree of overstrength and the effect of loading sequence on link performance. The following findings can be resumed:

a) The effect of material change seems to be minimal in terms of material overstrength. The average overstrength for short links is forty percent of the inelastic strength of the link V_n, where V_n contains factor of the probable yield stress R_y obtained from measurements on the test sections. The overstrength factor tends to be higher for shorter links.

b) The shapes with heavy flanges do not have higher overstrength factors. The relaxation on flange slenderness limits is supported by good results from tests, where links exceeded the required rotation level. The new proposed flange slenderness corresponds to a Class 2 in flexure.

c) The experiments shown that short links tested with the modified version of the moment resisting frame loading protocols (AISC protocol) developed web fracture close to the design inelastic rotation of 0.08 radians. Richards and Uang (2003) developed a new test loading protocol based on the cumulative and maximum rotation demands of the links, obtained from nonlinear time history analyses, where the analyses were performed for an ensemble of Los Angeles ground motions. Link specimens tested with the revised loading protocol achieved inelastic rotations of ± 0.12 radians. These values of the inelastic rotations of the links are determined for links that have the elastic deformations eliminated.

d) Contrary to the previous tests (Hjelmstad and Popov 1983; Kasai and Popov 1986a; Malley and Popov 1984), a number of shear link specimens developed the fracture of the link web, prior to web buckling. The fracture initiated at the end of filled weld from the connection of the stiffeners to link web. These observations were made for specimens tested with AISC loading protocol. Using the modified loading protocol proposed by Richards and Uang (2006) the same test specimens achieved link rotations above the code limit and did not exhibit any failure in the distance between the k-line and the stiffener weld termination.

2.1.3.2 Link model

The theoretical development of the link-element model is based on the approach proposed by Ricles and Popov (1987b; 1994). Their formulations of the link element successfully predicted both flexural and shear behavior of the link. The model includes shear and flexural yielding and takes into account an anisotropic strain hardening, where combined kinematic and isotropic hardening occurred in shear yielding, and only kinematic hardening for flexural yielding.

The element consists of a single linear elastic beam with non linear hinges at each end (Figure 2.3). The plastic deformations of the element are restrained to the end hinges, where the shear and flexural deformation take place. The axial deformations are restricted to the elastic beam segment between the hinges. Each hinge has zero length and is subdivided into three subhinges. The behavior of subhinges is described through a rigid-plastic force deformation and moment-rotation relationship. The subhinges are conceived to yield in a consecutive manner and thus produce a multilinear function for the general hinge (Figure 2.4). Experimental tests have shown that shear yielding in short links is not significantly influenced by the presence of the bending moment. Therefore, the theoretical subhinge yield surfaces, presented in Figure 2.4 (a), can be reduced to a rectangular yield surface for the element formulation as the one presented in Figure 2.4 (b). The influence of the axial force in a symmetrical chevron configuration is practically zero and therefore is not considered in the formulation of the link element.

In the new Standard S16S1-05 the steel used in energy-dissipating elements is recommended to have a minimum yielding stress F_y of 350 MPa. Thus the test results and the proposed link force-deformation models developed by Ricles (1994) and Ramadan and Ghobarah (1995) in which steel with a yielding stress F_y of 300 MPa was used would not be appropriate to be used for the present study. The available test data from Okazaki (2007) was studied by Jonathan Rozon (2009) and a multilinear shear force-deformation

function was derived to model the ductile shear link. This formulation of the shear link element will be used in the present study for the non linear time history analyses. The relationship for the shear and moment yielding are presented in Figure 2.5.

The recent experimental tests effectuated for ASTM A992 steel (Okazaki et al. 2004; Okazaki et al. 2005) imposed the need for a revision of the shear link force-deformation relationship. Together with the revision of the test loading protocol, a new multilinear force-deformation relationship for the shear link is given in Richards and Uang (2006). Their link element has the consecutive yielding values presented in Table 2.1 and it has the same theoretical basis as in Ramadan and Ghobarah (1995). Each plastic hinge from the link beam ends is modeled with three translational springs acting in parallel to develop the multilinear force-deformation relationship specific for the shear link element. The yield points and post-yield stiffness were calibrated using the test results for the ASTM A992 short links (Okazaki et al. 2004; Okazaki et al. 2005). The plastic flexural capacity was calculated for the expected yield stress of 379MPa, which is the numerical value for the theoretical probable yield stress R_yF_y.

Another link model was proposed by Ricles and Popov (1994) based on experimental tests realized with ASTM A36 steel. The values of the yielding points that they proposed for both shear and flexural yielding are presented in Table 2.1. They also proposed the values of the post-yielding stiffness to be used on the definition of the shear force-deformantion and bending moment-rotation relationships, which were afterwards adopted and used by other researchers. The difference with this model is that the initial shear yielding point is at $1.0V_p$, without accounting for the higher probable yielding R_yF_y.

Ramadan and Ghobarah (1995) developed an analytical model for the link element to be used in computer programs such as DRAIN 2DX. Their element was formulated based on the theoretical approach proposed by Ricles and Popov (1987b), using the same general hypotheses. The major difference that Ramadan and Ghobarah introduced is the

representation of the subhinges by means of translational and rotational spring elements. The element has four nodes, two internal and two external nodes, to represent the complete element. The internal nodes are slaved to the external nodes and the distance between each primary and slaved node is zero. The internal nodes enclose a beam-column element between them that is constrained to remain elastic. The inelastic response is to be concentrated at the link ends, where a set of three rotational and translational springs added in parallel model the multilinear inelastic behavior. This analytical model of the link beam is compatible with the most general purpose computer programs.

The Ramadan and Ghobarah model was calibrated using the existing test results from Hjelmstad and Popov (1983), Kasai and Popov (1986a; 1986b), and Ricles and Popov (1987b) for the steel grade 300 MPa. Their values of the shear and moments yielding points for the link model are presented in Table 2.1. The values of the forces at the initial yield were presented as $M_y=M_p$ and $V_y=0.9V_p$, where M_p is the moment plastic capacity and V_p is the plastic shear capacity of the link section.

A normalization for all three link elements formulation (Ramadan and Ghobarah 1995; Richards and Uang 2006; Ricles and Popov 1994) to the probable yield stress R_yF_y is presented in Table 2.1. The values for the shear yielding stages from Ricles and Popov were multiplied by R_y to account for the probable yield stress and the values from Ramadan and Ghobarah, with the factor $R_y/0.9$. These adjustments are effectuated to bring the initial yielding value to the probable stress of R_yF_y. A closer resemblance between Ricles element and Richard element is observed, considering that in the response of a link the important stages are: the initial yield shear force $V_y=R_yV_p$ and the maximum shear force, V_{max}, before the instability or buckling occurs in the link. Contrary, Ramadan and Ghobarah element show yielding stages that are different from the other two elements.

2.2 Canadian seismic design provisions for eccentrically braced frames

Canadian seismic design provisions for EBFs, are given in the latest editions of National Building Code of Canada (NBCC 2005) and the CAN/CSA-S16S1-05 Standard (CSA 2005; NBCC 2005). The structures studied herein are eccentrically braced frames with short shear links and only the provisions applicable to this system are presented in the following paragraphs.

2.2.1 Provisions of NBCC 2005

National Building Code of Canada defines only one level of ductility for the eccentrically braced frames characterized by the ductility-related force modification factor $R_d = 4.0$ and the overstrength-related force modification factor $R_o = 1.5$.

The NBCC 2005 describes two method of analysis for the calculation of the seismic force: the equivalent static force and the dynamic analysis method. The equivalent static force procedure is an empiric method of determining the distribution of the seismic force over the building height, based on the 100 percent of the structure's response on the fundamental mode of vibration. The response spectrum analysis used as a dynamic analysis method will yield a distribution of the lateral seismic force that includes the participation of higher modes of vibration. Both methods will be used in the study to calculate the seismic forces and then design the structures.

In the equivalent static force procedure, the design seismic lateral force V is calculated for a building fundamental period T_a equal to $0.025h_n$ for braced frames, where h_n is the building's height. The code also permits the use of the fundamental period of the structure determined from a dynamic analysis but not higher than the double of T_a.
The formula from the NBCC 2005 for the design base shear force is:

$$V = S(T_a)M_v W \frac{I_E}{R_d R_o} \quad [2\text{-}1]$$

with S (T_a) the spectral acceleration for the building fundamental period, M_v a coefficient that accounts for higher mode effects on base shear, I_E the earthquake importance factor of a structure and W the total seismic weight of the building. The coefficient R_d is a ductility related force modification factor that reflects the capability of the structure to dissipate energy though inelastic behavior and R_o is an overstrength related force modification factor that accounts for the reserve of strength generally present in a structure. The value of the seismic base shear force has two constraint limits: a maximum and a minimum value. The maximum value of the base shear is calculated with the formula:

$$V_{\max} = \frac{2}{3} S(0.2) W \frac{I_E}{R_d R_o} \quad [2\text{-}2]$$

The minimum base shear force that has to be considered in the seismic design is calculated as follows:

$$V_{\min} = S(2.0) M_V W \frac{I_E}{R_d R_o} \quad [2\text{-}3]$$

The maximum value of the base shear is restrictive for the low rise structures and the minimum base shear will apply to high rise structures. In the 2005 NBCC these types of limitations were imposed to soften the drastic changes on the spectral shapes of the NBCC 2005 which are now stepper than the spectral shape of NBCC 1995. For the short-period structures the reduction of the static base shear to two thirds is supported by the facts that the spectral accelerations values S(0.2) are higher in the new code and such structures have traditionally not suffered much damage during earthquakes. The long-

period forces in 2005 NBCC are generally lower than in the precedent building code thus the limitation of the spectral acceleration value to S(2.0) and the introduction of higher mode factor M_V which is a function of both spectral shape and type of structural system.

The distribution of the base seismic force V over the structure height is made according to:

$$F_x = \frac{(V - F_t)W_x h_x}{\Sigma W_i h_i} \qquad [2\text{-}4]$$

where W_x, W_i are the seismic weights at levels x and i respectively and h_x, h_i are the heights of the levels x and i. The force F_t is the concentrated force applied at the roof level to accounts for the effects of the higher modes on seismic force distribution and it is taken as $F_t = 0.07T_aV$ when T_a is larger than 0.7s. The torsional accidental moments must be calculated considering an eccentricity between the center of mass and the center of rigidity equivalent to $\pm 0.10D_{nx}$. The torsional sensitivity will be verified after the design of the EBF with a dynamic analysis for the 3D model of the building.

The dynamic analysis procedure that will be employed is the modal response spectrum method. The values of the spectral accelerations used in the modal response spectrum analysis are the values of the spectral accelerations $S_a(T)$ corresponding to the towns of Vancouver and Montreal. The effects of the torsional accidental moments developed at the same time with the seismic forces will be taken in account by assigning the same eccentricity mentioned for the static procedure. The results of this analysis are elastic shear forces with a total elastic shear at the base of the frame denoted V_e. In order to obtain the equivalent shear force to the statically calculated V, the elastic force V_e has to be multiplied with the risk coefficient I_E and then divided with the product R_dR_o. The formula for this dynamic shear force can be summarized as:

$$V_d = \frac{V_e I_E}{R_d R_o} \qquad [2\text{-}5]$$

For regular structures, the code permits a reduction of the dynamic shear force, which represents the minimum between the V_d and 0.8V, where V is the seismic force calculated with the equivalent static force procedure.

The deformations obtained from the linear dynamic analysis have to be multiplied with the factor V_d/V_e to find the more realistic estimates of inelastic deformations. The inter-storey drifts obtained from the calculated total deflections must to be smaller than $0.025h_s$ for the buildings of normal importance.

2.2.2 Provisions of CAN/CSA S16-05

The Clause 27 from CAN/CSA-S16-05 provides the special requirements to conduct the capacity design for the members and connections of the seismic force resisting system. The maximum anticipated seismic loads used in the process of capacity design are determined as described in the above paragraphs.

The minimum specified yield stress F_y of the steel used in the elements that are designed to dissipate the energy have to be lower or equal to 350 MPa. The probable yield stress is defined as $R_yF_y \geq 385MPa$, where R_y is 1.1 for steel G40.21.The width-to-thickness limits for the energy-dissipating elements are calculated using specified yield stress that should not be less than 350MPa.

2.2.2.1 Design of links

The sections used for the links in eccentrically braced frames have to be in general Class 1. Class 2 sections are permitted for links that develop pure shear behavior ($e \leq 1.6 M_p/V_p$) provided that the web is Class 1. Special attention is given to the link configuration in order to have a web of uniform depth without penetrations, splices, attachments or reinforcements (as double plates), except the stiffeners. The link stiffeners are vertically disposed plates having full-depth web development and they are attached to the web and the flanges of the link section with filled welds. A schematic illustration of this detailing can be found in Figure 2.7.

The links are designed for the coexisting forces that develop in it. The procedure employed to derive these forces from the lateral shears that act on the nodes of the structure is presented in Chapter 3.2.6. A restriction is imposed to the link length which can not be less than the depth of the link section. The other requirements for the link length do not apply herein because the axial force in the link P_f will be considered equal to zero.

According to Clause 27.7.2 the shear resistance of the link beam has to be taken as the minimum value between $\phi V_p'$ and $2\phi M_p'/e$, where:

$$V_p^{'} = V_p \sqrt{1 - \frac{P_f}{AF_y}} \qquad [2\text{-}6]$$

$$M_p^{'} = 1.18 M_p \left(1 - \frac{P_f}{AF_y}\right) \leq M_p \qquad [2\text{-}7]$$

The plastic resistance in shear of a section V_p is defined as $V_p=0.55wdF_y$ and the plastic moment resistance as $M_p=ZF_y$. The force P_f is the axial force in the link that can be either

tension or compression, the symbol A denotes the total area of the section and e is the length of the link. When the link is short enough ($e<1.6M_p/V_p$) the link will yield in shear and it is called a shear link. In this study all the links in the frame will be chosen to develop only shear behavior and the maximum shear resistances will be therefore the factored resistance $V_r=\phi 0.55wdF_y$, where ϕ is equal to 0.9. The links will be considered to have full lateral support provided at both top and bottom flanges at the end of the link.

During the earthquake activity the link segment will develop flexural, and/or shear plastic hinges and rotate relatively to the rest of the beam. The associated inelastic deformation is called the link rotation. The CAN/CSA-S16-05 specifies limitations on this inelastic rotation. For the links that yield in shear, as in the present study, the maximum inelastic link rotation is restricted to 0.08 radians. When verifying this requirement the code specifies to calculate the rotation by taking inelastic drift in the frame as 3 times the elastic drift, Δ_{el}, determined for the factored seismic loading at the design level:

$$\Delta_{in} = 3 \cdot \Delta_{el} \qquad [2\text{-}8]$$

The eccentrically braced frames are the only seismic resisting systems for which the verification of ductility is done directly through the calculation of inelastic link rotation. Limiting the links rotations to the code limit and maintaining a uniform value of these rotations through the frame's height is an aim of optimal design.

2.2.2.2 Design of other frame members

Prescription for the capacity design of the other frame members are given in the CAN/CSA-S16-05 such that the resistance of these members will be greater than the forces transmitted from the yielded link segment. The exterior parts of the beam, outside the link must have sufficient axial and bending capacity to resist forces developed in the

link beam sections are similar to the link segment sections). The beam resistance is taken as the factored resistance multiplied by R_y/ϕ and the link forces are equal to $1.30R_y$ times the nominal strength of the link ($1.30R_yV_p$). The outside beam has to be provided with sufficient lateral support to sustain the stability of the member under the forces transmitted from the link.

The diagonal brace and its end connections must be selected from section Class 1 or 2 and with a sufficient factored resistance to support the forces developed in the strain-hardened link, which shall be calculated as $1.30R_y$ times the nominal strength of the link. Special attention has to be given to the brace-to-beam connection such that the intersection of the brace and beam centerlines to be at the end of, or within, the link. Also the full end restrained (moment connection) of the braces with the beams is to be provided if the braces will sustain link end moments.

The column sections must be Class 1 or 2 and shall resist forces developed from the cumulative effect of yielding links and the gravity loads. The amplification coefficient for the columns is $1.15R_y$ times the nominal strength of the link, except for the top two storeys where this coefficient is $1.30R_y$. The column resistances shall satisfy the requirements of Clause 13.8 Axial Compression and Bending. The interaction equation for the columns will be taken as C_f/C_r without the moment contribution. The columns shall be chosen such that their interaction values shall not exceed 0.65 for the top column tier and 0.85 for the rest of columns in the EBF. The peak column moments are difficult to estimate only by static analysis because they are a function of inelastic drifts between adjacent storeys and column continuity. These moments could be evaluated using an inelastic dynamic analysis, therefore based on past analytical studies the above mentioned simplification of the interaction equation was proposed (Kasai and Han 1997a) to be used in the design of the EBF columns.

When the member strength and stability of the exterior beams, braces and columns is examined the equations of the Clause 13.8 and 13.9 will be used to compute the member capacity, depending on the type of section used. When using the above mentioned equations the member capacity will be examined for:

a) Cross-sectional strength,

b) Overall member strength, with the axial compressive resistance C_r calculated for the strong axis flexural buckling capacity, and

c) Lateral torsional buckling strength

2.3 Summary

As a result of the literature review effectuated the chevron type bracing for EBF was decided to be the most performing configuration and the short shear links the most stable and relaying ductile element for this type of frame. The new formulation of the shear link element that will be used for further nonlinear time history analysis was possible based on the recent experimental tests. The second part of the chapter presents the provisions of NBCC 2005 regarding the methods for the calculation of seismic forces followed by the seismic design requirements that the members of EBF have to satisfy in the capacity design process.

Table 2.1 Values of the shear forces and moments for the multilinear inelastic link element

	First subhinge yield value		Second subhinge yield value		Third subhinge yield value	
	Shear yield point	Moment yield point	Shear yield point	Moment yield point	Shear yield point	Moment yield point
J.M.Ricles and E.P.Popov (1994)	$1.0V_p$	$1.0M_p$	$1.26V_y$	$1.13M_p$	$1.40V_p$	$1.20M_p$
T.Ramadan and A.Ghobarah (1995)	$1.0V_y$	$1.0M_y$	$1.06V_y$	$1.03M_y$	$1.12V_y$	$1.06M_y$
P.W.Richards and C.-M.Uang (2006)	1.1Vp		1.30Vp		1.50Vp	

Table 2.2 Comparative summary of the shear yield values for the link element

	First subhinge yield value	Second subhinge yield value	Third subhinge yield value
J.M.Ricles and E.P.Popov (1994)	1.1Vp	1.386Vp	1.54Vp
T.Ramadan and A.Ghobarah (1995)	1.1Vp	1.30Vp	1.37Vp
P.W.Richards and C.-M.Uang (2006)	1.1Vp	1.30Vp	1.50Vp

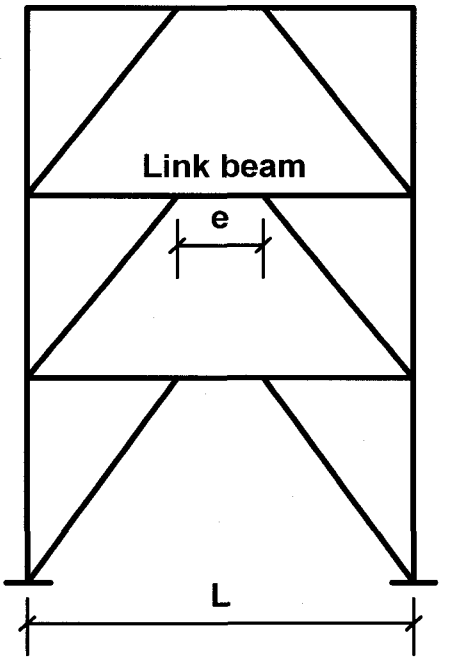

Figure 2.1 EBF configuration

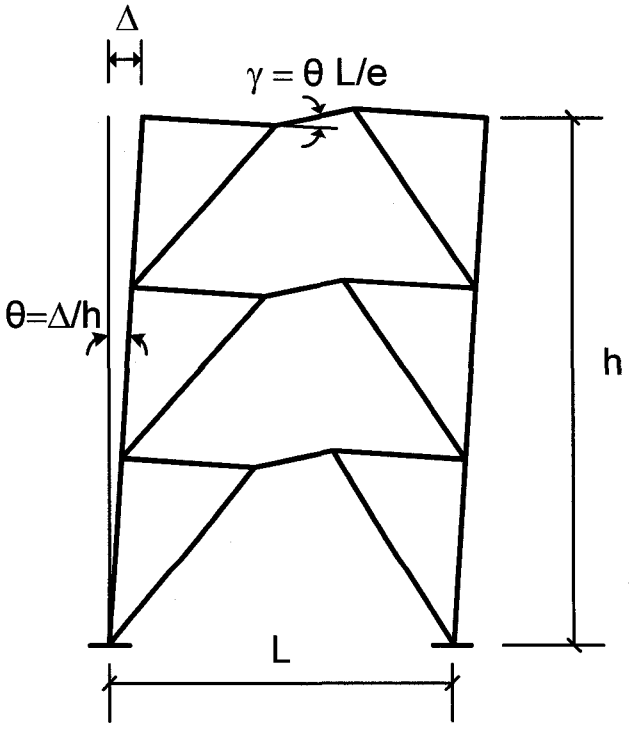

Figure 2.2 Rigid plastic collapse mechanisms

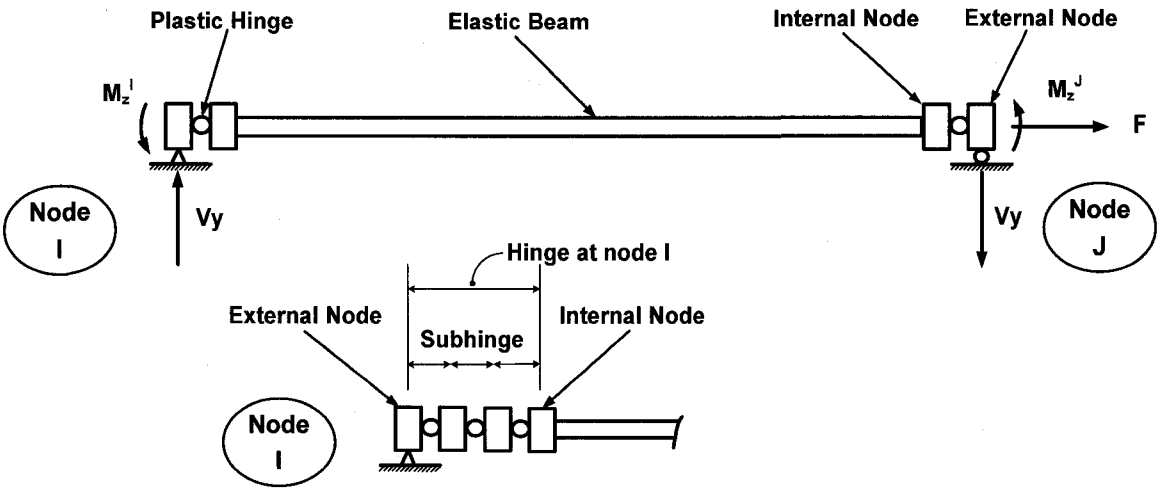

Figure 2.3 Link element (Ricles and Popov 1994)

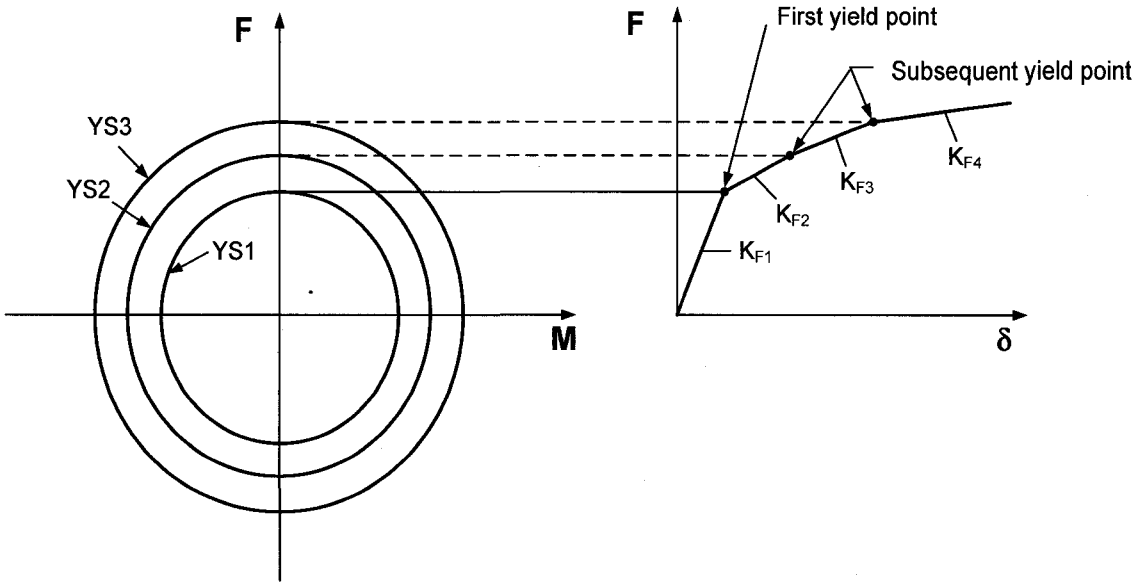

(a)

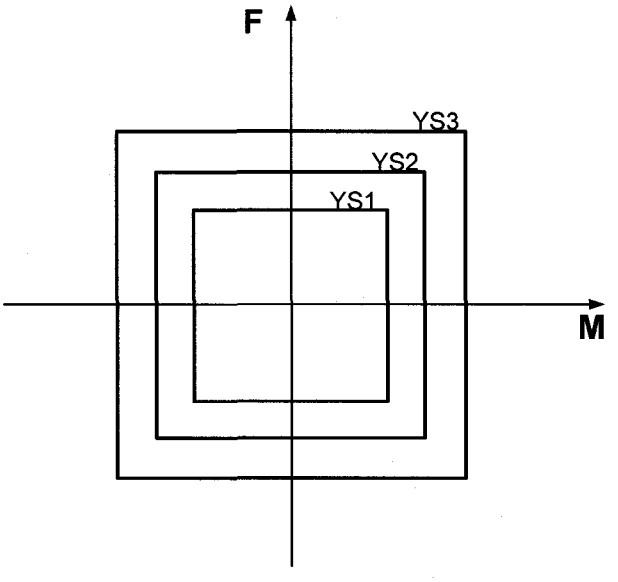

(b)

Figure 2.4 Strain hardening behavior of hinges: (a) Initial position of subhinge yield surfaces (b) Uncoupled yield surfaces for subhinges

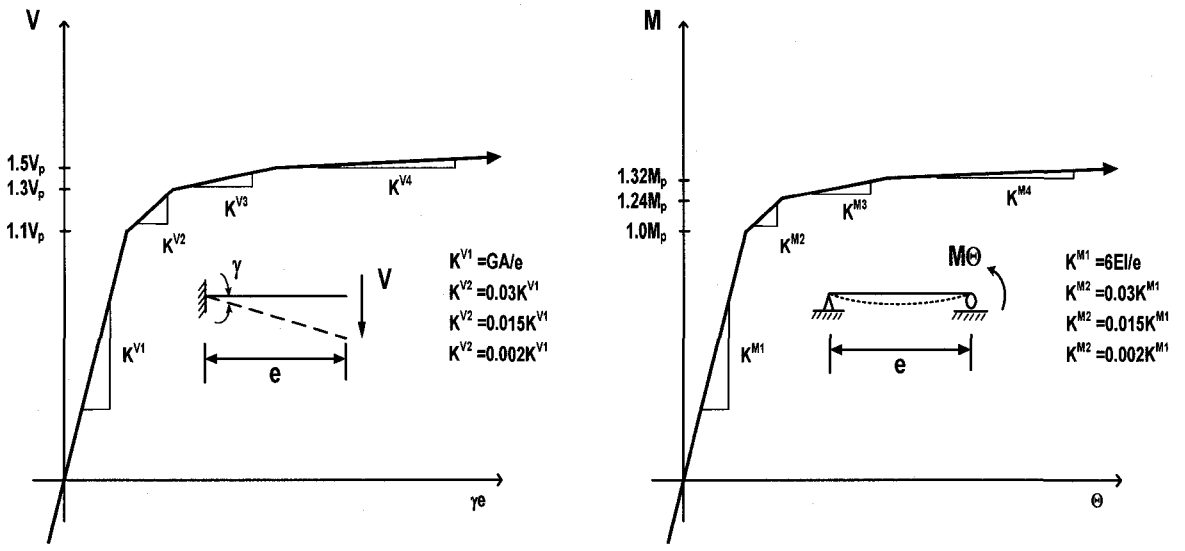

Figure 2.5 Shear link element: force-deformation relationship for combined translational spring action at each end

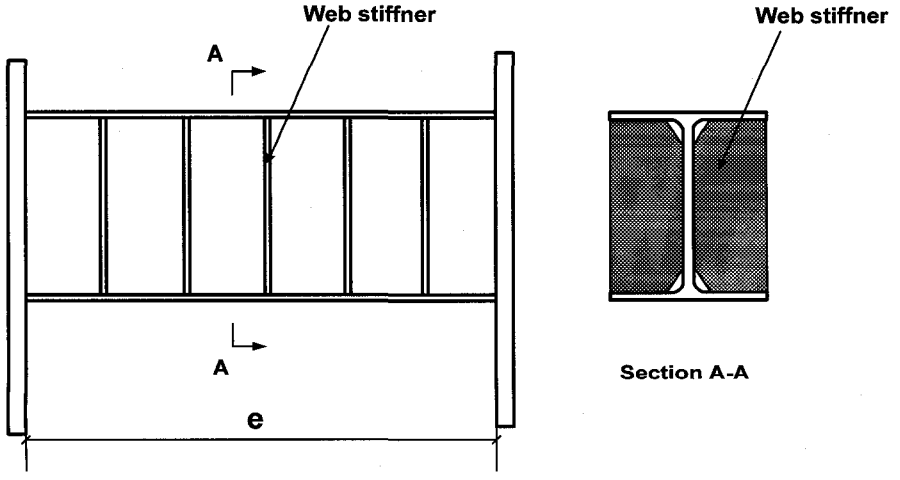

Figure 2.6 Link detailing

CHAPTER 3. DESIGN PROCEDURE

This chapter describes the steps that were performed to obtain EBF designs in accordance with the requirements of CSA-S16 standard. Two locations (Vancouver and Montreal) and three frame heights (14, 20 and 25 storeys) were considered. The geometry of the building and the loads are presented first, followed by the overview of design assumptions. The study carried out to establish the impact of two different lateral load distributions on the design is described. The importance of different design criteria is discussed and the appropriate design sequence is suggested.

3.1 Building geometry and loads

The buildings selected for this study have 14, 20 and 25 storeys in height. Two Canadian locations were considered, representative of seismic conditions in Eastern and Western Canada, namely Vancouver, British Columbia and Montreal, Quebec. The same building layout, shown in Fig.3.1, is adopted for all the structures. The framing consists of gravity columns and beams and two single bay EBFs located in the central core and placed in two orthogonal directions. The building is assumed to be of commercial usage. The frames are symmetrically located in the braced cores, thus eliminating the torsion in the building and allowing the investigation of two dimensional single plane braced frames. The equal mass was assigned at all storeys, with exception of the first and the top floor. Details concerning the calculation of the floor mass and the specific values used in the analysis can be found in Appendix A.

The elevation of the 14, 20 and 25 storey frames are shown in Figure 3.2. Identical bay widths of 9m were adopted for all the frames with typical storey heights of 3.7m, and the first storey where the height of 4.5m was selected. The link length of 800mm was

determined for all the frames based on the results of a parametric study. The reader is referred to the section 3.2.5 for a detailed explanation of this choice.

The design gravity and live loads for the single frame were adopted from Han (1998). Table 3.1 gives the values of the factored loads used for Vancouver and Table 3.2 for Montreal. The loads were applied as concentrated loads on the columns and as uniformly distributed loads on the beams. The top storey is the roof of the building and therefore the Tables 3.1 and 3.2 show the values of the snow load under the title "live load", since it was found that the combinations with snow load were critical.

In the CSA S16-01 Standard and the Subsection 4.1.8 of NBCC 2005 no height limit is defined for the eccentrically braced frames. Hence, the 25-storey building, 93.3m height can be considered appropriate for this study.

The seismic design base shear, V, was determined in accordance with the NBCC 2005 requirements, using the formulas discussed in section 2.2. Detailed calculation of the weight for each floor is presented in Appendix A. In the calculation of the seismic force, the specific acceleration and velocity coefficients for the ground conditions of a site Class C were considered for both Vancouver and Montreal. The earthquake importance factor I_E was assigned a value of 1.0 corresponding to the case of the of normal risk category.

The value of fundamental period, T_a, was taken as two times the empirical value suggested by the Canadian code. This assumption can be justified based on the fact that the period of a building calculated using established methods of mechanics is usually much longer than the period obtained applying the empirical formula of the code. Because the calculated period is extremely sensitive to the mass and stiffness modeling, the code limits the maximum value of the multiplication factor applied to the empirical period to 2.0 to avoid excessively long period estimates. For high buildings characterized by first period of vibration grater than 2 seconds, the use of $2T_a$ in the calculation of the

spectral acceleration $S_a(T)$ can lead to non-conservative seismic design forces. Therefore, in the equivalent static force procedure a minimum seismic design force V_{min}, is imposed. V_{min} is calculated using the spectral acceleration corresponding to the period of 2 seconds.

Tables 3.5 and 3.6 summarize the seismic load calculations for three frames located in Vancouver and Montreal respectively. As can be seen from those tables, the estimated design periods of the building are all longer than 2 seconds. Thus, the values for the seismic design forces V, given in Tables 3.5 and 3.6, correspond to the minimum permissible forces V_{min}. It is likely that a dynamic method used to determine the lateral seismic force will yield a lower value than the minimum seismic force determined with the empiric procedure. In such a case the NBCC 2005 allows to further reduce design seismic force up to 80 percent of the calculated value. This assumption will be verified later in section 3.4.

The base shear was distributed over the height of the building and the amplification due to accidental torsion was applied. The effects of accidental torsion resulted in the lateral shear amplification of 7%. Details regarding the calculation of the accidental torsion can be found in Appendix B. The notional loads are added to the lateral shear, and calculated in function of 0.5% of the seismic weight at every storey level.

The ratio of the maximum frame height (25 storey building) to the lesser width of the building plan (93.3m/36.0m) is less than 4, therefore the obligation to consider a dynamic analysis in order to determine the wind loads is not applicable. Thus, the wind load was calculated using the simplified procedure proposed in NBCC 2005. Two different load cases were considered. In the first one the wind is distributed on the entire façade of the building and in the second the wind is applied as pressure on the partial building surface in order to account for the torsional effects. The calculation showed that the wind with the torsion amplification yielded a more critical condition, thus this was the one used in

the design. Summary of the wind load for ultimate and serviceability limit state for Vancouver are presented in Table 3.3 and Montreal in Table 3.4.

The following load combinations were used in the design for ultimate and serviceability limit states:

(i) Ultimate limit states

1) 1.4D

2) 1.25D+1.5L+0.5S

3) 1.25D+1.5L+0.4W

4) 1.25D+1.5S+0.5L

5) 1.25D+1.5S+0.4W

6) 1.25D+1.4W+0.5L

7) 1.25D+1.4W+0.5L

8) 1.0D+1.0E+0.5L+0.25S

(Okazaki et al.) Serviceability limit state

9) 1.0W

10) 1.0L

3.2 Design procedure

Design process to obtain a seismic-resistant structure implies the verification of different design requirements related to strength, stiffness and ductility. In some cases it is possible to obtain designs that are efficient for all the major design requirements, but more frequently one of the design criteria would be critical. To optimize the design process it is desirable to use the sequence that would require the least modification between different design phases. Koboevic and Redwood (Koboevic and Redwood 1997) reported that for EBFs located in moderate seismic zones, it would be more appropriate to begin the design with strength and stiffness verifications rather than the requirements related to the

capacity design procedure (ductility design phase). In view of the increased flexibility of taller EBFs it is likely that the similar approach to design would be appropriate.

In order to minimize the number of iterations and in view of the importance of deflections in design of taller structure, following design sequence was adopted in this study:

- Initial selection of the link beam section is based on ductility design criteria, using the NBCC shear force distribution. Consequently, specific links are selected so that they have an adequate inelastic shear resistance for factored seismic loads.
- With imposed beam sections, the selection of the other members of the frame is done based on strength requirement. Selected beam sections are verified for all the NBCC load combinations and once the verification completed, other members of the frame are selected based on strength requirements.
- Selected frame sections are verified for stiffness and stability requirements, and modifications are done, if required. The stiffness parameters, as the total inter-storey drifts for the seismic load combination and the elastic drifts produced by service wind load, were verified to comply with the code limits. The global stability of the EBF frame is then checked using a P-Δ amplified seismic lateral force and the stability coefficient U2 is calculated and verified to be less than the code limit.
- Outer beam, braces and columns of the EBF, are verified for forces generated by fully yielded and strain-hardened links (capacity design), and the inelastic link rotation are calculated and compared against the code limits.

For all these design phases a distribution of the seismic force according to the equivalent static procedure was used.

3.2.1 Common features for EBF design

Following the preliminarily selection of the links sections, the sections of the links and outer beams were fixed and design of other members of the frame was done using the program Visual Design (VisualDesign 2007). The program Visual Design allows analyzing and designing of a steel frame in conformity with CSA/CAN S16-01. The optimization sections selection was done automatically in the program, in function of the cross-section area. The design was effectuated on a 2D model of the EBF.

The material grade used in the design and selected in the program Visual Design was G40.21.350W steel, with specific minimum yield strength F_y equal to 350 MPa.

The beams are modeled as pinned at the connection with the columns and they are fixed at the intersection with the brace and link beam (Figure 3.3). Lateral support was provided for the beam section, in order to avoid the flexural and lateral torsional buckling. Braces are designed as Class 1 or 2 HSS sections for the 14 storey structure and as W sections for the 20 and 25 storey structure. The option for W section was enforced by the lack of available sections and the necessity to use higher cross-sectional areas. Pinned connections are considered at the intersection of the braces with the columns, and rigid at the connection of the braces with the beams. The moment resisting brace to beam connection permits the redistribution of link end moment, assumption discussed further in the design (section 3.2.4.3). Columns are selected to have Class 1 or 2 sections, from W and WWF shapes for the EBFs having 14 storeys and from W, WWF, STE (plain square sections) shapes for the 20 and 25 storey frames. Columns are pinned at the base for the in-plane bending, and they are continuous over the entire and tiered into two or three storey segments.

3.2.2 Link selection

The link beams are selected based on ductility requirements, as specified in Clause 27.7.1 of CSA/CAN S16-01. The links were chosen to be Class 1 in compression and Class 1 or 2 in bending, as permitted in the S16-01. Link sections were first selected to have inelastic shear resistance as close as possible to the shear force induced by factored seismic loads.

The simple static approach used to derive the forces from the lateral seismic shear is presented in Figure 3.4, where the formula can be generalized as follows:

$$V_f = \frac{h_s}{L} V_{cum} \qquad \textbf{[3-1]}$$

The cumulated lateral shear, V_{cum} presented in Tables 3.5 and 3.6 in columns (c), (f), (i) is used to calculate V_f. The cumulated shear force includes an amplification to account for the P-Δ effects. This was calculated for an expected drift of 0.005 of the storey height h_s.

To calculate the inelastic shear resistance of the link the formula [2.4] from section 2.2.2.1 was used. The selected link sections, for both design locations studies are listed in Tables 3.7 and 3.8. The same tables indicate also the factors α, representing the link resistance-to-force demand ratio.

It was suggested in literature Popov and al. (1988; 1989) that , in order to obtain uniform energy dissipation and similar inelastic deformation in all the storeys, the effort should be made to select link sections so that a link resistance to force demand factor, α, remains uniform throughout the frame height.. In addition, α should be as close to unity as possible. Oftentimes, especially for taller EBFs it is difficult to maintain the link strength factor close to unity as because the link design may be governed by non-seismic load

combinations or stiffness considerations. Comparing the values from the Table 3.7 and 3.8 it can be observed that for links in Vancouver frames, α had an average value of 1.3 while for the Montreal frames α varies from 1.85 for the 14 storey frame to 1.55 for the 25 storey frame. For Vancouver the link factor could be kept at the value of 1.3 because the wind force combination controlled only locally the strength verification of the link, the same as the gravity combination controlled only the top storeys.

Another general trend that can be observed is that the top links for all designs had the highest α value. This can be explained by the fact that the link design was governed by other requirements. For Montreal, for instance, the heavier top link beams were necessary to obtain the links with pure shear yielding ($e \leq 1.6\ M_p/V_p$) as well as to comply with the requirements for the class of the section. The similar reasoning can be applied to Vancouver although in general lower values of α were obtained for the top links compared to Montreal.

For Vancouver, in all the three frames (14, 20 and 25 storey) the links are designed for the load combinations containing the gravity or seismic force in the top storey, and for combinations with the wind force in the middle portion and at the base of the frame. In the Montreal's case the larger values of the α factor are due to the wind force that governs the design in the middle portion and lower storeys or the gravity forces for the top storeys. It is anticipated that the overstrength introduced in the links will reduce the link deformations and consequently the capacity of the EBF to dissipate the energy introduced by an earthquake. In addition, following the capacity design principles this link overstrength will increase forces that need to be considered for design of other frame members, and thus results in larger brace and column sections. In the seismic zones with lower to moderate seismic activity, it is highly unlikely that the links will develop the same levels of strain hardening as for the higher seismic zones. Consequently, the high overstrength of the links combined with a less intense seismic solicitation can result in an

unjustifiably strong structure. These aspects will be discussed in further detail in Chapter 5 and 6.

In the next step links are verified for forces introduces by all other relevant load combinations, and stronger beam sections were selected if needed.

3.2.3 Design of other frame members

3.2.3.1 Strength design

Once the link sections were selected, the initial sizes of other frame members were determined to obtain the frame with adequate strength for factored load combinations defined in Section 3.1.

The section selection obtained after the strength design phase is presented in Tables 3.9 to 3.14. In order to facilitate the comparison between different design phases, the summary of the chosen sections is grouped by structure's height and location. The total mass by type of members is given at the bottom line of each table. The value featured as total mass of the structure contains the mass of the beams as well.

It is interesting to note that the critical load combinations for different frame elements were different for the eastern and western Canadian locations. For Vancouver, it was generally the seismic forces that controlled the design while for Montreal gravity and wind loads dominated member selection. A general tendency is that the combination containing 1.4 W governed the design of all the members at the bottom storeys, regardless the geographical location of the structures. The exterior beams at the top storeys were designed for the gravity combinations in the case of Montreal structures and for the seismic forces for the structures situated in Vancouver. The higher forces in the

top storey braces are produced by seismic loads, whereas the maximum forces in the top columns came from gravity or seismic load combinations.

3.2.3.2 Stiffness verification

In the next step, total inter-storey displacements were verified against the code limits for the load combinations including both the seismic and the wind loads. For the seismic loads the lateral deflections were calculated from the static analysis and multiplied by R_dR_o/I_E to obtain realistic estimates of the total deformations. Braces and columns sections were modified until the total inter-storey drifts met the code limit of 0.025 h_s, where h_s is the storey height. To assure the necessary stiffness of the frame the following strategy was adopted: columns beginning from bottom to top are modified first and followed by locally changes of the braces. It is usually expected that the braces and columns sections increase in size from the base to the top of the frame. However, for the 20 and 25 storey structures, especially for those situated in Vancouver, the local control of seismic drift requirements imposed heavier brace sections in the upper part of the frames.

The sections selections at the end of this design phase are shown in Tables 3.9 to 3.14. The presented sections for the EBF are those that satisfy the deflections limits only for the seismic load combination, because the increases in the mass due to wind requirements are virtually negligible.

A summary of the total inter-storey drifts obtained for the lateral seismic loads for both studied locations is given in Table 3.15. The NBCC design limits are also shown. For all the structures, regardless the geographic location of the building, the maximum values of displacements were observed in the upper storeys. The only exception is the 14 storey frame located in Montreal, were the sections selected after the strength verification, fully complied with stiffness requirements. The values of the total drifts for this structure are

presented in the Table 3.15 and as can be seen they are all below the design limit, with a maximum value at the 13th storey.

Verification of the displacement caused by the wind loads (serviceability limit state) was done for the EBF configuration meeting total seismic drift design limits. While all the three structures located in Vancouver inter-story drift values observed were lower than 1/500 h_s, the structures situated in Montreal had values of storey drifts larger than the design limit defined for wind loads. Required modifications of columns and braces resulted in minor mass increase compared to the mass increase due to the seismic drift requirement.

3.2.3.3 Verification of global stability (P-Δ effects)

The summary of the final selected sections for each structure studied is given in Tables 3.9 to 3.14. To verify the global stability of the structure the effects of vertical loads acting on the deformed structure (P-Δ effects) must be considered. The lateral loads acting in a deformed structure amplify the lateral displacements and induce additional forces in the structure. P-Δ effects can be very important for the seismic loads, in view of the large inelastic deformations anticipated and thus can not be ignored in the design. In the present study two methods are used to account for of P-Δ effects: (i) an iterative procedure in which the horizontal loads are amplified in function of the developed displacement at each storey and (Okazaki et al.) the NBCC 2005 procedure in which a factor U_2 is calculated using a one- step procedure and compared with a maximum admissible value.

The NBCC method of accounting for P-Δ effects is based on the calculation of a global stability factor U_2, where U_2 is defined as:

$$U_2 = 1 + \frac{\Sigma C_f R_d \Delta_f}{\Sigma V_f h_s} \qquad \textbf{[3-2]}$$

The stability coefficient U_2 is calculated as the amplification created by the moments due to gravity loads C_f acting on the structure deformed with the seismic displacement $R_d\Delta_f$. The factor R_d is used to multiply the elastic displacement Δ_f and not R_oR_d, because the resistance of the structure already includes the structure's overstrength (coefficient R_o) and thus the level of load where the inelastic action starts is V_{design} times R_o. The values of coefficient U_2 larger than 1.4 indicate that the structure is too flexible, and the frame need additional stiffness such as the coefficient U_2 does not exceed the value of 1.4.

In Visual Design program P-Δ effects for the seismic loads can not be automatically included in a 2D analysis, because the part from the mass of the building participating on the P-Δ effects can not be accounted in a 2D model. Therefore, an alternative iterative procedure to calculate the equivalent lateral loads P-Δ was used. The iterative method has the advantage to precisely calculate the additional lateral force that corresponds to a specific storey. An Excel worksheet was created to compute the additional horizontal seismic force denoted H, where the force is calculated with the formula $H = \Sigma C_f R_d \Delta_f / h_s$. In this formula C_f is the gravity load from the load combination 1.0D+1.0E+0.5L+0.25S for the corresponding storey level, R_d is the ductility-related force modification factor, Δ_f is the lateral elastic displacement obtained from a first order analysis and h_s is the storey height. The method is iterative and starts by the calculation of elastic displacements under the seismic loads. Equivalent horizontal forces, H1, are computed, added to the initial seismic load and a new set of displacements is calculated. With these new displacements, a new set of equivalent horizontal forces, Hi, are computed, added to the initial seismic loads and the displacements are recalculated. The procedure is performed until the set of H forces converges to a stable value. Five to six steps were generally needed to attain the convergence. Once the iterations completed, the strength of the members, the inter storey drifts and the U_2 value are verified against the NBCC design limits.

The deflections used for all the calculations correspond to the minimum seismic base shear V_{min}. The code does not specify if any adjustments should be made with the deflections when the period of the building is higher than 2.0 seconds, the limitation of the period is specifically imposed for the level of the forces (V_{min}) and thus the deflections are limited to those corresponding to the seismic force equal to minimum base shear.

To satisfy the global stability requirements it was necessary to modify all frame members including links. Although the allowance for P-Δ effects was made in initial link design, their impact was somewhat underestimated and consequently link sections had to be increased. This in turn increased the factor α as can be seen from Tables 3.7 and 3.8. While the modifications for the link sections were required only locally, a significant increase in the columns and braces sections was needed to control the displacements and the amplification of the forces caused by the P-Δ effects. It was observed that increasing the bottom columns sections was the most efficient way to control the inter storey drifts in the storeys above the modified sections. The adjustment of the braces sections was used to control locally the rigidity of the frame, especially for the middle storeys.

The values of the coefficient U_2 were calculated on the structure obtained after the calculation of the P-Δ forces, using these amplified seismic forces. Several sections modifications were needed to keep the value of U_2 in the code limit. These changes were especially done for the braces in the middle part of the EBF, where U_2 factor had the maximum values. It was also observed that for Montreal structures keeping the values of U_2 less than 1.4 was more difficult to realize than for the structures designed for Vancouver.

The same iterative method for the calculation of the second order effects is used in the case of the wind load combination. The displacements are computed with Visual Design

and an equivalent lateral force is calculated, using the load combination factors corresponding to dead and live loads. The procedure converged in two to three steps and the frame members modifications due to the wind P-Δ effects were minor compared to the modifications imposed during the stability verification for the seismic forces. Therefore, it was not considered a governing design criteria and it is not presented in detail herein.

3.2.4 Capacity design and verification of the inelastic rotation of the link

3.2.4.1 Outline of the procedure

The final step in the design procedure is the capacity design of the frame. The principle of the capacity design for EBF is to choose the links to be the weakest elements that develop a ductile behavior and to select the other elements to be sufficiently strong to sustain loads introduced by fully yielded and strain hardened links. Capacity design was selected to be the final deign step because it is believed that the previous steps (i.e. strength, stiffness, stability) are more demanding in the case of taller frames. The following sections present the method and principles used for design of beams outside of links, braces and columns.

The program Visual Design does not have the capacity design procedure implemented and thus an Excel worksheet was created carry out this final design step. Using an approximate static approach (Han 1998; Koboevic 2000; Redwood 1995), illustrated in Figure 3.4, the forces and moments introduced by the yielding links are calculates for the exterior beams, braces and columns. The calculation of the member forces starts from the top storeys and proceeds towards the lower storey levels. The formulas for each type of element will be discussed in more detail in the following sections.

For this study, it is considered that the exterior beam and link segment have the same section and are continuous, without any strengthening in the exterior beam section (i.e. additional plates).Thus, the connection between the outer beam, the link and the brace have to be a moment resisting connection. In this case, the beam must sustain high moments transmitted from a yielded link along with a significant axial force and thus, an inelastic behavior is very probable to develop in the beam. As it was earlier discussed in section 2.1.2, the previous studies (Koboevic 2000) considered the same assumptions on the design and it was observed that the inelastic beam rotations due to flexural deformations are in the acceptable limits. Therefore, the assumption agreed for this study that the beam can exhibit a nonlinear comportment during the earthquake.

3.2.4.2 Design considerations for link and outer beam

The link beam selection at the beginning of the design procedure was carried out so that the link has an adequate inelastic resistance to sustain seismic forces amplified to account for P-Δ effect thus no further modifications are necessary in the ductility phase of design.

The beams outside of the link have to be selected to resist the forces generated by fully yielding and strain hardening links. The Standard S16S01-05 specifies that this ultimate force $V_{u,}$ is equal to $1.3R_yV_p$, where R_y is the factor of the probable yield stress, equal to 1.1, and V_p is the plastic shear resistance. The beam resistance can be taken as the nominal resistance with a steel yield stress equal to R_yF_y. The ultimate shear force from the link is transmitted to the beam and brace as axial forces and moments, and thus these members have to be treated as beam-columns in the capacity design.

During experimental tests realized for the short links, it was observed that the axial forces in the links are usually small and therefore could be neglected in the design. The moment in the link beam developed at the connection with the outer beam and brace, and referred to as link end moment, can be calculated as:

$$M_{link} = V_u \frac{e}{2} \qquad \textbf{[3-3]}$$

In the following the link end moment M_{link} will be referred as M_{trans}, the moment transferred by the link. The beam shear force V_{beam} in the outer beam is:

$$V_{beam} = V_u \frac{e}{L-e} \qquad \textbf{[3-4]}$$

The beam axial force is determined to satisfy the horizontal equilibrium in the connection node. The type of axial effort in the beam, i.e. compression or tension depends on the direction of the seismic loads. Considering a left side direction, as shown in Figure 3.5, the value of the force will be positive for compression on the left side of the link and negative as for tension on the right side, and it is given as:

$$P_{beam} = P_{brace} \cos\beta = V_u \frac{L}{L-e} ctg\beta \qquad \textbf{[3-5]}$$

where β is the angle between brace and beam (Figure 3.5). The rigid connection between the outer beam and the brace permits the distribution of the moment transmitted from link, depending on the relative stiffness of the two members. Considering the high solicitation on the beam and to avoid increasing the section size due to the requirements for outer beam sectional behavior, it is assumed that the beam can develop an inelastic behavior. Thus the beam can sustain the combination of the bending moment and axial force to its full capacity and only the remaining moment will be transferred to the brace. The representation of the moment distribution is presented in Figure 3.5. Due to the presence of the concrete slab the top flange of the beam can be considered to be fully laterally supported and the verification for lateral torsional buckling does not apply.

The bending deformations in the members have two components: the first that results from the distribution of the link end moment, $M_{trans,}$ to the outer beam segment and the brace (see Figure 3.6 (a) and (b)) and the second originating from storey drifts (see Figure 3.6 (c), (d)). Kasai and Han (1997) have shown that when the lower end of the brace is pinned, the moments arising from storey drifts are small or non-existent. On the other hand, when the lower brace end is fixed to the column, moments arising from inter storey drifts have to be considered. In this study the beam to column connection is considered pinned since the flanges are not connected to the column. The brace bottom connection with the column is also treated as pinned because the typical connection does not include the connection of the flanges from the brace to the column section in order to transfer the moments. Therefore, the moments introduced by the storey drifts did not have to be included.

Regarding the axial forces in the beam and braces two situations can happen: the beam is in compression and the braces in tension or vice versa beam in tension – brace in compression. For Class 1 sections the second situation will always govern the design because it yields higher moments in the braces. For a typical storey the moment acting on the beam is:

$$M_{beam} = \min\left\{M_{trans,beam}, M_{p,beam}\right\} \qquad \textbf{[3-6]}$$

where

$$M_{trans,beam} = \left(\frac{3r}{\Psi\cos\beta + 3r}\right) M_{trans} \qquad \textbf{[3-7]}$$

And $M_{p,beam}$ is the plastic moment resistance of the outer beam segment. In the above formula, $r = (sI)_{beam}/(sI)_{brace}$ where s is a stiffness reduction factor in function of the axial force, I is the moment of inertia and Ψ is equal to 3 for a pinned brace lower end.

The presence of the axial force affects the flexural rigidity of an element, and this should be accounted for in the calculations. The formulas to calculate the stiffness reduction factor are taken from Trahair (1977) and can be summarized as follows:

In a typical storey

- for the beam segment, $s = (1\text{-}P/P_E)$, and
- for the brace with a fixed bottom end $s = (1\text{-}P/2P_E)$, and
- for the brace with a pinned bottom end $s = (1\text{-}P/P_E)$.

In the first storey if the effect of drift is considered the values of s are:

- for the brace $s = (1\text{-}P/4P_E)$ and
- for the beam $s = (1\text{-}P/P_E)$.

The bottom end of the first storey column is considered pin connected and the drift effect will not be included. Therefore, the s values for the brace in the first storey shall be taken as in a typical storey.

For Classe 1 or 2 I shaped section, according to CSA-S16-01, the beam plastic moments $M_{p,beam}$ can be calculated as follows, for tensile and compressive axial load in the beam:

$$M'_{p,beam} = \left(1 - \frac{T_{f,beam}}{AR_yF_y}\right) Z_x R_y F_y \qquad \textbf{[3-8]}$$

$$M'_{p,beam} = 1.18\left(1 - \frac{C_{f,beam}}{AR_yF_y}\right) Z_x R_y F_y \qquad \textbf{[3-9]}$$

The use of full yield strengths R_yF_y for the exterior beam is based on the specifications formulated in Clause 27.7.8 of the Standard CSA-S16-01 and discussed in section 2.2.2.2.

The beams member capacity is then verified for the interaction formulas of the Clause 13.8.2 (a) and (b). When calculating these interaction values, the maximum interaction value of the cross-sectional strength equal to 1.0 is accepted due to the fact that the beam is considered capable of resisting forces to its full capacity.

3.2.4.3 Brace design considerations

The procedure presented above accepts the possibility of outer beam yielding, requiring an elastic behavior from the brace. The brace sections obtained after the stability verification, described in section 3.2.3.3, were checked to have a sufficient factored resistance to sustain the forces developed by the fully yielded and strain-hardened link. The Clause 27.7.9 specifies that these forces are equal to 1.30 $R_y V_p$, the same as for the outer beams.

Applying the procedure adopted from Kasai and Han, the brace axial force P_{brace} can be determined from vertical equilibrium:

$$P_{brace}(left) = -P_{brace}(right) = V_u \frac{L}{L - e \sin\beta} \frac{1}{} \qquad \textbf{[3-10]}$$

Gravity axial force coming from the distributed gravity load on the beam is added to P_{brace}, considering the tributary area. The procedure adopted to distribute the link end moment between the outer beam and the brace is as follows:

- The flexural rigidities of the beam and brace were determined, taking into account the effect of the axial load on the stiffness (see section 3.2.4.2).
- The link end moment was distributed between the beam and the brace in proportion to their flexural rigidity.

- The moment assigned to the beam was verified to be smaller than the capacity of the beam with tensile axial load, if so the beam takes as much as beam can support and send the rest to the brace.
- The braces are verified for the determined forces and appropriate sections modifications are done if necessary.
- Following the braces modifications, the flexural rigidity of the beam and brace were recalculated and another redistribution of the moments for the changed section properties is done.

The part of the bending moment transferred to the brace assuming the above described procedure was obtained as:

$$M_{brace} = M_{trans} - M_{beam} \qquad \textbf{[3-11]}$$

In the above formula M_{trans} was determined with the forluma 3.3 and M_{beam} was determined with 3.6. The brace sections were then verified as beam-columns in conformity with Clause 13.8.3 (14 storey structure with HSS brace sections) and with Clause 13.8.2 (20 and 25 storey structures with W brace sections). When using these interaction equations the brace effective slenderness ratios were set to K_x= 1.0 for the in plane behavior and K_y= 0.9 for out of plane behavior.

Modifications of the braces from the bottom storeys for all the structures were necessary to grant the strength and stability of these members. The process of choosing the adequate braces sections converged for suitable solution in one to two steps of iterations.

3.2.4.4 Column design considerations

The columns have to be designed for the forces resulting from the yielding links together with gravity loads. The gravity forces in the columns arising from load combination no.2 1.25D+1.5L+0.5S are also calculated and the verification of the columns for these forces

is done. Depending on the magnitude of the forces coming from links, it is possible that for the top tier storeys the load combination with the gravity, live load and snow to control the column design.

The axial force in the column due to earthquake loads can be calculated as:

$$P_{col}^{i} = P_{col}^{i+1} + P_{brace}^{i+1} \sin\beta \pm V_{beam} \qquad \textbf{[3-12]}$$

where $P^{i+1}{}_{col}$ and $P^{i+1}{}_{brace}$ are the axial forces immediately above the column considered and V_{beam} is the shear force in the beam. The gravity axial force considering the loading on the appropriate tributary area is added to P_{col}. When calculating the forces transmitted from the links the coefficient 1.15 is applied to the ultimate force in the link and only for the top two storeys this coefficient is equal to 1.30, as it was taken for the other elements (i.e. beams and braces). The simple summation was used to evaluate the axial forces that develop in the columns based on the assumption that all the links from the EBF will yield at the same time. The column interaction equations C_f/C_r, describes in section 2.2.2.2, were used to verify the capacity of the columns for the seismic forces. The columns were also verified for the combination of gravity loads and they were checked as columns in axial compression only.

3.2.4.5 Verification of the inelastic link rotation

The verification of the inelastic link rotation concludes the design process. The structure compliant with strength, stiffness and capacity design requirements was used for a new static analysis in order to obtain the elastic inter storey drifts. The summary of the frames sections and the estimated values of inelastic link rotations are presented in Tables 3.16 and 3.17. To estimate of probable inelastic storey drifts the elastic inter storey drifts, determined for factored seismic loading plus the equivalent P-Δ forces, were calculated

using the formula 2.8., discussed in section 2.2.2.1. Following the inelastic drifts determination, the inelastic link rotations can be calculated using the above formula:

$$\gamma = \frac{L}{e}\frac{\Delta_{in}}{h_s} \qquad \textbf{[3-13]}$$

Where L is the span of the EBF, e is the length of the link segment, h_s is the storey height and Δ_{in} is the inelastic storey drift. This formula is based on a rigid plastic collapse mechanism that is supposed to form in the EBF, with the plastic deformations confined in the link segment.

The numerical values of γ are verified to be under the code limit (0.08 radians), the maximum admissible value for the pure shear links. Note that in the static analysis performed the columns were axial restrained when the determination of the displacements was performed, as specified in the Commentary of CAN/CSA-S16S01-05.

3.2.5 Parametric study of the link length

The length of the links for all the frames was fixed to 800mm. To verify the appropriateness of this choice, an additional study was done for the 14-storey structure, in order to investigate the sensitivity to the variation of the link's length. A shorter link of only 600 mm was chosen to carry out the same design steps and to observe how the final verification, the inelastic link rotation is changing. The shortness of the link brings more rigidity to the frame and enables us to select smaller beam sections. This also leads to the selection of smaller braces and columns, thus to an economy in the quantity of steel used in the frame. Although an improvement for the stiffness and stability verifications can be achieved, for the verification of the link rotation we can observe a significant increase of the inelastic link rotation γ. This increase is due to the higher ratio of the span of the frame to link length, L/e, by which the rotation of the storey, θ, is multiplied in order to

obtain the inelastic rotation of the link. It was also observed that imposing longer links will limit the possibility to choose optimal sections, especially for the upper storey. In the top tier, usually the selection of the section is based on the condition to have links that yield in shear ($e \leq 1.6\ M_p/V_p$) and a higher e value, length of the link, will impose stronger sections than necessary.

3.3 Discussion of the results

3.3.1 The14 storey structure

During the design process, many member sections were modified which resulted in increase of the structural mass. Note that the lightest sections compliant with design requirements were always selected. The Tables 3.9 and 3.10 present the selected columns and braces at the end of strength, stiffness and stability design phase, the total mass of each group of sections and the modal periods obtained. By examining the total masses of the braces and columns, it can be seen that the masses increased from strength to stiffness and thereafter from stiffness to stability phase.

As can be seen from Tables 3.9, the governing design criterion for Vancouver was the total inter-storey drift. The total mass of the braces increased by 83 percent, from strength to stiffness phase, and the mass increased more by 20 percent from stiffness to stability. The mass of the columns increases by 60 percent to satisfy the stiffness requirement and by 38 percent for stability. During the stability verification, where the total drifts of the frame were calculated for a higher seismic forces with the P-delta effects included, the total drifts in the top storeys control the design. In order to control the large displacements at the top storeys of the EBF, stronger braces are chosen only at these locations. The value of U_2 coefficient determined at the end of P-Δ iterations was under the permissible value of 1.40. If we examine the capacities of the braces in capacity design step versus the solicitation forces, the braces from the top half of the frame are

stronger than what it would be necessary to sustain the seismic forces, and in the lower part of the frame the brace section capacities are insufficient. Therefore the braces in storeys 1 to 4 were replaced with stronger sections. Capacity design did not introduce significant column section changes in the frame configuration, except for the storeys 11-12, where the columns were replaced with a W310x143 section due to section class condition. The median value of the C_f/C_r ratio for the columns is 0.63, when the admitted maximum value can be 0.85. As can be seen from the Table 3.16, the observed values of inelastic rotations of the links (for Vancouver are bellow the design limits is and conservative for the top storeys.

For the Montreal structure the selected member for all design phases are shown in the Table 3.10. The total inter-storey drifts produced by the seismic load combination were all below the NBCC limit. The structure configuration presented in Table 3.10 compliant with stiffness requirements is in fact the one for which the storey drifts under the wind load combination respect the code limitation on displacement of 1/500 h_s (7.4mm) for serviceability limit state. The mass increases for this phase are 35 percent for the braces and 12 percent for the columns. From the stiffness phase to stability these mass increases are much more significant (87 percent for the braces and 104 percent for the columns). At the verification of global frame stability for the structure from Montreal, it is the requirement for the U_2 value smaller than 1.4 that imposes the use of stronger columns. Examining the frame configuration in Table 3.10 it can be observed that the top storeys have lighter braces than for the Vancouver structure. For the Montreal structure, on the other hand, stability requirements imposed larges increase in structural mass. The stability requirements resulted in the frame configuration for Montreal that is not very different from the one in Vancouver regardless large difference in seismic base shear for the two locations. Minor changes in brace and column sections were required to meet ductility requirements. The braces at the bottom storeys 1 and 2 and the columns in storeys 9 and 10 had to be changed one size up. The columns have a median C_f/C_r ratio of 0.55, and only the columns in storeys 9-10 needed to be changed to meet design

requirements. The inelastic rotations of the link, presented in Table 3.17, have the maximum values of 0.04 radians in the lower half storeys. The total inter storey drifts calculated for the seismic combination including the P-Δ effects, were half of the code limits 0.025 h_s.

3.3.2 The 20 storey structure

Some of the trends observed for 14 storeys in Vancouver are similar to the structure with 20 storeys situated in Vancouver. The first is the large increase of the mass from strength to stiffness phase; the mass of the columns was doubled and the mass of the beams was increased by 10 percent. Two main reasons can explain this observation: the very large inter storey drifts in strength design phase, up to 2.5 times higher than the code limit, and the necessity to use the plain square sections (STE) for the columns. The drifts for the wind in the serviceability limit stat case are below the limits from NBCC. The mass increase to satisfy the stability requirement is similar to the one observed for the 14 storey structure: 36 percent for the braces and 25 percent for the columns. The modifications of the braces and columns after the P-Δ iterations were necessary in order to keep the total drifts in the code limit, thus it can be said that the total drift was the controlling parameter of the design. The coefficient U_2 attains maximum values of 1.37 at the middle storeys of the frame. During the capacity design the braces sections from storey 1 to 8 had to be changed. No modifications of the column sections were necessary. The columns that had more than sufficient resistance, with a median value of C_f/C_r ratio equal to 0.35. The inelastic rotations calculated for the links have values about 0.06 radians, thus remaining within the maximum permitted rotations of 0.08 radians.

The 20 storey frame situated in Montreal selected in the strength design phase, presented in Table 3.12, had seismic inter-storey drifts 1.5 times higher than the code limit. To comply with the stiffness requirement increases of 16 percent in the mass of the braces and 82 percent for the columns were needed. The frame sections selected after this step

are presented in Table 3.12. Similarly to the 14 storey frame the high displacements were obtained for the wind load combinations. The calculated wind drifts for the frame configuration, presented in Table 3.12, were around 10mm. Stability design requirements for the seismic load combination introduced an augmentation of 78 percent in the mass of the braces and 128 percent for the columns. The controlling parameter for the global stability was the maximum allowable value of U_2 factor, while the total drifts values, calculated for the P-Δ amplified seismic forces were all below 60mm. In the ductility design phase, only the modification of two bottom braces from W310x143 to W310x158 section was required. The median value of the C_f/C_r ratio for the columns is very close to the one found for the 20 storey Vancouver: 0.32. The inelastic link rotations were all under the value of 0.04 radians.

3.3.3 The 25 storey structure

The 25 storey Vancouver structure selected in the strength phase (see Table 3.13) had the total drifts due to seismic forces three times larger than the NBCC 2005 limit. The frame's selected sections obtained in the stiffness phase in presented in Table 3.13. As it can be seen stronger braces were selected at the top storeys to control the displacements which attained maximum values at these locations. For the braces 36 percent more steel was needed and for the column an increase of more than double in their mass was needed to control the seismic drifts. Compared to the 20 storeys Vancouver in the same design step, the increase of the column mass is almost the same. In the stability verification it was the necessity to limit the storey drifts produced by the lateral seismic force with P-Δ effects that controlled the design, while the stability coefficient U_2 reached a maximum value of 1.37. The braces in the bottom five storeys were changed in the capacity design phase. The average use of the columns' capacity in compression is about 0.27. The inelastic link rotations for all links were below the NBCC 2005 limit.

For 25 storey structure situated in Montreal, the specified sections for each design step and the total masses of each group of members are presented in Table 3.14. The drifts in the strength configuration were 1.8 times higher than the target limits. In order to restrain these drifts to 92.5 mm an increase of 11 percent in the mass for the braces and 127 percent increase for the columns was needed. The stability verification imposed a more severe increase in the masses of the braces and columns, 120 percent and 154 percent respectively. During the ductility design process no further modifications of the braces and columns were required with a C_f/C_r columns ratio having an average value of 0.22. The link rotations were all well below the design limits.

3.4 Second design using the spectral distribution of the seismic force

The six frames designed in the preceding sections, (14, 20 and 25 storeys) for the two Canadian locations Vancouver and Montreal, having the final sections selection as presented in Tables 3.16, 3.17, were used to perform three-dimensional dynamic analyses. The tall structures response can be significantly influenced by the higher modes of vibration and it is thus important to consider these effects more directly in the analysis. To examine this aspect an additional study, for the 14 storey structure, was carried out and the influence of the modes of vibrations on the spectral distribution of the seismic force is discussed. The results of this study are presented in Section 3.4.1.

The 3D response spectrum analyses were initiated using the structures proportioned on basis of equivalent static load profiles and fully compliant with all design requirements. The spectral forces obtained from these analyses were normalized to the empirical base shears and were used to perform a second design, following the same steps as in the first EBF design. The results of these two separate designs were compared to investigate the influence of spectral distribution in the selection of the EBF members.

The maximum modal responses were combined using the complete quadratic combination (CQC). Number of modes was selected to reach 95 percent of the participating mass of the building in both orthogonal directions. A damping of 5% of the critical damping for each mode was employed and accidental torsion is included by applying horizontal torsional moments at each storey level calculated as the horizontal seismic force at the level times 10% of the building plan dimension. P-Δ effects are not included in the 3-D analysis, but were accounted for in 2-D analysis once the spectral distribution of seismic force was obtained. In the Visual Design 3D model, the gravity columns were assumed to be continuous and the beams to be pin connected to the columns. The floors were modeled as rigid diaphragms at each level and the gravity loads used for the spectral analysis were uniformly distributed over the slabs areas. Four EBF frames, two in each direction, are positioned in the building configuration according to the building plan (Figure 3.1). The EBF frame configuration was the one obtained at the end of capacity design and the modeling is identical to that presented in Chapter 3.2.3.

The elastic base shear obtained from the analysis was reduced in accordance with NBCC 2005 provisions and the dynamic shear force V_d is compared to 0.8V, where V is determined using equivalent static force method. Note that the base shear force, V, was in fact the minimum base shear calculated for the period of 2.0 seconds, discussed in the previous chapter and identified as $V_{min.}$ As permitted in the code for the regular structures if V_d is smaller than 0.8V the base shear force will be taken equal to 0.8V. A summary of the base shear forces obtained following the equivalent static force procedure and the response spectrum method are presented in Table 3.18. The table presents the empirical base shear V, 80 % of V, the spectral value of the shear V_d and the design shear $V_{d,final}$ chosen as the maximum between the 0.8V and V_d. As it can be seen from the table for all but the 14 storey structure in Vancouver, the spectral values of the base shears were then 80 percents of the base shear obtained by the equivalent static force method. Thus, it can be concluded that the assumption of reducing the base shear force at 0.8V, described in section 3.1, is justifiable.

3.4.1 Sensibility to the frame configuration

The spectral design was done for frames configurations fully compliant with all design requirements and a further study using the 14 storey structure was considered necessary to see if the initial structure selection impacts the resulted forces. Note that the sections of the beams were the same for the all three structures and selected based on the adequate inelastic shear resistance for factored seismic loads. Three different approaches were considered to select brace and column sections:

a) braces and columns selected uniquely on basis of the strength requirement, configuration from Table 3.9 to 3.14; this design is referred to as Structure 1
b) braces and columns fully compliant with all the design requirements; Tables 3.16 to 3.17; this design is referred to as Structure 2
c) the same sections selected for all columns and braces respectively, the sections of these being identical with those chosen in first storey of the Structure 1; this design is referred to as Structure 3

The values of first periods for Vancouver are:

- 3.75 seconds for the structure 1,
- 2.61 seconds for the structure 2 and
- 3.36 seconds for the structure 3.

For Montreal structures the first periods are:

- 3.94 seconds for the structure 1
- 2.72 seconds for the structure 2 and
- 3.52 seconds for the structure 3.

The shear force distribution over the frame height obtained for three above-mentioned trial structures is shown in Figure 3.7 for Vancouver and 3.8 for Montreal. As can be seen, the magnitudes of the shear forces are found to be similar, thus it could be concluded that

the small variations of the frame sections do not have a significant impact on the spectral force distribution over the height.

3.4.2 Contribution of different vibration modes on the spectral force distribution

Another study was carried out to investigate the importance of the contribution of different vibration modes to the resulting spectral force. The purpose of this study was to determine the change, that each vibration mode brought, in the shape of the spectral force, and to establish a minimum number of vibration modes that need to be considered, in order to obtain a realistic spectral distribution. Analyses with 1 to 4 participating modes were done and the distribution of the spectral force obtained is plotted in Figures 3.9 and 3.10.

As can be expected, the spectral force obtained considering only the first mode has a linear distribution over the height and it resembles to the distribution obtained using equivalent static force method that provided basis to designs discussed in sections 3.2. The first mode distribution is clearly distinctive from the distributions with multiple modes participation and the differences decreases with the increase in the number of modes. More evident differences are observed in the force profiles calculated for the 14 storey Montreal, while for Vancouver the spectral force distributions are much closer regardless of the number of modes considered. Based on the results of these study it was concluded that, for both locations, it is important that at least the first two vibration modes be included in the seismic force calculation, in order to represent the shape specific for a spectral force distribution. However the spectral forces computed for the second design of the six frames, were calculated based on the first ten modes for each structure.

3.4.3 Particularities of design based on the spectral force distribution

New link sections were determined first for the loads introduced by spectral seismic forces. The selected sections are presented in Tables 3.20 and 3.21. The same design principles, as described in section 3.2., were followed and the effort was made to keep the link strength factors α similar to those obtained in design based on equivalent static force profile. Modified seismic force distribution resulted in 5% of reduction in the mass of the beams.

The braces and columns are initially selected based on the strength requirements for all the code defined load combinations. The results indicate that the wind combinations governed the selection of the braces and columns for all six structures. The exceptions were the top storeys of the frames where gravity loads governed design for Montreal's structures and the seismic load combination for Vancouver's structures. The total mass of the EBF frames is similar to the mass obtained using equivalent static force profiles, the highest differences being around 2%.

The stiffness design step brought a reduction in the mass of the frames of approximately 20% compared to the initial design, for the structures situated in Vancouver. For the structures situated in Montreal no significant changes were observed for 14 and 20 storey frames, however for 25 storeys the total mass was 23% higher compared to the initial design.

The verification for the stability of the frames introduced some changes compared to the initial design. While in the initial design all the three structures from Vancouver were controlled by the limitation of the inter storey drifts in the top storeys, now the design was governed by the stability coefficient U_2 for 14- and 20-storey frames. The exception

is 25 storey Vancouver where the inter storey drifts from the top storey reached first the code limit, before the coefficient U_2 become greater than 1.4. Another important difference was the necessity to use W sections for the braces in the 14 storey Montreal structure, as otherwise it was impossible to restrain the value of the stability coefficient U_2 to 1.40. In spite of the observed differences in design process, as can be seen from Tables 3.20 to 3.23, the total masses of the original and the modified design is very similar, reaching the maximum value of about 9 percent for 20-storey frame in Vancouver. Similar to the initial design, ductility requirements imposed minor changes of the brace sections and no columns modifications, for all six frames.

3.5 Conclusions

In this chapter a design procedure was applied in order to obtain EBFs that satisfy all code requirements. The initial frame configuration was selected based on strength, stiffness and stability requirements. Ductility design was performed afterwards as well as the verification of the inelastic rotations of the link. The established design sequence (strength, stiffness, stability and ductility design) are found to be appropriate for the range of frame heights and the locations studied. At each design step, the impact of different design criteria on section selection has been studied in detail and the following observations were made:

- In the strength design phase, wind load combination governed the design of frame members. As a direct consequence, high overstrength was introduced in the link beams of all frames situated in Montreal.
- In the stiffness design phase, an important increase in the mass of the structures designed for Vancouver was necessary in order to limit the total inter-storey drifts produced by the seismic forces. For the three structures in Montreal a smaller mass increases was observed in this design phase and was mainly required to limit the elastic inter-storey drifts caused by wind forces.

- The parameter that governed the design for the structures situated in Vancouver was the inter storey drift, calculated for the P-Δ amplified seismic force. For the Montreal structures, the stability verification was governed by the requirement to limit the coefficient U_2 to the NBCC limit.
- In the capacity design process (ductility design phase) only the braces at the base of the structures needed to be modified, while column had large reserves of strength due to the fact that other requirements (stiffness, stability) controlled the design.
- The inelastic link rotations verification did not govern the design of the frames. The new CSA S16S01–05 provision suggest to restrain axial deformations of the columns, when calculating the inter-storey drift that should be used in the empirical equation to calculate gamma (see section 3.2.4.5.). This is done to eliminate the chord drift that should not influence the inelastic link rotations. The higher the frame, the more important the deformation due to chord drift will be and the total elimination of this deformation is therefore questionable for high rise frames.

Secondary analyses to estimate link rotations that contain the deformations due to columns axial elongations yielded rotation values that go beyond the standard limit. Therefore it is of interest to see how dynamic total drifts and inelastic link rotations compare with the estimated design values.

The sequences of design steps described in section 3.2, are considered to be appropriate for the two location zones, as the section modifications were observed to follow a continuous increase in section capacities. Thus, the ductility design for tall EBF is not the governing design, but rather other design requirements as stiffness or stability govern the design for both western and eastern locations. For some frame members, other load combinations, which do not include the seismic load, dictate the selection of the EBF members.

Due to the necessity to satisfy other design requirements than the ductility design, a high overstrength is introduced in the members of all EBF frames and especially the columns were oversized as the height of the frame increases. Comparing the frames conceived for Montreal with those from Vancouver, the overstrength of the Montreal frames is much higher, a fact that reflects on the values of the estimated link rotations.

The variant design using the spectral distribution of the force was done to yield the possible differences in the frame member selection. The assumptions made in the calculation of the empirical seismic force, an estimated period of $2T_a$ and the reduction to 80% of the force are found to be justified, as the spectral analyses showed that the value of the spectral base shear was equal to 0.8V, where V was calculated for a period equal to $2T_a$. The complete EBF design regardless of the use of equivalent static force distribution or the spectral force distribution yield almost identical frame configurations, thus the seismic load distribution had negligible effect on frame design. Therefore it was decided that the structures designed using the empirical seismic force distribution will be employed for the nonlinear dynamic analyses

Table 3.1 Gravity and live loads on EBF (Vancouver)

Storey	Dead load			Live load		
	Column left (kN)	Beam (kN/m)	Column right (kN)	Column left (kN)	Beam (kN/m)	Column right (kN)
Top storey	42.07	11.31	42.07	84.13	8.37	84.13
1st and typical storey	230.85	22.95	230.85	123.12	16.56	123.12

Table 3.2 Gravity and live loads on EBF (Montreal)

Storey	Dead load			Live load		
	Column left (kN)	Beam (kN/m)	Column right (kN)	Column left (kN)	Beam (kN/m)	Column right (kN)
Top storey	42.07	11.31	42.07	127.22	14.28	127.22
1st and typical storey	230.85	22.95	230.85	123.12	16.56	123.12

Table 3.3 Wind load (Vancouver)

Storey	Reference height (m)	Wind load (kN)						Wind load with torsional amplification (kN)					
		SLS	ULS	SLS	ULS	SLS	ULS	SLS	ULS	SLS	ULS	ULS	SLS
25	93.3					47.05	62.73					54.94	73.25
24	89.6					93.33	124.44					109.00	145.33
23	85.9					92.56	123.41					108.10	144.13
22	82.2					91.76	122.35					107.17	142.89
21	78.5					90.94	121.26					106.21	141.61
20	74.8			43.86	58.49	90.10	120.13			51.22	68.30	105.22	140.29
19	71.1			86.84	115.79	89.22	118.96			101.42	135.22	104.19	138.93
18	67.4			85.93	114.57	88.31	117.74			100.36	133.81	103.13	137.51
17	63.7			84.98	113.31	87.36	116.48			99.25	132.33	102.03	136.03
16	60.0			84.00	112.00	86.38	115.17			98.10	130.80	100.88	134.50
15	56.3			82.97	110.63	85.35	113.80			96.90	129.20	99.67	132.90
14	52.6	39.49	52.65	81.89	109.19	84.27	112.36	46.11	61.48	95.64	127.52	98.42	131.22
13	48.9	77.83	103.77	80.76	107.68	83.14	110.85	90.89	121.19	94.32	125.76	97.09	129.46
12	45.2	76.64	102.18	79.57	106.09	81.94	109.26	89.50	119.33	92.92	123.90	95.70	127.60
11	41.5	75.37	100.50	78.30	104.40	80.68	107.57	88.02	117.37	91.45	121.93	94.22	125.63
10	37.8	74.03	98.70	76.96	102.61	79.33	105.78	86.45	115.27	89.88	119.84	92.65	123.54
9	34.1	72.58	96.78	75.52	100.69	77.89	103.86	84.77	113.03	88.19	117.59	90.97	121.29
8	30.4	71.03	94.71	73.96	98.61	76.34	101.78	82.95	110.60	86.38	115.17	89.15	118.87
7	26.7	69.34	92.45	72.27	96.36	74.64	99.53	80.98	107.97	84.40	112.53	87.17	116.23
6	23.0	67.47	89.96	70.40	93.87	72.78	97.04	78.79	105.06	82.22	109.62	84.99	113.33
5	19.3	65.38	87.17	68.31	91.08	70.69	94.25	76.35	101.80	79.78	106.37	82.55	110.07
4	15.6	62.98	83.98	65.91	87.89	68.29	91.05	73.56	98.07	76.98	102.64	79.76	106.34
3	11.9	60.15	80.20	63.08	84.11	65.46	87.28	70.25	93.66	73.67	98.23	76.45	101.93
2	8.2	60.23	80.31	63.17	84.22	65.54	87.39	70.35	93.79	73.77	98.36	76.54	102.06
1	4.5	66.75	88.99	69.99	93.33	72.63	96.84	77.94	103.93	81.74	108.98	84.81	113.08

Table 3.4 Wind load (Montreal)

Storey	Reference height (m)	Wind load (kN)						Wind load with torsional amplification (kN)					
		SLS	ULS	SLS	ULS	SLS	ULS	SLS	ULS	SLS	ULS	ULS	SLS
25	93.3					39.20	52.27					45.78	61.04
24	89.6					77.77	103.70					90.83	121.11
23	85.9					77.13	102.84					90.08	120.11
22	82.2					76.47	101.96					89.31	119.08
21	78.5					75.79	101.05					88.51	118.01
20	74.8			36.55	48.74	75.08	100.11			42.68	56.91	87.68	116.91
19	71.1			72.37	96.49	74.35	99.13			84.52	112.69	86.83	115.77
18	67.4			71.61	95.48	73.59	98.12			83.63	111.51	85.94	114.59
17	63.7			70.82	94.43	72.80	97.07			82.71	110.28	85.02	113.36
16	60.0			70.00	93.33	71.98	95.97			81.75	109.00	84.06	112.08
15	56.3			69.14	92.19	71.12	94.83			80.75	107.66	83.06	110.75
14	52.6	33.74	43.54	68.24	90.99	70.22	93.63	38.42	51.23	79.70	106.27	82.01	109.35
13	48.9	66.56	85.89	67.30	89.73	69.28	92.37	75.75	100.99	78.60	104.80	80.91	107.88
12	45.2	65.60	84.64	66.31	88.41	68.29	91.05	74.58	99.44	77.44	103.25	79.75	106.33
11	41.5	64.58	83.33	65.25	87.00	67.23	89.64	73.35	97.80	76.21	101.61	78.52	104.69
10	37.8	63.49	81.93	64.13	85.51	66.11	88.15	72.04	96.06	74.90	99.86	77.21	102.95
9	34.1	62.33	80.42	62.93	83.91	64.91	86.55	70.64	94.19	73.49	97.99	75.81	101.08
8	30.4	61.07	78.80	61.63	82.18	63.62	84.82	69.13	92.17	71.98	95.97	74.29	99.06
7	26.7	59.71	77.04	60.22	80.30	62.20	82.94	67.48	89.97	70.33	93.78	72.65	96.86
6	23.0	58.20	75.09	58.67	78.22	60.65	80.86	65.66	87.55	68.51	91.35	70.83	94.44
5	19.3	56.51	72.92	56.92	75.90	58.90	78.54	63.63	84.84	66.48	88.64	68.79	91.72
4	15.6	54.58	70.42	54.93	73.24	56.91	75.88	61.30	81.73	64.15	85.53	66.46	88.62
3	11.9	52.29	67.47	52.57	70.09	54.55	72.73	58.54	78.05	61.39	81.86	63.71	84.94
2	8.2	52.36	67.56	52.64	70.18	54.62	72.82	58.62	78.16	61.47	81.97	63.79	85.05
1	4.5	58.02	74.86	58.33	77.77	60.52	80.70	64.95	86.60	68.11	90.82	70.68	94.24

Table 3.5 Seismic loads calculation (Vancouver)

Storey	Height	Fourteen-storey frame			Twenty-storey frame			Twenty-five storey frame		
	h_x (m)	(a) W_x (kN)	(b) F_x / frame (kN)	(c) F_x^* / frame (kN)	(d) W_x (kN)	(e) F_x / frame (kN)	F_x^* / frame (kN)	(g) W_x (kN)	(h) F_x / frame (kN)	(i) F_x^* / frame (kN)
25	93.3							2293	727.11	628.14
24	89.6							7889	159.09	158.29
23	85.9							7889	152.46	152.62
22	82.2							7889	145.83	146.94
21	78.5							7889	139.20	141.27
20	74.8				2293	587.24	508.40	7889	132.58	135.59
19	71.1				7889	156.96	156.46	7889	125.95	129.92
18	67.4				7889	148.69	149.39	7889	119.32	124.25
17	63.7				7889	140.43	142.32	7889	112.69	118.57
16	60.0				7889	132.17	135.25	7889	106.06	112.90
15	56.3				7889	123.91	128.18	7889	99.43	107.22
14	52.6	2293	325.53	284.38	7889	115.65	121.11	7889	92.80	101.55
13	48.9	7889	165.81	164.04	7889	107.39	114.04	7889	86.17	95.87
12	45.2	7889	153.05	153.12	7889	99.13	106.97	7889	79.55	90.20
11	41.5	7889	140.30	142.21	7889	90.87	99.89	7889	72.92	84.53
10	37.8	7889	127.55	131.29	7889	82.61	92.82	7889	66.29	78.85
9	34.1	7889	114.79	120.37	7889	74.35	85.75	7889	59.66	73.18
8	30.4	7889	102.04	109.45	7889	66.09	78.68	7889	53.03	67.50
7	26.7	7889	89.28	98.54	7889	57.83	71.61	7889	46.40	61.83
6	23.0	7889	76.53	87.62	7889	49.56	64.54	7889	39.77	56.16
5	19.3	7889	63.77	76.70	7889	41.30	57.47	7889	33.14	50.48
4	15.6	7889	51.02	65.78	7889	33.04	50.40	7889	26.52	44.81
3	11.9	7889	38.26	54.86	7889	24.78	43.32	7889	19.89	39.13
2	8.2	7889	25.51	43.95	7889	16.52	36.25	7889	13.26	33.46
1	4.5	7954	12.86	33.28	7954	8.33	29.40	7954	6.68	27.99

Σ	104915	1486.30	1565.59	152249	2156.86	2272.25	191694	2715.80	2861.25
T_{NBCC} (sec)=	2Ta	2.63			3.74			4.67	
$7V_e$(kN)		17835.60			25882.33			32589.58	
V (kN)		2972.60			4313.72			5431.60	
Ft(kN)		545.17			1078.43			1357.90	

*Note: Fx is reduced to 80 percent of initial shear force, with a 7% amplification for accidental torsion and the notional loads added

Table 3.6 Seismic loads calculation (Montreal)

Storey	Height	Fourteen-storey frame			Twenty-storey frame			Twenty-five storey frame		
	h_x	(a) W_x	(b) F_x / frame	(c) F_x^* / frame	(d) W_x	(e) F_x / frame	F_x^* / frame	(g) W_x	(h) F_x / frame	(i) F_x^* / frame
	(m)	(kN)	(kN)	(kN)	(kN)	(kN)	(kN)	(kN)	(kN)	(kN)
25	93.3							2633	311.44	273.17
24	89.6							7889	67.26	79.69
23	85.9							7889	64.46	77.29
22	82.2							7889	61.66	74.89
21	78.5							7889	58.86	72.49
20	74.8				2633	252.18	222.45	7889	56.05	70.09
19	71.1				7889	66.33	78.89	7889	53.25	67.69
18	67.4				7889	62.84	75.90	7889	50.45	65.29
17	63.7				7889	59.35	72.91	7889	47.64	62.89
16	60.0				7889	55.86	69.92	7889	44.84	60.49
15	56.3				7889	52.37	66.94	7889	42.04	58.10
14	52.6	2633	141.42	127.64	7889	48.88	63.95	7889	39.24	55.70
13	48.9	7889	70.01	82.04	7889	45.39	60.96	7889	36.43	53.30
12	45.2	7889	64.62	77.43	7889	41.89	57.97	7889	33.63	50.90
11	41.5	7889	59.24	72.82	7889	38.40	54.98	7889	30.83	48.50
10	37.8	7889	53.85	68.21	7889	34.91	51.99	7889	28.03	46.10
9	34.1	7889	48.47	63.60	7889	31.42	49.01	7889	25.22	43.70
8	30.4	7889	43.08	58.99	7889	27.93	46.02	7889	22.42	41.30
7	26.7	7889	37.70	54.38	7889	24.44	43.03	7889	19.62	38.90
6	23.0	7889	32.31	49.77	7889	20.95	40.04	7889	16.82	36.50
5	19.3	7889	26.93	45.16	7889	17.46	37.05	7889	14.01	34.11
4	15.6	7889	21.54	40.55	7889	13.96	34.06	7889	11.21	31.71
3	11.9	7889	16.16	35.94	7889	10.47	31.08	7889	8.41	29.31
2	8.2	7889	10.77	31.33	7889	6.98	28.09	7889	5.61	26.91
1	4.5	7954	5.43	26.92	7954	3.52	25.28	7954	2.83	24.69
Σ		105255	631.53	834.76	152589	915.53	1210.52	192034	1152.25	1523.71

T_{NBCC} (sec)=	2Ta	2.63	3.74	4.67
V_e(kN)		7578.32	10986.37	13827.05
V (kN)		1263.05	1831.06	2304.51
Ft(kN)		232.53	457.77	576.13

*Note: Fx is reduced to 80 percent of initial shear force, with a 7% amplification for accidental torsion and the notional loads added

Table 3.7 Selection of the link beam sections (Vancouver)

Storey	Fourteen-storey frame		Twenty-storey frame		Twenty five-storey frame	
	Section	α (V_f/V_r)	Section	α (V_f/V_r)	Section	α (V_f/V_r)
25					W 250x58	1.34
24					W 310x52	1.25
23					W 310x74	1.24
22					W 360x79	1.21
21					W 410x74	1.28
20			W 250x58	1.65	W 460x82	1.30
19			W 250x58	1.23	W 460x89	1.26
18			W 310x67	1.27	W 460x97	1.26
17			W 360x72	1.24	W 530x101	1.29
16			W 410x67	1.28	W 530x109	1.29
15			W 410x74	1.27	W 610x113	1.32
14	W 200x42	2.14	W 460x82	1.30	W 610x113	1.25
13	W 200x52	1.44	W 460x89	1.27	W 610x125	1.27
12	W 250x58	1.31	W 530x92	1.32	W 610x140	1.35
11	W 310x67	1.35	W 530x101	1.33	W 610x140	1.29
10	W 360x72	1.31	W 530x109	1.33	W 610x140	1.25
9	W 360x79	1.27	W 530x109	1.27	W 610x153	1.30
8	W 410x74	1.36	W 610x113	1.32	W 610x153	1.26
7	W 460x68	1.30	W 610x113	1.26	W 610x153	1.23
6	W 410x85	1.30	W 610x125	1.30	W 610x195	1.31
5	W 460x89	1.31	W 610x125	1.26	W 610x195	1.28
4	W 530x74	1.31	W 610x140	1.36	W 610x195	1.26
3	W 530x85	1.34	W 610x140	1.32	W 610x195	1.23
2	W 530x101	1.37	W 610x140	1.29	W 610x195	1.21
1	W 610x113	1.28	W 610x153	1.13	W 610x241	1.17

Table 3.8 Selection of the link beam sections (Montreal)

Storey	Fourteen-storey frame		Twenty-storey frame		Twenty five-storey frame	
	Section	α (V_f/V_r)	Section	α (V_f/V_r)	Section	α (V_f/V_r)
25					W 200x42	2.22
24					W 200x42	1.63
23					W 250x39	1.52
22					W 250x58	1.47
21					W 250x67	1.44
20			W 200x42	2.72	W 310x67	1.44
19			W 200x42	1.89	W 310x74	1.44
18			W 250x39	1.71	W 360x79	1.50
17			W 250x58	1.63	W 410x67	1.49
16			W 310x67	1.79	W 410x74	1.53
15			W 310x74	1.75	W 460x74	1.47
14	W 200X42	4.63	W 360x72	1.61	W 460x82	1.52
13	W 200X42	2.61	W 360x79	1.61	W 460x89	1.54
12	W 250x45	2.53	W 410x74	1.78	W 460x97	1.59
11	W 250x58	1.97	W 460x74	1.69	W 460x97	1.52
10	W 250x67	1.85	W 460x82	1.75	W 530x92	1.48
9	W 360x64	1.86	W 460x89	1.75	W 530x101	1.53
8	W 360x72	1.85	W 460x89	1.66	W 530x109	1.58
7	W 360x79	1.84	W 530x92	1.76	W 530x109	1.52
6	W 410x67	1.83	W 530x92	1.68	W 610x113	1.60
5	W 410x74	1.88	W 530x101	1.74	W 610x113	1.56
4	W 460x68	1.83	W 530x101	1.67	W 610x125	1.62
3	W 460x82	1.88	W 530x109	1.73	W 610x125	1.58
2	W 460x82	1.79	W 610x113	1.82	W 610x140	1.71
1	W 530x101	1.81	W 610x125	1.55	W 610x153	1.48

Table 3.9 Sections of the fourteen-storey frame (Vancouver)

Storey	Strenght		Stiffness		Stability	
	Braces	Columns	Braces	Columns	Braces	Columns
14	HSS152x127x4.8	W 200x42	HSS203x203x11	W 200x59	HSS254x254x9.5	W 200x59
13	HSS203x152x6.4		HSS254x254x11		HSS305x305x13	
12	HSS203x152x6.4	W 310x79	HSS254x254x11	W 360x134	HSS305x305x13	W 360x134
11	HSS202x152x8.0		HSS254x254x11		HSS305x305x13	
10	HSS229x178x7.9	W 310x118	HSS254x254x11	W 360x237	HSS305x305x13	W 460x235
9	HSS229x178x7.9		HSS254x254x11		HSS305x305x13	
8	HSS229x178x7.9	WWF 350x155	HSS254x254x11	WWF 400x237	HSS305x305x13	WWF 450x308
7	HSS229x178x7.9		HSS254x254x13		HSS305x305x13	
6	HSS254x203x8.0	WWF 350x192	HSS254x254x13	WWF 450x308	HSS305x305x13	WWF 500x456
5	HSS254x203x8.0		HSS254x254x13		HSS305x305x13	
4	HSS254x203x8.0	WWF 400x243	HSS254x254x13	WWF 500x381	HSS305x305x13	WWF 600x551
3	HSS254x203x8.0		HSS254x254x13		HSS305x305x13	
2	HSS254x203x8.0	WWF500x306	HSS305x305x11	WWF 500x456	HSS305x305x11	WWF650x739
1	HSS305x203x9.5		HSS305x305x11		HSS305x305x11	
Mass [kg]	**7530**	**17291**	**13785**	**27583**	**16573**	**37937**
Total mass of the structure [kg]		**34367**		**50915**		**64056**
Modal period (2D) [seconds]		**3,92sec**		**3,23sec**		**2.86sec**

Table 3.10 Sections of the fourteen-storey frame (Montreal)

Storey	Strenght		Stiffness		Stability	
	Braces	Columns	Braces	Columns	Braces	Columns
14	HSS152x127x4.8	W 360x51	HSS152x127x4.8	W 360x51	HSS203x203x11	W 360x79
13	HSS152x127x4.8		HSS203x203x11		HSS305x305x11	
12	HSS178x127x6.4	W 310x79	HSS203x203x11	W 310x79	HSS305x305x11	W 310x118
11	HSS203x152x6.4		HSS203x203x11		HSS305x305x13	
10	HSS203x152x6.4	W 310x118	HSS254x203x9.5	W 310x118	HSS305x305x13	W 460x177
9	HSS203x152x8.0		HSS203x203x11		HSS305x305x13	
8	HSS203x152x8.0	WWF 350x137	HSS203x203x9.5	WWF 350x137	HSS305x305x13	WWF 500x381
7	HSS229x178x7.9		HSS203x203x9.5		HSS305x305x13	
6	HSS229x178x7.9	WWF 350x192	HSS203x203x9.5	WWF 400x243	HSS305x305x13	WWF 550x503
5	HSS229x178x7.9		HSS203x203x9.5		HSS305x305x13	
4	HSS254x203x8.0	WWF 450x228	HSS254x203x8.0	WWF 450x228	HSS305x305x13	WWF 600x680
3	HSS254x203x8.0		HSS254x203x8.0		HSS305x305x13	
2	HSS254x203x8.0	WWF 450x308	HSS254x203x8.0	WWF 500x381	HSS305x305x11	WWF650x598
1	HSS254x203x9.5		HSS254x203x9.5		HSS305x305x11	
Mass [kg]	**6517**	**16962**	**8808**	**18926**	**16499**	**38518**
Total mass of the structure [kg]		**31974**		**36228**		**63511**
Modal period (2D) [seconds]		**4.13sec**		**3.89sec**		**2.98sec**

Table 3.11 Sections of the twenty-storey frame (Vancouver)

Storey	Strenght		Stiffness		Stability	
	Braces	Columns	Braces	Columns	Braces	Columns
20	W 200x52	W 200x42	W 250x73	W 360x79	W 310x107	W 360x79
19	W 200x52		W 310x79		W 310x129	
18	W 250x58	W 250x101	W 310x79	W 360x216	W 310x129	W 360x287
17	W 310x67		W 310x79		W 310x129	
16	W 250x67		W 310x79		W 310x129	
15	W 250x73	W 310x179	W 310x79	W 360x382	W 310x129	W 360x463
14	W 250x73		W 310x86		W 310x129	
13	W 250x73		W 310x86		W 310x118	
12	W 250x73	WWF 350x238	W 310x86	Ste 400x400	W 310x118	Ste 400x400
11	W 250x73		W 310x97		W 310x118	
10	W 310x86		W 310x97		W 310x118	
9	W 310x107	WWF 400x362	W 310x107	Ste 400x400	W 310x129	Ste 450x450
8	W 310x107		W 310x107		W 310x129	
7	W 310x107		W 310x107		W 310x129	
6	W 310x107	WWF 450x503	W 310x107	Ste 450x450	W 310x129	Ste 550x550
5	W 310x107		W 310x107		W 310x143	
4	W 310x107		W 310x107		W 310x143	
3	W 310x107	WWF550x620	W 310x107	Ste 500x500	W 310x143	Ste 550x550
2	W 310x107		W 310x107		W 310x143	
1	W 310x129		W 310x129		W 310x143	
Mass [kg]	**19250**	**46119**	**21179**	**152234**	**28727**	**190239**
Total mass of the structure [kg]		**83649**		**191693**		**237246**
Modal period (2D) [seconds]		**5.19sec**		**3.70sec**		**3.37sec**

Table 3.12 Sections of the twenty-storey frame (Montreal)

Storey	Strenght		Stiffness		Stability	
	Braces	Columns	Braces	Columns	Braces	Columns
20	W 200x42	W 360x51	W 200x71	W 360x79	W 310x97	W 360x79
19	W 200x42		W 250x80		W 310x97	
18	W 200x42	W 360x101	W 250x80	W 360x147	W 310x97	W 360x237
17	W 200x52		W 250x80		W 310x118	
16	W 200x52		W 250x80		W 310x118	
15	W 200x52	W 360x162	W 310x74	W 360x262	W 310x118	W 360x347
14	W 250x58		W 310x74		W 310x158	
13	W 200x71		W 310x74		W 310x158	
12	W 200x71	WWF 350x212	W 310x74	WWF 400x303	W 310x158	Ste 400x400
11	W 250x73		W 310x79		W 310x158	
10	W 250x73		W 310x79		W 310x179	
9	W 250x73	WWF 400x303	W 310x79	WWF 450x342	W 310x179	Ste 450x450
8	W 250x73		W 310x79		W 310x179	
7	W 310x79		W 310x79		W 310x179	
6	W 310x79	WWF 450x409	W 310x79	WWF 450x503	W 310x179	Ste 500x500
5	W 310x86		W 310x86		W 310x158	
4	W 310x86		W 310x86		W 310x158	
3	W 310x97	WWF500x561	W 310x97	Ste 450x450	W 310x158	Ste 500x500
2	W 310x107		W 310x107		W 310x143	
1	W 310x107		W 310x107		W 310x143	
Mass [kg]	**15749**	**40494**	**18297**	**73616**	**32489**	**167570**
Total mass of the structure [kg]		**70785**		**106456**		**214601**
Modal period (2D) [seconds]		**5.71sec**		**4.88sec**		**3.55sec**

Table 3.13 Sections of the twenty-five storey frame (Vancouver)

Storey	Strenght		Stiffness		Stability	
	Braces	Columns	Braces	Columns	Braces	Columns
25	W 200x52	W 200x42	W 310x202	W 360x91	W 310x253	W 360x101
24	W 250x58		W 310x179		W 310x253	
23	W 310x67	W 310x86	W 310x143	W 360x237	W 310x253	W 360x262
22	W 250x73		W 310x129		W 310x202	
21	W 250x73	W 360x162	W 310x129	W 360x463	W 310x202	W 360x592
20	W 250x73		W 310x118		W 310x202	
19	W 250x73		W 310x118		W 310x202	
18	W 310x79	W 360x262	W 310x118	Ste 400x400	W 310x202	Ste 450x450
17	W 310x79		W 310x118		W 310x202	
16	W 310x86		W 310x118		W 310x202	
15	W 310x107	WWF 450x342	W 310x118	Ste 450x450	W 310x202	Ste 550x550
14	W 310x107		W 310x118		W 360x196	
13	W 310x107		W 310x118		W 360x196	
12	W 310x107	WWF 500x456	W 310x118	Ste 500x500	W 360x196	Ste 650x650
11	W 310x107		W 360x134		W 360x196	
10	W 310x107		W 360x134		W 360x196	
9	W 310x107	WWF 500x561	W 360x134	Ste 550x550	W 360x196	Ste 650x650
8	W 310x118		W 360x134		W 360x179	
7	W 310x118		W 360x134		W 360x179	
6	W 310x129	WWF 550x721	W 360x134	Ste 650x650	W 360x179	Ste 700x700
5	W 310x129		W 360x162		W 360x162	
4	W 310x129		W 360x162		W 360x162	
3	W 310x143	Ste 500x500	W 360x162	Ste 700x700	W 360x162	Ste 700x700
2	W 310x143		W 360x162		W 360x162	
1	W 360x162		W 360x162		W 360x162	
Mass [kg]	**28137**	**104282**	**38351**	**349780**	**54324**	**430751**
Total mass of the structure [kg]		**161850**		**417562**		**514506**
Modal period (2D) [seconds]		**6.18sec**		**4.13sec**		**3.79sec**

Table 3.14 Sections of the twenty-five storey frame (Montreal)

Storey	Strenght		Stiffness		Stability	
	Braces	Columns	Braces	Columns	Braces	Columns
25	W 200x42	W 360x51	W 250x73	W 360x51	W 250x73	W 360x79
24	W 200x42		W 310x97		W 310x118	
23	W 200x52	W 360x91	W 310x97	W 360x91	W 310x143	W 360x110
22	W 200x52		W 310x79		W 310x143	
21	W 250x58	W 360x162	W 310x79	W 360x196	W 310x226	W 360x347
20	W 250x67		W 310x79		W 310x226	
19	W 250x67		W 310x79		W 310x226	
18	W 250x73	W 360x216	W 310x86	W 360x347	W 310x226	Ste 450x450
17	W 250x73		W 310x86		W 310x226	
16	W 250x73		W 310x86		W 360x237	
15	W 310x79	WWF 400x303	W 310x79	WWF 400x303	W 360x237	Ste 550x550
14	W 310x79		W 310x79		W 360x237	
13	W 310x86		W 310x86		W 360x237	
12	W 310x97	WWF 450x409	W 310x97	Ste 400x400	W 360x237	Ste 550x550
11	W 310x97		W 310x97		W 360x237	
10	W 310x97		W 310x97		W 360x237	
9	W 310x107	WWF 500x561	W 310x107	Ste 450x450	W 360x216	Ste 650x650
8	W 310x107		W 310x107		W 360x216	
7	W 310x107		W 310x107		W 360x216	
6	W 310x107	WWF 500x651	W 310x107	Ste 450x450	W 360x216	Ste 700x700
5	W 310x107		W 310x107		W 360x216	
4	W 310x107		W 310x107		W 360x216	
3	W 310x107	WWF600x793	W 310x107	Ste 500x500	W 360x216	Ste 750x750
2	W 310x107		W 310x107		W 360x216	
1	W 310x129		W 310x129		W 360x216	
Mass [kg]	**23519**	**72133**	**26205**	**163833**	**57712**	**415339**
Total mass of the structure [kg]		**115722**		**210109**		**493122**
Modal period (2D) [seconds]		**7.17sec**		**5.50 sec**		**3.93 sec**

Table 3.15 Final seismic inter-storey drifts calculated for the frames complying with stiffness requirements (Vancouver)

Storey	Storey height hs (m)	VANCOUVER Anticipated total inter-storey drifts (mm)			MONTREAL Anticipated total inter-storey drifts (mm)			Maximum NBCC drift limit
		14 storey	20 storey	25 storey	14 storey	20 storey	25 storey	
25	93.3			92.51			90.69	92.5
24	89.6			92.15			91.68	92.5
23	85.9			91.18			90.35	92.5
22	82.2			91.16			90.40	92.5
21	78.5			91.35			90.49	92.5
20	74.8		91.42	90.64		91.42	89.11	92.5
19	71.1		90.97	88.46		91.45	86.84	92.5
18	67.4		90.37	88.04		91.54	83.98	92.5
17	63.7		90.04	86.39		90.13	82.68	92.5
16	60.0		89.24	84.79		87.39	79.61	92.5
15	56.3		88.16	83.03		86.73	76.33	92.5
14	52.6	91.03	83.58	81.82	75.67	85.46	70.37	92.5
13	48.9	91.20	80.09	79.04	84.67	83.05	62.13	92.5
12	45.2	91.80	78.61	75.72	80.30	80.17	59.07	92.5
11	41.5	90.25	75.33	71.36	79.04	75.68	58.06	92.5
10	37.8	89.42	73.21	68.38	79.39	70.65	55.76	92.5
9	34.1	88.12	69.83	65.25	72.91	65.58	52.19	92.5
8	30.4	85.79	66.32	62.56	70.15	60.29	49.77	92.5
7	26.7	81.10	63.44	58.93	64.20	53.12	47.58	92.5
6	23.0	75.24	59.94	53.83	61.26	48.11	44.42	92.5
5	19.3	68.20	56.76	48.47	56.26	40.98	41.47	92.5
4	15.6	63.37	52.09	44.75	49.31	34.82	37.80	92.5
3	11.9	54.57	48.78	41.80	42.39	30.66	34.84	92.5
2	8.2	43.54	44.64	38.63	36.75	26.51	30.70	92.5
1	4.5	40.31	45.20	42.75	30.99	28.73	30.07	112.5

Table 3.16 Summary of the selected sections after ductility design (Vancouver)

Storey	14 storey structure			20 storey structure			25 storey structure		
	Braces	Columns	γ (rad)	Braces	Columns	γ (rad)	Braces	Columns	γ (rad)
25							W 310x253	W 360x101	0.03
24							W 310x253		0.03
23							W 310x253	W 360x262	0.03
22							W 310x202		0.04
21							W 310x202	W 360x592	0.04
20				W 310x107	W 360x79	0.03	W 310x202		0.05
19				W 310x129		0.04	W 310x202		0.05
18				W 310x129	W 360x287	0.04	W 310x202	Ste 450x450	0.05
17				W 310x129		0.05	W 310x202		0.05
16				W 310x129		0.05	W 310x202		0.05
15				W 310x129	W 360x463	0.06	W 310x202	Ste 550x550	0.06
14	HSS254x254x9.5	W 200x59	0.03	W 310x129		0.06	W 360x196		0.06
13	HSS305x305x13		0.04	W 310x118		0.06	W 360x196		0.06
12	HSS305x305x13	W 310x143	0.04	W 310x118	Ste 400x400	0.07	W 360x196	Ste 650x650	0.06
11	HSS305x305x13		0.05	W 310x129		0.06	W 360x196		0.06
10	HSS305x305x13	W 460x235	0.05	W 310x143		0.06	W 360x196		0.06
9	HSS305x305x13		0.06	W 310x143	Ste 450x450	0.07	W 360x196	Ste 650x650	0.06
8	HSS305x305x13	WWF 450x308	0.06	W 310x143		0.07	W 360x179		0.07
7	HSS305x305x13		0.07	W 310x143		0.07	W 360x179		0.07
6	HSS305x305x13	WWF 500x456	0.07	W 310x158	Ste 550x550	0.06	W 360x179	Ste 700x700	0.06
5	HSS305x305x13		0.07	W 310x158		0.06	W 360x179		0.06
4	HSS356x305x13	WWF 600x551	0.07	W 310x179		0.06	W 360x179		0.07
3	HSS356x305x13		0.07	W 310x179	Ste 550x550	0.06	W 360x179	Ste 700x700	0.07
2	HSS305x305x13	WWF650x739	0.07	W 310x179		0.06	W 360x179		0.06
1	HSS305x305x13		0.07	W 310x179		0.06	W 360x196		0.06

Table 3.17 Summary of the selected sections after ductility design (Montreal)

Storey	14 storey structure			20 storey structure			25 storey structure		
	Braces	Columns	γ (rad)	Braces	Columns	γ (rad)	Braces	Columns	γ (rad)
25							W 250x73	W 360x79	0.02
24							W 310x118		0.03
23							W 310x143	W 360x110	0.03
22							W 310x143		0.03
21							W 310x226	W 360x347	0.02
20				W 310x107	W 360x79	0.02	W 310x226		0.03
19				W 310x107		0.03	W 310x226		0.03
18				W 310x107	W 360x237	0.03	W 310x226	Ste 450x450	0.03
17				W 310x118		0.03	W 310x226		0.03
16				W 310x118		0.03	W 360x237		0.03
15				W 310x118	W 360x347	0.03	W 360x237	Ste 550x550	0.03
14	HSS203x203x11	W 360x79	0.02	W 310x158		0.03	W 360x237		0.03
13	HSS305x305x11		0.02	W 310x158		0.03	W 360x237		0.03
12	HSS305x305x11	W 310x118	0.02	W 310x158	Ste 400x400	0.04	W 360x237	Ste 550x550	0.03
11	HSS305x305x13		0.03	W 310x158		0.04	W 360x237		0.04
10	HSS305x305x13	W 460x193	0.03	W 310x179		0.03	W 360x237		0.04
9	HSS305x305x13		0.03	W 310x179	Ste 450x450	0.04	W 360x216	Ste 650x650	0.04
8	HSS305x305x13	WWF 500x381	0.03	W 310x179		0.04	W 360x216		0.04
7	HSS305x305x13		0.04	W 310x179		0.04	W 360x216		0.04
6	HSS305x305x13	WWF 550x503	0.04	W 310x179	Ste 500x500	0.04	W 360x216	Ste 700x700	0.04
5	HSS305x305x13		0.04	W 310x158		0.04	W 360x216		0.04
4	HSS305x305x13	WWF 600x680	0.04	W 310x158		0.04	W 360x216		0.04
3	HSS305x305x13		0.04	W 310x158	Ste 500x500	0.04	W 360x216	Ste 750x750	0.04
2	HSS305x305x13	WWF650x598	0.04	W 310x158		0.04	W 360x216		0.04
1	HSS305x305x13		0.04	W 310x158		0.04	W 360x216		0.03

Table 3.18 Summary of the seismic forces obtained using equivalent static force procedure and modal response spectrum method

Location	Height (m)	V (kN)	0.8 V (kN)	V_e (kN)	V_d (kN)	$V_{d,final}$ (kN)	Controlling method
Vancouver	14	2972.60	2378.08	14435.00	2405.83	2405.83	spectral
	20	4313.72	3450.98	17321.40	2886.89	3450.98	empirical
	25	5431.60	4345.28	19766.20	3294.36	4345.28	empirical
Montreal	14	1263.05	1006.94	5355.77	892.629	1006.94	empirical
	20	1831.06	1464.85	6471.56	1078.59	1464.85	empirical
	25	2304.51	1843.61	7510.72	1251.79	1843.61	empirical

Table 3.19 Summary of the first periods of vibration

No. of storey	NBCC formula	Estimated period (2Ta)	Modal analysis (2D)	Modal analysis (3D)
Vancouver				
14	1.32	2.63	2.86	2.61
20	1.87	3.74	3.37	2.93
25	2.33	4.66	3.79	3.38
Montreal				
14	1.32	2.63	2.98	2.72
20	1.87	3.74	3.55	3.07
25	2.33	4.66	3.93	3.43

Table 3.20 Selection of the link beam sections – Spectral design(Vancouver)

Storey	Fourteen-storey frame		Twenty-storey frame		Twenty five-storey frame	
	Section	$\alpha=V_r/V_f$	Section	$\alpha=V_r/V_f$	Section	$\alpha=V_r/V_f$
25					W 250x39	4.84
24					W 250x58	1.50
23					W 310x67	1.28
22					W 360x79	1.29
21					W 410x67	1.22
20			W 250x39	5.10	W 460x74	1.24
19			W 250x58	1.62	W 460x82	1.24
18			W 250x67	1.22	W 460x89	1.20
17			W 310x74	1.25	W 460x97	1.21
16			W 360x79	1.22	W 530x101	1.25
15			W 410x74	1.30	W 530x109	1.27
14	W200x42	4.71	W 460x74	1.24	W 530x109	1.23
13	W200x59	1.68	W 460x82	1.25	W 610x113	1.28
12	W310x67	1.57	W 460x89	1.24	W 610x113	1.22
11	W310x74	1.44	W 460x97	1.26	W 610x125	1.25
10	W410x60	1.36	W 530x92	1.22	W 610x140	1.32
9	W410x67	1.41	W 530x101	1.24	W 610x140	1.27
8	W410x74	1.43	W 530x109	1.26	W 610x140	1.21
7	W460x68	1.37	W 610x113	1.31	W 610x153	1.26
6	W460x82	1.38	W 610x113	1.26	W 610x153	1.21
5	W460x89	1.36	W 610x125	1.29	W 610x195	1.29
4	W530x74	1.34	W 610x125	1.25	W 610x195	1.24
3	W530x85	1.35	W 610x140	1.33	W 610x195	1.21
2	W610x82	1.38	W 610x140	1.28	W 610x195	1.18
1	W610x113	1.30	W 610x153	1.17	W 610x241	1.22

Table 3.21 Selection of the link beam sections – Spectral design (Montreal)

Storey	Fourteen-storey frame		Twenty-storey frame		Twenty five-storey frame	
	Section	$\alpha=V_r/V_f$	Section	$\alpha=V_r/V_f$	Section	$\alpha=V_r/V_f$
25					W 200x42	4.70
24					W 200x42	1.80
23					W 250x58	1.86
22					W 250x67	1.78
21					W 250x67	1.59
20			W 200x42	5.88	W 310x67	1.63
19			W 200x42	2.00	W 310x67	1.48
18			W 250x39	1.75	W 310x74	1.53
17			W 250x58	1.75	W 360x79	1.63
16			W 250x67	1.75	W 410x67	1.67
15			W 310x67	1.79	W 410x74	1.74
14	W 200X42	6.86	W 310x67	1.63	W 460x74	1.69
13	W 200X42	2.39	W 360x72	1.72	W 460x82	1.76
12	W 250x45	2.44	W 360x79	1.76	W 460x82	1.65
11	W 250x58	2.06	W 410x67	1.77	W 460x89	1.67
10	W 250x58	1.82	W 410x67	1.65	W 530x92	1.77
9	W 250x67	1.86	W 460x74	1.77	W 530x92	1.69
8	W 310x67	1.92	W 460x74	1.66	W 530x101	1.73
7	W 360x57	1.90	W 460x82	1.73	W 530x109	1.76
6	W 360x72	1.83	W 460x89	1.74	W 530x109	1.67
5	W 360x79	1.84	W 460x97	1.79	W 610x113	1.73
4	W 460x60	1.82	W 530x92	1.73	W 610x113	1.65
3	W 460x68	1.90	W 530x101	1.74	W 610x125	1.67
2	W 460x82	1.88	W 530x109	1.73	W 610x140	1.74
1	W 530x101	1.81	W 610x125	1.55	W 610x153	1.48

Table 3.22 Summary of selected sections after ductility design - Spectral design (Vancouver)

Storey	14 storey structure			20 storey structure			25 storey structure		
	Braces	Columns	γ (rad)	Braces	Columns	γ (rad)	Braces	Columns	γ (rad)
25							W 310x79	W 360x79	0.01
24							W 310x143		0.03
23							W 310x158	W 360x134	0.04
22							W 310x158		0.04
21							W 310x158	W 360x382	0.05
20				W 310x79	W 360x79	0.01	W 310x179		0.05
19				W 310x118		0.03	W 310x179		0.05
18				W 310x118	W 360x216	0.04	W 310x179	Ste 400x400	0.05
17				W 310x118		0.04	W 310x179		0.05
16				W 310x129		0.05	W 310x202		0.05
15				W 310x129	W 360x421	0.05	W 310x202	Ste 450x450	0.05
14	HSS203x203x9.5	W 200x52	0.02	W 310x158		0.05	W 310x202		0.05
13	HSS305x305x11		0.03	W 310x158		0.05	W 360x216		0.05
12	HSS305x305x13	W 310x118	0.03	W 310x158	Ste 400x400	0.05	W 360x216	Ste 550x550	0.05
11	HSS305x305x13		0.04	W 310x158		0.05	W 360x216		0.05
10	HSS305x305x13	W 360x216	0.04	W 310x158		0.06	W 360x216		0.05
9	HSS305x305x13		0.05	W 310x158	Ste 450x450	0.06	W 360x216	Ste 650x650	0.05
8	HSS305x305x13	WWF 400x362	0.05	W 310x158		0.06	W 360x216		0.05
7	HSS305x305x13		0.05	W 310x143		0.06	W 360x196		0.06
6	HSS305x305x13	WWF 550x503	0.05	W 310x143	Ste 500x500	0.06	W 360x196	Ste 700x700	0.06
5	HSS305x305x13		0.06	W 310x158		0.06	W 360x196		0.06
4	HSS356x305x13	WWF 600x551	0.06	W 310x158		0.06	W 360x196		0.06
3	HSS356x305x13		0.06	W 310x179	Ste 500x500	0.06	W 360x196	Ste 750x750	0.06
2	HSS356x356x13	WWF 650x739	0.06	W 310x179		0.06	W 360x196		0.06
1	HSS356x305x13		0.07	W 310x179		0.06	W 360x196		0.06

Table 3.23 Summary of selected sections after ductility design - Spectral design (Montreal)

Storey	14 storey structure			20 storey structure			25 storey structure		
	Braces	Columns	γ (rad)	Braces	Columns	γ (rad)	Braces	Columns	γ (rad)
25							W 310x107	W 360x101	0.01
24							W 310x129		0.03
23							W 310x129	W 360x162	0.02
22							W 310x143		0.03
21							W 310x143	W 360x287	0.03
20				W 250x80	W 360x72	0.01	W 310x158		0.03
19				W 310x86		0.03	W 310x158		0.03
18				W 310x86	W 360x237	0.03	W 360x216	Ste 400x400	0.03
17				W 310x118		0.02	W 360x216		0.03
16				W 310x118		0.02	W 360x216		0.03
15				W 310x118	W 360x287	0.03	W 360x262	Ste500x500	0.03
14	W 250x80	W 360x79	0.01	W 310x158		0.02	W 360x262		0.03
13	W 250x101		0.02	W 310x158		0.02	W 360x262		0.03
12	W 310x107	W 310x118	0.02	W 310x179	Ste 400x400	0.02	W 360x262	Ste 600x600	0.03
11	W 310x107		0.02	W 310x179		0.03	W 360x262		0.03
10	W 310x107	W 460x177	0.03	W 310x179		0.03	W 360x262		0.03
9	W 310x143		0.02	W 310x179	Ste 450x450	0.03	W 360x262	Ste 700x700	0.03
8	W 310x143	WWF 500x381	0.03	W 310x179		0.03	W 360x262		0.03
7	W 310x143		0.03	W 310x179		0.03	W 360x216		0.03
6	W 310x143	WWF 550x503	0.03	W 310x179	Ste 550x550	0.03	W 360x216	Ste 700x700	0.03
5	W 310x143		0.03	W 310x179		0.03	W 360x216		0.04
4	W 310x143	WWF 600x680	0.03	W 310x179		0.03	W 360x162		0.04
3	W 310x118		0.04	W 310x143	Ste 550x550	0.04	W 360x162	Ste 750x750	0.04
2	W 310x118	WWF 650x598	0.04	W 310x143		0.04	W 360x162		0.04
1	W 310x129		0.04	W 310x143		0.04	W 360x162		0.04

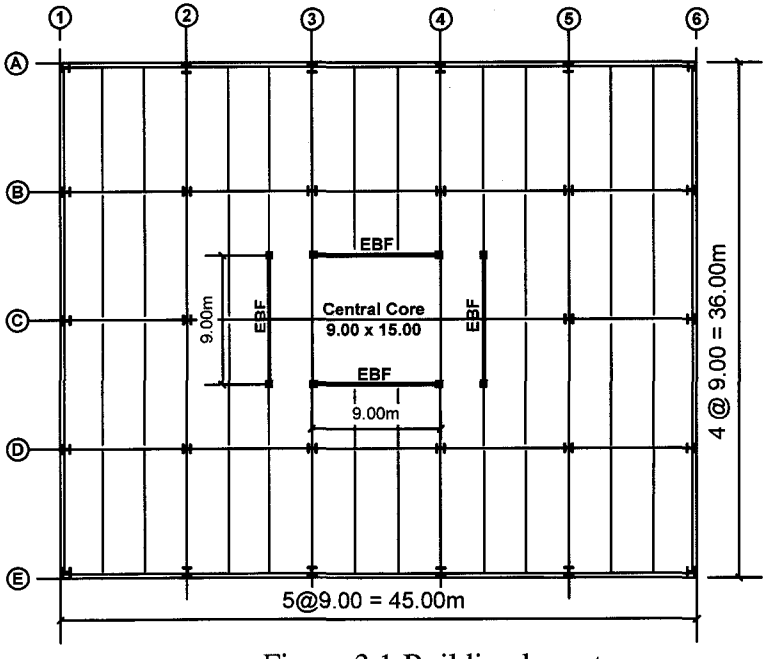

Figure 3.1 Building layout

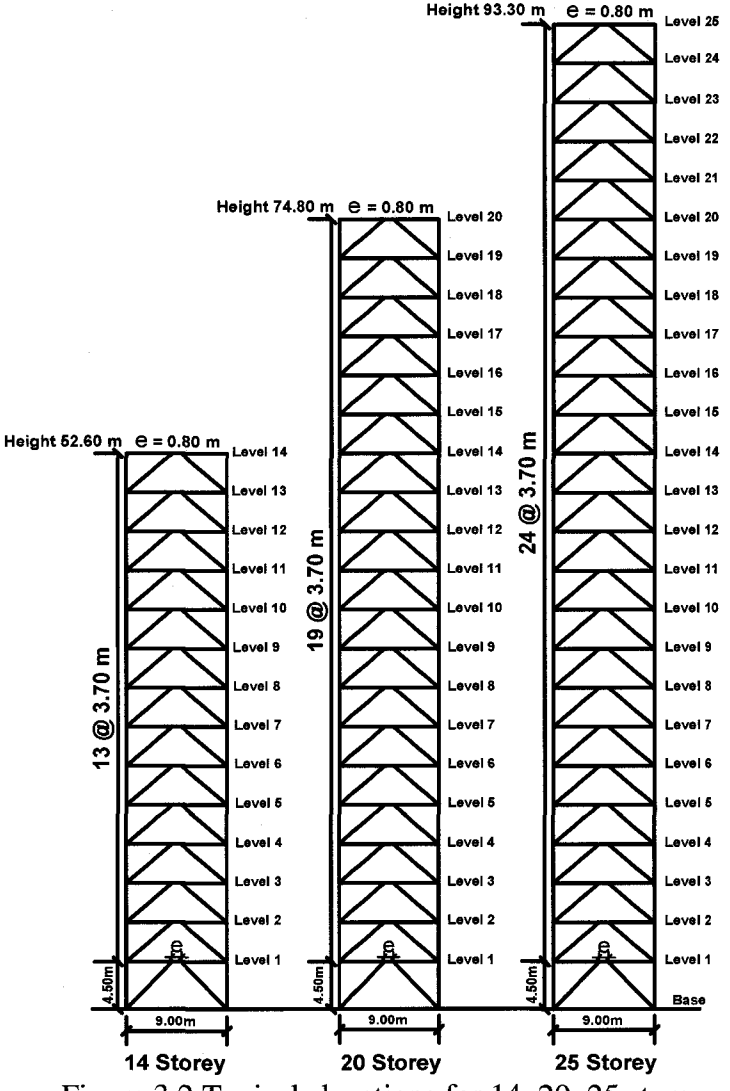

Figure 3.2 Typical elevations for 14, 20, 25 storey EBF

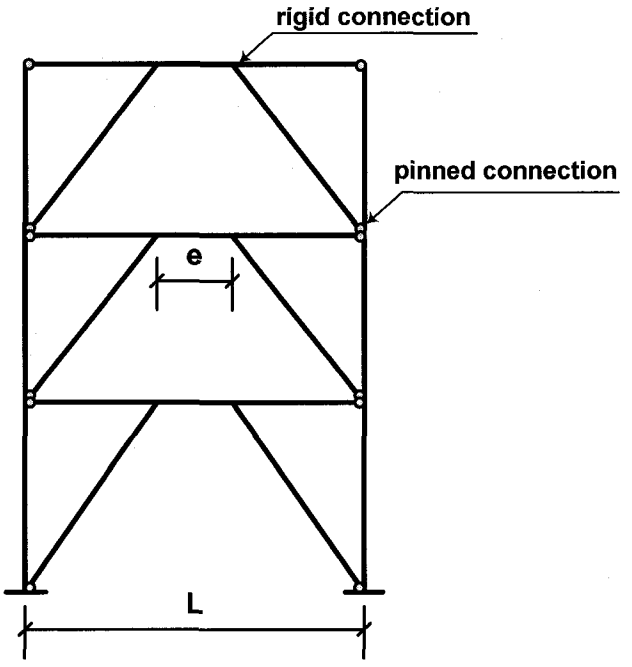

Figure 3.3 Members connections in the EBF model

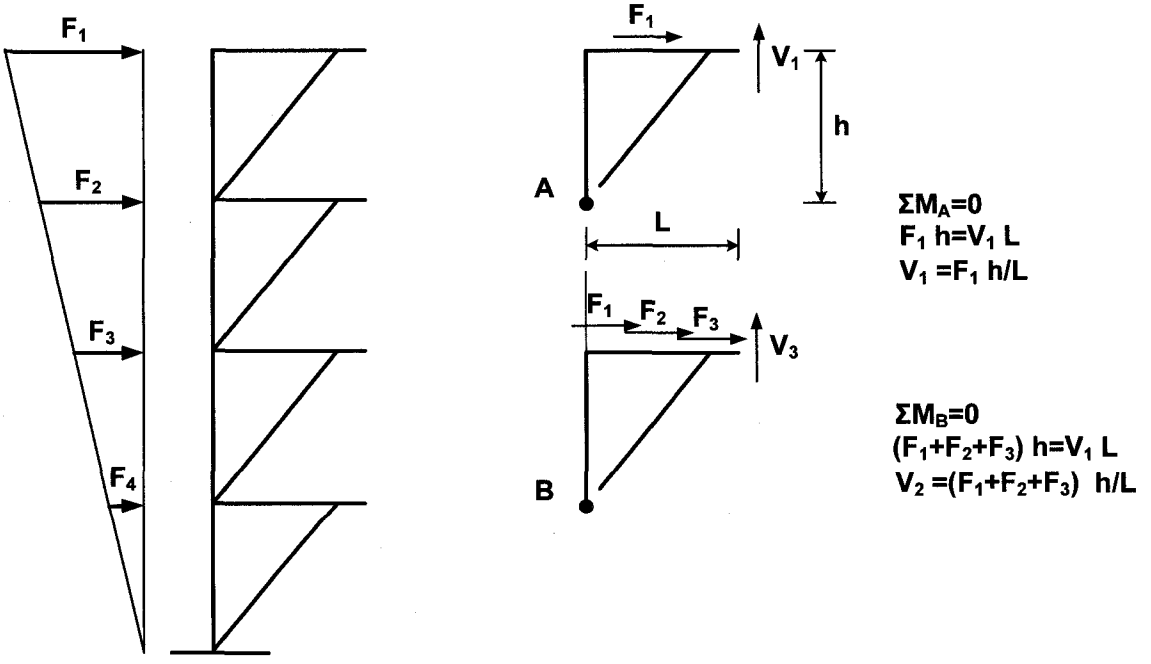

Figure 3.4 Simple static approach to obtain the link shear force

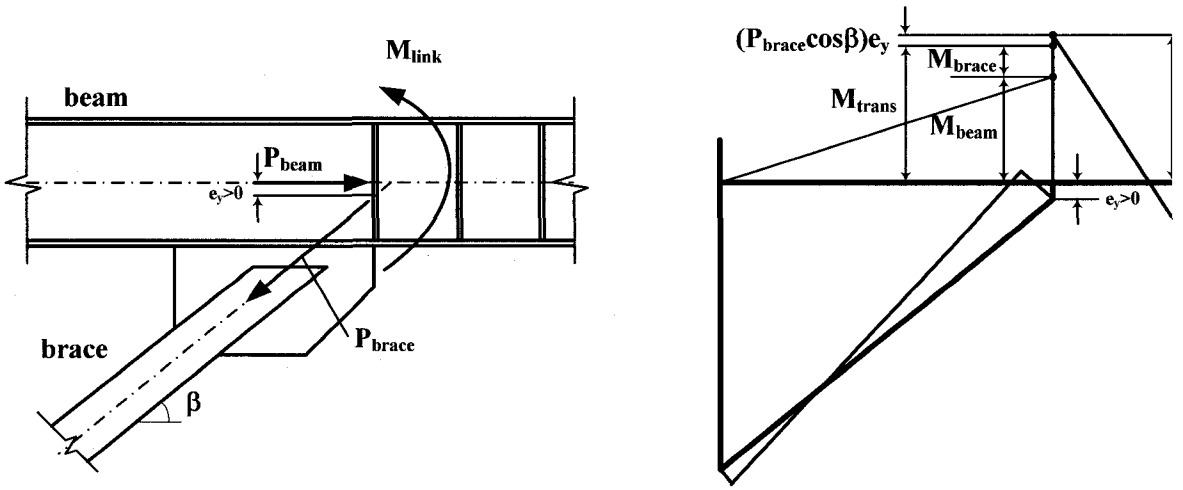

Figure 3.5 Distribution of link end moment between the brace and the outer beam segment

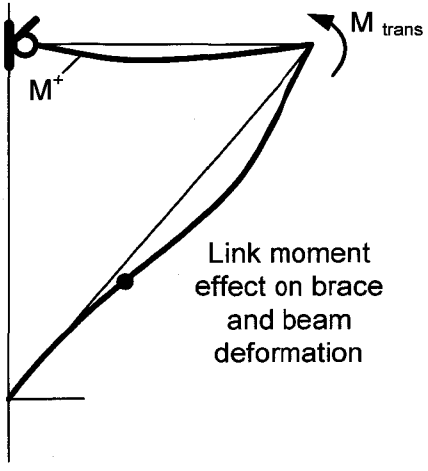

(a) All storeys with a fixed connection at lower end of brace

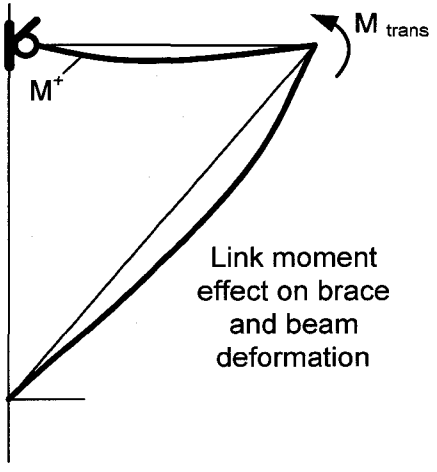

(b) All storeys with a pinned connection at lower end of brace

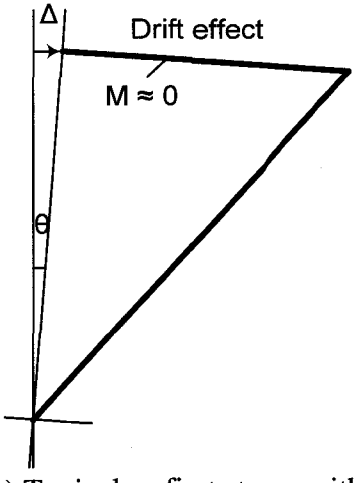

(c) Typical or first storey with a simple connection at lower end of brace

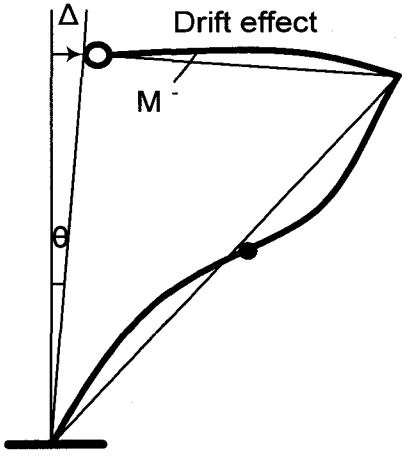

(d) 1st storey with a fixed connection at lower end of brace

Figure 3.6 Beam and brace moments with brace lower end conditions due to link moment (a), (b), and moment from drift (c), (d)

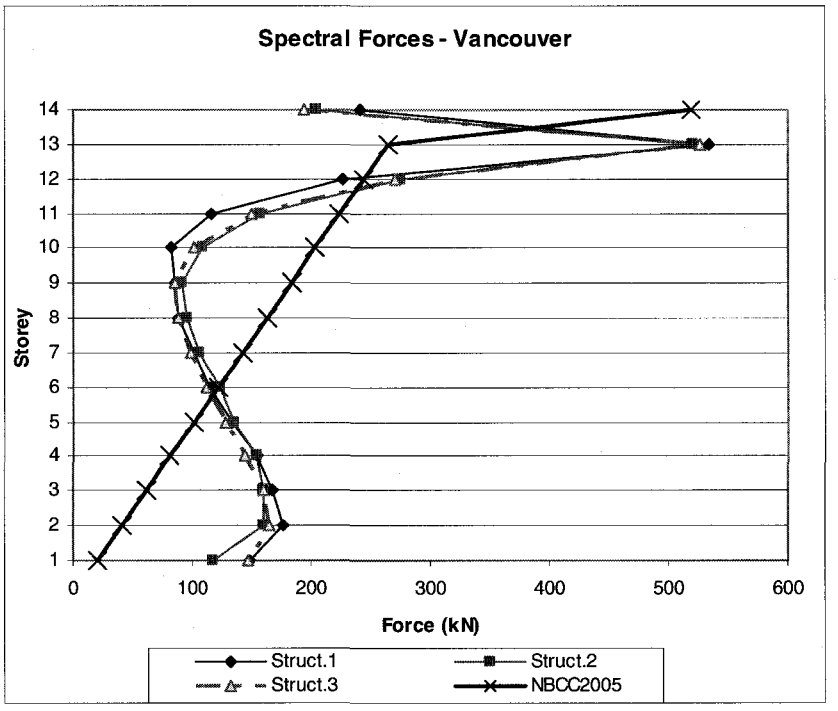

Figure 3.7 Seismic spectral force profile Vancouver

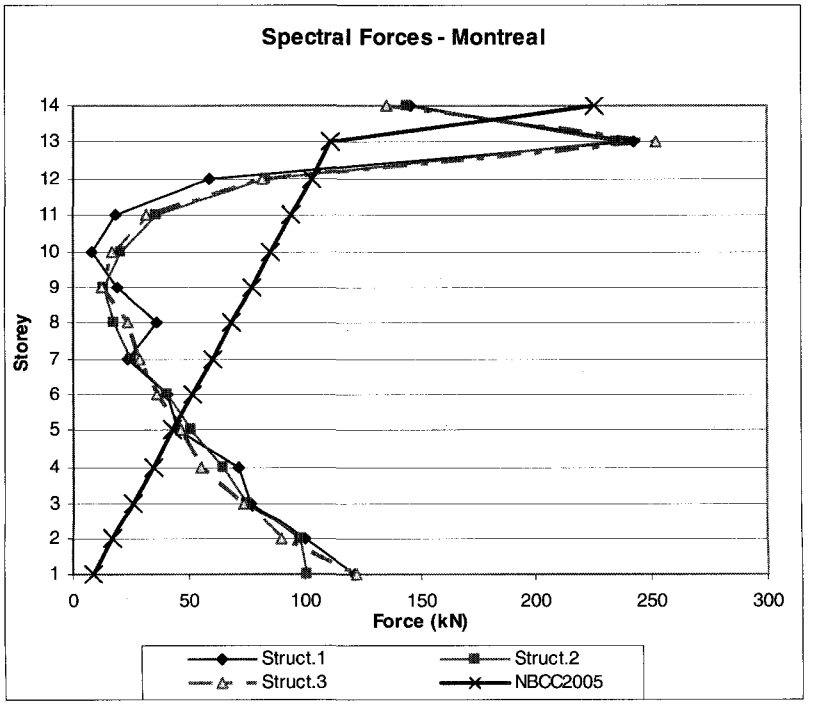

Figure 3.8 Seismic spectral force profile Montreal

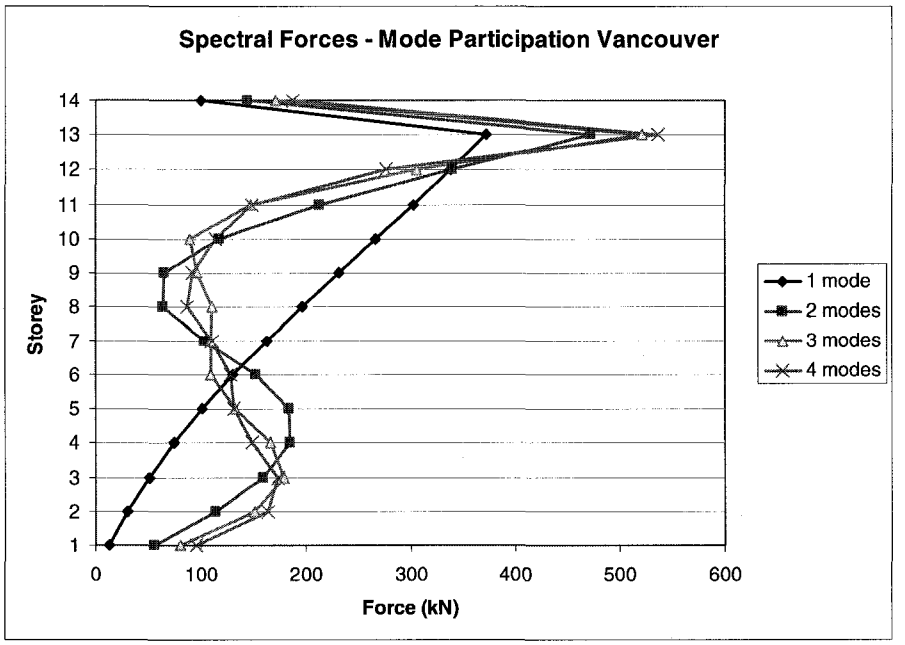

Figure 3.9 Contributions of higher modes to the seismic base shear (Vancouver)

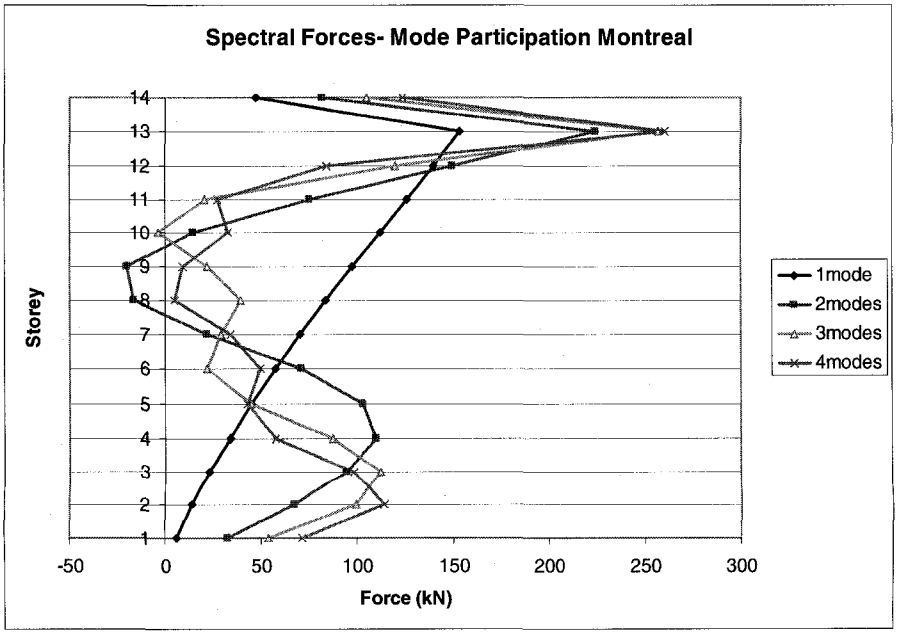

Figure 3.10 Contributions of higher modes to the seismic base shear (Montreal)

CHAPTER 4. CONSIDERATIONS FOR THE NONLINEAR DYNAMIC TIME HISTORY ANALYSIS

The first part of this chapter describes the methodology used to select the ground motions for the non-linear time history analyses. The elastic spectra of the historical and artificial records are computed and scaled to match the design acceleration spectra. The second part of the chapter presents a overview of the PC-ANSR1 computer program, followed by the details regarding the EBF modelization used in the present study. A description of the adopted and developed tools used for the post processing of the non-linear results concludes the chapter.

4.1 General considerations for the ground motions

NBCC 2005 requires the use of ground motion records for linear and non-linear time history analyses that are compatible with the median 2% in 50 year uniform hazard spectra (UHS), in order to represent the level of forces used in the design for the selected locations. Table 4.1 gives the 5% damped uniform hazard spectral ordinates for Vancouver and Montreal for firm ground conditions. It is considered that a ground motion is compatible with a given design spectrum if the response spectrum of the ground motion is in close match to the design spectrum for the period range of interest. The period range of interest should be established so that it contains all the periods of the modes that dominate the response of the studied buildings.

Different approaches can be used to obtain spectrum compatible ground motions. Historical records representative of design locations can be selected based, for instance, on the combination of magnitudes and epicentral distances that contribute most significantly to the seismic hazard of design location and then scaled to match design spectrum. Another approach could be to generate artificial records that are compatible

with the design spectra. The later approach is particularly interesting for the regions when there are no sufficient recordings of historical ground motions or when the available accelerograms do not correspond to the seismo-tectonic characteristics of the design location.

The first approach that uses the real records is appropriate when the ground motions correspond to the magnitude-distance (M-R) range and tectonic environment conditions at the site. The available earthquakes from North America, outside of California to meet these conditions are very few for either eastern or western Canada. Consequently, for the western Canada historical earthquakes from California region can be selected and scaled to correspond to the western Canadian conditions.

The use of California ground motions, according to Tremblay and Atkinson (2001), would be inappropriate due to the different site characteristics which affect the amplitude and frequency content of the accelerograms. Also for the eastern Canada there are no real ground motions available that can be used in the analyses because: the Californian ground motions are not compatible with the seismo-tectonic environment of the eastern Canada and the available eastern earthquakes (i.e. Saguenay earthquake) may be inappropriate to be used due to the high values of the low pass accelerograms filters, which cause the lost of the low frequency content. Thus, simulated artificial records were adopted as an alternative solution for the Montreal region. The advantage of these artificial records is that they represent the generalization of past events concerning the average amplitudes and frequency content as a function of magnitude and distance.

Recent studies (Naumoski N. 2006) investigated the effects of different types of seismic records on the structural response of medium-height buildings. It was found that artificial accelerograms compatible with the design spectrum, method described by Naumoski (2001) and real accelerations scaled to spectral area produce similar structural responses, but the simulated accelerograms using the method proposed by Atkinson and Beresnev

(1998) produce larger response results than the other records. Naumoski and al. (2006) also recommended the scaling of real accelerograms to spectral area as the preferred method to obtain spectrum-compatible accelerograms.

The elastic response spectra can offer relevant information on the amplitude and frequency content of each ground motion, and scaling based on the spectrum compatibility seems reasonable. However, the other characteristics of the earthquake records such as intensity, frequency, duration of strong motion, number of pulses, and the pulse intensity can have a great impact on the structural response, particularly in inelastic range. For these reasons, different characteristics of selected ground motions were closely examined in this study to justify the final record selection.

The ground motions were separated in short distance records (i.e. earthquakes recorded within a distance less than 50 km) and long distance records (i.e. earthquakes recorded from a distance longer than 50 km), to illustrate any possible differences in the motion characteristics and later in the response of the structures. The most appropriate way to highlight the characteristics of these earthquakes was to plot the response spectrum for each of them, in groups of short or long distance motions and compare their match with the NBCC spectrum.

4.1.1 Selection of the ground motion records and calculation of various parameters

For the purpose of this study, an ensemble of ten historical earthquake records was selected from PEER database for Vancouver plus an ensemble of ten artificial records from Atkinson's database. For Montreal only one sets of ten simulated ground motions were chosen, ground motions that were also taken from Atkinson's database. The scenario events, that make dominant contributions for the specified probability of exceedance of 2% in 50 years, are presented in Table 4.2 for the two locations. All the

ground motions are chosen to be representative of the site Class C conditions, with a characteristic shear wave velocity varying between 360 and 760 m/s.

The historical records are presented in Tables 4.3 and 4.5. These records were adopted from Lacerte (2005), with one revision for the earthquake number four from the group of short distance events. The initial selection of recorded ground motions for Vancouver is based on the combination of earthquake magnitude and epicentral distance, together with the site conditions corresponding to the conditions assumed in the design. The tables present the magnitude, the hypocentral distance, the peak horizontal acceleration (PHA), the peak horizontal velocity (PHV) of the original ground motions and the scaling factor S_f. The discussion regarding the scaling of the accelerations is enclosed in the section 4.1.2.

The parameters of a ground motion such as the PHA and a/v ratio can be related to the intensity of the event and are a good estimate for the initial selection of an event for certain location criteria match. The number of zero crossings and the predominant period of strong shaking are related to the frequency content of the motion. The lower number of zero crossings along with a longer period of strong shaking can have a higher impact on the response of the structure. It can also be the case for a ground motion with acceleration pulses. The characteristics for categorizing the strong shaking of an earthquake are the durations listed at number 6 to 10 in the following paragraph. These indices of duration also give information on the content and accumulation of the energy. For the reason that the mentioned parameters are sometimes difficult to match at an adequate tolerance, the closed match of the spectra to the UHS and a scaling factor close to 1.0 are also considered important selection criteria.

For the chosen records the elastic response spectra are plotted and the ground motion parameters are investigated to determine the suitability in the group ensemble. The indices to describe earthquake records were selected according to Christopoulos (1998)

and include the amplitude of the ground motion, the frequency content of the excitation and the duration and time of occurrence of maxima. To establish these indices several parameters were calculated:

1. PGA(g): Peak Ground Acceleration
2. Time of occurrence of the PGA (in seconds)
3. A/V ratio: the ratio of peak ground acceleration in units of g to peak ground velocity in m/s.
4. RMSA: Root Mean Square of acceleration: $a_{RMS} = \sqrt{\frac{1}{t_0}\int_0^{t_0}[a(t)]^2 \cdot dt}$, where a(t) is the acceleration and t_0 is the total duration of the accelerogram.
5. Arias intensity, Ia (Arias,1969): $I_a = \frac{\pi}{2g}\int_0^{t}[a(t)]^2 dt$, where a(t) is the acceleration and t is the total duration.
6. Bracketed duration: the time between the first and the last excursion of a specified level of acceleration (default is 5% of PGA).
7. Uniform duration: the total time during which the acceleration is larger than a given threshold value (default is 5% of PGA).
8. Hudser duration: the time necessary to accumulate 90% of the total energy (energy measured with the Arias Intensity).
9. Energy related duration: time necessary to attain 95% of the total energy. The energy is based on the Arias Intensity.
10. Trifunac-Brady duration (1975) or the significant duration: the time necessary to accumulate between 5 % and 95 % of the total energy (energy measured with the Aria's Intensity)
11. Number of zero crossings (NZC)
12. Predominant period: the ratio of the total duration to 2 times the number of zero crossings.

13. Spectral Intensity based on acceleration (ASI) the area under the pseudo-acceleration spectrum between periods of 0.1 s to 0.5 s for 5% of critical damping.
14. Spectral Intensity based on velocity (VSI): the area under the pseudo-velocity spectrum between periods of 0.1 s to 2.5 s for 5% of critical viscous damping.

The above mentioned indices and the elastic spectra were calculated using the program SeismoSignal (2007). The Tables 4.4 and 4.6 give the values of the calculated parameters for the short and long distance historical earthquakes for Vancouver respectively.

The simulated ground motions are adopted from Atkinson (1998)'s generated set of time histories and scaled using the "fine-tuning" factors recommended by the author. Trials from magnitude-distance combination different from the ones presented in Table 4.2 compose the ensembles of ground motions. Artificial records corresponding to magnitude-distance scenarios recommended by Atkinson were first selected, but to cover more broadly the contributions to seismic hazard at design location, other M-R combinations were included. It is believed that these combinations offer a better covering for the seismic hazard at the site locations. The characteristics of the two groups of artificial earthquakes for Vancouver and Montreal are presented in Tables 4.7 and 4.8.

The artificial ground motions are proposed for different combinations of M-R, where M is the earthquake magnitude and R is the epicentral distance, for different locations in Canada. The ten artificial motions chosen for Vancouver are in groups of two signals for each of the following M-R combinations: M=6.0 R=20km, M=6.5 R=30km, M=6.5 R=50km, M=7.2 R=30km and M=7.2 R=70km. Similar to the artificial motions for Vancouver, the ground motions for Montreal were selected in set of two from the following M-R combinations: M=6.0 R=30km, M=6.5 R=50km, M=7.0 R=50km, M=7.0 R=70km and M=7.0 R=100km.

4.1.2 Elastic spectra for the records

In the process of the scaling factor calculation for the ground excitations, the elastic spectrum of the earthquake is a key element to define the compatibility with the design spectrum. The final values of scaling parameters can greatly vary in function of the scaling method selected, which can have significant impact on the results, particularly inelastic displacements (Rozon 2009). The method used in this study to calculate the scaling factor for the historical records V11 to V20 is adopted from Rozon (2009). The method proposed combines the matching of the areas under the curves of the acceleration response spectrum of the motion and the NBCC response spectrum with the subjective selection of the range of periods for which this matching is done.

The ground motions were divided in two groups; the short distance accelerograms which are scaled to match the NBCC spectrum in the period range 0.2 s to 1.0 s and the long distance accelerograms which are calibrated for the period range 1.0 s to 2.5 s. For the selected period range, the area under the spectrum was calculated by numerical integration using the trapezoidal method between the two period integration bonds. The scaling factors obtained for short and long distance earthquakes are presented in Tables 4.3 and 4.5 respectively.

Figures 4.1 to 4.4 present the acceleration and velocity spectra of the scaled historical ground motions used for Vancouver calculated using a 5 % damping ratio. The figures containing the elastic spectra are differentiated by groups of records (i.e. short distance, long distance) and they also show the median spectra for each group of records, short or long distance records and the NBCC design spectrum for Vancouver. As it can be seen in Figures 4.1 for the short distance records scaled to the presented scaling factors (Table 4.3) have median spectra in close match with the NBCC spectrum for the period range 0.2 s to 1.0 s. Similar comment can be made for the long distance records, the calculated median spectra are in close match with the NBCC spectrum for the period range 1.0 s to 2.5 s.

The response spectrum of the ten scaled artificial records selected to be used for western Canada are presented in Figure 4.5. Figure 4.6 contains a comparison between the four groups of motions used for the Vancouver region: short distance historical, short distance artificial, long distance historical and long distance artificial. The four median spectra of each of these groups is presented together with the NBCC response spectrum. A close resemblance between the four spectra is observed for the period range 1.0 s to 2.5 s and higher acceleration values for the two groups of short distance records in the period range 0.2 s to 1.0 s. The median of the short distance historical records present a peak with 30 % higher than the NBCC spectrum for the period 0.2 s. Due to these differences it is possible that the Vancouver structures present some variations in the dynamic response and thus, it is considered necessary to distinguish between short and long distance records.

The acceleration spectra of the ten artificial motions that were chosen for eastern Canada are presented in Figure 4.7. The represented spectra were calculated for the scaled ground motions, where the scaling factors were presented in Table 4.8. All the ground motions show an adequate match with the design spectrum specific for Montreal, with no differences between short and long distance records.

4.2 Tools and the modeling assumptions for nonlinear time history dynamic analysis

4.2.1 Presentation of the program PC_ANSR1

The software used for the nonlinear structural analyses is a general purpose program named PC-ANSR1 developed at University of California, Berkeley by D.P.Mondkar and G.H.Powell (Mondkar and Powell 1975). Besides the nonlinear beam-column element which can be used to model the exterior beams, the braces and columns, the version of the program used in this study contains a special shear link element formulated by Ricles and Popov (1994). The shear link element from the program permits to appropriately

model inelastic behavior of shear links including the kinematic and isotropic strain hardening of the link.

The Newmark's method of constant average acceleration (β=0.25 and γ=0.50) was used to solve the integration of incremental equations of motion. The iterations to satisfy the equilibrium between two consecutive time steps were done using a constant stiffness method. A time step of 0.01 seconds or 0.005 seconds depending on the ground motion time step was used on the analyses.

4.2.2 EBF model for the nonlinear analyses

The EBF members were modeled using two types of elements available in PC-ANSR1: the shear link element and an inelastic beam-column element for the exterior beams, the braces and the columns. More details on the characteristics of the theoretical element types can be found in the section 2.1.3.

The material modeling accounts for combined kinematic and isotropic shear strain hardening as well as kinematic flexural strain hardening. The isotropic shear hardening is represented as the expansion of the yield surface as a function of the length of the plastic shear strain trajectory. The explicit function of the isotropic hardening (Ricles and Popov 1994) is expressed in function of the initial shear yield strength V_{y0}, ΔV_{max} the maximum shear yield strength after complete hardening and β a constant related to the expansion of the shear yield surface, determined from experimental data. The numerical values of these parameters were chosen to be the average value determined from the experimental results (Ricles and Popov 1994) and they are $2.68V_p$ for ΔV_{max} and 8.336 for β.

The two-dimensional beam-column element used to model the other members of the frame considers moment-axial force interaction and accounts for inelastic flexural deformation without considering the buckling. The stiffness properties of each element

are defined considering the effective dimensions of the sections and a strain hardening of 2 percent of the elastic stiffness. In the analysis it is assumed that the beams outside the link were modeled as inelastic elements, as long as the stability of the member is assured. This approach was adopted since the outside beam is less probable to remain elastic due to the high forces transmitted from yielding links.

The yielding values of the EBF members were calculated considering the provisions of CAN/CSA S16-05 discussed in section 2.2.2. Thus the first yielding level of the link was calculated considering a minimum yield stress equal to R_yF_y, and the following yielding levels as they were presented in Figure 2.5. The beam outside of link yielding value was the factored resistance multiplied by R_y/ϕ and for the braces and columns their flexural and compressive capacities were calculated using the factored resistances. A scale factor of 10 was assigned to the braces and columns in order to assure their elastic comportment during the analysis.

The frame was modeled considering the degree of freedom and connectivity conditions assumed in the initial design and described in section 3.2.1. The member also considers the reduction of their length due to the rigid offsets as: the gussets plates from the beam-brace connection and the eccentricities between the column centerline and the pin connection with the beam. In the analysis the axial deformations of the link segment were restrained and thus the link rotations presented herein exclude the elastic component coming from the axial link deformation.

The ANSR1 program does not feature the option to specify uniformly distributed loads as gravity loads on the beam-column element. Consequently, the gravity effects were taken into account on the columns by calculating and applying the total concentrated load at every storey. For the beams and braces initial forces resulting from these actions were applied as bending moments on the beams at the connection with the brace and as axial force on the braces. The initial member forces contribute to the beginning of plastic

action and geometric stiffness. For the modal analyses calculations, the mass of the building associated to one EBF was calculated from the total weight W and assigned as lumped at the nodes of the columns.

The damping coefficients for the elements of the EBF were calculated based on the natural periods of the elastic structure. For this EBF model a form of non-proportional damping is used in which a global mass-proportional damping is assigned to all members and the stiffness-proportional damping only for the beams, braces and columns. It was found from previous analytical studies (Ricles and Popov 1994) that assigning viscous damping to the links lead to development of larger axial forces in braces and columns due to unrealistic ultimate link forces. The damping coefficients are calculated using a 3 percent of critical damping for the first and third vibration modes.

The P-Δ effects were accounted in the nonlinear analyses by adding an adjacent column to the EBF structure. The column has no rigidity on bending and the nodes are slaved to the nodes of the EBF columns. The gravity axial loads representing the tributary loads for half of the building are assigned at the nodes of the columns.

4.3 Post-analysis processes

Several post-processing programs were used to extract the response parameters of interest obtained by nonlinear time-history analysis. Some of these programs were adopted from Koboevic (Koboevic 2000) and modified to comply with the current design provisions. Other programs were developed within the scope of the present project. All the programs were written in FORTRAN (Lahey/Fujitsu 2007).

The programs adapted from Koboevic were used to:

- Verify the strength and stability of the members of the frame other than links for each time step under the forces induced by the earthquake loads. This

verification was done for the members modeled to respond elastically to seismic excitation.

- Extract the maximum lateral forces acting on the EBF and their time of occurrence.
- Calculate the maximum total inter-storey drifts from the displacements output files.

Other similar programs were developed by the author to extract the following response parameters:

- The maximum positive and negative inelastic link rotations at their time of occurrence.
- The maximum positive and negative ultimate shear forces developed in the links.
- The maximum values of the accumulated inelastic rotations developed in the outside beams.
- The number of inelastic incursions in the braces and columns and the total time when these members were in the post yielding stage.

The programs were conceived to permit their usage for different time steps of data output and a different number of storeys for the frame.

4.4 Summary

This chapter presented the selection of the ground motions to be used in the following nonlinear dynamic analyses. Ten historical and ten artificial ground motions were selected for Vancouver and only ten artificial motions for Montreal due to the lack of historical available earthquakes for the east Canada. The ground motions were chosen to correspond to the magnitude-distance (M-R) range and tectonic environment conditions at the site and they were scaled such that their elastic spectra match the NBCC design spectrum. The spectra of different groups of motions was plotted and compared and it was concluded that distinguished structural dynamic responses could appear especially between the long and short distance records.

The second part of the chapter describes the program ANSR-1, which was selected to carry out the nonlinear analyses. The main parameters of the program were discussed together with the type of elements used in the modelization of the EBF. The distinguish characteristic of the EBF model was that the beams were modeled as inelastic elements versus the braces and columns which were modeled as elastic elements. The chapter concludes with the description of the tools for the post-processing analysis and their features.

Table 4.1 Uniform hazard spectral ordinates, S_a (g) for the design sites

Period (s)	Vancouver (crustal earthquake)	Montreal (crustal earthquake)
0.0	0.94	0.69
0.2	0.94	0.69
0.5	0.64	0.34
1.0	0.33	0.14
2.0	0.17	0.048
4.0	0.085	0.024

Table 4.2 Scenario events for the selection of compatible time histories

Location	City	Magnitude (M)	Hypocentral distance (km)
Eastern Canada	Short period event Montreal	6.0	30
	Long period event Montreal	7.0	70
Western Canada	Short period event Vancouver	6.5	30
	Long period event Vancouver	7.2	70

Table 4.3 Characteristics of short distance historical earthquakes

No	Event	Magn.	R (km)	Station	deg	PHA(g)	PHV(m/s)	Sf
V11	Jan. 17, 1994 Northridge	Mw 6.7	44	Castaic, Old Ridge Rd	90	0.568	0.518	**0.60**
V12	Jan. 17, 1994 Northridge	Mw 6.7	30	Santa Monica City Hall	360	0.369	0.251	**1.21**
V13	Jan. 17, 1994 Northridge	Mw 6.7	34	Los Angeles Baldwin Hills	360	0.167	0.176	**2.00**
V14	Apr.24,1984 Morgan Hill	Mw 6.2	37	Gilroy Array #4, San Ysidro School	270	0.224	0.193	**1.63**
V15	Jan. 17, 1994 Northridge	Mw 6.7	26	Pacific Palisades-Sunset	280	0.197	0.149	**2.55**

Table 4.4 Ground motion parameters of short distance historical earthquakes

No	PGA (g)	Time of PGA (s)	a/v	RMSA (g)	Arias Intensity (m/s)	Braketed duration (s)	Uniform duration (s)	Hudser duration (s)	Energy related duration (s)	Trifunac -Brady duration (s)	Number of zero crossing	Predominant period	ASI (g*s)	VSI (m)
V11	0.568	8.16	1.10	0.094	2.727	18.78	10.84	11.88	13.60	8.16	219	0.091	0.524	2.124
V12	0.369	9.90	1.47	0.0437	1.178	30.94	12.54	15.00	16.16	10.72	344	0.058	0.271	1.263
V13	0.167	10.56	0.95	0.0316	0.615	37.50	22.40	17.98	23.02	17.43	287	0.070	0.182	0.752
V14	0.224	3.95	1.16	0.0340	0.713	34.68	16.39	14.66	15.74	13.22	197	0.101	0.232	0.782
V15	0.197	10.73	1.32	0.0410	0.646	22.63	15.28	12.50	14.86	10.45	233	0.054	0.205	0.604

Table 4.5 Characteristics of long distance historical earthquakes

No	Event	Magn.	R (km)	Station	deg	PHA(g)	PHV(m/s)	Sf
V16	Apr. 25, 1992 Cape Mendocino	MW 7.0	52	Eureka - Myrtle & West	90	0.178	0.283	**1.13**
V17	Oct. 18, 1989 Loma Prieta	MW 7.0	54	Stanford Univ.	360	0.287	0.280	**1.27**
V18	Oct. 18, 1989 Loma Prieta	MW 7.0	100	Presidio	90	0.200	0.340	**1.55**
V19	Apr. 13, 1949 West.Wash.	MW 7.1	76	Olympia, Test Lab	86	0.280	0.170	**1.45**
V20	June 28, 1992 Landers	MW 7.3	93	Barstow	90	0.135	0.258	**1.89**

Table 4.6 Ground motion parameters of long distance historical earthquakes

No	PGA (g)	Time of PGA (s)	a/v	RMSA (g)	Arias Intensity (m/s)	Braketed duration (s)	Uniform duration (s)	Hudser duration (s)	Energy related duration (s)	Trifunac-Brady duration (s)	Number of zero crossing	Predominant period	ASI (g*s)	VSI (m)
V16	0.178	10.48	0.63	0.022	0.331	37.94	20.54	25.26	28.06	19.84	188	0.117	0.1298	0.949
V17	0.287	9.78	1.03	0.045	0.930	26.55	14.07	14.24	18.16	10.86	265	0.057	0.2733	1.191
V18	0.2	12.05	0.59	0.0238	0.262	27.04	9.73	14.74	17.83	8.25	244	0.061	0.1630	0.978
V19	0.28	19.62	1.65	0.0286	1.126	49.46	21.96	19.80	22.40	18.08	517	0.086	0.228	0.863
V20	0.135	16.08	0.52	0.0188	0.218	35.32	20.36	28.86	31.12	18.18	323	0.062	0.0858	0.575

Table 4.7 Characteristics of artificial earthquakes Vancouver

No	Event	Magn.	R (km)	PHA(g)	PHV(m/s)	Sf
W61	W60201	6.0	20	0.167	0.198	**2.0**
W62	W60202	6.0	20	0.203	0.338	**2.0**
W63	W65301	6.5	30	0.534	0.566	**1.0**
W64	W65302	6.5	30	0.537	0.613	**1.0**
W65	W65501	6.5	50	0.259	0.283	**1.1**
W66	W65502	6.5	50	0.279	0.309	**1.1**
W77	W72301	7.2	30	0.936	0.132	**0.5**
W78	W72302	7.2	30	0.649	0.084	**0.5**
W79	W72701	7.2	70	0.246	0.300	**1.0**
W70	W72702	7.2	70	0.259	0.240	**1.0**

Table 4.8 Characteristics of artificial earthquakes Montreal

No	Event	Magn.	R (km)	PHA(g)	PHV(m/s)	Sf
E61	E60301	6.0	30	0.43	0.171	**0.85**
E62	E60302	6.0	30	0.522	0.151	**0.85**
E63	E65501	6.5	50	0.409	0.164	**0.90**
E64	E65502	6.5	50	0.377	0.150	**0.90**
E71	E70501	7.0	50	0.509	0.195	**0.60**
E72	E70502	7.0	50	0.632	0.290	**0.60**
E73	E70701	7.0	70	0.301	0.149	**0.90**
E74	E70702	7.0	70	0.285	0.156	**0.90**
E75	E701001	7.0	100	0.243	0.150	**1.00**
E76	E701002	7.0	100	0.261	0.207	**1.00**

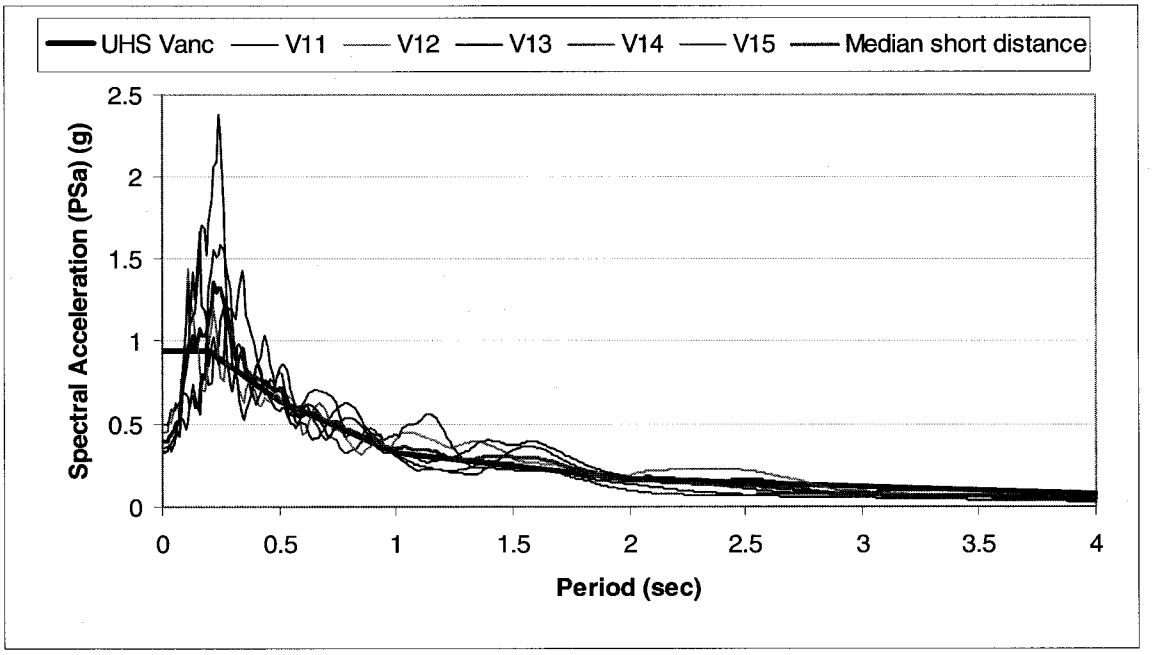

Figure 4.1 Scaled acceleration spectra for historical short distance records Vancouver

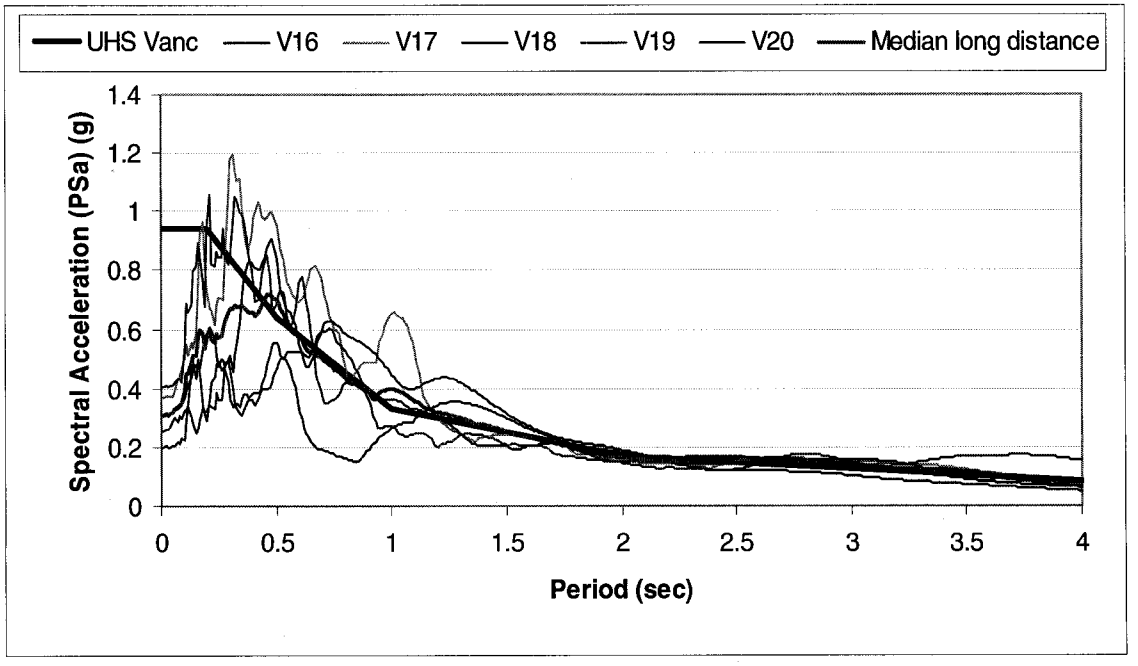

Figure 4.2 Scaled acceleration spectra for historical long distance records Vancouver

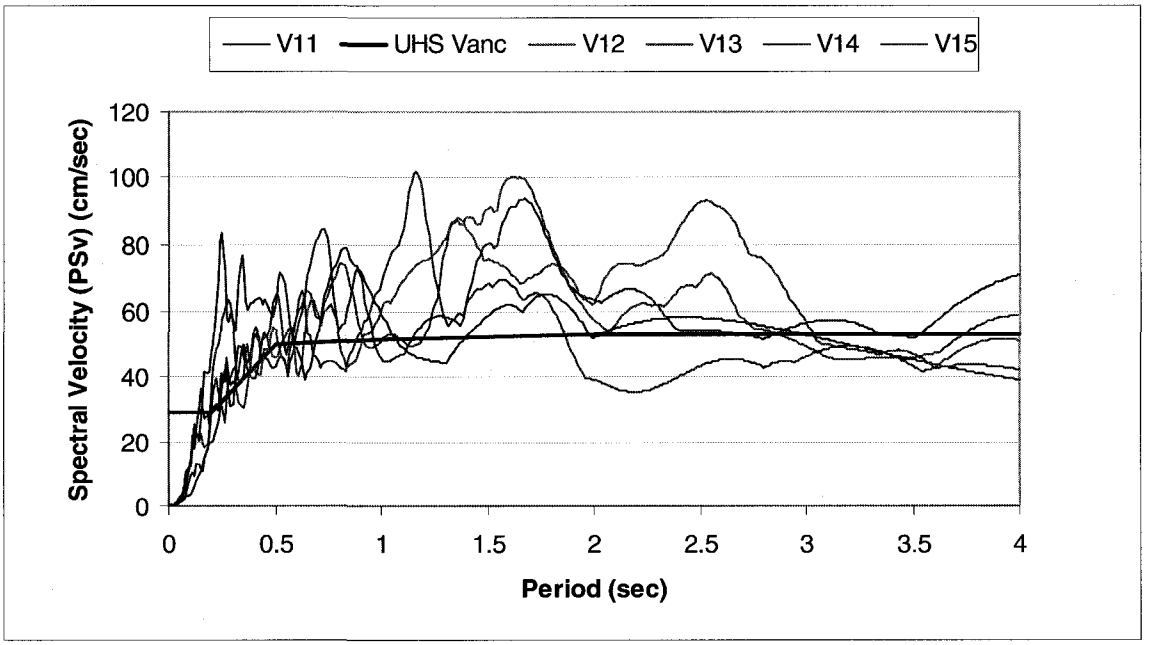

Figure 4.3 Scaled velocity spectra for historical short distance records

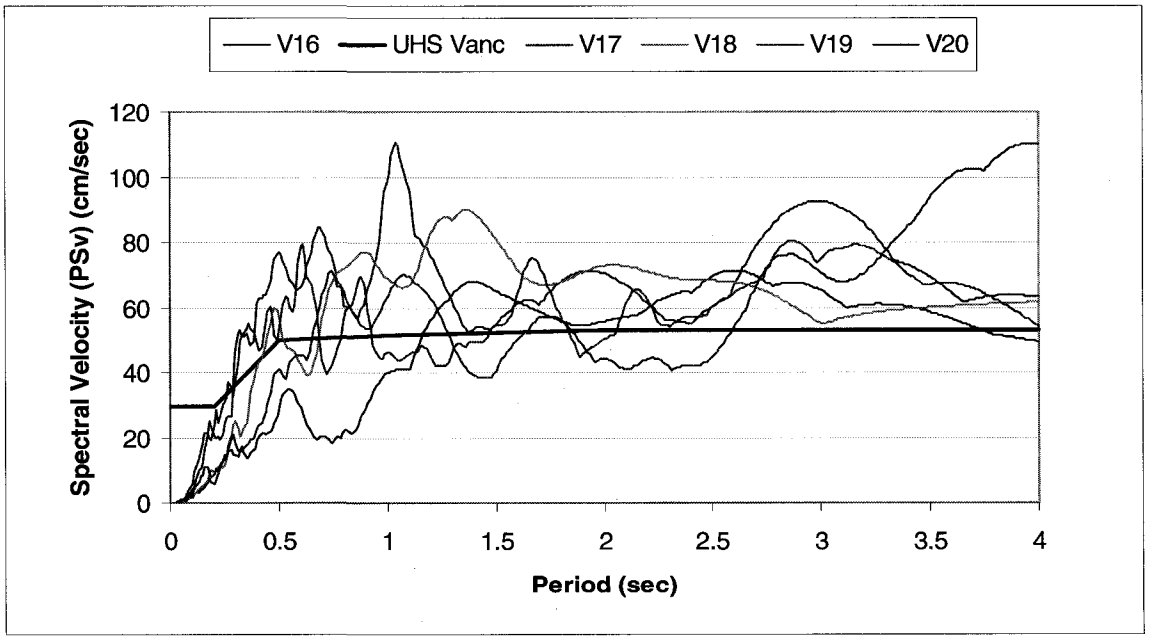

Figure 4.4 Scaled velocity spectra for historical long distance records Vancouver

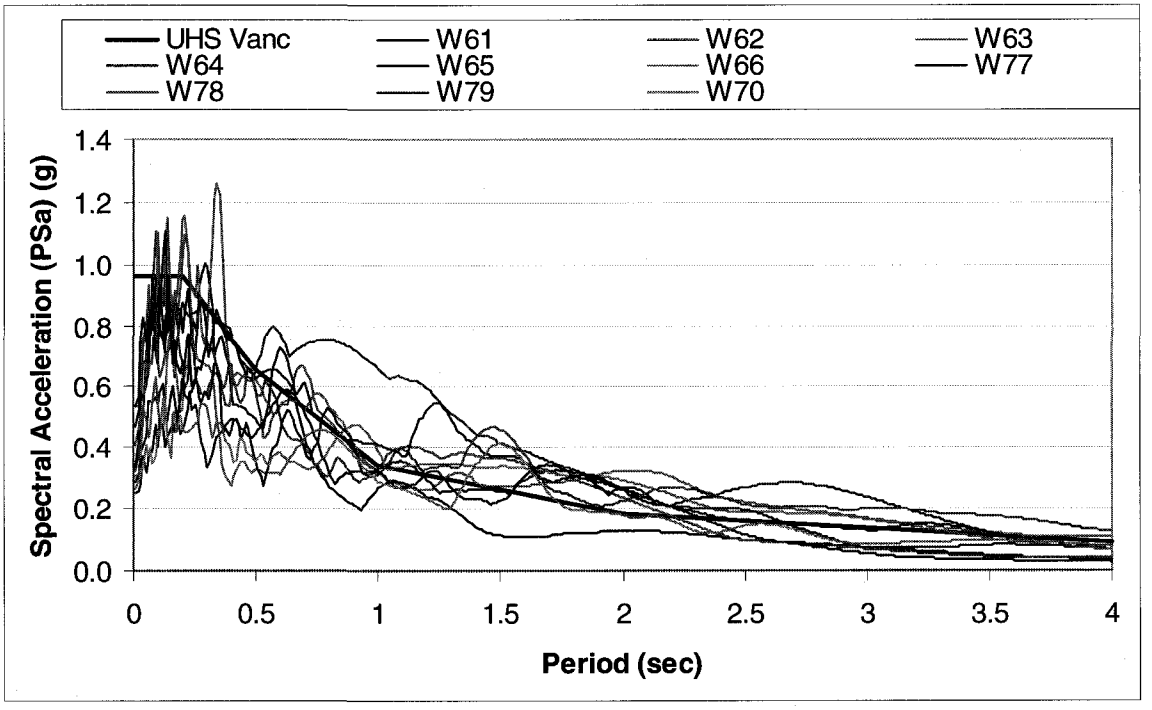

Figure 4.5 Scaled acceleration spectra for artificial records Vancouver

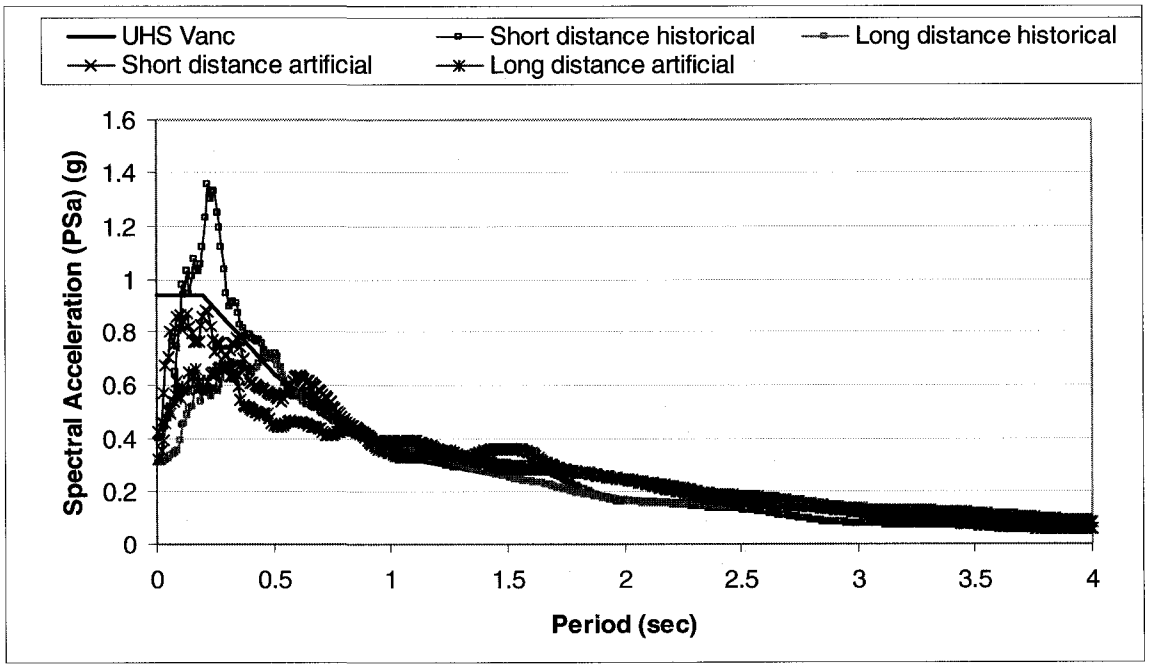

Figure 4.6 Comparison of median acceleration spectra for record groups Vancouver

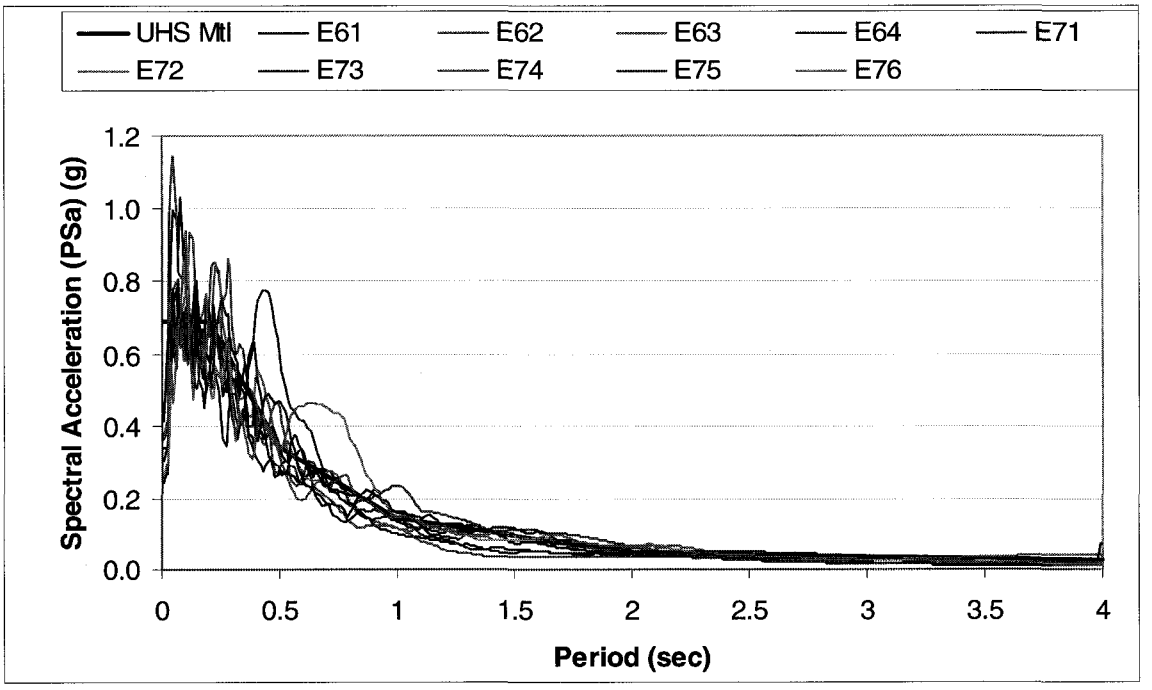

Figure 4.7 Scaled acceleration spectra for artificial records Montreal

CHAPTER 5. RESULTS OF THE NLTHA AND THE DISCUSSION OF THE EBF's SEISMIC BEHAVIOUR

The results of the nonlinear dynamic time history analyses are discussed in this chapter. The dynamic analyses were performed using the ground motions described in Chapter 4. The link performance is examined first in terms of normalized maximum shear force and maximum inelastic rotations. The behavior of the other frame members is analyzed with the tools described in Chapter 4 and the adequacy of the Standard S16S01-05 provisions is discussed. The global EBF response is examined through total inter-storey drifts and the seismic force profile on the frame. The relation between the inelastic link rotation and total inter-storey drift is studied and compared to the code method of estimating the link rotations. The results obtained in this study are presented in the form of the 50^{th} and the 84^{th} percentile of the values of the response parameters obtained, for a set of ground motions. The 50^{th} percentile values correspond to the demand imposed by the NBCC 2005 design spectra, and thus to the scaled ground motions. However the variability introduced by the peaks of individual ground motions is better illustrated by means of the 84^{th} percentile from the results.

5.1 Response of the links

To quantify the inelastic behavior of links two response parameters were investigated, the inelastic shear rotation of the link and the maximum normalized link shear force. The link inelastic rotation is an important response parameter since it is directly related to the ductility of the frame. In the current standard the inelastic rotation of the link is limited to 0.08 radians for the short links that yield in shear. The maximum inelastic rotations were examined for each structure in groups of ground motions at short distance versus ground motions at long distance, or the historical versus the artificial set.

It is likely that the maximum inelastic link rotation in a particular storey exhibits an extreme rotation in the positive or negative direction only, while in the other direction the value of the rotation is insignificant. Thus it is interesting to calculate the range of inelastic shear rotation or gamma range $\gamma_{range} = (|\gamma^{+}|+|\gamma^{-}|)$.

The maximum normalized link shear force is obtained by dividing the maximum shear force from NLTHA with the probable strength of the link value, where the probable shear resistance is equal to V_pR_y. The probable shear resistance was chosen as the norm to facilitate the study for coefficients of the forces transmitted from the links to the other members of the frame. Currently, these coefficients are 1.30 for exterior beams and braces and 1.30 for top tier columns and 1.15 to rest of the columns.

5.1.1 Fourteen storey structure

The maximum values of the inelastic link rotations are presented in Table 5.1 for Vancouver and Table 5.2 for Montreal. The results for Vancouver were arranged in groups of historical or artificial ground motions and differentiated by short or long distance motions. The division in groups was done to study the possible differences or to highlight the impact that a specific group of earthquakes can have on the global response. In the Figures 5.1 and 5.2 the graphic representation of the inelastic link rotations for the ensemble of all 20 ground motions is compared to the code limit. Analyzing these data the following observations can be made:

a) The maximum link rotations γ_{max} for the structure situated in Vancouver exceeded the design value in the upper storeys of the frame. The median values γ_{max} went beyond the code limit in the 12^{th} and 13^{th} storey, and the 84th percentile of the maximum inelastic rotation were almost double the code limit in top five storeys of the frame. In the lower half of the frame the values of the maximum link rotations were below the code limit 0.08 radians. For the frame located in Montreal both the 50th and 84th percentile of the inelastic

link rotations were below the maximum design values reaching about a third of the code limit 0.03radians. For Montreal the difference between the 50th and 84th percentile values was very small, but the structures exhibit the same tendency as the ones from Vancouver: higher link rotations in the upper storeys.

b) Comparing the values of the γ_{max} for different groups of ground motion (Table 5.1) larger inelastic rotations are observed for the 84th percentile in the group of short distance events for both historical and artificial records compared to the groups of long distance records. In reverse, the median values show no particular trends for any group of ground motions.

c) The increase of the inelastic rotations is noticed at the first storeys of the structure, with the 84th percentile values superior to 0.08 radians.

The maximum range of inelastic rotations as can be seen from Table 5.7, for Vancouver, have similar values for all subsets of ground motions, with slightly higher values observed for the historical events at short distance. Considering the results for the ensemble of the twenty accelerograms, the maximum range of link inelastic shear rotations have median values below the limit (0.16 radians = 2 x 0.08 radians) and 84th percentile have values around 0.16 radians only for the upper storeys. For Montreal (Table 5.8) the maximum relative link rotations have values much lower than the limit and the maximum values observed at the top storeys are four times smaller than the limit.

Tables C.1 and C.2, from Appendix C, present the results for the maximum normalized link shear force for Vancouver and Montreal, respectively. A close resemblance can be observed between the numerical values obtained for different groups of ground motions, the maximum differences for both the 50th and the 84th percentiles being about 10 percent. The Figure 5.3 presents the distribution of the 50th and the 84th percentiles of the link overstrength calculated from the data of all twenty events for Vancouver compared to the value of 1.3, the amplification force factor of the link as specified in the

Standard CSA S16S01-05. The maximum link shear forces follow the same tendency as the inelastic rotations, with higher values observed in the top five storeys. Here the median value of the link overstrength is 1.5, which corresponds to higher values observed in the experimental tests (Okazaki et al. 2005) for the short links. Figure 5.4 presents the link overstrength factors for the structure situated in Montreal. For this structure only in the top two storeys the amplification factor of 1.3 defined in S16S01-05 was attained. The links in the middle of the frame exhibit much less yielding and some don't even exhibit any inelastic behavior.

5.1.2 Twenty storey structure

The results obtained for the inelastic link rotations for Vancouver and Montreal are summarized in Tables 5.3 and 5.4. Figures 5.1 and 5.2 show the graphical representation of the 50th and 84th percentile for the ensemble of the twenty ground motions. The following observations can be made:

a) For the structure situated in Vancouver the median values of the maximum inelastic rotations are below the code limit for all the links, but the 84^{th} percentile value attains a maximum of 0.108 radians in the 15^{th} storey. For Montreal the median of the inelastic rotations is around 0.02 radians for the top storeys, with 84^{th} percentile that reach a maximum rotation of 0.073 radians in the 18^{th} storey. The rest of the storeys for the Montreal's structure have link rotations of 0.003 radians, which is far below the code limit.

b) While the median maximum link rotation is similar for all the groups of ground motions, the 84^{th} percentile have superior values introduced by the artificial events as it can be observed on the results of the structure located in Vancouver.

c) Previously, on the 14 storey structure Montreal and Vancouver it was observed that high inelastic rotations accumulate at the base of the frame. Similarly to the results obtained for 14 storey frame, the bottom storey links of 20 storey frames developed larger rotations at the base of the structure. For Vancouver structure the

base link rotations are higher compared to 14 storey frame, with a 50th percentile reaching 0.074 radians and 84th percentile 0.10 radians.

The ranges of the link rotations of the 20 storey structures have values inferior to the maximum permissible value of 0.16 radians. The data presented in Tables 5.9 and Table 5.10 show that the 84th percentile has maximum values of 0.12 radians in the upper storeys and 0.11 radians at the base of the frame for the Vancouver's structure, while for Montreal the 84th percentile have a maximum of 0.09 radians only in the upper storeys. As previously noted, the inelastic link activity for the structure situated in Montreal is minor compared to the links ductile behavior observed in the Vancouver structure.

The maximum normalized link force presented in Table C.3 for the links in 20 storeys Vancouver has values that are higher compared to the factor specified in the standard CSA S16-05 in six storeys in the upper half of the frame. The 50th percentile of normalized link force has values around 1.2 in the majority of the storeys, with greater values at the top that reach a maximum of 1.47 in the 17th storey. The distribution of 84th percentile follows the same tendency as the median with a general increase of 10%. As can be seen from the Table C.4, for the structure located in Montreal, the majority of the links present low levels of yielding and only the links from the top of the frame developed strain hardening with maximum values of 1.3.

5.1.3 Twenty-five storey structure

The inelastic link rotations, the relative link rotations and the overstrength factors for the two structures having 25 storeys exhibit the same tendencies as the structures with 20 storeys. The results obtained for the maximum inelastic rotations are presented in Tables 5.5 and Table 5.6 for Vancouver and Montreal respectively, while the Figures 5.1 and 5.2 show the 50th percentile and 84th percentile values calculated for the ensemble of the records. The following observations can be made:

a) The median of the link rotations for the Vancouver structure has maximum values of 0.05 radians in the upper storeys and around 0.015 radians for the other links from the frame. The 84th percentile of the inelastic rotations are close to the median values except for the top storeys, where the values are more than double the median values, reaching 0.12 radians. The link rotations for the Montreal's structure present very small deformations, except for the top storey, where the median values are 0.025 radians and the 84th percentile are 0.047 radians.
b) The maximum link inelastic rotations have similar values regardless the group of ground motions.
c) The increase of the inelastic link rotations, observed at the base of the frame, are less pronounced for the 25 storey structure located in Vancouver than in the case of the 20 storey structure presented before.

The relative link rotations for the 25 storey Vancouver are presented in Table 5.11 and for the 25 storey structure located in Montreal the values are shown in Table 5.12. The relative link rotations for all the storeys in the 25 storey structure located in Vancouver have values below the allowable relative rotation. The maximum of the 84th percentile is observed in storey 22 and it is equal to 0.133 radians. For Montreal the relative rotations are less than the rotations found in the Vancouver's case. The 84th percentile has maximum value in storey 23 and this is equal to 0.052 radians.

The maximum normalized link forces are presented in Table C.5 for Vancouver and in Table C.6 for Montreal. The 50th percentile and the 84th percentile, for the structure situated in Vancouver, of the link normalized forces have values less than 1.3 in the lower half of the frame. Similar to the previous presented structures the upper links develop higher forces reaching the value of 1.5, link normalized force. For Montreal the links do not develop the expected overstrength, with the exception of the top storeys where a maximum 84th percentile of 1.36 link normalized force is observed.

5.2 The response of other frame members

The behavior of the outer beam segments, the braces and the columns was monitored through the following two parameters: maximum value of axial force - bending moment interaction and the extent of overloading in the member. The later parameter was expressed through the number of inelastic excursions and the amount of inelastic rotations developed. Note that the beams outside the link segment were modeled to allow the inelastic behavior, but the braces and columns were considered to remain elastic during the entire motion. Thus for the beams the maximum accumulated rotation values can be examined and for the braces and columns the value of the interaction axial force-bending moment and the number of inelastic incursions and duration of the inelastic behavior.

A special attention was given to the columns axial forces and moments to verify the exactitude of the Standard S16S01-05 simplification in estimating the bending moments that are expected to develop.

5.2.1 Outer beam response

The segments of the beams outside the link were considered to have a nonlinear behavior with the yield point at R_yV_p. Thus the beams can develop plastic rotations at end where is the rigid connection with the link segment and the brace. This inelastic behavior of the exterior beams can be evaluated through the amount of maximum inelastic rotations accumulated. The ductility capacity of the exterior beams could be assessed by the analogy with the long links from eccentrically braced frames or with beams from moment resisting frames. The long links that yield essentially in flexure have the current code limitation of 0.02 radians and the beams of the MD type moment resisting frames are allowed to develop rotations of 0.03 radians.

The accumulated inelastic beam rotations observed in the 14 storey frame located in Vancouver are presented in Appendix C, Tables C.7 and C.8. In general, the yielding of the beams for this structure was observed infrequently, and if so, only the beams in two to six storeys were involved. The results summarized separately for the historical and artificial records are, in average, below the value of 0.02 radians and the yielding is concentrated in the beams in the lower half of the structure. Among historical events, the earthquake V20 imposes a greater demand on the exterior beams reaching the maximum rotation of 0.0311 radians in the 7^{th} storey. Among the artificial records, the earthquake W64 produces a maximum rotation of similar value (0.00345 rad) in the 4^{th} storey. It was also observed the occurrence of inelastic rotation in exterior beam did not coincide with the occurrence of the highest link rotations.

The 20 and 25 storey frames in Vancouver as well as the three frames in Montreal did not exhibit any yielding of the exterior beams. The combination of the bending moment transferred from the link and the corresponding axial force were low enough to exclude the plastic hinge formation in the beam.

The results obtained indicate that the yielding of outer beam segments was indeed limited. In view of these results and recognizing the beneficial effect that the acceptance of outer beam yielding has on design, the inclusion of the inelastic behavior of these elements in design process can be justified.

5.2.2 Brace response

An elastic and stable response of braces is important in order to maintain the global stability of an EBF. In the analytical model used in this study, the braces were represented by the elastic elements. In order to validate if the design procedures achieved desired brace response, the elastic demand imposed on braces was verified at each time step of loading history. Also, for a pair of braces at each storey, the number and the

duration of inelastic excursions for a given ground motion was counted using the Fortran programs developed. The results are presented in Tables C.9 to C.20 from the Appendix C.

The tables present the results obtained for all frames located in Vancouver, separately for historical or artificial events. A small amount of inelastic brace activity is observed for all the structures and it is in general concentrated at the bottom of the frame. For the 20 storey Vancouver it was also found that the braces from the middle storeys exhibit some inelastic behavior. The number of inelastic incursions varies from one to three with a total time of the yielding below 1.0 seconds. The braces from the structures located in Montreal did not exhibit any inelastic behavior.

To investigate the effectiveness of ductility design provisions of S16S01-05, the response ratios of the interaction axial force-bending moment equations are plotted in Figures 5.5 to 5.7. For Vancouver the graphic shows the 50^{th} percentile calculated for the historical records and the 50^{th} percentile for the artificial records. The values of the critical response ratios obtained in the ductility design step are also shown. For the frames designed in Montreal only the 50^{th} percentile for the group of the 10 artificial records is represented in graphics and compared with the values from the ductility design. The chosen interaction value of the ductility design represented in the figures is the one given by the equation 13.8.2 (b) for the overall member strength. This was considered to be the appropriate interaction equation because the non linear analyses were effectuated for a 2D frame model and therefore the response forces do not account for the lateral torsional buckling.

For the three structures situated in Vancouver the response of the braces was very close to the values calculated following the ductility design procedure, except for the upper storeys where the values obtained from NLTHA are 20 to 40 percent higher. Also some slightly higher values could be observed at the first storey, which is noticed to be similar

to the trend observed for the maximum link rotations. The structures situated in Montreal had the interaction values obtained from the NLTHA results smaller than the ones calculated during the ductility design, except for the upper storeys where the situation reversed. The interaction of the axial force – bending moment yields values of 25 percentages higher than those from ductility design. It can be said that the lack of inelastic link activity observed for Montreal structures, discussed in the preceding sections, reflects on the level of braces solicitation.

5.2.3 Columns' response

To monitor the behavior of the columns during the NLTHA the number and duration of inelastic incursions was calculated first and the maximum values of the response ratios of the axial force–bending moment interaction equations were compared to the values used in the ductility design phase. Secondly the axial forces and the bending moments obtained from the dynamic analyses were examined to validate the amplification factors specified by the Clause 27 of CSA/CAN S16S01-05, used to estimate the forces transmitted to columns by the yielding links.

Limited number of inelastic excursions in the columns was observed for the 14 storey structure situated in Vancouver, this one being the only structure in which the columns showed inelastic behavior. The inelastic incursions in the columns are presented in Tables C.21 to C.24 from Appendix C. Both for historical and artificial group of records the columns develop plastic hinges at one to two storeys during 1 to 2 inelastic incursions. The plastification of the columns happened for the four of historical ground motion and two of the artificial motions. The only exception to this behavior is the case of earthquake no V14 where 24 inelastic incursions were registered at the 11^{th} storey with a total time of 11.47 seconds. This behavior is associated with extremely high inelastic link rotations, observed at the same location, for the same earthquake.

The interactions of axial force-bending moment are presented in Figures 5.8 to 5.10 where the 50th percentile of the results from NLTHA is compared to the design values obtained in ductility design phase. The 50th percentile of the NLTH results for the historical and artificial records show a close resemblance to the design values for all the three structures in Vancouver. In general, slightly higher analytical values compared with the design values were observed in the upper half of the building. Contrary, in the lower half the values from the NLTHA are smaller than the estimated design values. This observation proves that the assumption used in the design phase that all the links from the entire frame yield at the same time is not true but practically conservative in the design phase. This tendency is even more evident for the frames designed in Montreal where the differences between the dynamic and the design results are more pronounced. While the results obtained from NLTHA and predicted design values in Vancouver differ by 10 % for the frames in Vancouver, the NLTHA results found for Montreal are 50 % lower than the values of estimated in the design.

5.2.3.1 Column axial forces

The axial forces developed in the columns during the time history analyses are presented in Tables 5.13 to 5.18 separately for the historical and artificial records. The tables show the 50th percentile and the 84th percentile for the each group of records. The tables also contain the axial forces in columns introduced by the load combination including the gravity loads (1.0D+0.5L+0.25S), and the forces calculated according to the capacity design procedure: 1.3 times the plastic capacity of the links in the top two storeys and 1.15 times the links plastic capacity for the other storeys. The axial factored resistance of the columns calculated according to the Clause 13.8.2 (c) from S16S1-2005 is also included in the tables to establish the upper bond of the possible axial columns forces.

For the 14 storey structure in Vancouver the 50th percentile of the NLTHA results were 20 percent lower than the design forces and the 84th percentile values were 15 % lower.

Similar observation was made for the 20 and 25 storeys Vancouver with slightly higher differences obtained between the design column forces and the forces developed during the ground motions. The factored capacity of the columns is close to the design and dynamic forces for the 14 storey structure but for the 20 storey and 25 storey structures it is two to three time larger than the demand.

The structures located in Montreal larger difference between the design column axial forces and the forces developed during the NLTHA were noted. For all three structures 14, 20 and 25 storeys, the design axial forces are more than two times bigger than the 84^{th} percentile of the values obtained in NLTHA. The difference between the capacity of the columns and the design or dynamic axial forces was similar to the structures situated in Vancouver, that is for the 14 storey structure the developed forces were close to the capacity limit and the difference was increasing with the increase in the number of storeys.

The values of the axial column forces developed during the NLTHA are, as expected, lower than the design forces as the capacity design procedure assumes the yielding of all links from the frame to a maximum force of 1.15 V_p. This tendency is normal since the links from the lower half of all structures did not develop their entire plastic capacity.

5.2.3.2 Column bending moments

In the design provisions of the S16S1-2005 the column bending moments are not calculated directly, but rather a certain portion of the column capacity is reserved to account for the bending moments in the interaction axial force-bending moment equation. The portion reserved for the moments is 0.35 from the moment plastic capacity M_p for the top two storeys and $0.15M_p$ for the other storeys. In the following paragraphs these design provisions for the column moment calculations are compared to the moments resulted from the NLTHA. It is therefore of interest to see how well the present Canadian

design procedures account for the contribution of bending moments in the columns of EBFs. The results of the NLTHA for the column bending moments are presented in Tables 5.19 to 5.24. The tables present the maximum values of the bending moments obtained at each storey in kNm (in absolute values) and also expressed as the percentage from the moment capacity M_p of the section.

As can be seen from Tables 5.19 to 5.24 for the 14 storey structure in Vancouver the 50th percentile values obtained for the column moments varied between the 15 and 35 percent of Mp , except for the group of historical records where the columns in the top four storeys reached moments of 0.30 Mp. The 84th percentile reflects values even higher in the upper half of the building with a maximum moment of 0.54M_p for the group of historical records. The moments developed in the 20 storey Vancouver structure are much closer the provisions recommended in Clause 27 and for the 50th percentile only a few storeys had values higher than 0.15M_p with a maximum of 0.19M_p in the 16th storey. The 84th percentile show values different from the 50th percentile which means that high variations in the moments can be expected depending on storey drifts and characteristics of individual ground motions. The maximum values for the 84th percentile are observed in the upper storeys with the highest value of 0.39M_p. In the 25 storey structure the 50th percentile have the maximum value of 0.19M_p in the 22nd storey and in the lower half of the frame the moments represent 0.03M_p. The 84th percentile from the results has higher values with a maximum of 0.30M_p in the 24th storey and percentages that attain 0.05M_p in the lower storeys.

For the 14 storey frame in Montreal, the 50th percentile reached the maximum values of 0.13Mp in the storey 14th and an average of 0.03 Mp in the lower storeys. Little difference was observed between the 84th percentile and 50th percentile values (up to 3 %). As it can be observed the moments developed during the NLTHA are much lower compared the estimated values used in the ductility design phase. The 20 storeys structure showed larger differences between 50th and 84th percentile and the highest 84th percentile

value is about $0.03M_p$ in the 19^{th} storey. In the bottom storey moments were very low reaching only 0.01Mp. The moments recorded for the 25 storey structure are similar to those observed in the 20 storey. They are below $0.15M_p$ at the upper storeys and as low as $0.01M_p$ in the lower half of the frame. Contrary to the structures designed for Vancouver, the bending moments in the columns of the structures in Montreal were very small and always under the estimated values used in the ductility design phase.

5.2.4 General observations on the behavior of outer beams, braces and columns

The inelastic behavior of outer beam segments was accepted and incorporated in design of EBFs studied. In order to represent this behavior and evaluate the extent of inelastic activity the exterior beams were modeled for the NLTHA as inelastic elements. Out of the six structures analyzed, only the beams of the 14-storey frame in Vancouver showed inelastic behavior. The inelastic behavior did not occur for all the events. When such response was observed it involved up to a maximum of six storeys with a medium value of inelastic beam rotation of 0.02 radians.

The inelastic behavior of the braces was observed for all the structures located in Vancouver, but in a small extent and concentrated at the bottom storeys. For the Montreal structures the braces did not show any inelastic behavior during the analyses. The graphics that presents the interaction of the axial force-bending moment over the frame height show values close to the values obtained in the design, except for the upper storeys where the interaction values are higher. This situation was observed for the Vancouver structures, but for the structures located in Montreal the interaction values obtained from NLTHA are smaller than the ones calculated in the ductility design, except for the upper storeys where the values are higher than those from the design.

The inelastic excursions in the columns are observed only for the 14 storey structure situated in Vancouver and the inelastic activity is observed for six out of twenty ground motions with plastic hinges that developed at one to two storeys. The axial force–bending moment interaction coefficients calculated for the forces obtained from the non-linear analyses were compared to those calculated in the ductility design phase. A close resemblance between the two values was observed for Vancouver and for Montreal with the exception of the bottom storeys for Montreal structures where the difference was substantial.

The axial forces in the columns developed during the dynamic analyses were lower than the values anticipated in the ductility design, the differences increasing with the increase of the number of storeys. For Montreal the differences between the dynamic and design forces were more pronounced than those found for Vancouver. Contrary to the tendency observed for the axial forces, the columns bending moments obtained from NLTHA are higher than those estimated in the design phase. For the structures situated in Vancouver the largest 84^{th} percentile values reached 0.5Mp for the 14 storey structure and diminished with the increase of the frame height. The frames designed for the eastern location developed moments that are within the code recommendations of $0.35M_p$. These moments reached $0.15M_p$ at the top storeys and moments that represent 0.01 to $0.05M_p$ in the other storeys.

5.3 Results for total inter storey drifts

The performance level of a structural system is directly related to the drift limit permitted in the NBCC for that building. For the "life-safe" performance level the new 2005 NBCC demands that the total drifts have to be lower than 2.5 % of the storey height.

The results for the inter-storey drifts obtained from the NLTHA are presented in Tables 5.25 to 5.30 together with the maximum inter storey drift permitted in the 2005 NBCC. The total drifts from the non linear analyses are grouped by types of ground motion as it

was done for the inelastic links rotations: historical and artificial records separated in short and long distance.

5.3.1 Fourteen storey structure

The total drifts for the 14 storey structure in Vancouver exceed the code limits for the group of historical records at short distance. The maximum drift of 118mm (84^{th} percentile value), was observed at the top storeys exceeding the code limit by 27 percent. The other groups of ground motions induced also high 84^{th} percentile values of total drift but all within the limit of 92.5mm. The short distance groups of records yielded higher total drifts at the top storeys compared to the long distance records for which the drifts were much more uniform over the height of the frame. A significant difference between the 50^{th} and the 84^{th} percentile was observed which indicates a high variability in the drifts values and thus an elevated sensitivity of the EBF's to storey deformations. Considering the group of all 20 ground motions the 50^{th} as the 84^{th} percentile are at about half of the code limit with higher values observed at the top storeys. The 84^{th} percentile of total drift has values in the range 25 to 72 mm and for the 50^{th} percentile they go from 20 to 49 mm.

The total drifts for the structure from Montreal have the 50^{th} percentile values close to the 84^{th} percentile and contrary to the structure from Vancouver the short and long distance values are similar one to another. The maximum 84^{th} percentile calculated for the group of all 10 artificial records is observed in the 11^{th} storey reaching 25 percent of the code limit. In general the drifts in the Montreal structure are much lowers than those from Vancouver with values between 10 and 15 mm.

5.3.2 Twenty storey structure

The total drifts for the 20 storey Vancouver presented in Table 5.27 were only grouped by historical or artificial records because the short and long distance groups presented no significant differences. The 50th percentile values obtained for the historical and artificial records were similar and varied between 15 to 47 mm, with slightly larger values at the middle portion of the frame. The 84th percentile values observed for the artificial records showed a different distribution with values that, in the top storeys were almost double the values obtained for the historical records results. But even in this situation the total drifts were all within the NBCC limit, with a maximum 84th percentile value of 77 mm in the 15th storey.

The maximum total drifts for 20 storeys Montreal had values similar to those observed for the 14 storey structure. The 50th percentile varied between 7 mm in the lower storeys and a maximum of 17 mm at the 18th storey while the 84th percentile went from 7 mm to 37 mm at the storey 18. The maximum value represents about 40 % from the code limit a value but it is higher than the one predicted in the design.

5.3.3 Twenty-five storey structure

Table 5.29 shows the total drifts obtained for the 25 storey Vancouver grouped in three categories historical, artificial and the entire group of the 20 ground motions. The artificial ground motions generated inter storey drifts higher than those yielded from the historical motions. The difference is especially seen in the 84th percentile were the artificial group have a maximum of 67 mm drift in the 20th storey compared to a maximum of 48 mm for the group of historical records, drift that occurred in the 19th storey. In general the maximum drifts for the 25 storey structure are below the code limit and the 50th percentile from the entire set of results represent less than the half of the NBCC drift limit.

The total drifts for Montreal structure, presented in Table 5.30, have a 50^{th} percentile value of maximum 17 mm drift in the upper storeys with a corresponding 84^{th} percentile that reach 24 mm. These values represent about a quart of the permitted drift thus the frame is over strengthen for the level of seismic activity specific for the eastern location. The drifts in the middle and lower storey from this structure are maintained to 10 % for the NBCC limit 92.5 mm.

5.4 Lateral force distribution

The structures analyzed in this study were designed for a base shear and a distribution of lateral force as recommended in the 2005 NBCC. The approach presented in the building code is based on the calculation of the seismic force for the first mode of vibration as the regular buildings response is in the first mode of vibration and to account for the contribution of the higher modes a potion of the base shear as a concentrated force is applied at the top of the building. The concentrated force denoted F_t and the formula of calculation were discussed in Section 2.2.1. The forces calculated following the NBCC empirical approach is noted as $NBCC_{linear}$. For terms of comparison the lateral seismic forces for the same structures obtained from spectral analyses and scaled to the $NBCC_{linear}$ base shear is also presented in the study of the lateral force distribution. This spectral force is designate as $NBCC_{spectral}$. The Figures 5.11 to 5.13 present the distribution over the building's height of the $NBCC_{linear}$, $NBCC_{spectral}$, and the lateral force obtained from the non linear analyses as the difference between two subsequent storeys and scaled to the level of $NBCC_{linear}$.

The actual values of the shear forces on the structures obtained from the NLTHA are also presented in tables (Tables C.25 to C.30, Appendix C) together with the empirical lateral force $NBCC_{linear}$, and the spectral force $NBCC_{spectral}$. The lateral shear force will be discussed in the following paragraphs through the level of the force developed in the

structure and the distribution over the frame's height compared to the $NBCC_{linear}$ and $NBCC_{spectral}$. The tables present the values of the dynamic lateral forces as the 50^{th} and 84^{th} percentile for the historical group of ground motion, the artificial group and the entire group of ground motions. The maximum values of the dynamic forces from all the earthquakes are also presented on the tables and all of these values represent the elastic response of the frames.

5.4.1 Fourteen storey structure

Table C.25 contain the shear forces on the structure for the 14 storey Vancouver compared to the design forces obtained in the analyses described in Chapter 3. The elastic values of the forces developed during the ground motions are in general double compared to the both linear and spectral design forces. The only difference is observed at the top storeys were the spectral forces are lower than the other groups. From the Figure 5.11 (a) it can be observed that the lateral force distribution is in general, in good agreement except the fact that the non linear results succeed to reflect in a better way the influences of the superior modes.

The NLTH forces for the Montreal structure are similar to those from Vancouver with values that are the double of the design values and with higher ratios at the top storeys that can reach 3 to 4 times the corresponding storey design force. Regarding the distribution over the height of the lateral shear the Figure 5.11 (b) the non linear shears are closer to the $NBCC_{spectral}$ distribution than to the $NBCC_{linear}$, and a much stronger influence of the higher modes of vibration is seen compared to the Vancouver structure.

5.4.2 Twenty storey structure

The NLTH storeys shears for the 20 storey Vancouver are around 1.8 times higher than the forces from the design, but the upper storeys have ratios of dynamic to design force

higher the 2.0. The lateral distribution is showed in Figure 5.12 (a) and it presents a good sufficient good match between the dynamic, the $NBCC_{linear}$ and $NBCC_{spectral}$ distribution. Discrepancies are observed at the top and bottom storeys and especially between the dynamic and linear distribution, with a closer match between the spectral and dynamic forces.

The shear dynamic forces of the structure from Montreal represent in general the double of the forces used for the design of the frame, with higher values at the top storeys that reach three times their corresponding amount of the design force. The distribution of the lateral forces as it is presented in Figure 5.12 (b) shows a closer resemblance of the dynamic distribution to the $NBCC_{spectral}$ than to the $NBCC_{linear}$. The lack of smoothness on the form of the lateral dynamic force is similar to the one observed for the 14 storey frame with even more changes on the sign of the force.

5.4.3 Twenty-five storey structure

Table C.29 contains the values of the storey shears for the 25 storey structure from Vancouver. The values of the storey shears are similar to those found in the other structures but with ratios of the dynamic to design values around 1.5 and only at the top storeys the factor is 2 for the linear distribution forces and 3 for the spectral forces. The distribution of the lateral force on the storeys follows the tendency observed for the other Vancouver structures, a similar distribution on the middle with differences at the top and bottom storeys, but it is also observed a higher influence of the superior modes with changes on the amount of the force.

The NLTH shear forces found for the Montreal 25 storey structure are presented in Table C.30 and their values are similar to those found for the 25 storey Vancouver. They have closer values to the ones from design at the middle and bottom at the frame with values around 50 % higher, but the top storeys shear forces are three times higher than the

corresponding design values. The distribution of the force over the frame height presents a high variation compared to the corresponding $NBCC_{spectral}$ and the $NBCC_{linear}$. In this case the influence of higher modes of vibration causes the appearance of a negative value at the middle storeys.

5.5 Relation between the link inelastic shear rotation γ and the inter-storey drift Δ

The verification of inelastic shear rotations, γ, is an important phase in seismic design of eccentrically braced frames. As explained in Section 3.2.4.5, at design stage γ is calculated as a function of the total inter-storey drift, Δ_i, the storey height, h_s, the length of the link, e, and the width of the braced bay, L, assuming the rigid-plastic behavior of the frame. The value of Δ_i is taken equal to three times the elastic inter-storey drift, Δ_{el}, computed under the factored seismic loads. This Δ_i estimate is obtained applying the equal displacement principle ($\Delta_i = R_d\Delta_e$) , assuming that inelastic link rotations first develop when the storey shear reaches the design value amplified by the overstrength (R_oV_p). In view of the importance of this design parameter on EBF seismic design, the study was carried out to understand better the relationship between the inelastic shear rotations of the link and total inter-storey drifts.

For all structures studied, the maximum link rotation γ and the maximum inter storey drift Δ at every storey level were collected for each acceleration record. The results showed a strong positive correlation between the two parameters. For most of the cases studied, the maximum values of the two parameters occurred at the same location and at the same time. These findings further confirmed the physical relationship between the two parameters.

For every storey of each frame studied, the ratio of the maximum γ_{max} and the total maximum Δ_{max} was calculated. The results for maximum γ_{max} and maximum Δ_{max} were

obtained based on maximum values found for all records. Tables 5.31 and 5.32 summarize the results obtained for Vancouver and Montreal structure respectively. For Vancouver, the results are shown separately for 10 historical and 10 artificial records, as well as for the complete set of 20 records. The tendency of results obtained for historical and artificial records was found to be very similar and thus the results shown for the whole record ensemble were considered representative.

As can be seen in Tables 5.31 and 5.32 for all frames studied the ratio of the maximum γ_{max} / maximum Δ_{max} for top storey link is much smaller in comparison to other storeys. This is not surprising in view of lower amount of inelastic activity observed in the analysis. Regarding the vertical distribution of the obtained ratios, different profiles were observed for Vancouver and Montreal structures. While for Vancouver structures, somewhat higher values were observed in the upper and lower storeys of the frame, for Montreal, the larger ratios were observed in the upper floors while those in the lower storeys were very small.

For the Vancouver structures mean values of the ratio of the maximum γ_{max} / maximum Δ_{max} obtained for 14-, 20- and 25- storeys frame, excluding the results for top story link, were 0.0024, 0.0022 and 0.0019 respectively. Using the same principle, for Montreal frames, mean values were calculated excluding the storeys that showed the similar behavior to the top storey link, i.e. all the results less or equal to 0.0005 were excluded. Following values were obtained: 0.0012 for 14-storey frame, 0.0014 for 20-storey frame and 0.0013 for 25-storey frame. Taking the conservative values and neglecting the slight variation of the ratio γ_{max} / Δ_{max} following relationships can be written: (i) for Vancouver, $\gamma = 0.0023\ \Delta$, and for Montreal, $\gamma = 0.0014\ \Delta$. It can be seen that the factor multiplying the total drifts is sensitive to design location, but less sensitive to the height of the frame. The reader is reminded that the ductility demand imposed on Montreal structures was much smaller compared to those located in Vancouver.

To determine more precisely the relationship between γ and Δ, another approach was also considered for both studied locations. In this approach, for selected location and the frame height, the pairs of values of the inter-storey drifts and the link rotations were defined. For the three Vancouver frames, the pairs of values, excluding the top storey were determined for the complete ensemble of ground motions and plotted in Figures 5.14, 5.15 and 5.16. A linear relationship (best-fit line) was determined for each of three graphs. Similar relationships were found for the three structures and thus the cumulative results are presented for all the three frames. The linear relation extracted for these graphics can be written as:

$$\Delta/h_s = 0.10\gamma + 0.0033 \qquad [5\text{-}1]$$

In the above relation Δ represents the total inter-storey drift, h_s is the storey height and γ is the inelastic link rotation. The coefficient of 0.10 by which γ is multiplied could be approximated with the ratio of e/L which is equal to 0.0889 in this study. The constant 0.0033 is an inferior limit of drift index above which the inelastic rotations appears (drift index at yield). Expressing γ as a function of Δ, and introducing e/L the previous relationship can be written as follows:

$$\gamma = (L/e)*(\Delta/h_s - 0.0033) \qquad [5\text{-}2]$$

This relationship is representative of the rigid-plastic deformation mechanism (see Figure 2.2), at yield drift of 0.3 percent.

The same approach was applied to relate total inter-storey drifts and link inelastic rotations for Montreal frames. The values of the links rotations that were less or equal to 0.005rad were excluded from the calculation. Similarly to Vancouver, it was determined that variation of the linear relationship in function of frame height was small. Figure 5.17 present plots of the pairs total inter-storey drifts – link inelastic rotations for all structures

designed in Montreal. The following linear relation Δ - γ was established on basis of cumulative results obtained:

$$\Delta/h_s = 0.098\gamma + 0.0024 \qquad [5\text{-}3]$$

For structures located in Montreal the inferior limit of the drift above which the inelastic rotations occurs is set to 0.24 % h_s. Although the relationship [5-3] slightly differs from the [5-2] it is anticipated that the latter could be used to obtain conservative estimated of inelastic link rotations for structures in Montreal.

The Figure 5.17 compares the link inelastic rotations obtained from non-linear time-history analysis for Vancouver structures, with the values predicted using the formula 5.2. A solid line represents the perfect prediction. For the majority of cases, the proposed equation gives satisfactory and conservative results. Although this type of relationship cannot be easily integrated into capacity design procedures, as the prior knowledge of total inter-storey drift is required, the results can be useful in the context of performance-based design. For instance, two interesting results can be obtained from the equation [5-2]: (a) the first inelastic link deformation occurs at an inter-storey drift index of 0.33% and (b) the link maximum design rotation (0.08rad) is attained at drift index of 1.01%.

5.6 Summary

The maximum inelastic link rotations for the Vancouver structures have all went beyond the code limit in the top and sometimes in the bottom storeys, while the other storeys developed inelastic rotations, but in the limit of 0.08 radians. Following the link rotation tendency the factor of amplification for the force developed in the link was found to be close to the CAN/CSA S16-05 specified factor, with slightly higher values at the top storeys. Contrary to the strong inelastic activity observed in the Vancouver structures, for Montreal the frames developed plastic rotations only at the top storey and the values

stayed within the code limit. The middle and bottom storeys remained in general in the elastic range, fact that reflects on the factor of the force developed in the link, which is below 1.0 for the lower storeys.

The response of the beams, braces and columns was analyzed carefully to locate the inelastic activity or to validate the code specifications from the ductility design versus the dynamic results. The inelastic activity in the exterior beams is very low and present only on the 14 storey Vancouver and it is isolated and in a small extend for the braces and columns. The response of the braces in the NLTHA present higher values compared to those from the ductility design for the Vancouver structures, but values that are smaller for the structures designed in Montreal. Similar to the braces behavior, the columns from the Vancouver structures developed higher moments than estimated in the design and thus a higher response factor, while the frames designed for Montreal had moments that stayed in the limits recommended in the Canadian steel code.

The total inter-storey drifts developed during the ground motion excitations have similar tendency as the inelastic link rotations: high values for the Vancouver structures and especially at the top storeys and low values for the structures from Montreal. The lateral force profiles were compared to the empirical and spectral distributions of the force and a closer resemblance is observed with the spectral lateral load than with the empirical distribution and also significant differences with the two design loads at the storeys from the top and bottom of the frame.

The interconnection between the drift and the link rotation was analyzed in detail and a strong positive γ-Δ relation was established for the two specific locations. A formula in function of the L/e (frame span/ link length) was developed and the link rotations predicted with the formula were compared with the NLTHA link rotation values. The new link rotation formula yielded adequate and conservative estimates for the registered inter storey drifts.

Table 5.1 Maximum inelastic link rotations 14 storey frame in Vancouver

Storey	Historical records(5)-short distance		Artificial records(5)-short distance		Historical records(5)-long distance		Artificial records(5)-long distance		Historical records(10)		Artificial records(10)		All records(20)	
	γ_{max}		γ_{max}		γ_{max}		γ_{max}		γ_{max}		γ_{max}		γ_{max}	
	50^{th}	84^{th}	50^{th}	84^{th}	50^{th}	84^{th}	50^{th}	84^{th}	50^{th}	84^{th}	50^{th}	84^{th}	50^{th}	84^{th}
14	0.003	0.004	0.004	0.004	0.004	0.006	0.004	0.004	0.004	0.004	0.004	0.004	0.004	0.004
13	0.131	0.231	0.126	0.170	0.099	0.112	0.069	0.071	0.102	0.186	0.072	0.148	0.097	0.164
12	0.074	0.306	0.083	0.154	0.093	0.121	0.104	0.122	0.084	0.204	0.089	0.126	0.088	0.157
11	0.065	0.210	0.059	0.163	0.068	0.117	0.097	0.110	0.067	0.158	0.081	0.111	0.069	0.124
10	0.056	0.126	0.068	0.193	0.135	0.162	0.098	0.105	0.060	0.164	0.083	0.121	0.066	0.157
9	0.047	0.110	0.073	0.158	0.081	0.120	0.085	0.109	0.062	0.120	0.079	0.109	0.068	0.118
8	0.031	0.066	0.041	0.089	0.038	0.048	0.070	0.077	0.035	0.049	0.054	0.078	0.040	0.074
7	0.020	0.056	0.034	0.040	0.029	0.057	0.049	0.072	0.026	0.056	0.041	0.056	0.036	0.056
6	0.021	0.037	0.025	0.040	0.030	0.067	0.063	0.080	0.023	0.049	0.042	0.069	0.030	0.063
5	0.015	0.040	0.018	0.043	0.030	0.064	0.052	0.105	0.026	0.044	0.042	0.083	0.034	0.074
4	0.014	0.028	0.012	0.049	0.053	0.056	0.047	0.104	0.031	0.054	0.035	0.086	0.031	0.060
3	0.018	0.022	0.009	0.067	0.044	0.067	0.053	0.103	0.028	0.052	0.032	0.109	0.029	0.080
2	0.023	0.027	0.009	0.083	0.044	0.081	0.060	0.098	0.032	0.055	0.032	0.099	0.032	0.096
1	0.032	0.039	0.017	0.102	0.058	0.108	0.070	0.094	0.046	0.074	0.043	0.102	0.046	0.086

Table 5.2 Maximum inelastic link rotations 14 storey frame in Montreal

Storey	Artificial records(5)-short distance		Artificial records(5)-long distance		Artificial records(10)	
	γ_{max}		γ_{max}		γ_{max}	
	50^{th}	84^{th}	50^{th}	84^{th}	50^{th}	84^{th}
14	0.003	0.003	0.003	0.003	0.003	0.003
13	0.021	0.027	0.027	0.033	0.024	0.031
12	0.007	0.012	0.023	0.028	0.018	0.027
11	0.018	0.019	0.033	0.041	0.023	0.037
10	0.015	0.018	0.013	0.015	0.014	0.018
9	0.005	0.006	0.004	0.008	0.005	0.008
8	0.004	0.005	0.004	0.004	0.004	0.005
7	0.003	0.003	0.003	0.004	0.003	0.004
6	0.003	0.003	0.003	0.003	0.003	0.003
5	0.003	0.003	0.003	0.003	0.003	0.003
4	0.003	0.003	0.003	0.004	0.003	0.004
3	0.003	0.003	0.003	0.004	0.003	0.003
2	0.003	0.004	0.005	0.007	0.004	0.006
1	0.004	0.005	0.006	0.009	0.005	0.008

Table 5.3 Maximum inelastic link rotations 20 storey frame in Vancouver

Storey	Historical records(5)-short distance		Artificial records(5)-short distance		Historical records(5)-long distance		Artificial records(5)-long distance		Historical records(10)		Artificial records(10)		All records(20)	
	γ_{max}		γ_{max}		γ_{max}		γ_{max}		γ_{max}		γ_{max}		γ_{max}	
	50^{th}	84^{th}	50^{th}	84^{th}	50^{th}	84^{th}	50^{th}	84^{th}	50^{th}	84^{th}	50^{th}	84^{th}	50^{th}	84^{th}
20	0.002	0.002	0.002	0.003	0.002	0.003	0.002	0.002	0.002	0.003	0.002	0.003	0.002	0.003
19	0.031	0.043	0.049	0.086	0.036	0.044	0.017	0.040	0.033	0.045	0.032	0.076	0.033	0.058
18	0.057	0.076	0.049	0.117	0.040	0.057	0.039	0.091	0.051	0.069	0.044	0.127	0.047	0.082
17	0.060	0.076	0.053	0.117	0.050	0.063	0.042	0.120	0.054	0.070	0.053	0.145	0.053	0.074
16	0.067	0.074	0.062	0.140	0.043	0.055	0.066	0.136	0.051	0.068	0.064	0.159	0.062	0.084
15	0.043	0.051	0.108	0.153	0.063	0.079	0.088	0.137	0.052	0.065	0.090	0.169	0.060	0.108
14	0.020	0.026	0.078	0.130	0.070	0.099	0.082	0.115	0.029	0.086	0.080	0.131	0.055	0.098
13	0.032	0.034	0.054	0.107	0.065	0.084	0.069	0.090	0.035	0.068	0.061	0.091	0.046	0.087
12	0.016	0.022	0.031	0.062	0.042	0.057	0.042	0.061	0.026	0.049	0.033	0.063	0.031	0.058
11	0.012	0.018	0.018	0.032	0.036	0.042	0.031	0.046	0.016	0.037	0.021	0.044	0.018	0.040
10	0.016	0.017	0.016	0.026	0.039	0.070	0.024	0.071	0.017	0.052	0.019	0.044	0.017	0.050
9	0.008	0.014	0.017	0.037	0.040	0.087	0.024	0.085	0.011	0.066	0.021	0.057	0.018	0.062
8	0.005	0.013	0.008	0.039	0.033	0.060	0.022	0.080	0.017	0.045	0.020	0.046	0.018	0.047
7	0.008	0.012	0.006	0.032	0.027	0.041	0.021	0.070	0.018	0.031	0.021	0.040	0.019	0.035
6	0.009	0.013	0.003	0.021	0.033	0.040	0.020	0.058	0.015	0.035	0.019	0.036	0.018	0.036
5	0.010	0.014	0.003	0.020	0.030	0.043	0.022	0.049	0.014	0.035	0.020	0.037	0.016	0.039
4	0.009	0.016	0.003	0.022	0.018	0.034	0.020	0.027	0.014	0.019	0.017	0.029	0.016	0.022
3	0.012	0.024	0.006	0.034	0.021	0.052	0.032	0.054	0.015	0.037	0.021	0.053	0.019	0.051
2	0.017	0.031	0.023	0.058	0.043	0.069	0.051	0.091	0.024	0.057	0.043	0.080	0.036	0.078
1	0.023	0.053	0.052	0.093	0.076	0.094	0.089	0.141	0.053	0.089	0.083	0.114	0.074	0.100

Table 5.4 Maximum inelastic link rotations 20 storey frame in Montreal

Storey	Artificial records(5)-short distance		Artificial records(5)-long distance		Artificial records(10)	
	γ_{max}		γ_{max}		γ_{max}	
	50^{th}	84^{th}	50^{th}	84^{th}	50^{th}	84^{th}
20	0.003	0.004	0.003	0.003	0.003	0.003
19	0.018	0.023	0.022	0.036	0.019	0.029
18	0.023	0.025	0.048	0.083	0.025	0.073
17	0.013	0.016	0.032	0.078	0.018	0.063
16	0.004	0.009	0.011	0.014	0.008	0.013
15	0.003	0.008	0.006	0.010	0.005	0.011
14	0.005	0.009	0.010	0.013	0.008	0.012
13	0.004	0.005	0.006	0.011	0.005	0.008
12	0.003	0.003	0.004	0.004	0.003	0.004
11	0.003	0.003	0.003	0.006	0.003	0.005
10	0.003	0.003	0.003	0.003	0.003	0.003
9	0.003	0.003	0.003	0.003	0.003	0.003
8	0.003	0.003	0.003	0.003	0.003	0.003
7	0.003	0.003	0.003	0.003	0.003	0.003
6	0.003	0.003	0.003	0.003	0.003	0.003
5	0.002	0.003	0.002	0.003	0.002	0.003
4	0.003	0.003	0.003	0.003	0.003	0.003
3	0.002	0.003	0.003	0.003	0.003	0.003
2	0.002	0.003	0.003	0.003	0.003	0.003
1	0.003	0.005	0.004	0.005	0.004	0.006

Table 5.5 Maximum inelastic link rotations 25 storey frame in Vancouver

Storey	Historical records(5)-short distance		Artificial records(5)-short distance		Historical records(5)-long distance		Artificial records(5)-long distance		Historical records(10)		Artificial records(10)		All records(20)	
	γ_{max}		γ_{max}		γ_{max}		γ_{max}		γ_{max}		γ_{max}		γ_{max}	
	50^{th}	84^{th}	50^{th}	84^{th}	50^{th}	84^{th}	50^{th}	84^{th}	50^{th}	84^{th}	50^{th}	84^{th}	50^{th}	84^{th}
25	0.002	0.002	0.003	0.003	0.002	0.002	0.002	0.002	0.002	0.003	0.002	0.003	0.002	0.003
24	0.018	0.026	0.020	0.051	0.024	0.045	0.008	0.029	0.021	0.033	0.014	0.053	0.017	0.048
23	0.041	0.084	0.056	0.098	0.046	0.106	0.025	0.074	0.044	0.095	0.038	0.106	0.043	0.100
22	0.043	0.096	0.057	0.111	0.056	0.095	0.043	0.113	0.050	0.104	0.052	0.129	0.051	0.120
21	0.028	0.098	0.047	0.102	0.040	0.060	0.060	0.114	0.039	0.063	0.054	0.125	0.046	0.070
20	0.039	0.087	0.081	0.127	0.039	0.074	0.040	0.132	0.039	0.075	0.064	0.141	0.041	0.103
19	0.031	0.070	0.091	0.126	0.057	0.099	0.050	0.142	0.045	0.100	0.071	0.131	0.049	0.119
18	0.029	0.053	0.073	0.101	0.065	0.093	0.068	0.124	0.043	0.077	0.071	0.112	0.054	0.105
17	0.020	0.050	0.054	0.079	0.050	0.069	0.071	0.082	0.036	0.061	0.063	0.083	0.050	0.071
16	0.010	0.043	0.035	0.053	0.036	0.044	0.045	0.054	0.027	0.048	0.042	0.055	0.036	0.056
15	0.012	0.028	0.023	0.038	0.019	0.058	0.036	0.043	0.019	0.044	0.035	0.041	0.022	0.044
14	0.010	0.023	0.019	0.031	0.016	0.064	0.031	0.041	0.016	0.037	0.030	0.034	0.022	0.035
13	0.011	0.022	0.013	0.015	0.016	0.055	0.026	0.034	0.014	0.028	0.018	0.027	0.016	0.027
12	0.007	0.016	0.005	0.014	0.012	0.044	0.019	0.027	0.009	0.025	0.013	0.021	0.013	0.023
11	0.004	0.015	0.005	0.019	0.009	0.040	0.017	0.026	0.008	0.024	0.015	0.022	0.010	0.024
10	0.003	0.016	0.005	0.018	0.011	0.039	0.016	0.026	0.010	0.023	0.014	0.023	0.011	0.025
9	0.005	0.015	0.003	0.015	0.012	0.036	0.015	0.021	0.010	0.021	0.012	0.020	0.012	0.020
8	0.006	0.015	0.003	0.016	0.014	0.033	0.013	0.018	0.010	0.019	0.013	0.017	0.012	0.018
7	0.009	0.017	0.003	0.017	0.015	0.030	0.017	0.021	0.012	0.018	0.015	0.021	0.015	0.020
6	0.009	0.015	0.003	0.016	0.015	0.022	0.021	0.026	0.010	0.020	0.015	0.025	0.012	0.024
5	0.008	0.014	0.003	0.017	0.016	0.017	0.019	0.031	0.010	0.017	0.017	0.029	0.012	0.022
4	0.017	0.019	0.010	0.021	0.016	0.021	0.021	0.038	0.017	0.020	0.016	0.035	0.017	0.024
3	0.022	0.029	0.017	0.031	0.019	0.026	0.021	0.051	0.021	0.029	0.021	0.042	0.021	0.034
2	0.033	0.041	0.024	0.040	0.020	0.033	0.020	0.069	0.026	0.037	0.022	0.054	0.022	0.045
1	0.044	0.054	0.035	0.051	0.022	0.048	0.026	0.092	0.035	0.052	0.031	0.071	0.031	0.054

Table 5.6 Maximum inelastic link rotations 25 storey frame in Montreal

Storey	Artificial records(5)-short distance		Artificial records(5)-long distance		Artificial records(10)	
	γ_{max}		γ_{max}		γ_{max}	
	50^{th}	84^{th}	50^{th}	84^{th}	50^{th}	84^{th}
25	0.003	0.003	0.003	0.003	0.003	0.003
24	0.018	0.020	0.013	0.025	0.015	0.020
23	0.022	0.028	0.031	0.054	0.026	0.047
22	0.009	0.025	0.033	0.041	0.025	0.039
21	0.004	0.012	0.024	0.027	0.021	0.026
20	0.004	0.010	0.014	0.019	0.010	0.018
19	0.004	0.007	0.012	0.021	0.007	0.016
18	0.004	0.004	0.005	0.012	0.004	0.008
17	0.003	0.003	0.006	0.008	0.005	0.007
16	0.003	0.003	0.004	0.006	0.003	0.005
15	0.003	0.003	0.003	0.008	0.003	0.005
14	0.003	0.003	0.003	0.005	0.003	0.004
13	0.003	0.003	0.003	0.004	0.003	0.003
12	0.002	0.003	0.003	0.005	0.003	0.003
11	0.002	0.003	0.003	0.005	0.003	0.003
10	0.002	0.003	0.003	0.005	0.003	0.003
9	0.002	0.002	0.002	0.003	0.002	0.002
8	0.002	0.002	0.003	0.003	0.002	0.003
7	0.002	0.002	0.003	0.003	0.002	0.003
6	0.002	0.002	0.003	0.003	0.002	0.003
5	0.002	0.003	0.003	0.003	0.002	0.003
4	0.002	0.002	0.003	0.003	0.002	0.003
3	0.002	0.002	0.003	0.003	0.003	0.003
2	0.002	0.002	0.003	0.003	0.002	0.003
1	0.002	0.003	0.004	0.006	0.003	0.005

Table 5.7 Maximum inelastic relative link rotations 14 storey frame in Vancouver

Storey	Historical records(5)-short distance		Artificial records(5)-short distance		Historical records(5)-long distance		Artificial records(5)-long distance		Historical records(10)		Artificial records(10)		All records(20)	
	max γ_{range}		max γ_{range}		max γ_{range}		max γ_{range}		max γ_{range}		max γ_{range}		max γ_{range}	
	50^{th}	84^{th}	50^{th}	84^{th}	50^{th}	84^{th}	50^{th}	84^{th}	50^{th}	84^{th}	50^{th}	84^{th}	50^{th}	84^{th}
14	0.006	0.008	0.007	0.007	0.008	0.010	0.007	0.007	0.007	0.008	0.007	0.007	0.007	0.008
13	0.156	0.241	0.131	0.177	0.109	0.127	0.074	0.095	0.112	0.202	0.108	0.152	0.112	0.168
12	0.121	0.313	0.129	0.182	0.128	0.162	0.107	0.147	0.125	0.214	0.117	0.161	0.124	0.181
11	0.082	0.213	0.080	0.179	0.084	0.131	0.100	0.129	0.083	0.165	0.090	0.136	0.083	0.150
10	0.077	0.138	0.077	0.198	0.138	0.173	0.100	0.130	0.079	0.173	0.089	0.148	0.079	0.171
9	0.059	0.115	0.077	0.165	0.102	0.123	0.087	0.130	0.066	0.123	0.082	0.140	0.072	0.125
8	0.035	0.078	0.046	0.098	0.052	0.055	0.072	0.095	0.051	0.057	0.059	0.100	0.051	0.084
7	0.024	0.071	0.042	0.055	0.041	0.070	0.065	0.086	0.036	0.072	0.048	0.076	0.045	0.073
6	0.031	0.046	0.032	0.067	0.039	0.074	0.065	0.092	0.035	0.056	0.054	0.089	0.039	0.086
5	0.018	0.053	0.023	0.059	0.044	0.068	0.056	0.112	0.040	0.053	0.052	0.086	0.045	0.076
4	0.020	0.034	0.016	0.057	0.057	0.062	0.057	0.109	0.041	0.060	0.044	0.088	0.041	0.064
3	0.021	0.029	0.011	0.070	0.053	0.070	0.055	0.105	0.036	0.058	0.040	0.111	0.037	0.082
2	0.027	0.031	0.012	0.086	0.048	0.083	0.062	0.100	0.035	0.059	0.042	0.101	0.036	0.098
1	0.040	0.049	0.021	0.105	0.068	0.113	0.072	0.106	0.050	0.081	0.053	0.111	0.050	0.095

Table 5.8 Maximum inelastic relative link rotations 14 storey frame in Montreal

Storey	Artificial records(5)-short distance		Artificial records(5)-long distance		Artificial records(10)	
	max γ_{range}		max γ_{range}		max γ_{range}	
	50^{th}	84^{th}	50^{th}	84^{th}	50^{th}	84^{th}
14	0.006	0.006	0.006	0.006	0.006	0.006
13	0.031	0.036	0.040	0.047	0.035	0.043
12	0.012	0.021	0.030	0.034	0.027	0.032
11	0.020	0.029	0.043	0.052	0.036	0.047
10	0.018	0.020	0.017	0.024	0.018	0.022
9	0.009	0.010	0.007	0.011	0.008	0.011
8	0.007	0.008	0.007	0.007	0.007	0.008
7	0.006	0.006	0.006	0.007	0.006	0.007
6	0.006	0.006	0.006	0.006	0.006	0.006
5	0.006	0.006	0.006	0.006	0.006	0.006
4	0.006	0.006	0.006	0.007	0.006	0.007
3	0.006	0.006	0.006	0.007	0.006	0.006
2	0.006	0.007	0.008	0.010	0.007	0.009
1	0.007	0.009	0.011	0.014	0.008	0.014

Table 5.9 Maximum inelastic relative link rotations 20 storey frame in Vancouver

Storey	Historical records(5)-short distance		Artificial records(5)-short distance		Historical records(5)-long distance		Artificial records(5)-long distance		Historical records(10)		Artificial records(10)		All records(20)	
	max γ_{range}		max γ_{range}		max γ_{range}		max γ_{range}		max γ_{range}		max γ_{range}		max γ_{range}	
	50^{th}	84^{th}	50^{th}	84^{th}	50^{th}	84^{th}	50^{th}	84^{th}	50^{th}	84^{th}	50^{th}	84^{th}	50^{th}	84^{th}
20	0.004	0.004	0.004	0.004	0.004	0.004	0.003	0.004	0.004	0.005	0.004	0.004	0.004	0.004
19	0.038	0.051	0.052	0.089	0.044	0.052	0.024	0.052	0.039	0.053	0.047	0.090	0.042	0.070
18	0.059	0.086	0.084	0.122	0.059	0.072	0.051	0.101	0.059	0.077	0.058	0.141	0.059	0.089
17	0.070	0.084	0.090	0.153	0.082	0.089	0.076	0.124	0.073	0.091	0.077	0.164	0.076	0.099
16	0.073	0.087	0.098	0.150	0.070	0.079	0.078	0.149	0.072	0.086	0.089	0.167	0.077	0.098
15	0.050	0.056	0.117	0.156	0.070	0.086	0.093	0.159	0.056	0.072	0.105	0.172	0.067	0.123
14	0.026	0.038	0.081	0.134	0.073	0.102	0.084	0.130	0.040	0.089	0.083	0.142	0.057	0.102
13	0.035	0.043	0.057	0.117	0.073	0.089	0.071	0.098	0.046	0.075	0.064	0.099	0.052	0.095
12	0.019	0.031	0.034	0.072	0.044	0.059	0.044	0.065	0.035	0.051	0.039	0.066	0.035	0.062
11	0.023	0.025	0.026	0.036	0.038	0.044	0.033	0.056	0.026	0.039	0.026	0.055	0.026	0.052
10	0.019	0.023	0.023	0.037	0.041	0.075	0.026	0.075	0.020	0.057	0.025	0.053	0.023	0.053
9	0.012	0.021	0.020	0.058	0.042	0.092	0.027	0.089	0.019	0.069	0.024	0.070	0.022	0.081
8	0.008	0.019	0.011	0.059	0.036	0.068	0.024	0.082	0.021	0.052	0.022	0.063	0.022	0.064
7	0.011	0.018	0.007	0.049	0.041	0.050	0.032	0.073	0.026	0.043	0.028	0.050	0.027	0.048
6	0.012	0.019	0.006	0.038	0.038	0.049	0.032	0.061	0.019	0.041	0.028	0.044	0.023	0.043
5	0.015	0.020	0.006	0.027	0.039	0.054	0.031	0.053	0.017	0.047	0.026	0.042	0.021	0.050
4	0.015	0.020	0.006	0.024	0.026	0.042	0.024	0.029	0.018	0.028	0.021	0.030	0.019	0.030
3	0.017	0.029	0.009	0.036	0.023	0.054	0.034	0.057	0.022	0.040	0.024	0.055	0.023	0.054
2	0.021	0.041	0.026	0.060	0.045	0.071	0.053	0.095	0.034	0.060	0.046	0.082	0.040	0.080
1	0.039	0.070	0.056	0.095	0.078	0.108	0.091	0.151	0.063	0.104	0.086	0.116	0.076	0.112

Table 5.10 Maximum inelastic relative link rotations 20 storey frame in Montreal

Storey	Artificial records(5)-short distance		Artificial records(5)-long distance		Artificial records(10)	
	max γ_{range}		max γ_{range}		max γ_{range}	
	50^{th}	84^{th}	50^{th}	84^{th}	50^{th}	84^{th}
20	0.005	0.006	0.005	0.005	0.005	0.005
19	0.024	0.035	0.029	0.043	0.029	0.043
18	0.027	0.036	0.058	0.089	0.058	0.089
17	0.015	0.019	0.041	0.086	0.041	0.086
16	0.006	0.010	0.013	0.020	0.013	0.020
15	0.006	0.010	0.010	0.015	0.010	0.015
14	0.008	0.012	0.014	0.016	0.014	0.016
13	0.007	0.008	0.011	0.013	0.011	0.013
12	0.005	0.006	0.007	0.007	0.007	0.007
11	0.005	0.005	0.006	0.009	0.006	0.009
10	0.005	0.005	0.006	0.006	0.006	0.006
9	0.005	0.005	0.006	0.006	0.006	0.006
8	0.005	0.005	0.006	0.006	0.006	0.006
7	0.004	0.005	0.005	0.005	0.005	0.005
6	0.005	0.005	0.005	0.006	0.005	0.006
5	0.004	0.005	0.004	0.006	0.004	0.006
4	0.005	0.005	0.005	0.006	0.005	0.006
3	0.004	0.005	0.005	0.006	0.005	0.006
2	0.004	0.004	0.005	0.006	0.005	0.006
1	0.005	0.008	0.006	0.008	0.006	0.008

Table 5.11 Maximum inelastic relative link rotations 25 storey frame in Vancouver

Storey	Historical records(5)-short distance		Artificial records(5)-short distance		Historical records(5)-long distance		Artificial records(5)-long distance		Historical records(10)		Artificial records(10)		All records(20)	
	max γ_{range}		max γ_{range}		max γ_{range}		max γ_{range}		max γ_{range}		max γ_{range}		max γ_{range}	
	50^{th}	84^{th}	50^{th}	84^{th}	50^{th}	84^{th}	50^{th}	84^{th}	50^{th}	84^{th}	50^{th}	84^{th}	50^{th}	84^{th}
25	0.004	0.004	0.005	0.005	0.004	0.004	0.003	0.004	0.004	0.005	0.004	0.005	0.004	0.005
24	0.029	0.036	0.028	0.054	0.031	0.050	0.011	0.037	0.030	0.042	0.021	0.056	0.027	0.050
23	0.056	0.091	0.082	0.102	0.065	0.112	0.034	0.088	0.061	0.106	0.050	0.113	0.055	0.112
22	0.070	0.107	0.070	0.141	0.071	0.103	0.050	0.121	0.071	0.112	0.065	0.152	0.070	0.133
21	0.043	0.103	0.079	0.118	0.059	0.066	0.062	0.117	0.050	0.069	0.066	0.137	0.060	0.084
20	0.042	0.090	0.092	0.133	0.058	0.077	0.047	0.134	0.043	0.077	0.078	0.145	0.053	0.109
19	0.043	0.083	0.095	0.129	0.066	0.102	0.051	0.145	0.056	0.103	0.073	0.134	0.056	0.121
18	0.035	0.066	0.077	0.105	0.070	0.095	0.069	0.127	0.048	0.084	0.073	0.115	0.064	0.107
17	0.022	0.058	0.057	0.084	0.070	0.073	0.072	0.084	0.042	0.072	0.065	0.085	0.055	0.078
16	0.015	0.050	0.038	0.062	0.038	0.058	0.048	0.057	0.036	0.058	0.048	0.060	0.043	0.059
15	0.024	0.032	0.025	0.045	0.028	0.061	0.038	0.052	0.025	0.046	0.038	0.047	0.032	0.047
14	0.019	0.035	0.022	0.037	0.025	0.067	0.033	0.050	0.024	0.039	0.033	0.040	0.033	0.042
13	0.014	0.029	0.015	0.021	0.022	0.057	0.030	0.040	0.022	0.037	0.022	0.031	0.022	0.033
12	0.010	0.020	0.007	0.025	0.016	0.046	0.022	0.029	0.013	0.031	0.019	0.025	0.015	0.025
11	0.007	0.021	0.006	0.029	0.015	0.043	0.020	0.029	0.013	0.030	0.017	0.030	0.014	0.030
10	0.006	0.022	0.007	0.028	0.018	0.042	0.019	0.028	0.014	0.030	0.016	0.029	0.015	0.030
9	0.008	0.020	0.006	0.024	0.017	0.040	0.018	0.024	0.013	0.028	0.017	0.024	0.015	0.024
8	0.008	0.020	0.006	0.024	0.019	0.040	0.019	0.023	0.013	0.026	0.019	0.024	0.017	0.024
7	0.012	0.023	0.006	0.024	0.022	0.037	0.020	0.024	0.017	0.024	0.020	0.025	0.020	0.024
6	0.012	0.019	0.006	0.022	0.020	0.027	0.023	0.028	0.015	0.022	0.020	0.026	0.018	0.025
5	0.013	0.018	0.006	0.022	0.019	0.027	0.022	0.033	0.014	0.025	0.019	0.031	0.016	0.029
4	0.019	0.022	0.012	0.027	0.019	0.029	0.024	0.040	0.019	0.025	0.021	0.036	0.020	0.032
3	0.024	0.031	0.019	0.037	0.025	0.036	0.026	0.054	0.025	0.036	0.025	0.043	0.025	0.038
2	0.035	0.043	0.027	0.046	0.034	0.040	0.033	0.073	0.035	0.041	0.030	0.055	0.034	0.048
1	0.047	0.058	0.038	0.058	0.043	0.052	0.051	0.099	0.047	0.056	0.045	0.073	0.047	0.059

Table 5.12 Maximum inelastic relative link rotations 25 storey frame in Montreal

Storey	Artificial records(5)-short distance		Artificial records(5)-long distance		Artificial records (10)	
	max γ_{range}		max γ_{range}		max γ_{range}	
	50^{th}	84^{th}	50^{th}	84^{th}	50^{th}	84^{th}
25	0.006	0.006	0.005	0.005	0.005	0.006
24	0.023	0.026	0.024	0.037	0.023	0.031
23	0.026	0.030	0.038	0.063	0.030	0.052
22	0.012	0.027	0.041	0.052	0.036	0.048
21	0.008	0.015	0.028	0.035	0.022	0.031
20	0.007	0.012	0.023	0.025	0.014	0.023
19	0.007	0.010	0.015	0.025	0.010	0.020
18	0.006	0.006	0.008	0.015	0.007	0.011
17	0.005	0.006	0.009	0.013	0.008	0.012
16	0.005	0.006	0.007	0.010	0.006	0.009
15	0.005	0.006	0.006	0.010	0.006	0.008
14	0.005	0.006	0.006	0.008	0.006	0.007
13	0.005	0.005	0.006	0.008	0.005	0.006
12	0.004	0.005	0.006	0.008	0.005	0.006
11	0.004	0.005	0.005	0.008	0.005	0.006
10	0.004	0.005	0.006	0.008	0.005	0.006
9	0.004	0.004	0.004	0.005	0.004	0.004
8	0.004	0.004	0.005	0.006	0.004	0.005
7	0.004	0.004	0.005	0.005	0.004	0.005
6	0.004	0.004	0.005	0.005	0.004	0.005
5	0.004	0.005	0.005	0.006	0.004	0.006
4	0.004	0.004	0.005	0.006	0.004	0.006
3	0.004	0.004	0.005	0.006	0.005	0.006
2	0.004	0.004	0.005	0.005	0.004	0.005
1	0.004	0.005	0.007	0.009	0.006	0.008

Table 5.13 Axial forces in the columns (kN) for the 14 storeys frame in Vancouver

Storey	$P_{col}^{gravity}$	Ductility Design SS (1.15Vp)	Results from NLTHA Historical records		Results from NLTHA Artificial records		Capacity of the section
			50^{th}	84^{th}	50^{th}	84^{th}	C_{ry} eq.13.8.2. (c)
14	123	163	124	126	124	126	1497
13	556	977	703	742	709	760	1497
12	989	1980	1516	1590	1527	1609	4754
11	1422	3090	2455	2670	2504	2583	4754
10	1855	4367	3686	4005	3648	3845	7341
9	2288	5760	4885	5113	4876	5187	7341
8	2721	7254	6108	6516	6212	6519	11526
7	3154	8933	7662	8041	7493	8016	11526
6	3587	10667	9135	9455	8859	9587	17452
5	4020	12507	10577	11068	10359	11155	17452
4	4453	14437	12228	12765	12062	12691	21438
3	4886	16449	13567	14457	13419	14225	21438
2	5319	18570	15320	16160	15341	15845	28880
1	5752	20976	16588	17855	16941	17866	28880

Table 5.14 Axial forces in the columns (kN) for the 14 storeys frame in Montreal

Storey	$P_{col}^{gravity}$	Ductility Design SS (1.15Vp)	Results from NLTHA Artificial records		Capacity of the section
			50^{th}	84^{th}	C_{ry} eq.13.8.2. (c)
14	141	180	145	147	1885
13	574	995	725	748	1885
12	1007	1998	1504	1533	3896
11	1440	3096	2380	2421	3896
10	1873	4198	3323	3382	5990
9	2306	5383	4169	4298	5990
8	2739	6678	4986	5160	14530
7	3171	8071	5831	5964	14530
6	3604	9555	6563	6796	19455
5	4037	11124	7156	7503	19455
4	4470	12804	7470	8041	26419
3	4903	14538	7999	8736	26419
2	5336	16373	8612	9291	23405
1	5769	18372	9692	9918	23012

Table 5.15 Axial forces in the columns (kN) for the 20 storeys frame in Vancouver

Storey	$P_{col}^{gravity}$	Ductility Design SS (1.15Vp)	Results from NLTHA Artificial records		Results from NLTHA Historical records		Capacity of the section
			50^{th}	84^{th}	50^{th}	84^{th}	C_{ry} eq.13.8.2.(c)
20	123	178	126	127	124	126	1885
19	556	1307	675	735	693	760	1885
18	989	2487	1478	1628	1571	1690	10468
17	1422	3763	2578	2785	2613	2859	10468
16	1855	5163	3841	3959	3910	4129	10468
15	2288	6732	5160	5427	5247	5415	17024
14	2721	8420	6586	6981	6790	7028	17024
13	3154	10262	8330	8597	8126	8550	17024
12	3587	12200	10019	10463	9610	10260	46886
11	4020	14302	11523	12259	11430	12023	46886
10	4453	16524	13581	14250	12825	13465	46886
9	4886	18853	15146	16102	14666	15939	60471
8	5319	21195	16827	17958	16165	17828	60471
7	5752	23687	18085	19561	17566	19825	60471
6	6185	26189	19763	21715	19415	21523	92319
5	6618	28818	22126	23999	20820	23354	92319
4	7051	31466	24062	26220	22651	25206	92319
3	7484	34328	26139	28431	24147	26425	92319
2	7917	37190	27310	30561	25917	28583	92319
1	8349	40298	29606	32395	27790	30718	90394

Table 5.16 Axial forces in the columns (kN) for the 20 storeys frame in Montreal

Storey	$P_{col}^{gravity}$	Ductility Design SS (1.15Vp)	Results from NLTHA Artificial Records (kN)		Capacity of the section
			50^{th}	84^{th}	Cry eq.13.8.2. (c)
20	141	180	142	143	1885
19	574	1135	686	724	1885
18	1007	2132	1456	1502	8588
17	1440	3151	2314	2364	8588
16	1873	4262	3209	3348	8588
15	2306	5535	4022	4319	12671
14	2739	6895	4822	5278	12671
13	3171	8288	5747	6093	12671
12	3604	9782	6658	7072	46886
11	4037	11460	7521	7958	46886
10	4470	13177	8199	8984	46886
9	4903	15019	8717	9904	60471
8	5336	16943	9420	10743	60471
7	5769	18881	10170	11373	60471
6	6202	20973	10802	12166	75616
5	6635	23075	11604	12766	75616
4	7068	25288	12267	13350	75616
3	7501	27510	12950	13814	75616
2	7934	29852	13740	14472	75616
1	8367	32551	14309	15518	73619

Table 5.17 Axial forces in the columns (kN) for the 25 storeys frame in Vancouver

Storey	$P_{col}^{gravity}$	Ductility Design SS (1.15Vp)	Results from NLTHA - Artificial records		Results from NLTHA - Historical records		Capacity of the section
			50^{th}	84^{th}	50^{th}	84^{th}	Cry eq.13.8.2. (c)
25	123	178	123	125	123	125	2967
24	556	1317	666	723	734	765	2967
23	989	2626	1579	1728	1669	1764	9558
22	1422	3994	2800	2987	2752	2862	9558
21	1855	5488	4021	4312	4196	4326	23263
20	2288	7176	5488	5797	5611	5808	23263
19	2721	9018	6929	7266	7090	7348	23263
18	3154	10953	8764	8972	8599	8974	60471
17	3587	13021	10536	10971	10385	10549	60471
16	4020	15244	12476	12897	12035	12633	60471
15	4453	17586	14564	15358	14187	14750	92319
14	4886	20077	16447	17321	15862	16537	92319
13	5319	22580	18558	19378	17569	18892	92319
12	5752	25228	20788	21689	19098	20982	130403
11	6185	28090	22691	23844	20927	22942	130403
10	6618	30951	24776	25814	22759	24955	130403
9	7051	33828	26755	28115	24517	26876	130403
8	7484	36876	29248	30575	26156	28785	130403
7	7917	39924	30117	32636	27611	30565	130403
6	8349	42992	31925	34799	29511	32357	151786
5	8782	46289	35354	37763	31225	34054	151786
4	9215	49586	37359	40314	32813	35777	151786
3	9648	52883	39354	42974	34008	37777	151786
2	10081	56181	41176	45512	35192	40620	151786
1	10514	59793	43175	48125	37107	43180	150075

Table 5.18 Axial forces in the columns (kN) for the 25 storeys frame in Montreal

Storey	$P_{col}^{gravity}$	DuctilityDesign SS (1.15Vp)	Results from NLTHA		Capacity of the section
			50^{th}	84^{th}	Cry eq.13.8.2. c)
25	141	180	143	144	1885
24	574	1135	716	737	1885
23	1007	2132	1481	1532	3233
22	1440	3151	2317	2371	3233
21	1873	4254	3220	3307	12671
20	2306	5437	4113	4298	12671
19	2739	6711	5032	5311	12671
18	3171	8078	5814	6236	60471
17	3604	9562	6798	7202	60471
16	4037	11131	7586	8058	60471
15	4470	12809	8339	8819	92319
14	4903	14526	9094	9769	92319
13	5336	16368	9984	10717	92319
12	5769	18303	10746	11494	92319
11	6202	20359	11587	12354	92319
10	6635	22417	12367	13336	92319
9	7068	24519	13011	14086	130403
8	7501	26741	13465	14814	130403
7	7934	29070	14115	15740	130403
6	8367	31413	14790	16592	151786
5	8800	33904	15475	17348	151786
4	9233	36406	15946	17779	151786
3	9666	39035	16661	18438	174734
2	10099	41683	17572	18878	174734
1	10532	44791	18358	19368	173087

Table 5.19 Bending moments in the columns (kNm) for the 14 storey frame in Vancouver

Storey	Capacity of the section (kNm)	Results from NLTHA Artificial records (kNm)		Column moments (% from Mp)		Results from NLTHA Historical records (kNm)		Column moments (% from Mp)	
	Mp	50^{th}	84^{th}	50^{th}	84^{th}	50^{th}	84^{th}	50^{th}	84^{th}
14	229	56	86	24	38	63	94	28	41
13	229	81	102	35	45	81	124	35	54
12	847	116	227	14	27	200	348	24	41
11	847	159	241	19	28	265	353	31	42
10	2044	214	318	10	16	305	525	15	26
9	2044	337	442	16	22	426	686	21	34
8	2552	330	457	13	18	370	703	14	28
7	2552	200	739	8	29	278	328	11	13
6	4235	319	521	8	12	347	459	8	11
5	4235	314	646	7	15	376	629	9	15
4	6230	466	763	7	12	426	783	7	13
3	6230	571	845	9	14	425	777	7	12
2	8820	573	1045	6	12	502	1100	6	12
1	8820	471	1056	5	12	407	997	5	11

Table 5.20 Bending moments in the columns (kNm) for the 14 storey frame in Montreal

Storey	Capacity of the section (kNm)	Results from NLTHA Artificial records (kNm)		Column moments (% from Mp)	
	Mp	50^{th}	84^{th}	50^{th}	84^{th}
14	501	63	81	13	16
13	501	49	70	10	14
12	683	57	78	8	11
11	683	63	105	9	15
10	1663	80	132	5	8
9	1663	81	132	5	8
8	3535	92	117	3	3
7	3535	109	134	3	4
6	5180	128	168	2	3
5	5180	163	200	3	4
4	7420	199	270	3	4
3	7420	241	286	3	4
2	7385	219	261	3	4
1	7385	216	266	3	4

Table 5.21 Bending moments in the columns (kNm) for the 20 storey frame in Vancouver

Storey	Capacity of the section (kNm)	Results from NLTHA Artificial records (kNm)		Column moments (% from Mp)		Results from NLTHA Historical records (kNm)		Column moments (% from Mp)	
	Mp	50^{th}	84^{th}	50^{th}	84^{th}	50^{th}	84^{th}	50^{th}	84^{th}
20	501	72	110	14	22	72	107	14	21
19	501	90	194	18	39	86	135	17	27
18	2034	229	336	11	17	194	365	10	18
17	2034	282	442	14	22	328	424	16	21
16	2034	389	578	19	28	354	542	17	27
15	3458	421	657	12	19	337	535	10	15
14	3458	325	604	9	17	321	445	9	13
13	3458	294	455	9	13	342	430	10	12
12	5600	239	544	4	10	264	557	5	10
11	5600	214	479	4	9	198	504	4	9
10	5600	171	552	3	10	178	322	3	6
9	7973	239	433	3	5	237	404	3	5
8	7973	288	414	4	5	257	463	3	6
7	7973	257	457	3	6	266	487	3	6
6	14558	301	674	2	5	322	607	2	4
5	14558	417	953	3	7	445	790	3	5
4	14558	505	1000	3	7	595	854	4	6
3	14558	855	1149	6	8	621	1166	4	8
2	14558	1279	1704	9	12	549	1238	4	9
1	14558	1271	1759	9	12	566	1254	4	9

Table 5.22 Bending moments in the columns (kNm) for the 20 storey frame in Montreal

Storey	Capacity of the section (kNm)	Results from NLTHA Artificial records (kNm)		Col.moments (% from Mp)	
	Mp	50^{th}	84^{th}	50^{th}	84^{th}
20	501	44	63	9	13
19	501	52	137	10	27
18	1642	108	176	7	11
17	1642	126	279	8	17
16	1642	93	279	6	17
15	2499	69	102	3	4
14	2499	78	118	3	5
13	2499	52	109	2	4
12	5600	53	87	1	2
11	5600	57	78	1	1
10	5600	58	74	1	1
9	7973	80	85	1	1
8	7973	87	95	1	1
7	7973	87	101	1	1
6	10938	118	135	1	1
5	10938	123	152	1	1
4	10938	137	157	1	1
3	10938	138	155	1	1
2	10938	136	154	1	1
1	10938	120	143	1	1

Table 5.23 Bending moments in the columns (kNm) for the 25 storey frame in Vancouver

Storey	Capacity of the section(kNm)	Results from NLTHA - Artificial records		Col.moments (%Mp)		Results from NLTHA - Historical records		Col.moments (%Mp)	
	Mp	50^{th}	84^{th}	50^{th}	84^{th}	50^{th}	84^{th}	50^{th}	84^{th}
25	658	50	108	8	16	62	76	9	12
24	658	86	163	13	25	100	195	15	30
23	1841	167	271	9	15	188	231	10	13
22	1841	249	417	14	23	345	464	19	25
21	4585	438	506	10	11	444	631	10	14
20	4585	444	565	10	12	374	604	8	13
19	4585	460	632	10	14	357	529	8	12
18	7973	532	701	7	9	467	640	6	8
17	7973	591	729	7	9	500	799	6	10
16	7973	505	584	6	7	464	531	6	7
15	14558	395	536	3	4	440	586	3	4
14	14558	379	567	3	4	373	700	3	5
13	14558	533	789	4	5	482	679	3	5
12	24030	573	838	2	3	540	720	2	3
11	24030	510	696	2	3	533	735	2	3
10	24030	551	674	2	3	558	742	2	3
9	24030	538	753	2	3	640	732	3	3
8	24030	523	709	2	3	535	829	2	3
7	24030	613	972	3	4	643	1029	3	4
6	30013	807	1051	3	4	871	1380	3	5
5	30013	563	1156	2	4	907	1568	3	5
4	30013	599	1337	2	4	866	1615	3	5
3	30013	680	1586	2	5	956	1467	3	5
2	30013	601	1836	2	6	898	1386	3	5
1	30013	538	1627	2	5	786	1443	3	5

Table 5.24 Bending moments in the columns (kNm) for the 25 storey frame in Montreal

Storey	Capacity of the section (kNm)	Results from NLTHA		Col.moments (%Mp)	
	Mp	50^{th}	84^{th}	50^{th}	84^{th}
25	501	38	50	8	10
24	501	33	61	7	12
23	721	48	58	7	8
22	721	52	91	7	13
21	2499	94	130	4	5
20	2499	99	124	4	5
19	2499	86	123	3	5
18	7973	86	125	1	2
17	7973	84	113	1	1
16	7973	85	114	1	1
15	14558	143	182	1	1
14	14558	147	187	1	1
13	14558	146	171	1	1
12	14558	140	168	1	1
11	14558	156	162	1	1
10	14558	183	216	1	1
9	24030	292	357	1	1
8	24030	301	367	1	2
7	24030	296	343	1	1
6	30013	303	382	1	1
5	30013	311	388	1	1
4	30013	296	428	1	1
3	36914	337	442	1	1
2	36914	353	457	1	1
1	36914	313	397	1	1

Table 5.25 Maximum total drifts for the 14 storey frame in Vancouver

Storey	Historical records(5)-short distance		Artificial records(5)-short distance		Historical records(5)-long distance		Artificial records(5)-long distance		Historical records (10)		Artificial records (10)		All records (20)		All records	NBCC 2005
	Δ_{total}		Δ_{total}		Δ_{total}		Δ_{total}		Δ_{total}		Δ_{total}		Δ_{total}		Δ_{total}	Δ_{total}
	50^{th}	84^{th}	50^{th}	84^{th}	50^{th}	84^{th}	50^{th}	84^{th}	50^{th}	84^{th}	50^{th}	84^{th}	50^{th}	84^{th}	max	max
14	19.8	20.4	20.3	23.3	23.0	23.6	20.3	23.5	20.0	23.1	20.3	23.6	20.2	23.5	24.8	92.5
13	64.8	93.4	66.6	72.8	50.6	55.3	43.8	44.4	51.8	80.0	44.5	67.1	49.2	67.5	95.9	92.5
12	40.3	118.1	47.0	72.8	50.3	59.6	56.7	63.9	46.8	84.0	49.3	66.3	48.7	71.5	158.4	92.5
11	38.2	91.2	35.0	77.4	45.1	59.9	51.0	59.9	41.7	75.1	46.4	60.2	43.4	62.3	120.0	92.5
10	36.3	61.2	39.5	86.5	65.5	73.1	53.0	58.6	37.7	74.0	46.3	62.1	39.3	71.3	125.7	92.5
9	31.5	52.7	41.7	72.2	46.0	60.3	46.1	57.6	36.3	60.4	43.9	58.7	40.1	60.4	107.1	92.5
8	25.1	42.9	31.1	49.1	30.8	35.5	41.2	47.4	30.4	35.7	35.6	47.8	31.0	46.4	65.0	92.5
7	20.6	38.0	29.9	31.1	27.7	38.4	36.8	41.3	27.2	38.0	31.4	37.5	30.1	38.0	50.3	92.5
6	21.6	30.4	24.4	31.5	27.3	39.1	36.7	44.4	25.4	33.3	31.3	40.3	27.2	37.8	59.6	92.5
5	20.3	27.9	20.7	30.9	24.9	36.7	32.5	49.5	23.6	30.3	29.6	43.3	25.5	41.1	57.8	92.5
4	17.0	23.4	16.7	31.2	32.3	33.2	29.2	48.2	24.1	32.7	25.7	43.9	24.1	33.4	61.0	92.5
3	16.5	18.9	12.7	35.4	26.3	34.9	30.4	45.9	22.0	29.7	23.2	48.6	22.7	39.1	55.6	92.5
2	17.3	19.0	11.9	39.6	27.1	38.2	31.5	44.6	21.8	30.0	22.2	44.6	21.8	44.0	62.3	92.5
1	23.4	26.9	16.9	52.6	36.0	55.4	39.9	51.0	29.1	42.0	28.1	53.9	29.1	46.7	81.0	112.5

Table 5.26 Maximum total drifts for the 14 storey frame in Montreal

Storey	Artificial records(5)-short distance		Artificial records(5)-long distance		Artificial records(10)		All records	NBCC 2005
	Δ_{total}		Δ_{total}		Δ_{total}		Δ_{total}	Δ_{total}
	50^{th}	84^{th}	50^{th}	84^{th}	50^{th}	84^{th}	max	max
14	12.4	13.0	12.9	13.3	12.9	13.2	13.4	92.5
13	17.8	19.4	20.7	22.9	19.6	21.7	25.9	92.5
12	15.0	16.4	20.6	22.9	17.8	21.7	25.8	92.5
11	16.9	17.4	23.1	25.9	18.0	24.7	26.2	92.5
10	15.1	16.5	15.5	16.5	15.3	16.6	17.3	92.5
9	11.0	11.8	11.8	12.8	11.7	12.1	14.8	92.5
8	10.5	11.1	9.7	12.0	10.1	11.7	12.4	92.5
7	9.1	10.2	9.1	10.2	9.1	10.3	10.8	92.5
6	8.2	9.7	9.0	9.5	9.0	9.5	9.9	92.5
5	7.9	8.7	8.7	9.4	8.5	9.1	10.0	92.5
4	8.0	8.4	8.8	10.0	8.3	9.6	11.0	92.5
3	7.5	8.0	8.4	9.6	8.1	8.7	12.3	92.5
2	7.6	8.4	8.8	10.0	8.5	9.3	11.8	92.5
1	9.4	10.2	10.9	12.5	10.1	11.8	13.9	112.5

Table 5.27 Maximum total drifts for the 20 storey frame in Vancouver

Storey	Historical records (10)		Artificial records (10)		All records (20)		All records	NBCC 2005
	Δ_{total}		Δ_{total}		Δ_{total}		Δ_{total}	Δ_{total}
	50^{th}	84^{th}	50^{th}	84^{th}	50^{th}	84^{th}	max	max
20	15.5	17.0	16.0	18.4	16.0	18.1	20.3	92.5
19	24.8	29.8	25.3	43.0	25.3	36.6	48.3	92.5
18	32.2	37.8	30.9	59.9	31.5	41.0	80.4	92.5
17	33.9	39.8	33.3	67.1	33.4	39.9	96.6	92.5
16	33.4	39.2	39.0	74.7	35.6	44.2	101.5	92.5
15	31.0	38.9	46.8	76.4	38.8	56.6	93.2	92.5
14	26.4	47.0	44.3	63.2	36.5	49.7	90.7	92.5
13	28.5	43.2	36.8	49.9	31.0	48.0	78.8	92.5
12	27.4	33.9	27.2	40.6	27.4	38.2	57.5	92.5
11	22.3	29.2	23.4	34.6	23.1	32.0	38.7	92.5
10	20.3	32.6	21.8	32.7	21.3	35.1	54.0	92.5
9	17.9	37.1	22.2	36.7	20.3	37.8	65.9	92.5
8	18.9	30.7	21.0	32.1	19.9	32.3	64.5	92.5
7	18.9	24.4	20.8	28.4	20.1	26.1	54.8	92.5
6	17.4	26.2	20.2	26.0	19.0	26.3	42.9	92.5
5	15.9	24.5	18.9	25.2	17.5	25.8	31.2	92.5
4	14.8	18.1	17.8	21.8	15.8	19.7	33.9	92.5
3	15.3	22.7	17.2	28.4	16.9	28.0	36.8	92.5
2	18.0	29.0	23.8	36.1	21.7	35.7	47.8	92.5
1	30.7	44.7	42.9	55.3	39.9	50.3	84.2	112.5

Table 5.28 Maximum total drifts for the 20 storey frame in Montreal

Storey	Artificial records (10) Δ_{total}		All records Δ_{total}	NBCC 2005 Δ_{total}
	50^{th}	84^{th}	max	max
20	8.9	10.4	11.1	92.5
19	15.2	21.0	28.9	92.5
18	17.1	36.7	45.8	92.5
17	14.7	31.9	40.0	92.5
16	11.6	15.2	19.0	92.5
15	10.5	14.4	18.2	92.5
14	10.8	13.8	15.3	92.5
13	9.2	12.1	13.7	92.5
12	8.5	10.0	12.1	92.5
11	8.0	10.1	12.0	92.5
10	7.3	9.4	10.1	92.5
9	7.3	8.9	9.6	92.5
8	7.2	8.3	10.1	92.5
7	6.8	7.4	9.9	92.5
6	6.4	7.4	10.2	92.5
5	6.3	7.3	9.6	92.5
4	6.5	7.2	9.3	92.5
3	6.5	7.3	8.8	92.5
2	6.5	7.2	8.1	92.5
1	8.3	9.6	11.5	112.5

Table 5.29 Maximum total drifts for the 25 storey frame in Vancouver

Storey	Historical records (10)		Artificial records (10)		All records (20)		All records	NBCC 2005
	Δ_{total}		Δ_{total}		Δ_{total}		Δ_{total}	Δ_{total}
	50^{th}	84^{th}	50^{th}	84^{th}	50^{th}	84^{th}	max	max
25	14.9	16.4	17.1	18.4	15.4	17.9	19.6	92.5
24	22.3	26.3	21.8	31.6	22.1	28.0	38.7	92.5
23	29.0	46.4	29.7	49.7	29.0	47.1	61.2	92.5
22	30.3	48.2	33.1	62.6	31.4	52.0	74.9	92.5
21	28.5	35.9	36.0	61.9	29.9	41.6	87.7	92.5
20	29.0	38.9	36.8	67.0	30.6	54.7	85.7	92.5
19	29.9	48.1	40.9	63.4	33.2	58.3	79.6	92.5
18	28.3	41.6	41.0	56.6	31.6	52.6	65.5	92.5
17	27.9	37.0	37.6	45.1	32.6	43.6	50.2	92.5
16	24.2	31.9	30.2	36.3	27.7	34.8	41.0	92.5
15	21.5	29.5	28.8	32.3	23.1	30.8	48.2	92.5
14	20.5	26.9	27.4	28.8	22.7	28.1	55.9	92.5
13	19.8	23.6	22.2	25.2	21.5	24.9	53.3	92.5
12	16.7	22.9	19.8	23.4	18.9	24.0	48.0	92.5
11	15.6	22.2	20.3	23.0	17.2	23.9	46.2	92.5
10	15.3	21.5	19.3	22.8	17.1	23.3	45.5	92.5
9	15.0	20.3	17.9	21.3	16.9	21.7	43.6	92.5
8	15.4	20.0	18.1	20.0	17.1	20.1	39.9	92.5
7	15.9	18.7	18.5	20.4	17.3	19.9	33.3	92.5
6	14.0	18.0	17.5	20.4	16.4	20.0	24.8	92.5
5	13.3	17.4	17.0	21.4	15.4	18.6	23.7	92.5
4	15.1	16.7	16.3	22.5	15.5	20.9	28.9	92.5
3	17.0	18.9	16.8	24.3	17.0	22.4	36.4	92.5
2	18.4	22.5	16.1	27.7	16.6	23.3	43.8	92.5
1	23.4	30.3	21.9	38.2	21.9	31.4	60.1	112.5

Table 5.30 Maximum total drifts for the 25 storey frame in Montreal

Storey	Artificial records (10) Δ_{total}		All records Δ_{total}	NBCC 2005 Δ_{total}
	50^{th}	84^{th}	max	max
25	9.5	11.1	11.7	92.5
24	13.8	16.4	22.0	92.5
23	17.1	23.8	29.8	92.5
22	17.2	20.8	27.0	92.5
21	13.9	16.7	18.2	92.5
20	10.8	13.7	13.8	92.5
19	8.6	13.5	16.7	92.5
18	8.2	11.1	14.1	92.5
17	8.4	11.0	12.0	92.5
16	7.9	9.8	11.0	92.5
15	7.5	9.9	11.1	92.5
14	7.0	8.8	11.2	92.5
13	6.9	8.3	12.7	92.5
12	6.6	7.7	13.3	92.5
11	6.2	7.1	13.5	92.5
10	5.8	6.3	12.7	92.5
9	6.0	6.4	11.6	92.5
8	5.5	6.0	10.1	92.5
7	5.4	5.9	8.8	92.5
6	5.3	6.2	8.2	92.5
5	5.3	6.2	7.8	92.5
4	5.4	6.0	7.4	92.5
3	5.6	6.0	7.4	92.5
2	5.3	6.3	7.6	92.5
1	6.5	8.1	10.2	112.5

Table 5.31 Relation of the inelastic link rotation γ to the inter storey drift Δ – Vancouver

Storey	NLTHA (Max γ_{max}/Max Δ_{max}) at each storey								
	Historical records	Artificial records	All records (20)	Historical records	Artificial records	All records (20)	Historical records	Artificial records	All records (20)
25							0.0002	0.0002	0.0002
24							0.0019	0.0019	0.0019
23							0.0024	0.0022	0.0024
22							0.0024	0.0023	0.0024
21							0.0025	0.0023	0.0025
20				0.0002	0.0002	0.0002	0.0025	0.0023	0.0025
19				0.0016	0.0022	0.0022	0.0023	0.0023	0.0023
18				0.0020	0.0022	0.0022	0.0021	0.0022	0.0022
17				0.0022	0.0023	0.0023	0.0019	0.0018	0.0019
16				0.0020	0.0024	0.0024	0.0018	0.0016	0.0018
15				0.0018	0.0024	0.0024	0.0017	0.0015	0.0017
14	0.0004	0.0002	0.0004	0.0020	0.0023	0.0023	0.0019	0.0016	0.0019
13	0.0025	0.0024	0.0025	0.0021	0.0022	0.0022	0.0018	0.0015	0.0018
12	0.0027	0.0023	0.0027	0.0016	0.0020	0.0020	0.0018	0.0012	0.0018
11	0.0025	0.0024	0.0025	0.0014	0.0015	0.0015	0.0017	0.0011	0.0017
10	0.0024	0.0024	0.0024	0.0018	0.0020	0.0020	0.0018	0.0011	0.0018
9	0.0023	0.0024	0.0024	0.0020	0.0022	0.0022	0.0018	0.0010	0.0018
8	0.0019	0.0020	0.0020	0.0018	0.0022	0.0022	0.0017	0.0010	0.0017
7	0.0016	0.0019	0.0019	0.0017	0.0021	0.0021	0.0015	0.0012	0.0015
6	0.0020	0.0019	0.0020	0.0016	0.0019	0.0019	0.0012	0.0013	0.0013
5	0.0020	0.0023	0.0023	0.0016	0.0017	0.0017	0.0012	0.0015	0.0015
4	0.0018	0.0024	0.0024	0.0018	0.0014	0.0018	0.0014	0.0017	0.0017
3	0.0021	0.0024	0.0024	0.0020	0.0019	0.0020	0.0017	0.0021	0.0021
2	0.0023	0.0024	0.0024	0.0022	0.0023	0.0023	0.0019	0.0023	0.0023
1	0.0021	0.0021	0.0021	0.0020	0.0022	0.0022	0.0018	0.0020	0.0020
50th	0.0021	0.0024	0.0024	0.0018	0.0022	0.0022	0.0018	0.0017	0.0019

Table 5.32 Relation of the inelastic link rotation γ to the inter storey drift Δ – Montreal

Storey	NLTHA (Max γ_{max}/Max Δ_{max}) at each storey Artificial records		
25			0.0004
24			0.0020
23			0.0021
22			0.0019
21			0.0017
20		0.0005	0.0015
19		0.0020	0.0016
18		0.0023	0.0013
17		0.0022	0.0009
16		0.0011	0.0008
15		0.0011	0.0009
14	0.0003	0.0014	0.0005
13	0.0017	0.0012	0.0008
12	0.0013	0.0005	0.0009
11	0.0018	0.0007	0.0010
10	0.0012	0.0005	0.0009
9	0.0007	0.0004	0.0005
8	0.0005	0.0005	0.0005
7	0.0004	0.0005	0.0005
6	0.0004	0.0005	0.0005
5	0.0004	0.0005	0.0005
4	0.0005	0.0005	0.0005
3	0.0008	0.0005	0.0005
2	0.0009	0.0005	0.0005
1	0.0009	0.0008	0.0008
50^{th}	0.0012	0.0014	0.0013

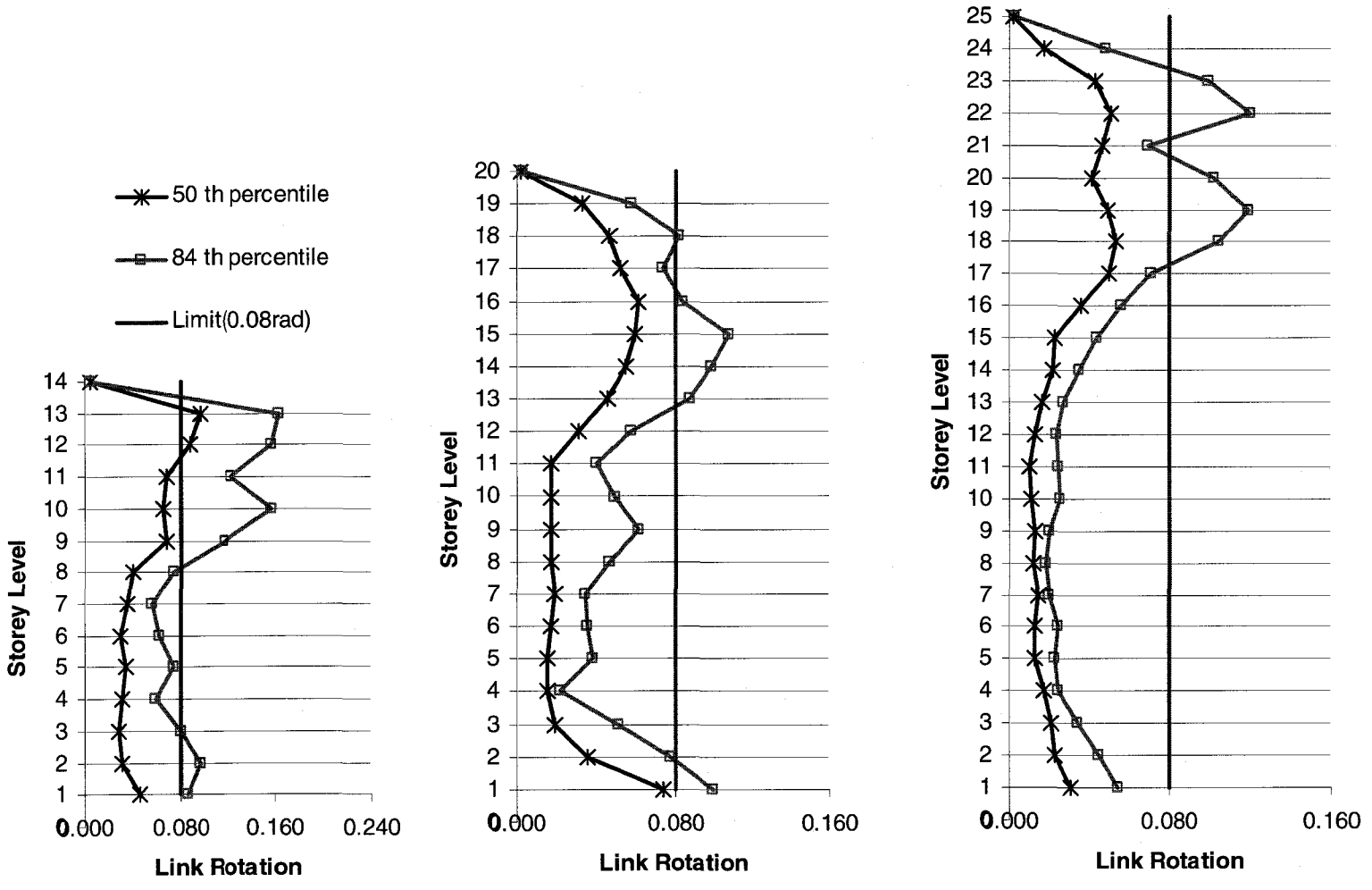

Figure 5.1 Inelastic link rotations Vancouver

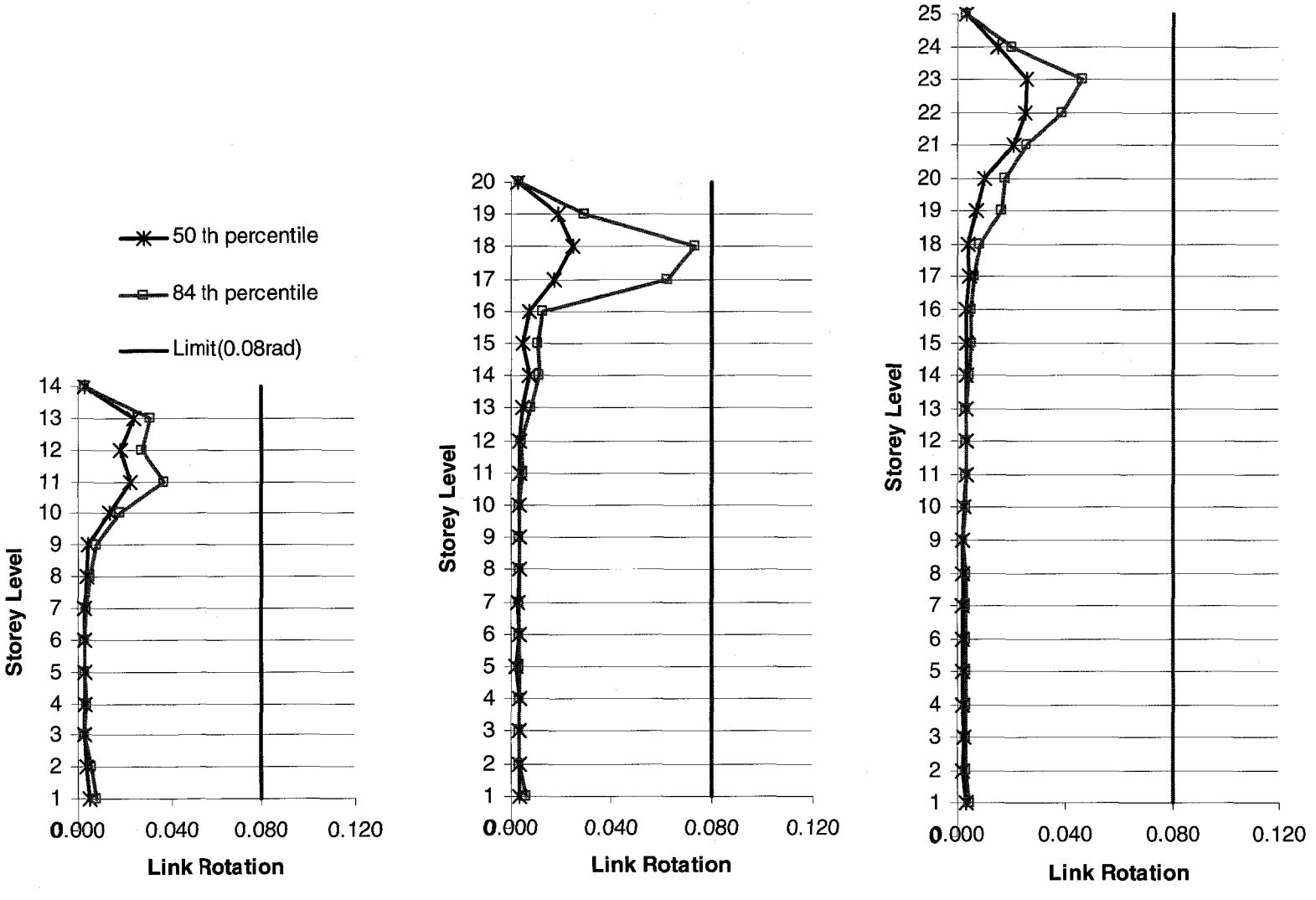

Figure 5.2 Inelastic link rotations Montreal

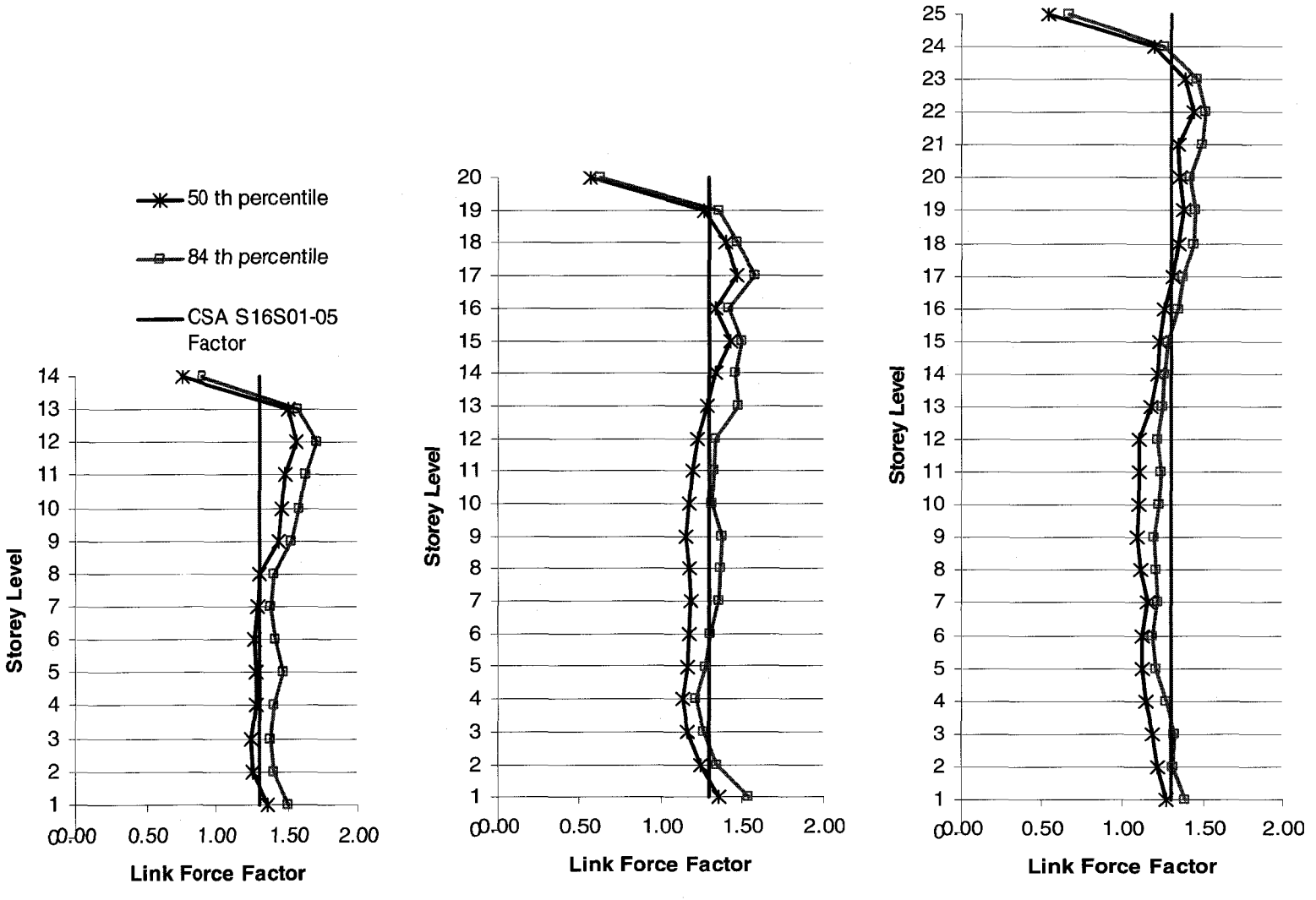

Figure 5.3 Maximum link shear force factor Vancouver

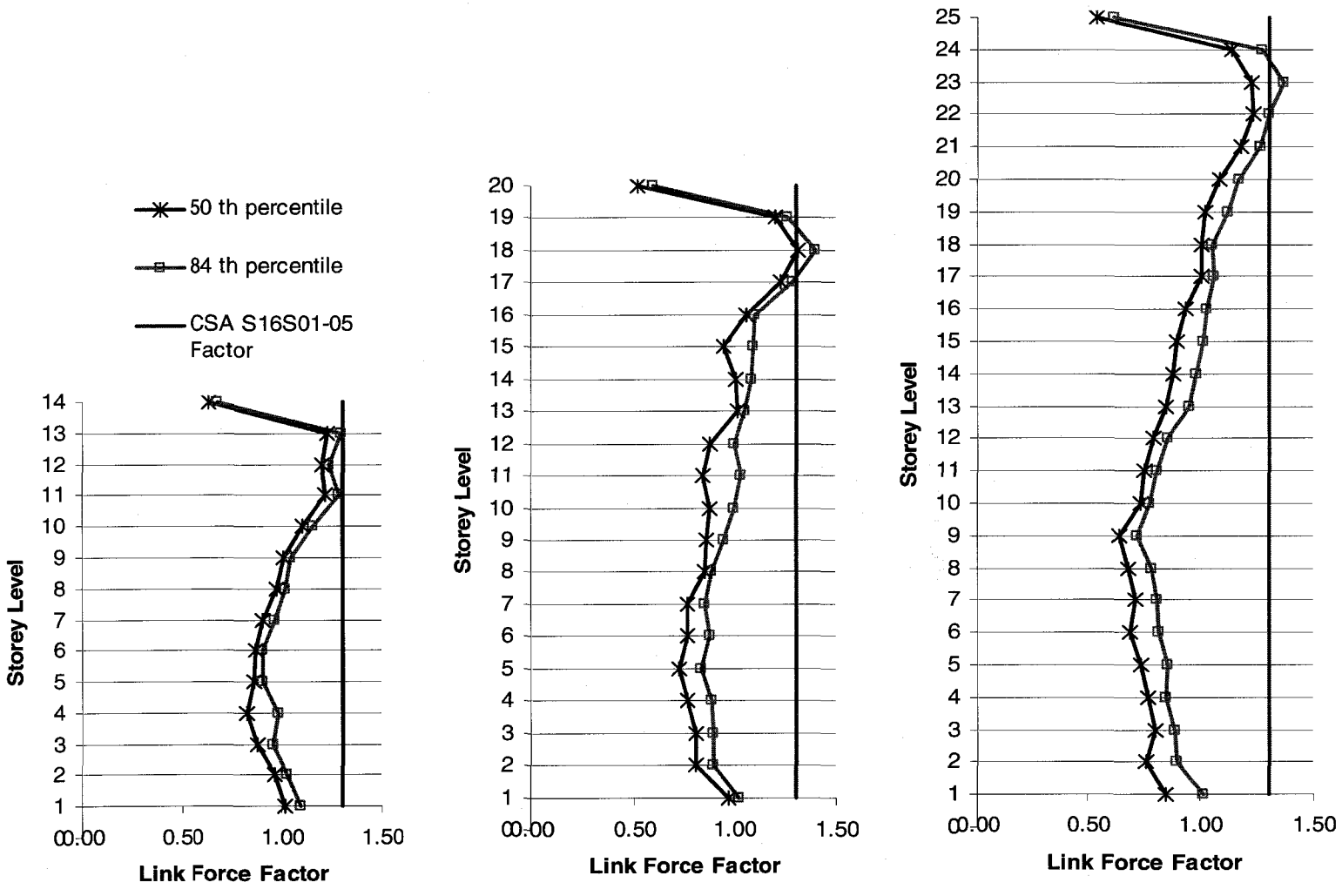

Figure 5.4 Maximum link shear force factor Montreal

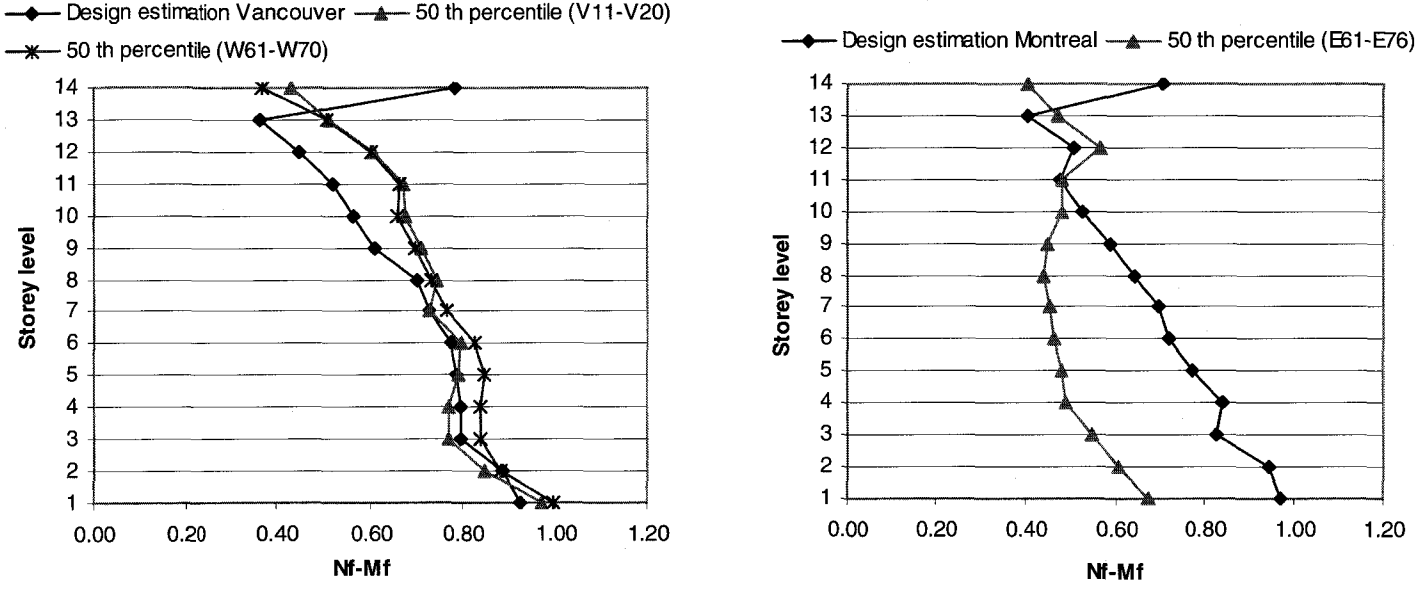

Figure 5.5 Capacity of the braces (14 storeys): Comparison between design estimates and results obtained from dynamic analysis

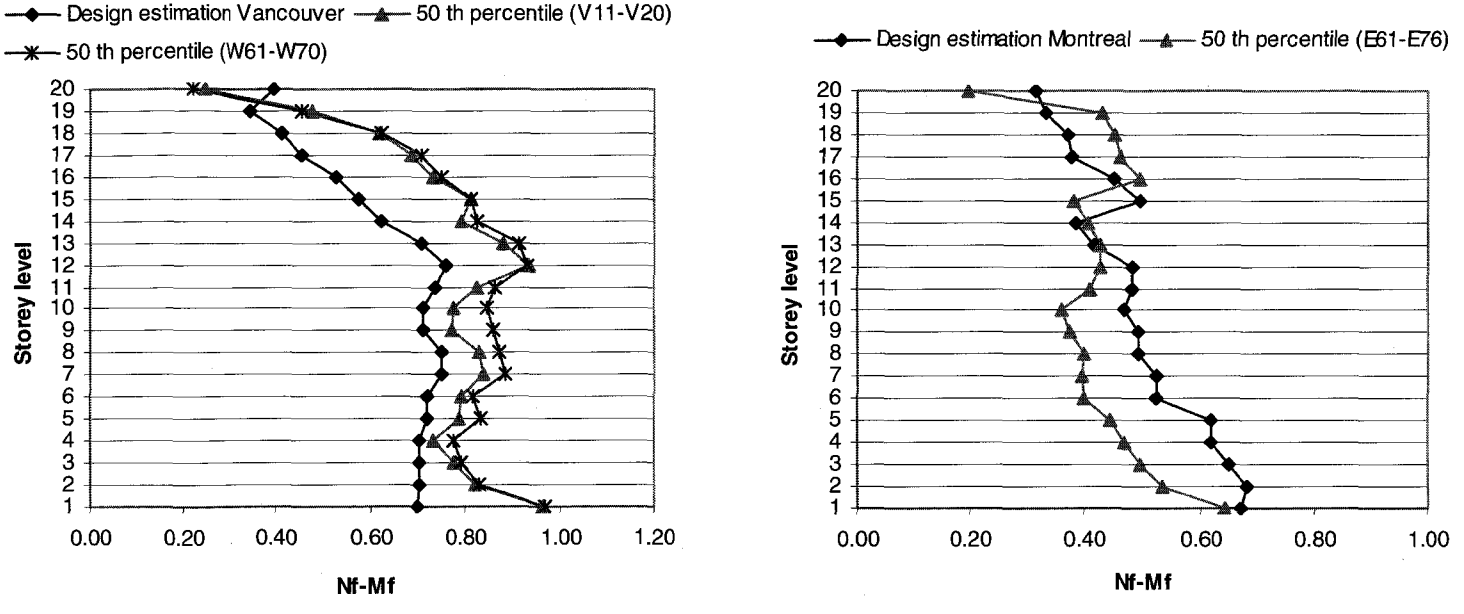

Figure 5.6 Capacity of the braces (20 storeys): Comparison between design estimates and results obtained from dynamic analysis

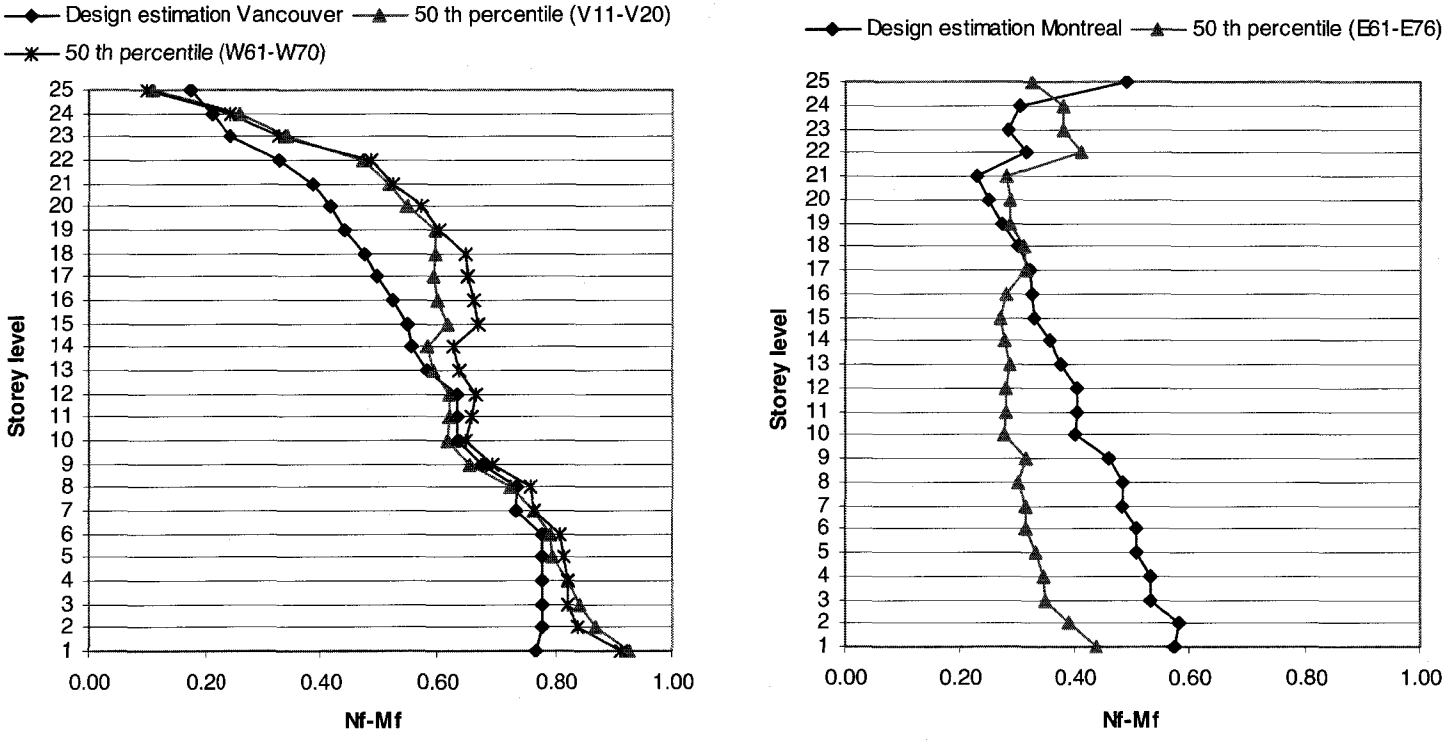

Figure 5.7 Capacity of the braces (25 storeys): Comparison between design estimates and results obtained from dynamic analysis

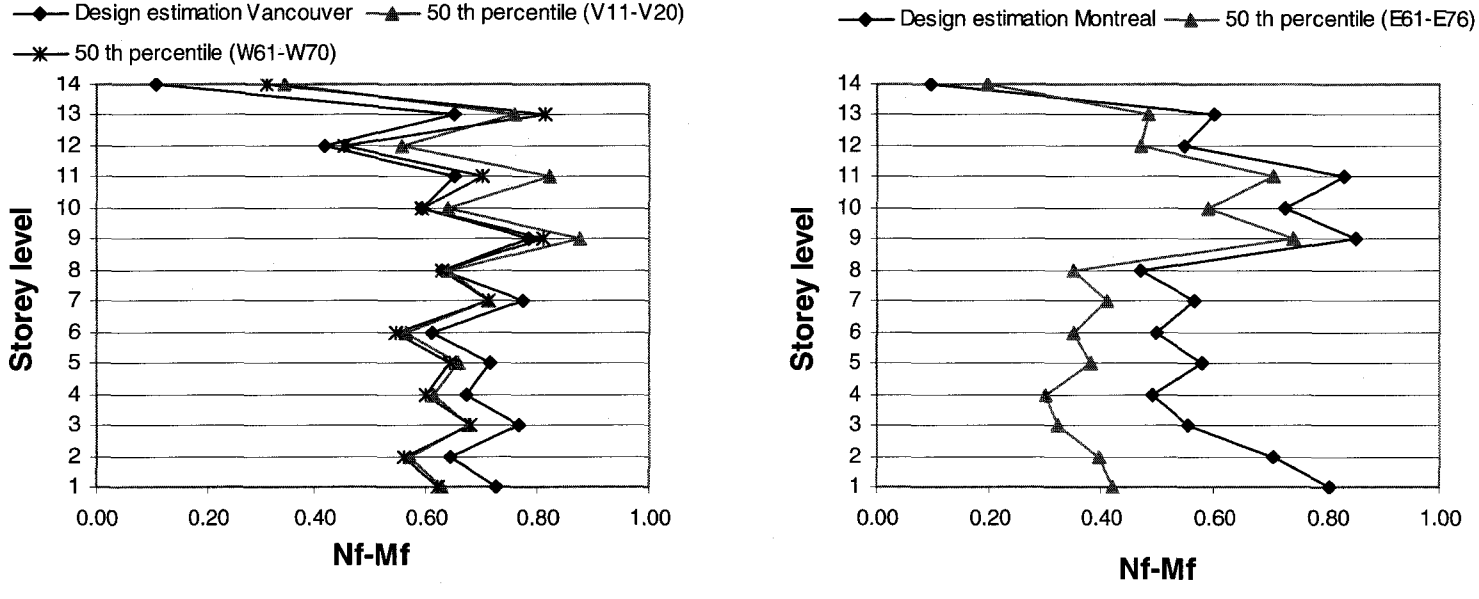

Figure 5.8 Capacity of the columns (14storeys): Comparison between design estimates and results obtained from dynamic analysis

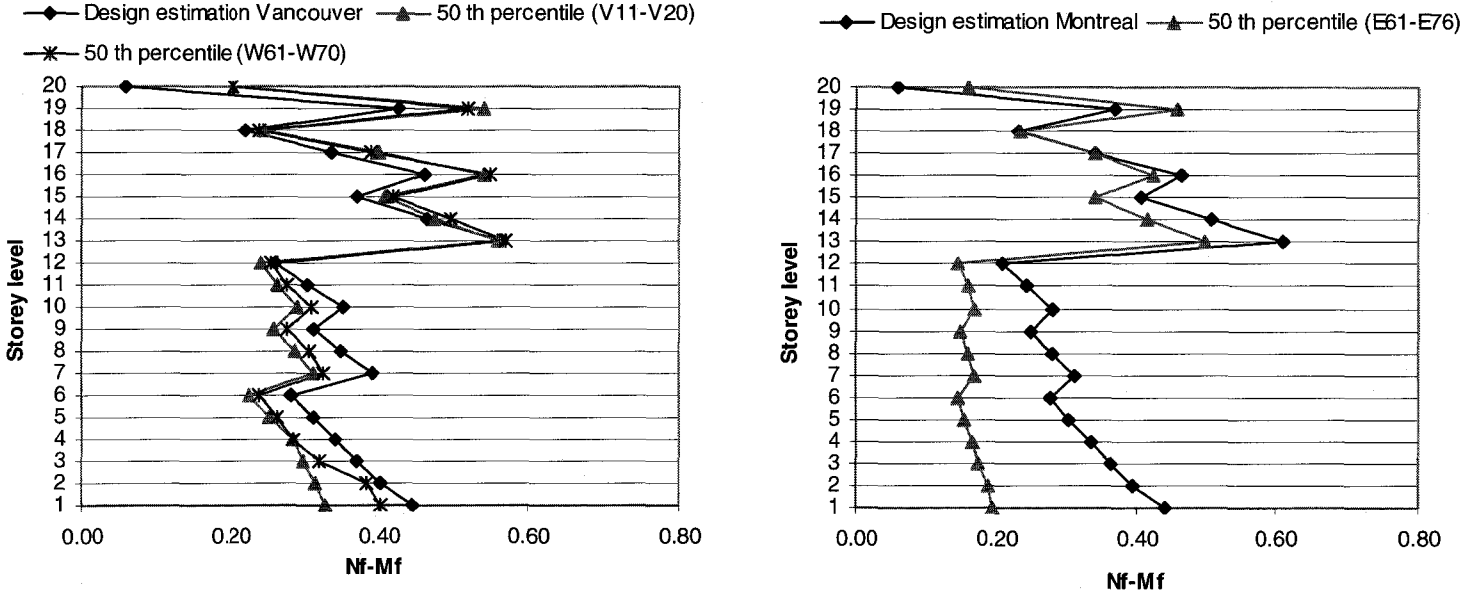

Figure 5.9 Capacity of the columns (20storeys): Comparison between design estimates and results obtained from dynamic analysis

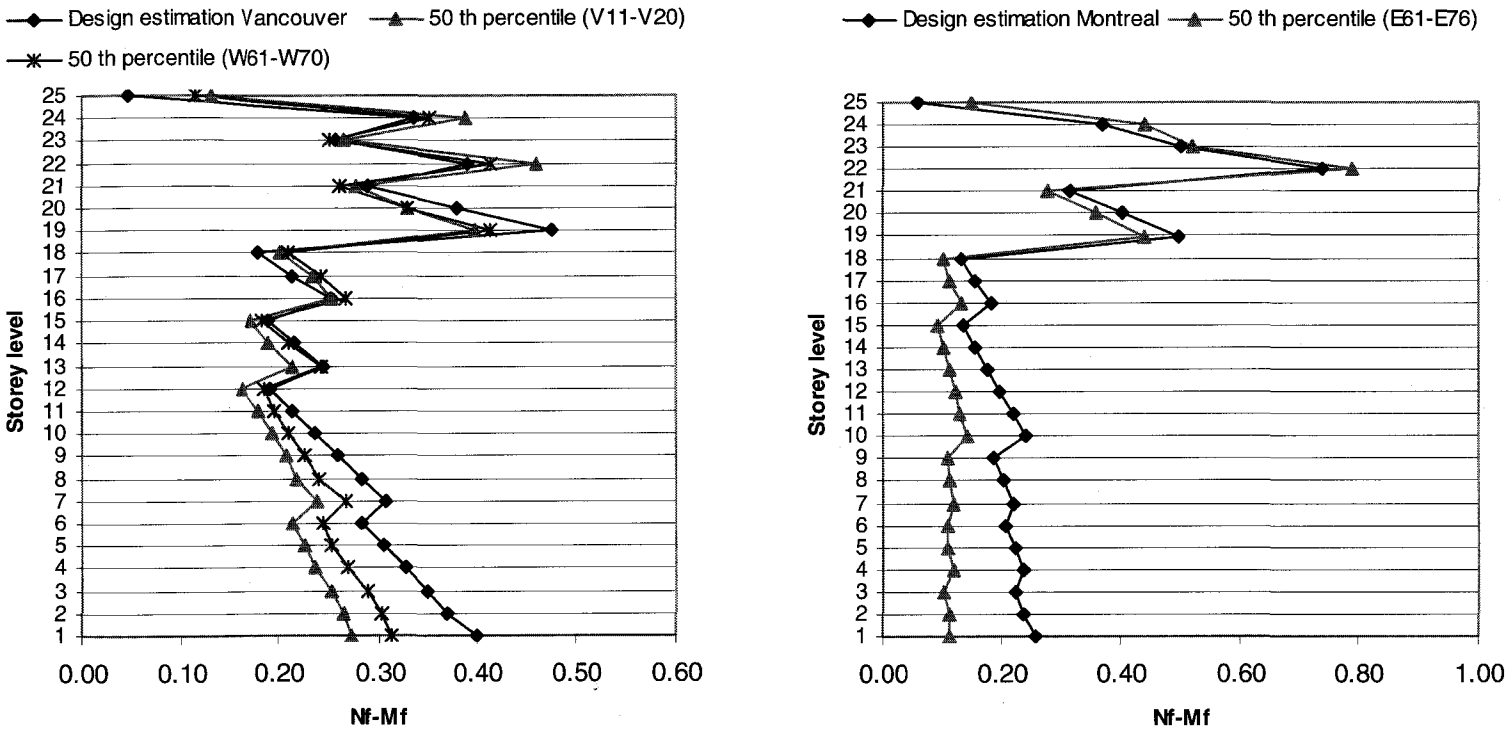

Figure 5.10 Capacity of the columns (25 storeys): Comparison between design estimates and results obtained from dynamic analysis

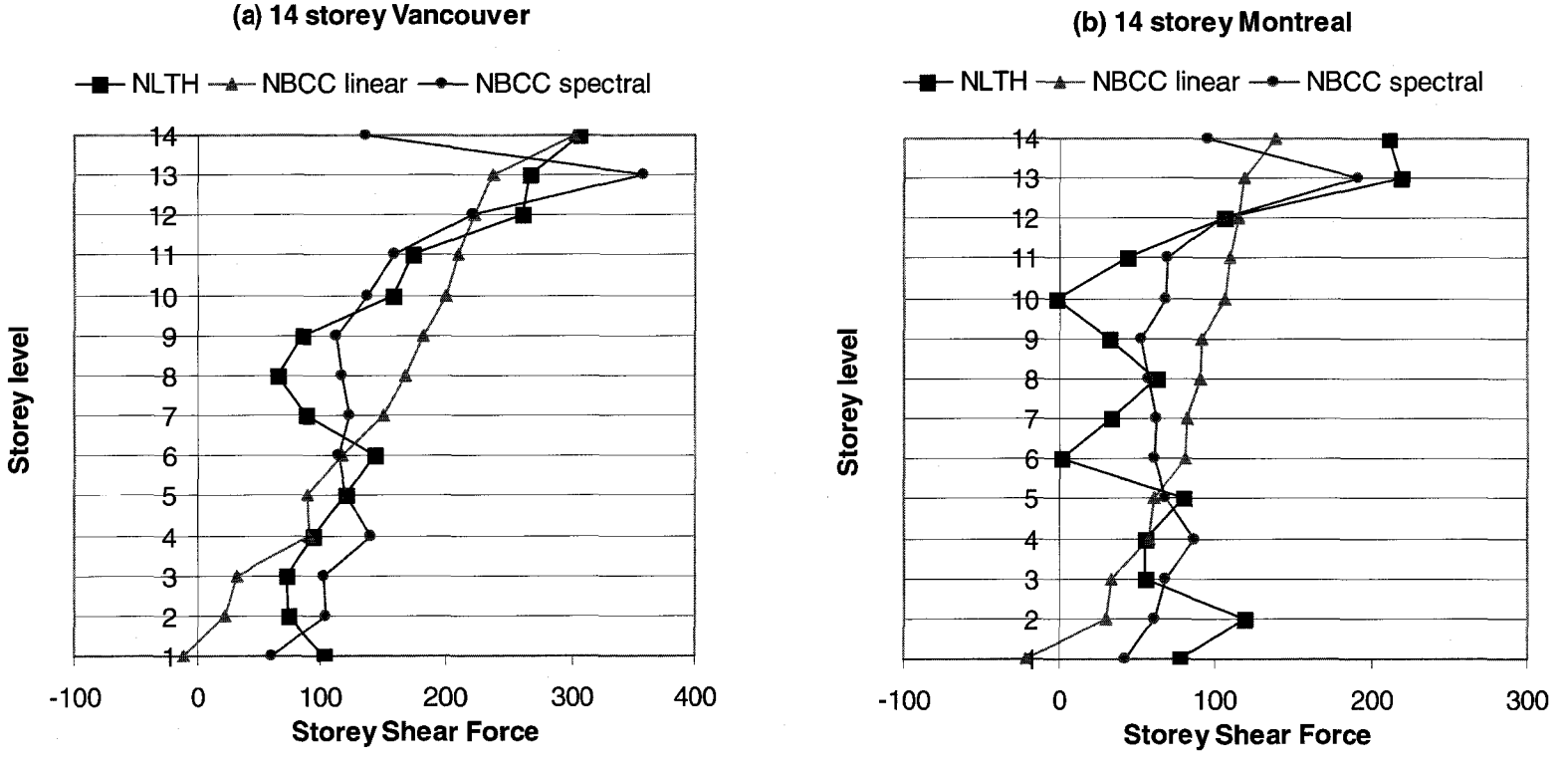

Figure 5.11 Lateral shear force distribution (14 storey structures)

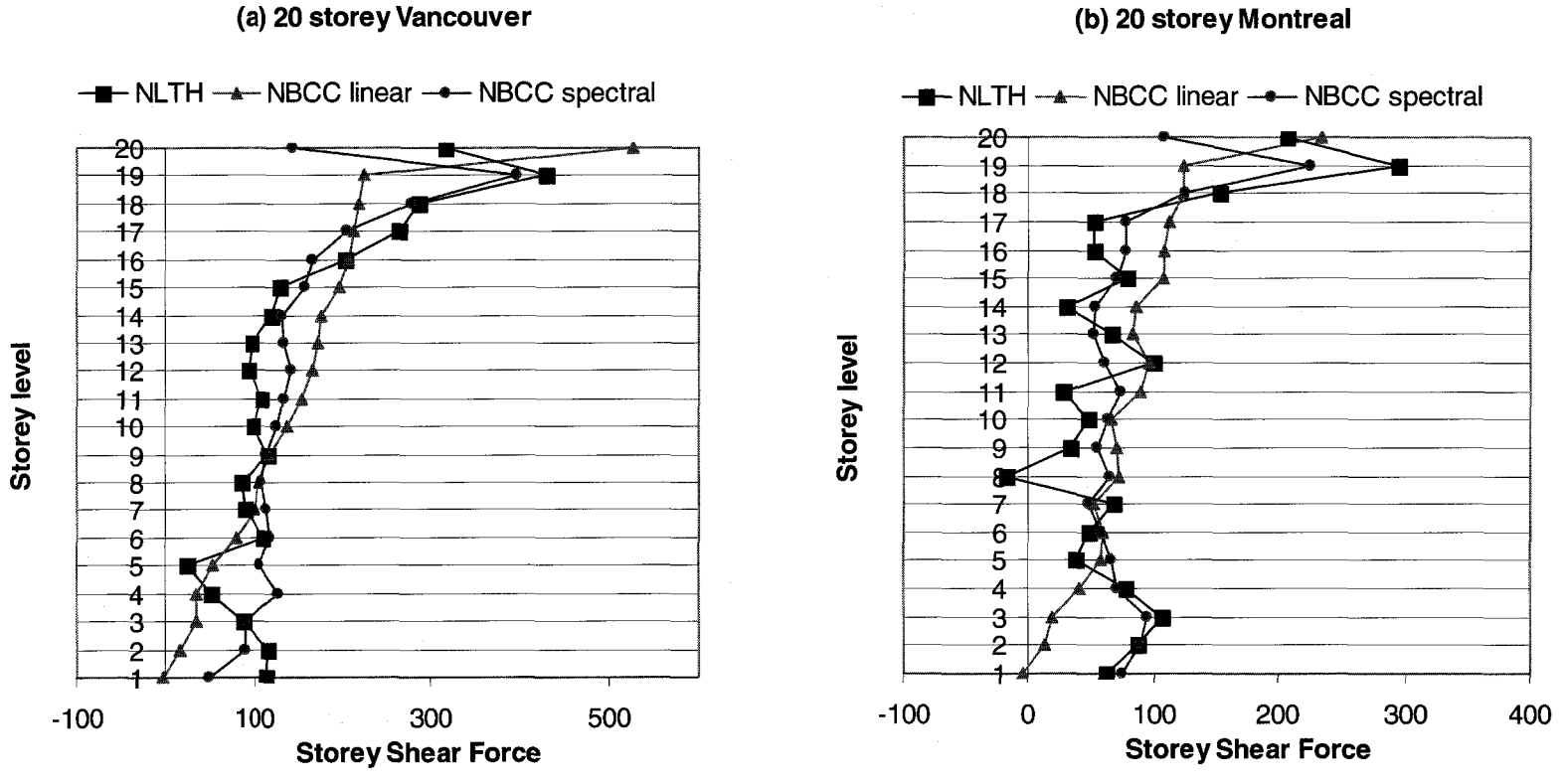

Figure 5.12 Lateral shear force distribution (20 storey structures)

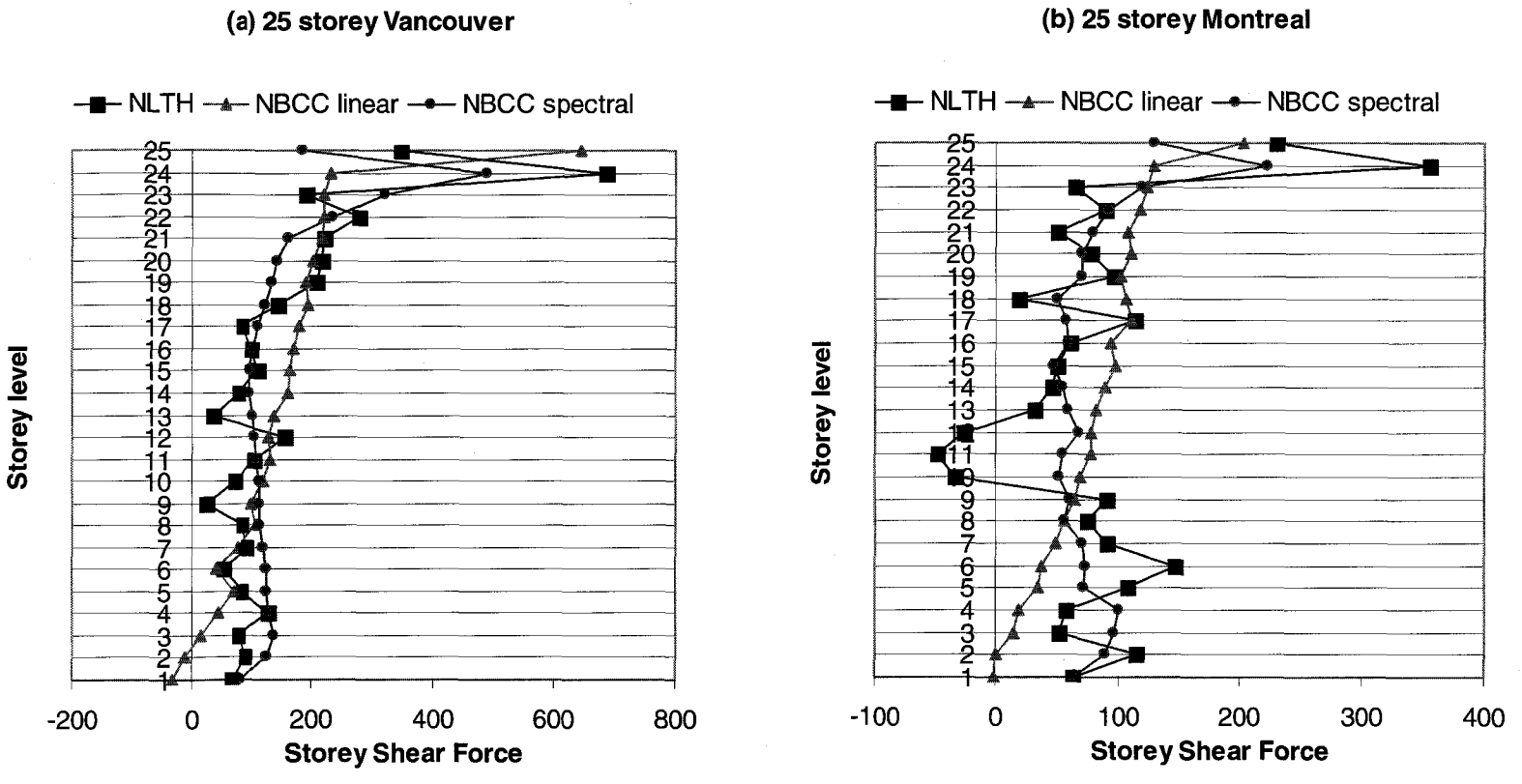

Figure 5.13 Lateral shear force distribution (25 storey structures)

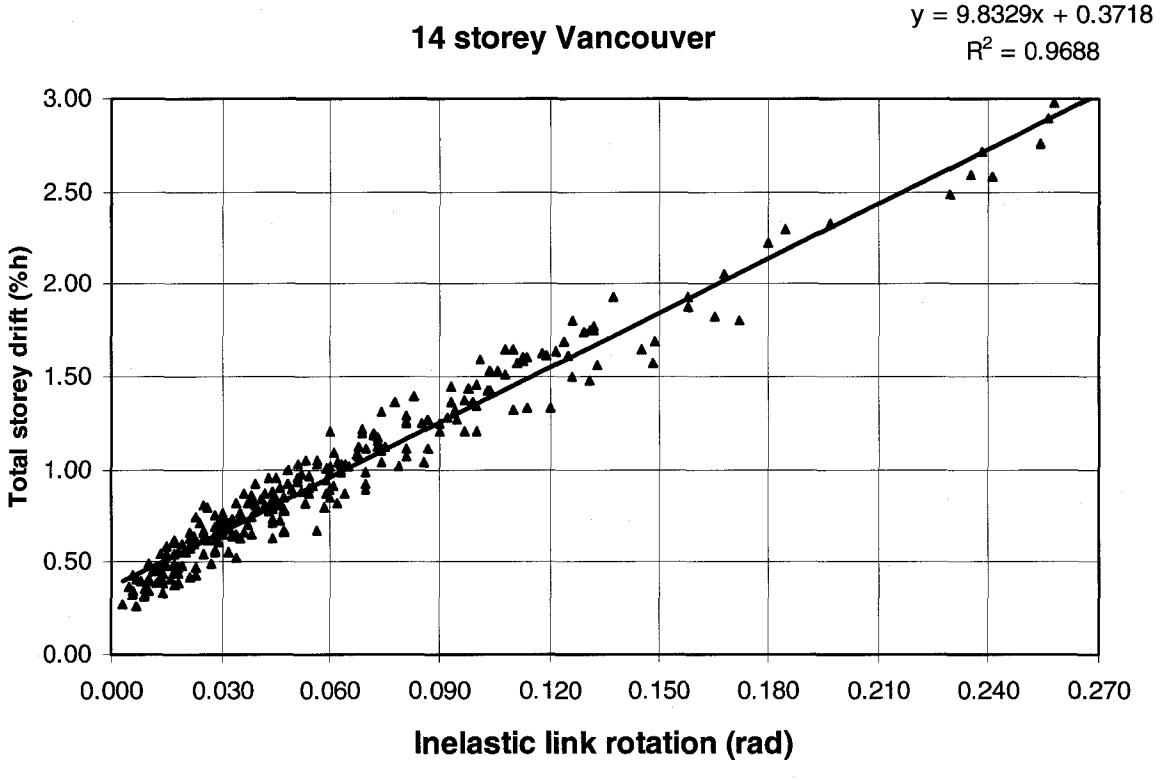

Figure 5.14 Relation between the link inelastic shear rotation and the total inter-storey drift (14 storey Vancouver)

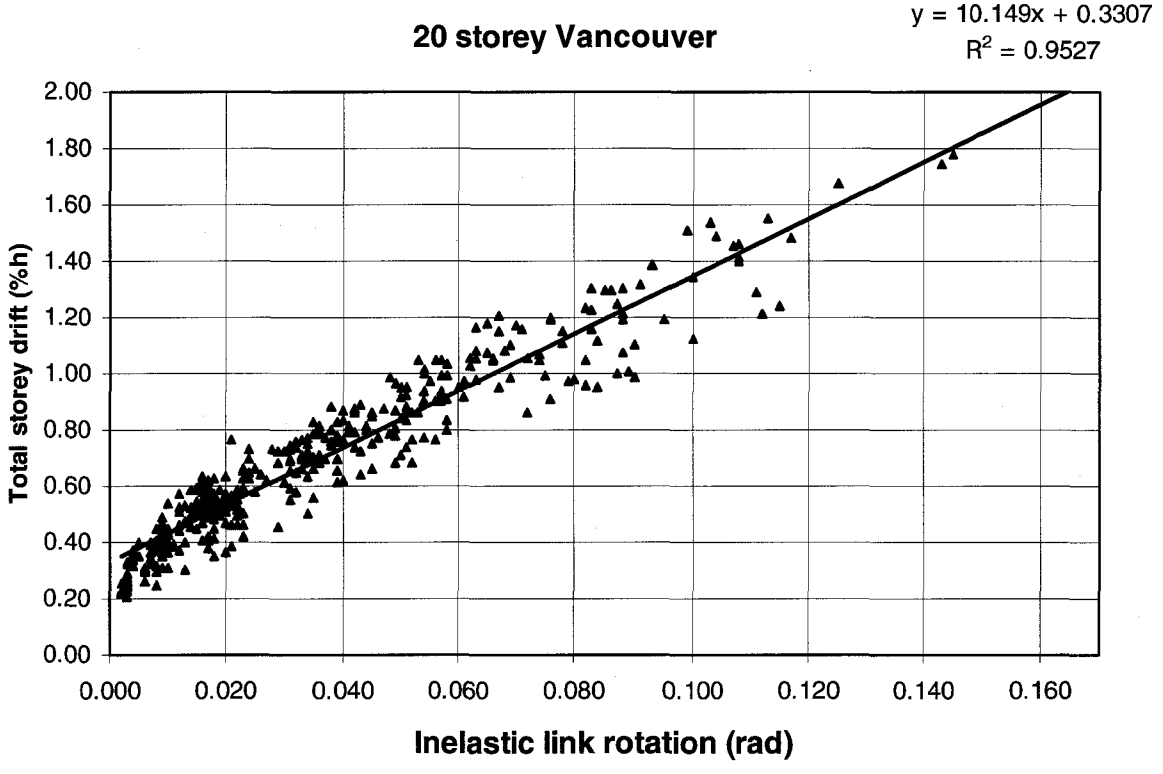

Figure 5.15 Relation between the link inelastic shear rotation and the total inter-storey drift (20 storey Vancouver)

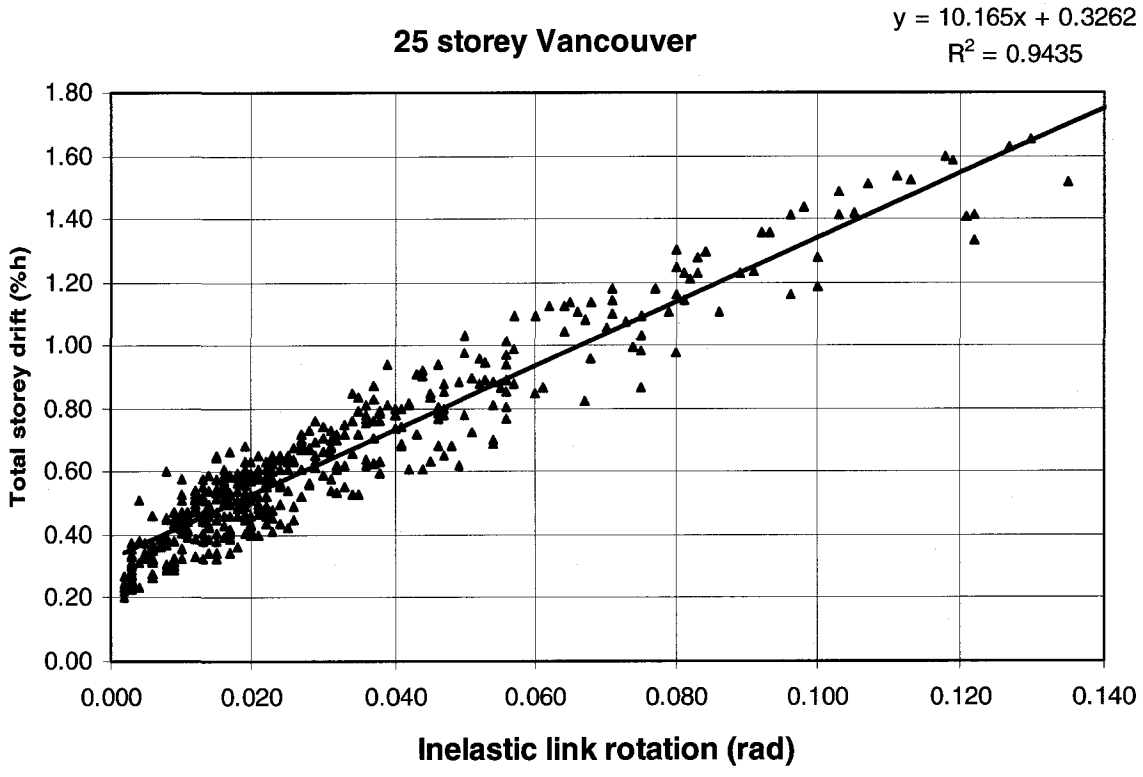

Figure 5.16 Relation between the link inelastic shear rotation and the total inter-storey drift (25 storey Vancouver)

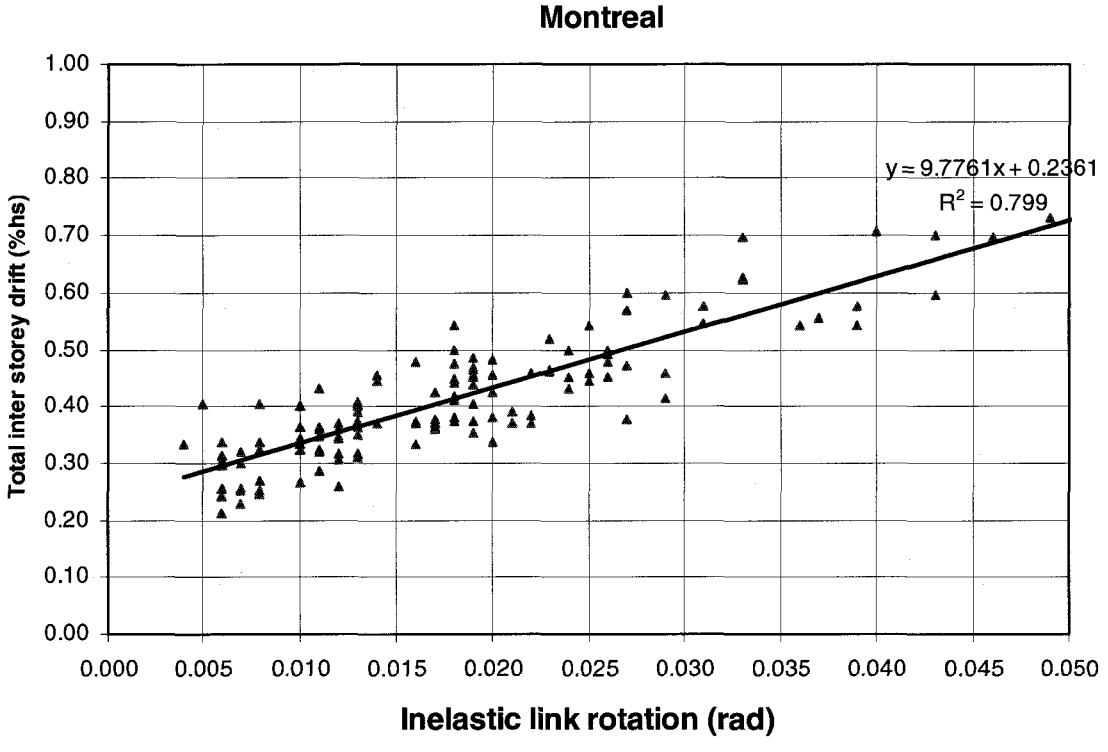

Figure 5.17 Relation between the link inelastic shear rotation and the total inter-storey drift (Montreal)

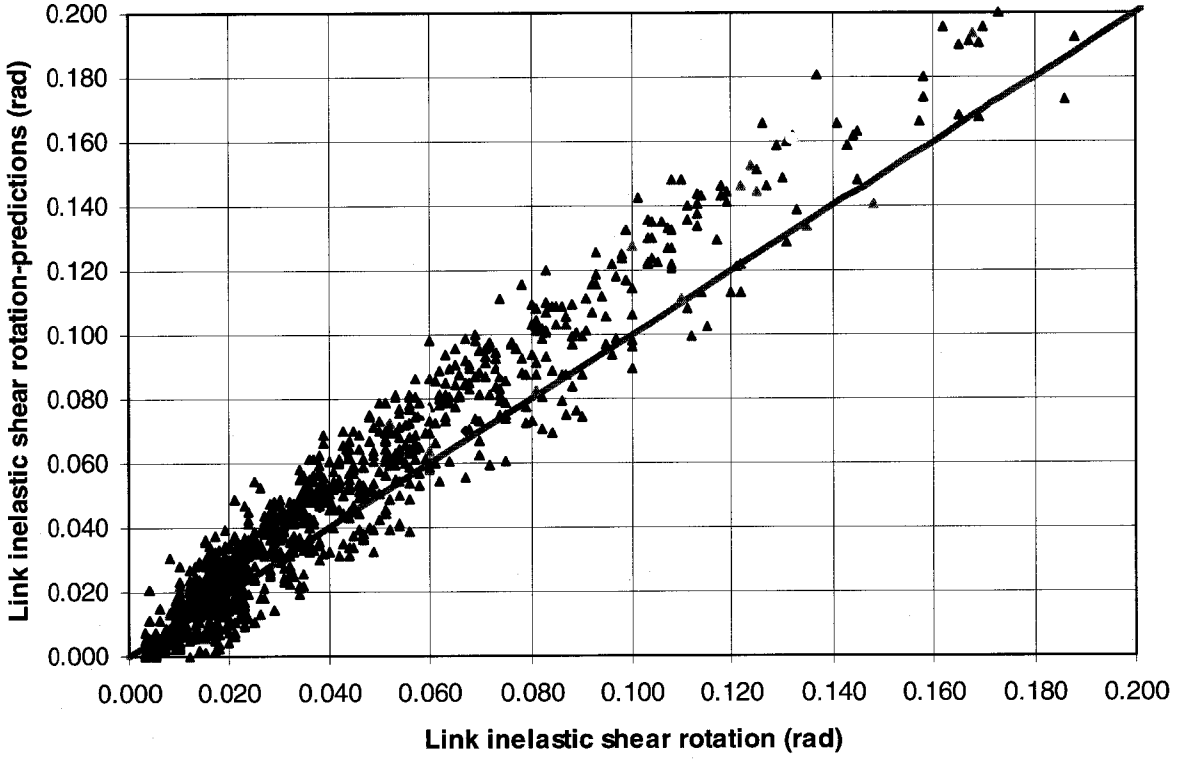

Figure 5.18 Comparison between the analytic and the predicted link inelastic shear rotation

CHAPTER 6. SUMMARY AND CONCLUSIONS

6.1 Summary

This project has investigated the design demand and the seismic behavior of the taller eccentrically braced frames (EBFs) in the context of the NBCC 2005 and the CSA-S16S1-05 seismic provisions. A total of six buildings with chevron-type EBFs with shear-critical links were designed for two Canadian locations: Vancouver and Montreal. Design procedures were described and applied to the 14-, 20-and 25-storey frames. The importance of different design criteria was discussed and the appropriate design sequence was suggested. The seismic response of the frames was investigated using the non-linear time-history analysis to assess if the design procedures achieved desired frame response. The analyses were done for the sets of earthquake records calibrated to match design spectra at studied locations. Historical and artificial records were selected for Vancouver, while for Montreal only artificial records were considered, due to the lack of the appropriate historical recordings, typically rich in high frequencies. The behavior of the system was monitored through the response of links and the global frame behavior. Following response parameters were examined: inelastic link rotation, maximum normalized shear force, response of the outer beams, braces response ratios, columns moments and axial forces, values of the inter storey drifts and lateral force distribution and the study of the relation between the inelastic link rotation and the inter storey drift.

6.2 Conclusions on the design procedure

(i) Seismic design of EBFs according to Canadian design procedures includes three phases: capacity, stiffness, and strength design. It is important to establish an appropriate design sequence to minimize the number of iterations required. The approaches to design discussed in literature had been mainly established based on the

observations made for lower to medium height frames. In taller EBFs larger deflections are anticipated and thus providing the adequate stiffness and global structural stability could become important design consideration. Following design sequence was established as the most appropriate for the taller EBFs:

(1) select link section based on ductility requirements; (2) design other frame members based on strength requirement;(3) verify total-drift requirement and global stability; (4) perform verifications frame members other than links applying capacity design and (5) verify link inelastic rotation. It was found that these steps are appropriate for both locations: the high and moderate seismic zones.

(ii) Initial design assumptions to calculate the seismic force based on a period equal to $2T_a$ is found to be appropriate for the design of tall eccentrically braced frames. In all cases seismic design base shear was governed by the minimum value defined in NBCC 2005,V_{min}, based on S_a (2.0). NBCC generally does not impose the period restriction when deflections are calculated, however it is not clear what rules should be applied are when V_{min} controls the design. In view of this, all displacements were calculated limiting the period to $2T_a$.

(iii) The selected length of the link influence significantly seismic behavior of the frame. Based on the results of parametric study carried out at the beginning of the project the link length of 600 mm was chosen and a complete design of the frame was done following the design steps explained in Chapter 3. Although the shorter link increases the rigidity to the frame and leads to the selection of smaller sections for the other frame members, the rotations of the link segments are much higher since they are in direct proportion to the ratio of the frame width to link length, L/e. For EBFs with short, shear links it is considered appropriate to use links that have lengths up to about 10 percent of the frame width.

(iv) Due to the importance of deflections in taller frames, seismic forces should be amplified to account for P-delta effects for initial link selection. In this study the initial calculations were based on expected drift index of 0.5%. It was found for the frames studied that the appropriate value of the inter-storey drifts varied in function

of the frame location but not in function of the frame height. Based on the results presented in this study following values can be established: 2.0% for Vancouver and 1% for Montreal.

(v) When sizing links, special attention was given to maintain the ratio of link shear resistance-to-link shear force demand as uniform as possible and close to one. Due to the importance of design criteria other than inelastic strength (i.e. wind load, gravity load), it was not possible to achieve this objective. For the structure situated in Vancouver the ratio was about 1.3 and for the structures in Montreal the ratio ranged from 1.55 to 1.85. This high ratio observed for Montreal structures is mainly due to the fact that link design was governed by wind load combinations.

(vi) For all frames studied it was found that the controlling design requirements were the stiffness and the global stability of the frame. Comparison of structural mass obtained in different steps of design process indicate that for the frames in Vancouver, total-drift requirements governed the design, while for the frames in Montreal global structural stability ($U_2 \leq 1.4$) was the main criterion. Note that, in spite of an important difference in seismic solicitations in two locations studied, the mass obtained for frames with equal height was virtually the same.

(vii) In none of the cases studied here the modification of frame section sizes was required to comply with design limits imposed on link shear rotations ($\gamma \leq 0.08$ rad). In the calculation of γ the recommendations from the Commentary S16-01 were followed and the contribution of the chord drifts to the total drift was eliminated. It was observed however, that had the chord drift not eliminated, the γ criterion would have became important in design.

(viii) To investigate the impact of lateral load distribution on final frame design, two variant designs were obtained for seismic forces calculated using the equivalent static method and the response spectrum method. It was concluded that the two load distributions yielded almost identical frame configurations. Following these observations, the study of structural response was carried out on frames designed for equivalent static load force profiles.

(ix) It was of interest to establish if the lateral force distribution obtained using response spectrum analysis was sensitive to the frame configuration selected. A study was carried out on the 14-storey frame designed for Vancouver. Three different designs were examined: (i) frame members compliant with strength requirements, (Okazaki et al.) frame members compliant with all design criteria and (iii) identical sections for the braces and columns in all the storeys. Although the structures had different periods of vibration and different levels of the base shear, the spectral force distribution over the frame's height was similar. It was concluded that, within the range of sections commonly used in type of the frames studied, the variations in the frame sections do not have a significant impact on the spectral force distribution over the height of the structure. This further supported the decision to use frames designed for equivalent lateral force method in study of the seismic response.

6.3 Conclusions relative to the study of EBFs' seismic behavior

(i) The inelastic link rotations exceeded the design limit of 0.08 rad in the upper storeys for all the structures situated in Vancouver while for the structures in Montreal the maximum link rotations represent about a third of the design limit. The maximum range of link rotations calculated as the maximum positive plus the maximum negative rotations for a link were all smaller than the permissible value of two times the design limit (0.16 rad).

(ii) The link overstrength factor followed the same trend as the link rotations with median values of 1.5 at the top storeys for the structures from Vancouver. For Montreal the overstrength factor reached the value assumed in design (1.3) only in the top storey while the other links remained elastic.

(iii)The inelastic activity in the outer beam segments of 14-storey frame in Vancouver was concentrated at the lower storeys beams and was not related to the occurrence of the maximum link rotations. The plastic beams rotations developed infrequently, only for small number of the ground motions, and were in general bellow 0.02 radians. 20-

and 25-storeys frames in Vancouver as well as all structures in Montreal did not exhibit any inelastic beam activity. In view of these results, the design approach to accept the limited plastification of the outer beam segment is justifiable, particularly as it can bring more economical design solutions in some cases.

(iv)The braces showed few inelastic incursions concentrated at the bottom level of the frame for limited periods of time and this only for the structures in Vancouver. In general, the stress ratios obtained from non-linear time-history analysis (NLTHA) compared well with the stress ratios predicted in design. For Vancouver, the only exceptions were the upper storeys where the analytical results were 20 to 40 percentages higher. For Montreal structure the analytical values were in general smaller than the design values.

(v) The stress ratios in the columns obtained from NLTHA were higher at the top storeys than in the rest of the structure for the structures designed in Vancouver and much lower than the estimated design response ratios. The axial forces developed in the columns were generally lower than those calculated in the design phase and the differences increased with the increase in the number of storeys. The bending moments developed in the columns of the structures from Vancouver were higher in the upper storeys than the estimated design value of $0.3M_p$ and they decreased with the increase in the frame's height. For Montreal the bending moments in columns represent maximum values of $0.15M_p$ at the top storeys and between $0.01M_p$ and $0.03M_p$ in the other storeys, values that are lower than the moments estimated in the design.

(vi)The inter storey drifts show similar vertical distribution as the inelastic link rotations with higher values observed in the upper storeys and lower in the rest of the structure. For the structures situated in Vancouver the design limit of 0.025 h_s was exceeded only in the 14 storey structure for the group of historical short distance records, while for the frames in Montreal, it remained well below the design limit (three to four times smaller).

(vii) The distribution of the dynamic lateral force corresponded well to the distribution of the spectral force with stronger higher modes impact for taller frames and for the frames located in Montreal.

(viii) The NLTHA results demonstrate that the higher modes influenced significantly the response. It can also be remarked that the structures situated in Vancouver reached the anticipated level of seismic performance while for the structures designed for Montreal the seismic demand was much smaller mainly due to the increased overstrength imposed by design criteria other than the capacity design requirements.

(ix)The maximum link rotation and the total inter-storey drift showed a very strong positive correlation. A linear relation between the two parameters was established based on the results obtained from NLTHA. This equation is representative of the rigid-plastic deformation mechanism commonly used in design standards. The equation was evaluated for the frames geometry studied herein and it yielded satisfactory and conservative estimates of link rotations.

6.4 Recommendations

Although useful results showing the seismic performance of tall eccentrically braced frames were obtained in this project, further studies and research work are necessary to improve the frame models and better evaluate the seismic performance of this system. It should also be noted that the conclusions from this study are limited to a particular geometry and dynamic characteristics of EBFs studied. Some of the subjects that should be further investigated include:

- The sensitivity of the seismic response to the modeling assumptions considering the inclusion of the P-delta effects should be investigated. In this study, the modeling of P-delta effects was achieved by adding one fictitious column, connected by means of axially-rigid links to the rest of the frame. Some previous studies reported on concentrically braced frames suggest that using

three fictitious columns to represent typical gravity columns in the building (inside, outside and corner columns) may yield less conservative results.

- The potential for dynamic instability that can develop at the upper storeys caused by long-duration strong ground motions with large pulse-type input. The present study included limited number of ground motions of this type, which resulted in very high values of response parameters for all structures.
- Further experimental testing is also necessary to verify the seismic response obtained thought the analytical studies.

REFERENCES

Atkinson, G. a. B. I. A. (1998). "Compatible ground-motion time histories for new national seismic hazard maps." *Canadian Journal of Civil Engineering*, 25, 305-318.

Bosco, M., Marino, E. M., Neri, F., and Rossi, P. P. (2004). "Seismic behaviour of EBFs coupled to moment resisting frames." *13th Conference on Earthquake Engineering*.

Christopoulos, C. (1998). "A study on the characteristics of vertical accelerations and their effects on civil engineering structures," dissertation, Ecole Polytechnique, Montreal

CSA. (2005). "S16S1-05 Supplement No.1 to CAN/CSA-S16-01, Limit State Design of Steel Structures." C. S. Association, ed., Rexdale, ON.

Engelhardt, M. D., and Popov, E. P. (1989). "Tests on brace and link connections for EBFs." 549-558.

Engelhardt, M. D., Tsai, K. C., and Popov, E. P. (1992). "Stability of beams in eccentrically braced frames." *Proceedings of Engineering Mechanics*, 1043-1046.

Ghobarah, A., and Ramadan, T. (1990). "Behavior of links of various lengths in eccentrically braced frames." *Proceedings of the US National Conference on Earthquake Engineering*, 1017.

Han, X. M. (1998). "Design and behavior of eccentrically braced frames in moderate seismic zones," dissertation, McGill University, Montreal, QC, .

Hjelmstad, K. D., and Popov, E. P. (1983). "Cyclic behavior and design of link beams." *Journal of Structural Engineering*, 109(10), 2387-2403.

Kasai, K., and Han, X. (1997a). "New EBF design method and application: redesign and analysis of US-Japan EBF." *International Conference on Behavior of Steel Structures in Seismic Areas STESSA' 1997.*

Kasai, K., and Popov, E. P. (1986a). "Cyclic web buckling control for shear link beams." *Journal of Structural Engineering*, 112(3), 505-523.

Kasai, K., and Popov, E. P. (1986b). "A study of seismically resistant eccentrically braced frames." *UCB/EERC-86/01*, University of California, Berkeley, California.

Kasai , K. a. H., X. "New EBF design method and application: redisign and analysis of US-Japan EBF." *International Conference on Behavior of Steel Structures in Seismic Areas STESSA' 1997*, Kyoto, Japan.

Koboevic, S. (2000). "An approach to seismic design of eccentrically braced frames," McGill university, Montreal.

Koboevic, S., and Redwood, R. (1997). "Design and seismic response of shear critical eccentrically braced frames." *Canadian Journal of Civil Engineering*, 24(5), 761-771.

Lacerte, M. (2005). "Utilisation de la surcapacite des diagonales pour l'amelioration du comportement sismique de contreventements en acier de type split-X," dissertation, Ecole Polytechnique, Montreal.

Lahey/Fujitsu. (2007). "LF Fortran v7.1." Lahey/Fujitsu Fortran 95 compiler.

Malley, J. O., and Popov, E. P. (1984). "Shear Links in Eccentrically Braced Frames." *Journal of Structural Engineering*, 110(9), 2275-2295.

Marino, E. M., Muratore, M., and Rossi, P. (2003). "Pushover analysis in the evaluation of the seismic response of steel frames." *STESSA2003: Proceedings of the Conference on behavior of steel structures in seismic areas.*

Mondkar, D. P., and Powell, G. H. (1975). "ANSR-1 General purpose computer program for analysis of non-linear structural response ", University of California, Berkeley.

Naumoski N., S. M., Lan Lin and Kambiz Amiri-Hormozaki. (2006). "Evaluation of the effects of spectrum-compatible seismic excitations on the response of medium-height reinforced concrete frame buildings." *Canadian Journal of Civil Engineering*, 33, 1304-1319.

NBCC. (2005). "National Building Code of Canada 2005." 12th edition, N. R. C. o. Canada, ed., Ottawa, ON.

Okazaki, T., Arce, G., Ryu, H.-C., and Engelhardt, M. (2004). "Recent research on link performance in steel eccentrically braced frames." *13th World Conference on Earthquake Engineering*

Okazaki, T., Arce, G., Ryu, H.-C., and Engelhardt, M. D. (2005). "Experimental study of local buckling, overstrength, and fracture of links in eccentrically braced frames." *Journal of Structural Engineering*, 131(10), 1526-1535.

Okazaki, T., and Engelhardt, M. D. (2007). "Cyclic loading behavior of EBF links constructed of ASTM A992 steel." *Journal of Constructional Steel Research*, 63(6), 751-765.

Okazaki, T., Engelhardt, M. D., Nakashima, M., and Suita, K. (2006). "Experimental performance of link-to-column connections in eccentrically braced frames." *Journal of Structural Engineering*, 132(8), 1201-1211.

Popov, E. P., and Engelhardt, M. D. (1988). "Seismic eccentrically braced frames." *Journal of Constructional Steel Research*, 10, 321-354.

Popov, E. P., Engelhardt, M. D., and Ricles, J. M. (1989). "Eccentrically braced frames: U.S. practice." *Engineering Journal of the American Institute of Steel Construction*, 26(2), 66-80.

Ramadan, T., and Ghobarah, A. (1995). "Analytical model for shear-link behavior." *Journal of Structural Engineering*, 121(11), 1574-1580.

Redwood, R. (1995). "Earthquake resistant design of structures - notes on design of steel structures, Dept. of Civil Engineering and Applied Mechanics, McGill University."

Richards, P. W., and Uang, C.-M. (2003). "Development of Testing Protocol for Short Links in Eccentrically Braced Frames." *SSRP-2003/08*, University of California, San Diego, California.

Richards, P. W., and Uang, C.-M. (2006). "Testing protocol for short links in eccentrically braced frames." *Journal of Structural Engineering*, 132(8), 1183-1191.

Ricles, J. M., and Popov, E. P. (1987b). "Dynamic analysis of seismically resistant eccentrically braced frames." *Report No.UCB/EERC-87/07*, University of California, Berkeley, California

Ricles, J. M., and Popov, E. P. (1994). "Inelastic Link Element for EBF Seismic Analysis." *Journal of Structural Engineering*, 120(2), 441-463.

Rossi PP, L. A. (2007). "Influence of the link overstrength factor on the seismic behavior of eccentrically braced framens." *Journal of Constructional Steel Research.*

Rozon, J. (2009). "Étude du comporteent global des cadres à contreventement excentrique de faible et moyenne hauteur," Ecole Polytechnique de Montreal, Montreal.

SeismoSignal. (2007). "Earthquake Engineering Software Solutions." SeismoSoft S.R.L., Greece.

VisualDesign. (2007). "Structural analysis program." CivilDesign Inc., Longueuil (QC).

APPENDIX A Calculation of the storey loads

Gravity Load Calculation:

Roof Load: (in Montreal region)

Live load: Snow load Ss = 2.6 kPa (1.8 kPa in Vancouver region)

Associated Rain load, Sr = 0.4 kPa

Roof Dead load + Steel allowance (20 ton for roof) = 0.7 + 0.12 = 0.82 kPa

Live load: S= 25% x (2.6 x 0.8 + 0.4) = 0.62 kPa

Floor Load: (65mm concrete floor on 75mm composite steel floor)

Live load: 2.4 kN/m² (reduced according to tributary area)

3.6 kN/m² (for braced core area which is assumed to serve as equipment area)

Dead load: 4.5 kN/m² (including partitions)

Curtain wall weight: 1 kN/m²

Exterior wall weight of each storey:

1st storey =664.2 kN

Typical storey =599.4 kN

Roof =299.7 kN

Total weight of each floor:

1st storey =7954.2 kN (Assume steel weight included in 4.5 kPa)

Typical storey =7889.4 kN (Assume steel weight included in 4.5 kPa)

Roof =2632.5 kN (include 20 tons steel weight and 25%snow)

Roof (in Vancouver region) =2293 kN

APPENDIX B Calculation of the seismic force amplification due to accidental torsion

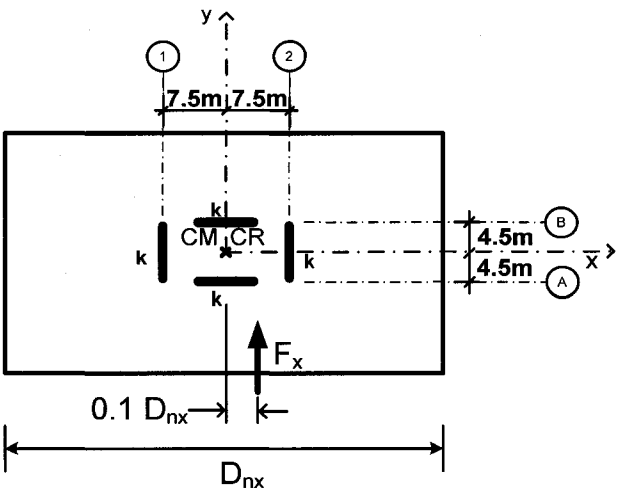

The seismic frames resisting systems is oriented after two orthogonal axes; it has two identical EBF in each of the principal directions that are symmetrically positioned in the plan, thus the building can be considered regular with the center of mass (CM) identical to the center of rigidity (CR) of the building. CM ≡ CR

Accidental torsion $e_x=\pm 0.1\ D_{nx}=4.5m$ $(D_{nx}=45m)$

Calculation of the force from accidental torsion:

$$P_{xj}=\frac{F\cdot e_x\cdot k_{xj}\cdot y_i}{\Sigma k_{yi}\cdot x_i^2+\Sigma k_{xi}\cdot y_i^2}$$

1. $e_x=+4.5m$

Line	k_y	x	$k_y x^2$
1	k	-12	144k
2	k	3	9k
		Σ	153k

Line	k_x	y	$k_x y^2$
A	k	-4.5	20.25k
B	k	4.5	20.25k
		Σ	40.5k

193.5k

$$P_{x1} = \frac{F_x \cdot 4.5 \cdot k \cdot (-12)}{193.5k} = F_x \cdot (-0.062)$$

$$P_{x1} = \frac{F_x \cdot 4.5 \cdot k \cdot (3)}{193.5k} = F_x \cdot (0.015)$$

2. e_x=-4.5m

Line	k_y	x	$k_y x^2$
1	k	-3	9k
2	k	12	144k
		Σ	153k

Line	k_x	y	$k_x y^2$
A	k	-4.5	20.25k
B	k	4.5	20.25k
		Σ	40.5k

193.5k

$$P_{x1} = \frac{F_x \cdot 4.5 \cdot k \cdot (-3)}{193.5k} = F_x \cdot (-0.015)$$

$$P_{x1} = \frac{F_x \cdot 4.5 \cdot k \cdot (12)}{193.5k} = F_x \cdot (0.062)$$

For the calculation of the seismic force amplification due to accidental torsion a rounded percentage equal to 7% will be used in the design.

APPENDIX C Additional NLTHA results

Additional results from non linear time histories that are not presented as a part of Chapter 5, but are referred there.

Table C.1 Maximum link overstrength factor 14 storey frame in Vancouver

Storey	Historical records(5)-short distance		Artificial records(5)-short distance		Historical records(5)-long distance		Artificial records(5)-long distance		Historical records (10)		Artificial records (10)		All records (20)	
	V_{max}/V_p		V_{max}/V_p		V_{max}/V_p		V_{max}/V_p		V_{max}/V_p		V_{max}/V_p		V_{max}/V_p	
	50^{th}	84^{th}	50^{th}	84^{th}	50^{th}	84^{th}	50^{th}	84^{th}	50^{th}	84^{th}	50^{th}	84^{th}	50^{th}	84^{th}
14	0.71	0.86	0.80	0.93	0.81	0.94	0.73	0.82	0.80	0.89	0.71	0.90	0.75	0.90
13	1.55	1.57	1.48	1.55	1.45	1.62	1.48	1.55	1.54	1.59	1.48	1.56	1.51	1.57
12	1.58	1.64	1.63	1.72	1.51	1.72	1.59	1.71	1.56	1.71	1.57	1.67	1.56	1.71
11	1.50	1.59	1.62	1.64	1.51	1.63	1.53	1.63	1.50	1.64	1.47	1.63	1.48	1.63
10	1.44	1.51	1.46	1.60	1.48	1.53	1.50	1.61	1.45	1.48	1.50	1.61	1.46	1.59
9	1.43	1.49	1.37	1.54	1.45	1.57	1.44	1.55	1.43	1.50	1.44	1.56	1.43	1.53
8	1.22	1.42	1.26	1.40	1.34	1.39	1.29	1.40	1.31	1.41	1.29	1.40	1.30	1.40
7	1.19	1.35	1.28	1.40	1.34	1.42	1.31	1.41	1.25	1.36	1.31	1.42	1.29	1.38
6	1.23	1.28	1.22	1.45	1.32	1.42	1.34	1.45	1.25	1.35	1.34	1.44	1.27	1.42
5	1.12	1.25	1.17	1.44	1.32	1.38	1.34	1.50	1.26	1.32	1.34	1.50	1.28	1.48
4	1.14	1.28	1.09	1.37	1.30	1.36	1.33	1.42	1.27	1.31	1.33	1.42	1.28	1.41
3	1.17	1.22	1.05	1.34	1.32	1.36	1.30	1.39	1.23	1.33	1.30	1.39	1.24	1.39
2	1.19	1.22	1.06	1.31	1.34	1.40	1.28	1.39	1.24	1.37	1.28	1.39	1.25	1.40
1	1.36	1.38	1.15	1.48	1.39	1.48	1.37	1.57	1.36	1.43	1.37	1.59	1.36	1.51

Table C.2 Maximum link overstrength factor 14 storey frame in Montreal

Storey	Artificial records(5)-short distance		Artificial records(5)-long distance		Artificial records(10)	
	V_{max}/V_p		V_{max}/V_p		V_{max}/V_p	
	50^{th}	84^{th}	50^{th}	84^{th}	50^{th}	84^{th}
14	0.67	0.68	0.64	0.66	0.64	0.68
13	1.21	1.26	1.25	1.29	1.22	1.29
12	1.03	1.14	1.23	1.25	1.20	1.24
11	1.13	1.19	1.24	1.33	1.22	1.29
10	1.10	1.12	1.10	1.19	1.10	1.16
9	1.02	1.03	1.01	1.05	1.01	1.04
8	0.98	1.01	0.96	1.01	0.97	1.01
7	0.90	0.94	0.90	0.98	0.90	0.97
6	0.80	0.87	0.89	0.91	0.87	0.90
5	0.79	0.86	0.87	0.94	0.86	0.90
4	0.80	0.85	0.88	1.01	0.83	0.98
3	0.84	0.89	0.93	1.00	0.88	0.96
2	0.91	0.98	1.01	1.04	0.96	1.03
1	0.99	1.02	1.05	1.09	1.01	1.09

Table C.3 Maximum link overstrength factor 20 storey frame in Vancouver

Storey	Historical records(5)-short distance		Artificial records(5)-short distance		Historical records(5)-long distance		Artificial records(5)-long distance		Historical records(10)		Artificial records(10)		All records(20)	
	V_{max}/V_p		V_{max}/V_p		V_{max}/V_p		V_{max}/V_p		V_{max}/V_p		V_{max}/V_p		V_{max}/V_p	
	50^{th}	84^{th}	50^{th}	84^{th}	50^{th}	84^{th}	50^{th}	84^{th}	50^{th}	84^{th}	50^{th}	84^{th}	50^{th}	84^{th}
20	0.57	0.63	0.60	0.65	0.57	0.62	0.42	0.49	0.57	0.62	0.53	0.63	0.56	0.63
19	1.27	1.37	1.34	1.35	1.30	1.36	1.20	1.28	1.29	1.37	1.26	1.36	1.27	1.36
18	1.41	1.47	1.45	1.47	1.39	1.45	1.29	1.43	1.40	1.48	1.41	1.47	1.40	1.47
17	1.44	1.57	1.52	1.58	1.47	1.55	1.40	1.55	1.47	1.58	1.50	1.58	1.47	1.58
16	1.34	1.39	1.40	1.41	1.34	1.37	1.33	1.44	1.34	1.38	1.38	1.42	1.34	1.42
15	1.29	1.47	1.41	1.51	1.45	1.46	1.50	1.64	1.38	1.47	1.45	1.58	1.43	1.50
14	1.28	1.31	1.37	1.38	1.33	1.47	1.37	1.48	1.30	1.42	1.37	1.43	1.34	1.46
13	1.22	1.27	1.30	1.41	1.35	1.48	1.32	1.50	1.27	1.41	1.31	1.48	1.29	1.48
12	1.15	1.22	1.22	1.32	1.31	1.36	1.26	1.33	1.22	1.34	1.24	1.33	1.23	1.34
11	1.11	1.20	1.19	1.27	1.25	1.37	1.22	1.32	1.20	1.30	1.20	1.32	1.20	1.33
10	1.11	1.16	1.18	1.28	1.25	1.36	1.24	1.31	1.15	1.29	1.21	1.32	1.17	1.32
9	1.06	1.14	1.14	1.36	1.25	1.39	1.30	1.39	1.15	1.32	1.23	1.39	1.16	1.38
8	1.02	1.11	1.05	1.35	1.23	1.39	1.28	1.38	1.17	1.29	1.21	1.39	1.18	1.37
7	1.06	1.13	1.03	1.31	1.28	1.34	1.27	1.38	1.17	1.29	1.22	1.37	1.19	1.36
6	1.08	1.16	1.00	1.23	1.30	1.32	1.26	1.34	1.14	1.30	1.18	1.32	1.17	1.31
5	1.10	1.17	0.99	1.27	1.22	1.33	1.25	1.31	1.13	1.27	1.22	1.28	1.17	1.28
4	1.11	1.15	0.96	1.16	1.16	1.29	1.19	1.23	1.13	1.22	1.16	1.21	1.14	1.22
3	1.15	1.19	1.03	1.19	1.18	1.31	1.22	1.28	1.17	1.25	1.17	1.27	1.17	1.27
2	1.15	1.25	1.19	1.29	1.28	1.34	1.29	1.37	1.23	1.31	1.25	1.36	1.25	1.35
1	1.33	1.41	1.30	1.48	1.42	1.55	1.35	1.51	1.38	1.49	1.35	1.52	1.36	1.54

Table C.4 Maximum link overstrength factor 20 storey frame in Montreal

Storey	Artificial records(5)-short distance		Artificial records(5)-long distance		Artificial records(10)	
	V_{max}/V_p		V_{max}/V_p		V_{max}/V_p	
	50^{th}	84^{th}	50^{th}	84^{th}	50^{th}	84^{th}
20	0.53	0.67	0.51	0.60	0.52	0.60
19	1.15	1.26	1.24	1.26	1.20	1.26
18	1.22	1.29	1.36	1.41	1.31	1.39
17	1.07	1.14	1.29	1.30	1.23	1.29
16	0.95	1.05	1.07	1.12	1.06	1.10
15	0.86	1.02	1.00	1.08	0.95	1.09
14	0.97	1.05	1.03	1.08	1.00	1.08
13	0.99	1.01	1.04	1.06	1.01	1.05
12	0.82	0.87	0.98	1.00	0.88	1.00
11	0.77	0.84	0.97	1.03	0.85	1.03
10	0.73	0.83	0.93	1.02	0.88	0.99
9	0.77	0.83	0.91	0.97	0.86	0.95
8	0.82	0.84	0.88	0.91	0.86	0.88
7	0.76	0.79	0.75	0.92	0.76	0.85
6	0.76	0.79	0.78	0.95	0.77	0.88
5	0.71	0.76	0.74	0.90	0.73	0.84
4	0.70	0.82	0.79	0.92	0.77	0.89
3	0.66	0.83	0.82	0.90	0.81	0.89
2	0.66	0.84	0.83	0.88	0.81	0.89
1	0.82	0.99	1.00	1.02	0.97	1.03

Table C.5 Maximum link overstrength factor 25 storey frame in Vancouver

Storey	Historical records(5)-short distance		Artificial records(5)-short distance		Historical records(5)-long distance		Artificial records(5)-long distance		Historical records (10)		Artificial records (10)		All records (20)	
	V_{max}/V_p		V_{max}/V_p		V_{max}/V_p		V_{max}/V_p		V_{max}/V_p		V_{max}/V_p		V_{max}/V_p	
	50^{th}	84^{th}	50^{th}	84^{th}	50^{th}	84^{th}	50^{th}	84^{th}	50^{th}	84^{th}	50^{th}	84^{th}	50^{th}	84^{th}
25	0.54	0.63	0.64	0.71	0.60	0.63	0.43	0.53	0.57	0.64	0.51	0.71	0.55	0.67
24	1.23	1.27	1.23	1.25	1.21	1.23	1.05	1.15	1.21	1.27	1.13	1.25	1.20	1.26
23	1.40	1.47	1.40	1.44	1.38	1.40	1.26	1.40	1.39	1.45	1.36	1.44	1.39	1.46
22	1.45	1.53	1.50	1.52	1.42	1.51	1.27	1.47	1.45	1.51	1.44	1.52	1.45	1.52
21	1.30	1.45	1.43	1.50	1.38	1.41	1.34	1.49	1.33	1.42	1.35	1.50	1.34	1.50
20	1.30	1.41	1.39	1.43	1.36	1.37	1.38	1.51	1.33	1.38	1.38	1.46	1.36	1.42
19	1.30	1.48	1.38	1.41	1.38	1.41	1.44	1.54	1.36	1.45	1.39	1.47	1.38	1.45
18	1.32	1.45	1.37	1.39	1.34	1.40	1.37	1.47	1.33	1.44	1.37	1.43	1.35	1.44
17	1.19	1.31	1.30	1.35	1.35	1.42	1.37	1.47	1.27	1.36	1.34	1.41	1.32	1.38
16	1.10	1.27	1.24	1.33	1.28	1.36	1.32	1.38	1.24	1.30	1.31	1.34	1.27	1.34
15	1.16	1.22	1.19	1.28	1.24	1.35	1.28	1.34	1.20	1.27	1.25	1.29	1.24	1.28
14	1.16	1.23	1.17	1.22	1.22	1.34	1.26	1.34	1.22	1.25	1.22	1.27	1.22	1.26
13	1.10	1.20	1.11	1.24	1.17	1.31	1.21	1.29	1.16	1.24	1.19	1.27	1.18	1.26
12	1.06	1.12	1.02	1.21	1.11	1.29	1.16	1.23	1.07	1.21	1.14	1.22	1.11	1.22
11	1.00	1.12	1.02	1.23	1.13	1.28	1.15	1.23	1.08	1.21	1.12	1.23	1.10	1.24
10	0.97	1.11	1.02	1.23	1.14	1.27	1.14	1.23	1.07	1.21	1.11	1.23	1.10	1.23
9	0.99	1.09	1.00	1.20	1.12	1.26	1.12	1.21	1.06	1.19	1.11	1.20	1.10	1.20
8	1.02	1.13	0.97	1.19	1.14	1.28	1.14	1.20	1.08	1.22	1.14	1.20	1.12	1.21
7	1.06	1.19	0.96	1.20	1.17	1.29	1.18	1.20	1.12	1.21	1.17	1.21	1.16	1.22
6	1.06	1.15	0.93	1.17	1.14	1.26	1.18	1.19	1.09	1.20	1.15	1.19	1.13	1.19
5	1.10	1.12	1.00	1.17	1.14	1.30	1.17	1.22	1.10	1.24	1.16	1.20	1.12	1.21
4	1.11	1.15	1.07	1.22	1.16	1.34	1.19	1.29	1.14	1.26	1.19	1.27	1.15	1.28
3	1.19	1.20	1.14	1.22	1.24	1.33	1.25	1.35	1.19	1.29	1.18	1.31	1.19	1.33
2	1.22	1.24	1.18	1.28	1.22	1.36	1.25	1.34	1.22	1.30	1.22	1.30	1.22	1.31
1	1.32	1.33	1.23	1.37	1.27	1.37	1.27	1.42	1.29	1.35	1.25	1.39	1.27	1.39

Table C.6 Maximum link overstrength factor 25 storey frame in Montreal

Storey	Artificial records(5)-short distance		Artificial records(5)-long distance		Artificial records (10)	
	V_{max}/V_p		V_{max}/V_p		V_{max}/V_p	
	50^{th}	84^{th}	50^{th}	84^{th}	50^{th}	84^{th}
25	0.57	0.62	0.53	0.57	0.54	0.62
24	1.15	1.20	1.13	1.30	1.14	1.27
23	1.19	1.24	1.30	1.40	1.22	1.36
22	1.04	1.15	1.29	1.32	1.23	1.30
21	1.00	1.09	1.21	1.30	1.17	1.26
20	0.97	1.07	1.14	1.19	1.08	1.17
19	0.96	1.03	1.09	1.17	1.02	1.12
18	0.94	1.00	1.01	1.10	1.00	1.06
17	0.89	0.90	1.02	1.08	1.00	1.06
16	0.82	0.90	1.01	1.05	0.93	1.03
15	0.79	0.90	0.95	1.04	0.89	1.01
14	0.74	0.88	0.93	1.03	0.88	0.98
13	0.74	0.85	0.91	1.00	0.85	0.95
12	0.70	0.76	0.83	0.91	0.80	0.86
11	0.70	0.74	0.80	0.87	0.75	0.81
10	0.70	0.75	0.76	0.85	0.74	0.78
9	0.61	0.66	0.67	0.80	0.64	0.72
8	0.62	0.71	0.72	0.85	0.68	0.79
7	0.64	0.74	0.75	0.86	0.72	0.81
6	0.62	0.75	0.74	0.84	0.69	0.82
5	0.64	0.77	0.78	0.89	0.74	0.86
4	0.63	0.75	0.82	0.88	0.77	0.85
3	0.63	0.74	0.86	0.92	0.80	0.88
2	0.57	0.68	0.88	0.92	0.76	0.89
1	0.67	0.77	1.00	1.03	0.85	1.01

Table C.7 Maximum inelastic accumulated rotations in the exterior beams – historical records

Storey	Inelastic accumulated rotation, θ (rad)									
	V11	V12	V13	V14	V15	V16	V17	V18	V19	V20
14	0.00000	0.00000	0.00000	0.00000	0.00000	0.00000	0.00000	0.00000	0.00000	0.00000
13	0.00000	0.00000	0.00000	0.00000	0.00000	0.00000	0.00000	0.00000	0.00000	0.00000
12	0.00000	0.00000	0.00000	0.00000	0.00000	0.00000	0.00000	0.00000	0.00000	0.00000
11	0.00000	0.00000	0.00000	0.00000	0.00000	0.00000	0.00000	0.00000	0.00000	0.00000
10	0.00000	0.00000	0.00000	0.00000	0.00000	0.00000	0.00000	0.00000	0.00000	0.00000
9	0.00000	0.00000	0.00000	0.00000	0.00000	0.00000	0.00000	0.00000	0.00000	0.00000
8	0.00000	0.00000	-0.00049	0.00000	0.00000	0.00000	0.00000	0.00000	0.00000	-0.00009
7	0.00000	0.00172	-0.00041	0.00000	0.00000	-0.00063	0.00000	0.00000	-0.00079	0.00311
6	0.00000	0.00000	0.00000	0.00000	0.00000	0.00000	0.00000	0.00000	0.00000	0.00113
5	0.00000	0.00000	0.00000	0.00000	0.00000	0.00000	0.00000	0.00000	0.00000	0.00068
4	0.00000	0.00030	0.00000	0.00000	0.00000	0.00051	0.00059	0.00059	-0.00080	0.00237
3	0.00000	0.00000	0.00000	0.00000	0.00000	0.00000	0.00066	-0.00009	0.00000	-0.00056
2	0.00000	0.00000	0.00000	0.00000	0.00000	0.00000	0.00000	0.00000	0.00000	0.00000
1	0.00000	0.00000	0.00000	0.00000	0.00000	0.00000	0.00000	0.00000	0.00000	0.00000

Table C.8 Maximum inelastic accumulated rotations in the exterior beams – artificial records

Storey	Inelastic accumulated rotation, θ (rad)									
	W61	W62	W63	W64	W65	W66	W77	W78	W79	W70
14	0.00000	0.00000	0.00000	0.00000	0.00000	0.00000	0.00000	0.00000	0.00000	0.00000
13	0.00000	0.00000	0.00000	0.00000	0.00000	0.00000	0.00000	0.00000	0.00000	0.00000
12	0.00000	0.00000	0.00000	0.00000	0.00000	0.00000	0.00000	0.00000	0.00000	0.00000
11	0.00000	0.00000	0.00000	0.00000	0.00000	0.00000	0.00000	0.00000	0.00000	0.00000
10	0.00000	0.00000	0.00000	0.00000	0.00000	0.00000	0.00000	0.00000	0.00000	0.00000
9	0.00000	0.00000	0.00000	0.00000	0.00000	0.00000	0.00000	0.00000	0.00000	0.00000
8	0.00000	0.00000	0.00082	0.00000	0.00000	0.00000	0.00000	-0.00208	0.00000	0.00000
7	0.00008	0.00000	0.00001	0.00200	0.00000	0.00035	0.00103	0.00200	0.00000	0.00019
6	0.00000	0.00000	0.00000	-0.00154	0.00000	0.00008	0.00000	0.00070	0.00000	0.00000
5	0.00000	0.00000	0.00000	-0.00179	0.00000	0.00000	0.00084	-0.00134	0.00000	0.00000
4	0.00000	0.00030	0.00071	-0.00345	0.00000	-0.00089	0.00196	-0.00283	0.00116	-0.00048
3	0.00000	0.00000	0.00000	-0.00117	0.00000	-0.00040	-0.00069	0.00093	0.00002	0.00000
2	0.00000	0.00000	0.00000	0.00000	0.00000	0.00000	0.00000	0.00000	0.00000	0.00000
1	0.00000	0.00000	0.00000	-0.00096	0.00000	0.00000	0.00027	0.00241	0.00000	0.00000

Table C.9 Number of inelastic incursions in the braces (14 storeys Vancouver)-historical records

Storey	V11	V12	V13	V14	V15	V16	V17	V18	V19	V20
14	–	–	–	–	–	–	–	–	–	–
13	–	–	–	–	–	–	–	–	–	–
12	–	–	–	–	–	–	–	–	–	–
11	–	–	–	–	–	–	–	–	–	–
10	–	–	–	–	–	–	–	–	–	–
9	–	–	–	–	–	–	–	–	–	–
8	–	–	–	–	–	–	–	–	–	–
7	–	–	–	–	–	–	–	–	–	–
6	–	–	–	–	–	–	–	–	–	–
5	–	–	–	–	–	–	–	–	–	–
4	–	–	–	–	–	–	–	–	–	–
3	–	–	–	–	–	–	–	–	–	–
2	–	–	–	–	1	–	–	–	–	–
1	–	1	–	1	1	–	4	2	–	3

Table C.10 Accumulated time for the inelastic incursions in braces (14 storeys Vancouver)-historical records

Storey	V11	V12	V13	V14	V15	V16	V17	V18	V19	V20
14	–	–	–	–	–	–	–	–	–	–
13	–	–	–	–	–	–	–	–	–	–
12	–	–	–	–	–	–	–	–	–	–
11	–	–	–	–	–	–	–	–	–	–
10	–	–	–	–	–	–	–	–	–	–
9	–	–	–	–	–	–	–	–	–	–
8	–	–	–	–	–	–	–	–	–	–
7	–	–	–	–	–	–	–	–	–	–
6	–	–	–	–	–	–	–	–	–	–
5	–	–	–	–	–	–	–	–	–	–
4	–	–	–	–	–	–	–	–	–	–
3	–	–	–	–	–	–	–	–	–	–
2	–	–	–	–	–	–	–	–	–	–
1	–	0.04	–	0.08	0.05	–	0.51	0.20	–	0.89

Table C.11 Number of inelastic incursions in the braces (14 storeys Vancouver)-artificial records

Storey	W61	W62	W63	W64	W65	W66	W77	W78	W79	W70
14	–	–	–	–	–	–	–	–	–	–
13	–	–	–	–	–	–	–	–	–	–
12	–	–	–	–	–	–	–	–	–	–
11	–	–	–	–	–	–	–	–	–	–
10	–	–	–	–	–	–	–	–	–	–
9	–	–	–	–	–	–	–	–	–	–
8	–	–	–	–	–	–	–	–	–	–
7	–	–	–	–	–	–	–	–	–	–
6	–	–	–	1	–	–	–	–	–	–
5	–	–	–	1	–	–	–	–	–	–
4	–	–	–	1	–	–	–	–	–	–
3	–	–	–	–	–	–	–	–	–	–
2	–	–	–	–	–	–	–	–	–	–
1	–	–	1	3	–	1	3	6	–	–

Table C.12 Accumulated time for the inelastic incursions in braces (14 storeys Vancouver)-artificial records

Storey	W61	W62	W63	W64	W65	W66	W77	W78	W79	W70
14	–	–	–	–	–	–	–	–	–	–
13	–	–	–	–	–	–	–	–	–	–
12	–	–	–	–	–	–	–	–	–	–
11	–	–	–	–	–	–	–	–	–	–
10	–	–	–	–	–	–	–	–	–	–
9	–	–	–	–	–	–	–	–	–	–
8	–	–	–	–	–	–	–	–	–	–
7	–	–	–	–	–	–	–	–	–	–
6	–	–	–	0.08	–	–	–	–	–	–
5	–	–	–	0.13	–	–	–	–	–	–
4	–	–	–	0.13	–	–	–	–	–	–
3	–	–	–	–	–	–	–	–	–	–
2	–	–	–	–	–	–	–	–	–	–
1	–	–	0.07	0.63	–	0.18	0.52	1.34	–	–

Table C.13 Number of inelastic incursions in the braces (20 storeys Vancouver)-historical records

Storey	V11	V12	V13	V14	V15	V16	V17	V18	V19	V20
20	–	–	–	–	–	–	–	–	–	–
19	–	–	–	–	–	–	–	–	–	–
18	–	–	–	–	–	–	–	–	–	–
17	–	–	–	–	–	–	–	–	–	–
16	–	–	–	–	–	–	–	–	–	–
15	–	–	–	–	–	–	–	–	–	–
14	–	–	–	–	–	–	–	–	–	–
13	–	–	–	–	–	–	–	–	1	1
12	–	–	–	–	–	–	–	–	2	3
11	–	–	–	–	–	–	–	–	–	1
10	–	–	–	–	–	–	–	–	–	–
9	–	–	–	–	–	1	–	–	–	–
8	–	–	–	–	–	–	–	–	–	1
7	–	–	–	–	–	–	–	–	–	1
6	–	–	–	–	–	–	–	–	–	–
5	–	–	–	–	–	–	–	–	–	–
4	–	–	–	–	–	–	–	–	–	–
3	–	–	–	–	–	–	–	–	–	–
2	–	–	–	1	1	–	1	–	–	–
1	–	–	–	1	–	–	2	–	3	3

Table C.14 Accumulated time for the inelastic incursions in braces (20 storeys Vancouver)-historical records

Storey	V11	V12	V13	V14	V15	V16	V17	V18	V19	V20
20	–	–	–	–	–	–	–	–	–	–
19	–	–	–	–	–	–	–	–	–	–
18	–	–	–	–	–	–	–	–	–	–
17	–	–	–	–	–	–	–	–	–	–
16	–	–	–	–	–	–	–	–	–	–
15	–	–	–	–	–	–	–	–	–	–
14	–	–	–	–	–	–	–	–	–	–
13	–	–	–	–	–	–	–	–	0.06	0.35
12	–	–	–	–	–	–	–	–	0.13	0.88
11	–	–	–	–	–	–	–	–	–	0.13
10	–	–	–	–	–	–	–	–	–	–
9	–	–	–	–	–	0.07	–	–	–	–
8	–	–	–	–	–	–	–	–	–	0.49
7	–	–	–	–	–	–	–	–	–	0.40
6	–	–	–	–	–	–	–	–	–	–
5	–	–	–	–	–	–	–	–	–	–
4	–	–	–	–	–	–	–	–	–	–
3	–	–	–	–	–	–	–	–	–	–
2	–	–	–	0.05	0.02	–	0.14	–	–	–
1	–	–	–	0.02	–	–	0.37	–	0.22	1.59

Table C.15 Number of inelastic incursions in the braces (20 storeys Vancouver)-artificial records

Storey	W61	W62	W63	W64	W65	W66	W77	W78	W79	W70
20	–	–	–	–	–	–	–	–	–	–
19	–	–	–	–	–	–	–	–	–	–
18	–	–	–	–	–	–	–	–	–	–
17	–	–	–	–	–	–	–	–	–	–
16	–	–	–	–	–	–	–	–	–	–
15	–	–	–	–	–	–	1	–	–	–
14	–	–	–	–	–	–	–	–	–	–
13	–	–	–	1	–	–	1	1	–	–
12	–	–	–	1	–	–	1	3	–	–
11	–	–	–	–	–	–	–	–	–	–
10	–	–	–	–	–	–	–	–	–	–
9	–	–	–	–	–	–	–	–	–	–
8	–	–	–	1	–	–	1	1	–	–
7	–	–	–	2	–	–	1	1	–	–
6	–	–	–	–	–	–	–	–	–	–
5	–	–	–	–	–	–	–	–	–	–
4	–	–	–	–	–	–	–	–	–	–
3	–	–	–	–	–	–	–	–	–	–
2	–	–	–	–	–	–	–	–	–	–
1	–	–	1	1	–	–	2	2	–	–

Table C.16 Accumulated time for the inelastic incursions in braces (20 storeys Vancouver)-artificial records

Storey	W61	W62	W63	W64	W65	W66	W77	W78	W79
20	–	–	–	–	–	–	–	–	–
19	–	–	–	–	–	–	–	–	–
18	–	–	–	–	–	–	–	–	–
17	–	–	–	–	–	–	–	–	–
16	–	–	–	–	–	–	–	–	–
15	–	–	–	–	–	–	0.03	–	–
14	–	–	–	–	–	–	–	–	–
13	–	–	–	0.38	–	–	0.52	0.10	–
12	–	–	–	0.41	–	–	0.20	0.07	–
11	–	–	–	–	–	–	–	–	–
10	–	–	–	–	–	–	–	–	–
9	–	–	–	–	–	–	–	–	–
8	–	–	–	0.24	–	–	0.07	0.35	–
7	–	–	–	0.13	–	–	0.07	0.11	–
6	–	–	–	–	–	–	–	–	–
5	–	–	–	–	–	–	–	–	–
4	–	–	–	–	–	–	–	–	–
3	–	–	–	–	–	–	–	–	–
2	–	–	–	–	–	–	–	–	–
1	–	–	0.08	0.22	–	–	0.39	0.53	–

Table C.17 Number of inelastic incursions in the braces (25 storeys Vancouver)-historical records

Storey	V11	V12	V13	V14	V15	V16	V17	V18	V19	V20
25	–	–	–	–	–	–	–	–	–	–
24	–	–	–	–	–	–	–	–	–	–
23	–	–	–	–	–	–	–	–	–	–
22	–	–	–	–	–	–	–	–	–	–
21	–	–	–	–	–	–	–	–	–	–
20	–	–	–	–	–	–	–	–	–	–
19	–	–	–	–	–	–	–	–	–	–
18	–	–	–	–	–	–	–	–	–	–
17	–	–	–	–	–	–	–	–	–	–
16	–	–	–	–	–	–	–	–	–	–
15	–	–	–	–	–	–	–	–	–	–
14	–	–	–	–	–	–	–	–	–	–
13	–	–	–	–	–	–	–	–	–	–
12	–	–	–	–	–	–	–	–	–	–
11	–	–	–	–	–	–	–	–	–	–
10	–	–	–	–	–	–	–	–	–	–
9	–	–	–	–	–	–	–	–	–	–
8	–	–	–	–	–	–	–	–	–	–
7	–	–	–	–	–	–	–	–	–	–
6	–	–	–	–	–	–	–	–	–	–
5	–	–	–	–	–	–	–	–	–	–
4	–	–	–	–	–	–	–	–	–	–
3	–	–	–	–	–	–	–	–	–	1
2	–	–	–	–	–	–	–	–	–	1
1	–	–	–	–	–	–	–	–	–	1

Table C.18 Accumulated time for the inelastic incursions in braces (25 storeys Vancouver)-historical records

Storey	V11	V12	V13	V14	V15	V16	V17	V18	V19	V20
25	–	–	–	–	–	–	–	–	–	–
24	–	–	–	–	–	–	–	–	–	–
23	–	–	–	–	–	–	–	–	–	–
22	–	–	–	–	–	–	–	–	–	–
21	–	–	–	–	–	–	–	–	–	–
20	–	–	–	–	–	–	–	–	–	–
19	–	–	–	–	–	–	–	–	–	–
18	–	–	–	–	–	–	–	–	–	–
17	–	–	–	–	–	–	–	–	–	–
16	–	–	–	–	–	–	–	–	–	–
15	–	–	–	–	–	–	–	–	–	–
14	–	–	–	–	–	–	–	–	–	–
13	–	–	–	–	–	–	–	–	–	–
12	–	–	–	–	–	–	–	–	–	–
11	–	–	–	–	–	–	–	–	–	–
10	–	–	–	–	–	–	–	–	–	–
9	–	–	–	–	–	–	–	–	–	–
8	–	–	–	–	–	–	–	–	–	–
7	–	–	–	–	–	–	–	–	–	–
6	–	–	–	–	–	–	–	–	–	–
5	–	–	–	–	–	–	–	–	–	–
4	–	–	–	–	–	–	–	–	–	–
3	–	–	–	–	–	–	–	–	–	0.32
2	–	–	–	–	–	–	–	–	–	0.24
1	–	–	–	–	–	–	–	–	–	0.02

Table C.19 Number of inelastic incursions in the braces (25 storeys Vancouver)-artificial records

Storey	W61	W62	W63	W64	W65	W66	W77	W78	W79	W70
25	–	–	–	–	–	–	–	–	–	–
24	–	–	–	–	–	–	–	–	–	–
23	–	–	–	–	–	–	–	–	–	–
22	–	–	–	–	–	–	–	–	–	–
21	–	–	–	–	–	–	–	–	–	–
20	–	–	–	–	–	–	–	–	–	–
19	–	–	–	–	–	–	–	–	–	–
18	–	–	–	–	–	–	–	–	–	–
17	–	–	–	–	–	–	–	–	–	–
16	–	–	–	–	–	–	–	–	–	–
15	–	–	–	–	–	–	–	–	–	–
14	–	–	–	–	–	–	–	–	–	–
13	–	–	–	–	–	–	–	–	–	–
12	–	–	–	–	–	–	–	–	–	–
11	–	–	–	–	–	–	–	–	–	–
10	–	–	–	–	–	–	–	–	–	–
9	–	–	–	–	–	–	–	–	–	–
8	–	–	–	–	–	–	–	–	–	–
7	–	–	–	–	–	–	–	–	–	–
6	–	–	–	–	–	–	–	–	–	–
5	–	–	–	–	–	–	–	–	–	–
4	–	–	–	–	–	–	–	–	–	–
3	–	–	–	–	–	–	–	1	–	–
2	–	–	–	–	–	–	–	–	–	–
1	–	–	–	1	–	–	1	1	–	–

Table C.20 Accumulated time for the inelastic incursions in braces (25 storeys Vancouver)-artificial records

Storey	W61	W62	W63	W64	W65	W66	W77	W78	W79	W70
25	–	–	–	–	–	–	–	–	–	–
24	–	–	–	–	–	–	–	–	–	–
23	–	–	–	–	–	–	–	–	–	–
22	–	–	–	–	–	–	–	–	–	–
21	–	–	–	–	–	–	–	–	–	–
20	–	–	–	–	–	–	–	–	–	–
19	–	–	–	–	–	–	–	–	–	–
18	–	–	–	–	–	–	–	–	–	–
17	–	–	–	–	–	–	–	–	–	–
16	–	–	–	–	–	–	–	–	–	–
15	–	–	–	–	–	–	–	–	–	–
14	–	–	–	–	–	–	–	–	–	–
13	–	–	–	–	–	–	–	–	–	–
12	–	–	–	–	–	–	–	–	–	–
11	–	–	–	–	–	–	–	–	–	–
10	–	–	–	–	–	–	–	–	–	–
9	–	–	–	–	–	–	–	–	–	–
8	–	–	–	–	–	–	–	–	–	–
7	–	–	–	–	–	–	–	–	–	–
6	–	–	–	–	–	–	–	–	–	–
5	–	–	–	–	–	–	–	–	–	–
4	–	–	–	–	–	–	–	–	–	–
3	–	–	–	–	–	–	–	0.23	–	–
2	–	–	–	–	–	–	–	–	–	–
1	–	–	–	0.06	–	–	0.09	0.40	–	–

Table C.21 Number of inelastic incursions in the columns (14 storeys Vancouver)-historical records

Storey	V11	V12	V13	V14	V15	V16	V17	V18	V19	V20
14	–	–	–	–	–	–	–	–	–	–
13	–	–	1	2	–	–	–	–	–	–
12	–	–	–	–	–	–	–	–	–	–
11	–	–	–	24	–	–	–	–	–	–
10	–	–	–	–	–	–	–	–	–	–
9	–	–	1	–	–	–	1	–	–	2
8	–	–	–	–	–	–	–	–	–	–
7	–	–	–	–	–	–	–	–	–	–
6	–	–	–	–	–	–	–	–	–	–
5	–	–	–	–	–	–	–	–	–	–
4	–	–	–	–	–	–	–	–	–	–
3	–	–	–	–	–	–	–	–	–	–
2	–	–	–	–	–	–	–	–	–	–
1	–	–	–	–	–	–	–	–	–	–

Table C.22 Accumulated time for the inelastic incursions in columns (14 storeys Vancouver)-historical records

Storey	V11	V12	V13	V14	V15	V16	V17	V18	V19	V20
14	–	–	–	–	–	–	–	–	–	–
13	–	–	0.09	0.16	–	–	–	–	–	–
12	–	–	–	–	–	–	–	–	–	–
11	–	–	–	11.47	–	–	–	–	–	–
10	–	–	–	–	–	–	–	–	–	–
9	–	–	0.11	–	–	–	0.11	–	–	0.20
8	–	–	–	–	–	–	–	–	–	–
7	–	–	–	–	–	–	–	–	–	–
6	–	–	–	–	–	–	–	–	–	–
5	–	–	–	–	–	–	–	–	–	–
4	–	–	–	–	–	–	–	–	–	–
3	–	–	–	–	–	–	–	–	–	–
2	–	–	–	–	–	–	–	–	–	–
1	–	–	–	–	–	–	–	–	–	–

Table C.23 Number of inelastic incursions in the columns (14 storeys Vancouver)-artificial records

Storey	W61	W62	W63	W64	W65	W66	W77	W78	W79	W70
14	–	–	–	–	–	–	–	–	–	–
13	–	–	–	–	–	–	–	–	–	–
12	–	–	–	–	–	–	–	–	–	–
11	–	–	–	–	–	–	–	–	–	–
10	–	–	–	–	–	–	–	–	–	–
9	–	–	–	1	–	–	–	–	–	–
8	–	–	–	–	–	–	–	–	–	–
7	–	–	–	1	–	–	–	1	–	–
6	–	–	–	–	–	–	–	–	–	–
5	–	–	–	–	–	–	–	–	–	–
4	–	–	–	–	–	–	–	–	–	–
3	–	–	–	–	–	–	–	–	–	–
2	–	–	–	–	–	–	–	–	–	–
1	–	–	–	–	–	–	–	–	–	–

Table C.24 Accumulated time for the inelastic incursions in columns (14 storeys Vancouver)-artificial records

Storey	W61	W62	W63	W64	W65	W66	W77	W78	W79	W70
14	–	–	–	–	–	–	–	–	–	–
13	–	–	–	–	–	–	–	–	–	–
12	–	–	–	–	–	–	–	–	–	–
11	–	–	–	–	–	–	–	–	–	–
10	–	–	–	–	–	–	–	–	–	–
9	–	–	–	0.71	–	–	–	–	–	–
8	–	–	–	–	–	–	–	–	–	–
7	–	–	–	0.17	–	–	–	0.38	–	–
6	–	–	–	–	–	–	–	–	–	–
5	–	–	–	–	–	–	–	–	–	–
4	–	–	–	–	–	–	–	–	–	–
3	–	–	–	–	–	–	–	–	–	–
2	–	–	–	–	–	–	–	–	–	–
1	–	–	–	–	–	–	–	–	–	–

Table C.25 Lateral shear force for the 14 storey frame in Vancouver

Storey	Historical records(10)		Artificial records(10)		All records(20)		All records	NBCC $_{linear}$	NBCC$_{spectral}$
	NLTH Shear Force		NLTH Shear Force		NLTH Shear Force		NLTH Shear Force	Design Shear Force	Design Shear Force
	50^{th}	84^{th}	50^{th}	84^{th}	50^{th}	84^{th}	max		
14	588	655	494	630	517	649	794	302	137
13	1182	1260	1117	1175	1127	1215	1319	539	494
12	1636	1773	1582	1712	1568	1766	1863	761	716
11	1959	2157	1929	2044	1929	2136	2237	971	874
10	2266	2418	2235	2454	2207	2471	2620	1171	1012
9	2556	2622	2536	2706	2437	2652	3068	1354	1125
8	2627	2775	2685	2820	2626	2791	3262	1522	1243
7	2775	3017	2903	2960	2838	2979	3556	1672	1366
6	2941	3178	3072	3306	2941	3282	3963	1790	1480
5	3117	3518	3472	3689	3165	3536	4071	1880	1601
4	3411	3591	3648	3930	3383	3737	4064	1971	1741
3	3444	3728	3779	4038	3472	3891	4207	2002	1844
2	3580	3974	3822	4248	3603	4050	4371	2024	1949
1	3928	4115	3830	4369	3879	4271	4552	2012	2010

Table C.26 Lateral shear force for the 14 storey frame in Montreal

Storey	Artificial records(10) NLTH Shear Force		All records NLTH Shear Force	$NBCC_{linear}$ Design Shear Force	$NBCC_{spectral}$ Design Shear Force
	50^{th}	84^{th}	max		
14	466	499	523	138	92
13	982	1017	1050	257	278
12	1216	1266	1285	372	376
11	1225	1371	1538	482	449
10	1282	1365	1493	587	515
9	1391	1443	1478	679	557
8	1421	1593	1642	769	611
7	1461	1673	1713	851	669
6	1587	1677	1742	932	726
5	1650	1868	2056	995	790
4	1780	2002	2116	1053	874
3	2017	2134	2169	1087	956
2	2326	2415	2443	1118	1032
1	2504	2600	2823	1097	1081

Table C.27 Lateral shear force for the 20 storey frame in Vancouver

Storey	Historical records (10)		Artificial records (10)		All records (20)		All records	$NBCC_{linear}$	$NBCC_{spectral}$
	NLTH Shear Force		NLTH Shear Force		NLTH Shear Force		NLTH Shear Force	Design Shear Force	Design Shear Force
	50^{th}	84^{th}	50^{th}	84^{th}	50^{th}	84^{th}	max		
20	550	609	457	598	502	607	718	526	148
19	1348	1466	1293	1454	1342	1454	1582	753	554
18	1877	2002	1827	1942	1856	1997	2177	972	837
17	2306	2468	2257	2380	2275	2459	2633	1186	1046
16	2629	2781	2707	2840	2642	2819	3014	1393	1215
15	2841	2964	3012	3252	2849	3207	3430	1590	1377
14	3061	3131	3243	3336	2985	3270	3626	1768	1513
13	3253	3456	3340	3582	3170	3480	3893	1942	1650
12	3369	3686	3386	3541	3326	3673	4089	2108	1794
11	3394	3801	3602	3796	3559	3849	4203	2262	1931
10	3562	3953	3881	4123	3647	4024	4661	2401	2060
9	3601	4180	4022	4420	3656	4201	4928	2521	2177
8	3838	4348	4057	4765	3821	4350	5130	2625	2288
7	4001	4503	4190	4891	3937	4512	5233	2725	2405
6	4112	4702	4328	4892	4145	4629	5301	2803	2524
5	4273	4824	4541	4931	4310	4793	5436	2856	2632
4	4414	4973	4736	4950	4424	4923	5573	2889	2764
3	4620	5089	4769	4976	4627	5085	5622	2924	2854
2	4875	5193	4928	5110	4875	5163	5696	2940	2943
1	5080	5408	5089	5536	5080	5545	6294	2937	2992

Table C.28 Lateral shear force for the 20 storey frame in Montreal

Storey	Artificial records(10) NLTH Shear Force		All records NLTH Shear Force	$NBCC_{linear}$ Design Shear Force	$NBCC_{spectral}$ Design Shear Force
	50^{th}	84^{th}	max		
20	380	411	581	235	108
19	930	996	1032	358	334
18	1199	1298	1405	481	459
17	1232	1399	1541	593	536
16	1368	1499	1590	701	613
15	1468	1655	1755	808	683
14	1613	1715	1933	894	736
13	1742	1847	2043	978	788
12	1805	2042	2058	1073	848
11	1786	2096	2234	1162	921
10	1946	2190	2374	1227	985
9	2065	2254	2402	1297	1039
8	2124	2218	2572	1369	1102
7	2119	2352	2762	1420	1150
6	2157	2444	2924	1478	1207
5	2200	2516	3015	1535	1273
4	2345	2671	3088	1575	1343
3	2575	2882	3272	1593	1438
2	2789	3056	3315	1606	1528
1	2992	3178	3421	1600	1602

Table C.29 Lateral shear force for the 25 storey frame in Vancouver

Storey	Historical records(10) NLTH Shear Force		Artificial records(10) NLTH Shear Force		All records(20) NLTH Shear Force		All records NLTH Shear Force	$NBCC_{linear}$ Design Shear Force	$NBCC_{spectral}$ Design Shear Force
	50^{th}	84^{th}	50^{th}	84^{th}	50^{th}	84^{th}	max		
25	567	635	464	619	501	592	729	647	158
24	1742	1804	1652	1745	1739	1823	1982	877	608
23	2111	2193	1963	2137	1994	2141	2334	1096	926
22	2495	2680	2450	2581	2475	2632	2913	1316	1172
21	2775	2920	2894	3040	2814	3005	3616	1531	1374
20	3132	3206	3292	3423	3183	3389	3774	1732	1539
19	3352	3618	3695	3615	3465	3826	4076	1923	1694
18	3551	3928	3867	3857	3784	4051	4337	2115	1853
17	3552	4192	4029	4115	4002	4254	4449	2293	1995
16	3788	4309	4252	4296	4213	4324	4725	2462	2105
15	3921	4414	4345	4358	4244	4528	5251	2626	2222
14	4059	4430	4454	4419	4223	4687	5652	2788	2342
13	4271	4798	4614	4471	4489	4719	5744	2926	2435
12	4322	5112	4613	4751	4412	5015	5924	3054	2554
11	4511	5178	4655	4954	4535	5049	6052	3188	2658
10	4508	5305	4675	5171	4582	5206	6281	3308	2753
9	4583	5504	4885	5284	4802	5276	6474	3410	2869
8	4818	5758	5056	5418	4895	5418	6542	3520	2988
7	5274	5771	5194	5603	5033	5645	6450	3593	3105
6	5474	5833	5383	5698	5138	5699	6420	3633	3210
5	5653	5915	5516	5777	5347	5876	6470	3703	3287
4	5666	5999	5575	6022	5470	6112	6688	3747	3396
3	5829	6015	5618	6233	5790	6251	6758	3762	3555
2	6057	6324	5808	6357	5889	6452	7194	3750	3667
1	6040	6366	6116	6604	6061	6684	7520	3719	3715

Table C.30 Lateral shear force for the 25 storey frame in Montreal

Storey	Artificial records(10) NLTH Shear Force		All records NLTH Shear Force	$NBCC_{linear}$ Design Shear Force	$NBCC_{spectral}$ Design Shear Force
	50^{th}	84^{th}	max		
25	385	420	493	202	135
24	983	1070	1138	331	371
23	1115	1187	1339	454	497
22	1242	1349	1388	572	594
21	1401	1440	1598	679	677
20	1433	1580	1789	790	751
19	1530	1756	1847	891	824
18	1700	1791	1846	998	877
17	1792	1997	2052	1108	937
16	1838	2107	2135	1202	1000
15	1847	2197	2207	1299	1049
14	1885	2279	2481	1388	1105
13	1995	2336	2812	1469	1167
12	1984	2288	2976	1545	1238
11	1972	2200	3148	1623	1295
10	2043	2139	3217	1691	1350
9	2008	2303	3218	1756	1413
8	2082	2439	3286	1811	1473
7	2240	2603	3256	1860	1546
6	2355	2869	3278	1898	1623
5	2528	3067	3394	1931	1699
4	2809	3170	3558	1949	1805
3	2840	3263	3788	1963	1906
2	2875	3472	4044	1962	2000
1	3003	3587	4190	1961	2066